



**Hybrid silica materials derived from proline
sulfonamides, imidazolium salts and
(NHC)AuX complexes as supported
catalysts**

Meritxell Ferré Romeu

Tesi Doctoral

Estudis de Doctorat en Química

Directora:

Dra. Roser Pleixats i Rovira

Departament de Química

Facultat de Ciències

2015

Memòria presentada per aspirar al Grau de Doctor per:

Merixell Ferré Romeu

Vist i plau:

Roser Pleixats i Rovira

Bellaterra, 28 d'Abril de 2015

ACKNOWLEDGEMENTS

The present work has been carried out at the *Unitat de Química Orgànica de Departament de Química* from *Universitat Autònoma de Barcelona* under the supervision of Prof. Roser Pleixats i Rovira whom I will always be grateful of her confidence, her availability for meeting me and giving me advice as well as all the time she has dedicate me to follow up my work. Furthermore, a collaboration with the group of *Architectures Moléculaires et Matériaux Nanostructurés* at *Institut Charles Gerhardt de Montpellier* in *ENSCM* has been done during these years where Dr. Michel Wong Chi Man offered me the chance of working in his research group. In the same manner, Dr. Xavier Cattoën taught me everything I needed to do the experiments. Thus, I would like to thank them all the help and guidance that they gave me during my stages. Likely, I would like to thank all the Professors of our group who have contributed to develop this thesis with their suggestions and recommendations.

I would also like to thank all my labmates from C7/423, C7/419, C7/415 and C7/416 who have contributed to this work with their companionship and their kindness, specially Dra. Amàlia Monge who helped me from my first day in the group and taught me all the tricks she knew and she still gives me advice. Likewise, I would like to thank Achraf and Ana all their hospitality while I was in France.

També vull agrair a tots els meus amics del grup "Il Cazzo": la Roser, el Joseju, el Marc i el Nico per compartir aquests anys amb mi; junts hem viscut viatges i moments que recordaré sempre i espero que en vinguin molts més. D'altra banda, als meus amics Bea, Lúdia, Toni, Marta, Jess, Ana, Lara i Cris que sempre et fan somriure i t'animen a seguir endavant.

No hi ha prou paraules per agrair a tota la meva família el seu suport i interès per saber com va tot i en què et poden ajudar, sobretot a la meva mare, a la meva àvia i a l'Àlex, ells són casa meva i sempre estan disposats a fer el que calgui, incondicionalment. Gràcies per estimar-me tant i dedicar-me tant d'esforç. No puc deixar d'esmentar com m'agradaria que el meu pare fos aquí i poder-li agrair tot el que em va donar i ensenyar. Gràcies per ajudar-me a arribar fins aquí, per a mi, sempre seràs un referent i el motiu de fer les coses bé. Finalment, li he de donar gràcies al Jordi, per estar cada dia al meu costat, saber-me escoltar i donar-me ànims per continuar avançant. Gràcies per fer-me tan feliç i voler compartir aquest temps amb mi.

Thank you all very much! / Moltes gràcies a tots!

FINANCIAL AND TECHNICAL SUPPORT

I would like to thank *Universitat Autònoma de Barcelona* for giving me the *Personal Investigador en Formació* scholarship as well as the financial support received from Spain (Projects CTQ2009-07881, CTQ2011-22649 and *Consolider Ingenio* 2010 (CSD2007-0006)) which have done this thesis possible.

Finally, the technical support from *Servei d'Anàlisi Química de la UAB*, *Servei de Ressonància Magnètica Nuclear de la UAB*, *Serveis Científico-Tècnics de la UB* and *University of Montpellier II* is acknowledged as well.

Als meus pares

TABLE OF CONTENTS

PREFACE	i
Abbreviations.....	viii
Abstract.....	x
Resum.....	xi
Resumen.....	xii
CHAPTER 1.	
INTRODUCTION TO ORGANIC-INORGANIC HYBRID SILICA MATERIALS	3
1. Hybrid silica materials	3
2. Preparation of organic-inorganic hybrid silica materials	5
<i>Synthetic strategies towards hybrid materials</i>	5
2.1 Post-functionalization methods (<i>building block approach</i>).....	5
2.2 The Sol-Gel process (<i>in situ formation of the components</i>).....	7
2.2.1 The Sol-Gel process	7
2.2.2 Co-condensation and bridged silsesquioxanes.....	9
2.2.3 Mesostructuring of organosilicas	10
3. Characterization of hybrid silica materials	15
3.1 ²⁹ Si and ¹³ C Solid State Nuclear Magnetic Resonance (SSNMR)	15
3.2 Vibrational Spectroscopy (IR and Raman)	18
3.3 Thermogravimetric analysis	19
3.4 Elemental Analysis	20
3.5 Surface area analysis	20
3.6 Powder X-Ray Diffraction	24
3.7 Electron Microscopy	26
CHAPTER 2.	
ORGANOSILICAS DERIVED FROM PROLINE SULFONAMIDES AND PROLINE TETRAZOLES. APPLICATIONS IN ASYMMETRIC ORGANOCATALYSIS	29
1. INTRODUCTION	31
1.1 Introduction to asymmetric organocatalysis	31
1.2 Organocatalysis classification. Activation modes	33

Table of Contents

1.3 Enamine catalysis in α -functionalization of carbonyl compounds.....	37
1.4 Organocatalysts based on proline derivatives.....	40
1.4.1 Proline sulfonamides as asymmetric organocatalysts.....	42
1.4.2 Proline tetrazoles as asymmetric organocatalysts	45
1.5 Supported organocatalysts based on proline derivatives. Catalyst recovery and recycling.....	46
2. OBJECTIVES	54
3. RESULTS AND DISCUSSION.....	55
3.1. Preparation and catalytic applications of hybrid silica materials M1 and M2 derived from a silylated proline sulfonamide	55
3.1.1 Preparation of hybrid silica material M1	55
3.1.2 Assay of M1 in asymmetric organocatalysis	58
3.1.2.1 Catalytic tests of M1 in the direct aldol reaction.....	58
3.1.2.2 Catalytic tests of M1 in the aza-Diels Alder reaction.....	64
3.1.3 Preparation of organosilica M2	65
3.1.4 Assay of M2 in asymmetric organocatalysis	66
3.1.4.1 Catalytic tests of M2 in the direct aldol reaction.....	66
3.1.5 Immobilization effect on the supported catalysts	68
3.2 Preparation and catalytic applications of hybrid silica materials M3, M4, and M6 derived from monosilylated <i>trans</i> -4-hydroxyproline sulfonamide	69
3.2.1 Preparation of the organosilicas M3, M4 and M6.....	69
3.2.2 Assay of M3, M4 and M6 in asymmetric organocatalysis.....	72
3.2.2.1 Catalytic tests of M3, M4 and M6 in the direct aldol reaction	72
3.2.2.2 Catalytic tests of M3 and M6 in the aza-Diels Alder reaction	77
3.3 Attempts to prepare an organosilica derived from a proline tetrazole.....	78
4. CONCLUSIONS	83
5. EXPERIMENTAL SECTION	85
5.1 General remarks.....	85
5.2 Preparation of hybrid silica materials derived from proline sulfonamides ...	87
5.2.1 Synthesis of (<i>S</i>)-1-((benzyloxy)carbonyl)pyrrolidine-2-carboxylic acid, 4.	87
5.2.2 Synthesis of (<i>S</i>)-1-benzyl 2-(4-nitrophenyl) pyrrolidine-1,2-dicarboxylate, 5.....	87
5.2.3 Synthesis of 4-vinylbenzenesulfonamide, 6.	88
5.2.4 Synthesis of (<i>S</i>)-benzyl 2-(((4-vinylphenyl)sulfonyl)carbamoyl)pyrrolidine-1-carboxylate, 7.....	89

5.2.5 Synthesis of (<i>S</i>)-benzyl 2-(((4-(2-(triethoxysilyl)ethyl)phenyl)sulfonyl)carbamoyl)pyrrolidine-1-carboxylate, 8.....	90
5.2.6 Synthesis of (<i>S</i>)- <i>N</i> -((4-(2-(triethoxysilyl)ethyl)phenyl)sulfonyl)pyrrolidine-2-carboxamide, 1.....	91
5.2.7 Preparation of the hybrid silica material M1.....	91
5.2.8 Preparation of hybrid silica material M2.....	92
5.2.9 Synthesis of (2 <i>S</i> ,4 <i>R</i>)-1-benzyl 2-(4-nitrophenyl) 4-hydroxypyrrolidine-1,2-dicarboxylate, 20.....	93
5.2.10 Synthesis of (2 <i>S</i> ,4 <i>R</i>)-benzyl 4-hydroxy-2-(tosylcarbamoyl)pyrrolidine-1-carboxylate, 21.....	94
5.2.11 Synthesis of (2 <i>S</i> ,4 <i>R</i>)-benzyl 2-(tosylcarbamoyl)-4-(((3-(triethoxysilyl)propyl)carbamoyl)oxy)pyrrolidine-1-carboxylate, 22.....	95
5.2.12 Synthesis of (3 <i>R</i> ,5 <i>S</i>)-5-(tosylcarbamoyl)pyrrolidin-3-yl (3-(triethoxysilyl)propyl)carbamate, 2.....	95
5.2.13 Preparation of hybrid silica material M3.....	96
5.2.14 Preparation of hybrid silica material M4.....	97
5.2.15 Preparation of mesostructured silica of SBA-15 type, M5.....	97
5.2.16 Preparation of hybrid silica material M6.....	98
5.2.17 Preparation of (<i>S</i>)-benzyl 2-(tosylcarbamoyl)pyrrolidine-1-carboxylate, 9.....	98
5.2.18 Preparation of (<i>S</i>)- <i>N</i> -tosylpyrrolidine-2-carboxamide, 10.....	99
5.3 Catalytic tests with proline sulfonamide derived organosilicas.....	100
5.3.1 Intermolecular aldol reactions.....	100
5.3.2 Intramolecular aldol condensation (Robinson annulation).....	102
5.3.3 Aza-Diels Alder reaction.....	103
5.3.3.1 Preparation of <i>N</i> -(4-chlorobenzylidene)-4-methoxyaniline, 18.....	103
5.3.3.2 Catalytic tests.....	104
5.4 Attempt to prepare a monosilylated proline tetrazole 3.....	105
5.4.1 Preparation of (2 <i>S</i> ,4 <i>R</i>)-1-benzyl 2-(prop-2-yn-1-yl) 4-(prop-2-yn-1-yloxy)pyrrolidine-1,2-dicarboxylate, 23.....	105
5.4.2 Preparation of (2 <i>S</i> ,4 <i>R</i>)-1-((benzyloxy)carbonyl)-4-(prop-2-yn-1-yloxy)pyrrolidine-2-carboxylic acid, 24.....	106
5.4.3 Preparation of (2 <i>S</i> ,4 <i>R</i>)-benzyl 2-carbamoyl-4-(prop-2-yn-1-yloxy)pyrrolidine-1-carboxylate, 25.....	107
5.4.4 Preparation of (2 <i>S</i> ,4 <i>R</i>)-benzyl 2-cyano-4-(prop-2-yn-1-yloxy)pyrrolidine-1-carboxylate, 26.....	108
5.4.5 Preparation of (2 <i>S</i> ,4 <i>R</i>)-benzyl 4-(prop-2-yn-1-yloxy)-2-(1 <i>H</i> -tetrazol-5-yl)pyrrolidine-1-carboxylate, 27.....	108
5.4.6 Preparation of (3-azidopropyl)triethoxysilane, (Az-PTES).....	109

Table of Contents

5.4.7 General procedure for click reactions under microwave heating.....	110
5.4.8 Procedure for Bn protection of NH groups of proline tetrazole 27.....	110

CHAPTER 3.

ORGANOSILICAS DERIVED FROM IMIDAZOLIUM AND IMIDAZOLINIUM SALTS. APPLICATIONS IN CATALYSIS.....	113
1. INTRODUCTION	115
1.1 Introduction to NHC carbenes as organocatalysts	115
1.2 NHC-catalyzed transformations	116
1.2.1 Ambiphilicity or Umpolung	117
1.2.1.1 <i>Classical Umpolung</i> (a ¹ to d ¹).....	119
1.2.1.2 <i>Conjugate umpolung</i> (a ³ to d ³)	121
1.2.2 Basicity.....	126
1.3 Organocatalysis by 1-alkyl-3-methylimidazolium cation	127
1.4 Supported NHC pre-catalysts	128
1.5 Imidazolium and imidazolinium derived organosilicas. Precedents in the group	133
2. OBJECTIVES	136
3. RESULTS AND DISCUSSION.....	138
3.1 Immobilization of imidazolium and imidazolinium salts.....	138
3.1.1 Hybrid silica material derived from a mono-silylated <i>N</i> -mesityl imidazolium salts	138
3.1.1.1 Preparation of the hybrid silica material M7.....	138
3.1.1.2 Capping of surface silanol groups of hybrid silica material M7	141
3.1.2 Hybrid silica materials derived from a bis-silylated <i>N,N'</i> -dimesityl imidazolinium salt.....	143
3.1.2.1 Preparation of the hybrid silica material M9.....	143
3.1.2.2 Capping of surface silanol groups of hybrid silica material M9	146
3.2 Catalytic tests of materials M7, M8 and M10.	146
3.2.1 Catalytic tests of materials M8 and M10 in NHC type reactions.....	147
3.2.1.1 Benzoin condensation.....	147
3.2.1.2 Annulation reactions of enals and vinyl ketones	149
3.2.2 Assay of M7 in imidazolium-based catalysis.....	150
3.2.2.1 Chemoselective <i>N-tert</i> -butyloxycarbonylation of amines	150
4. CONCLUSIONS	154
5. EXPERIMENTAL SECTION	155

5.1. General remarks	155
5.2 Preparation of hybrid silica materials	157
5.2.1 Preparation of 1-mesitylimidazole, 35.....	157
5.2.2 Preparation of 1-mesityl-3-[3-(triethoxysilyl)propyl]-1 <i>H</i> -imidazol-3-ium chloride, 33.	157
5.2.3 Preparation of hybrid silica material M7	158
5.2.4 Preparation of hybrid silica material M8.....	158
5.2.5 Preparation of <i>N,N'</i> -(1 <i>E</i> ,2 <i>E</i>)-(ethane-1,2-diylidene)-bis(2,4,6-trimethylaniline), 36.	159
5.2.6 Preparation of (4 <i>R</i> , 5 <i>S</i>)- <i>N,N'</i> -dimesitylocta-1,7-diene-4,5-diamine, 37.	159
5.2.7 Preparation of (4 <i>S</i> , 5 <i>R</i>)-4,5-diallyl-1,3-dimesityl-4,5-dihydroimidazolium chloride, 38.....	160
5.2.8 Preparation of (4 <i>R</i> , 5 <i>S</i>)-1,3-dimesityl-4,5-bis[3-(triethoxysilyl)-propyl]-4,5-dihydroimidazolium chloride, 34.....	161
5.2.9. Preparation of organosilica M9	161
5.2.10. Preparation of organosilica M10	162
5.3 Catalytic tests	163
5.3.1 Assays in NHC-based catalytic reactions	163
5.3.1.1 Benzoin condensation.....	163
<i>General procedure for homogeneous catalysis.</i>	163
<i>General procedure for heterogeneous catalysis.</i>	163
5.3.1.2 Annulation of enals and vinyl ketones	164
<i>General procedure for homogeneous catalysis.</i>	164
5.3.2 Assays in imidazolium-based catalytic reactions	164
5.3.2.1 Chemoselective <i>N-tert</i> -butyloxycarbonylation of amines.	164

CHAPTER 4.

HYBRID SILICA MATERIAL DERIVED FROM A [(NHC)AuCl] COMPLEX. APPLICATIONS AS RECYCLABLE CATALYST.....

1. INTRODUCTION	169
1.1 Gold catalysis	169
1.2 General mechanism of gold(I) catalysis	170
1.3 NHC-Au(I) complexes.....	171
1.4 Reactivity of NHC-Au(I) complexes.....	174
1.4.1 Allylic ester rearrangement (alkene activation)	174

Table of Contents

1.4.2 NHC-Au-OH as precatalyst	176
1.4.3 NHC-Au(I) catalysis in aqueous media	177
1.4.4 Catalytic cycloisomerization of γ -alkynoic acids into enol-lactones in aqueous media	179
1.5 Supported NHC-Au(I) catalysts.....	180
1.6 Precedents in the research group on the immobilization of NHC-metal complexes.....	182
2. OBJECTIVES	184
3. RESULTS AND DISCUSSION.....	186
3.1 Immobilization of NHC-Au(I) complexes	186
3.1.1 Hybrid silica material M11 derived from a disilylated bis-mesityl NHC-Au complex	186
3.1.1.1. Preparation of the disilylated NHC-Au-Cl monomer 46.....	186
3.1.1.2 Preparation of hybrid silica material M11	189
3.1.2 Studies towards the formation of hybrid silica material M13 derived from a disilylated bis-SIPr (NHC)-Au complex	191
3.1.2.1 Attempts for the preparation of the disilylated NHC-Au-Cl monomer 53.....	192
3.2 Applications of M11 as recyclable catalyst.....	194
3.2.1. Rearrangement of allylic acetates	194
3.2.2 Cycloisomerization of γ -alkynoic acids	199
4. CONCLUSIONS	206
5. EXPERIMENTAL SECTION	207
5.1. General remarks.....	207
5.2 Immobilization of (NHC)AuCl complexes	209
5.2.1 Synthesis of ((4 <i>R</i> ,5 <i>S</i>)-4,5-diallyl-1,3-dimesitylimidazolidin-2-yl)gold(I) chloride, 47	209
5.2.2 Preparation of ((4 <i>R</i> ,5 <i>S</i>)-1,3-dimesityl-4,5-bis(3-(triethoxysilyl)propyl)imidazolidin-2-yl)gold(I) chloride, 46, from gold complex 47	210
5.2.3 First preparation of ((4 <i>R</i> ,5 <i>S</i>)-1,3-dimesityl-4,5-bis(3-(triethoxysilyl)propyl)imidazolidin-2-yl)gold(I) chloride, 46, from silylated dihydroimidazolium salt 34.....	211
5.2.4 Synthesis of [Au(tht)Cl], 48.	211
5.2.5 Second preparation of ((4 <i>R</i> ,5 <i>S</i>)-1,3-dimesityl-4,5-bis(3-(triethoxysilyl)propyl)imidazolidin-2-yl)gold(I) chloride, 46, from silylated dihydroimidazolium salt 34.....	212
5.2.6 Preparation of hybrid silica material M11	212
5.2.7 Preparation of glyoxal bis[(2,6-diisopropylphenyl)imine], 49.....	213

5.2.8 Preparation of (4 <i>R</i> , 5 <i>S</i>)- <i>N,N'</i> -dimesitylocta-1,7-diene-4,5-diamine, 50.....	213
5.2.9 First attempt to prepare (4 <i>S</i> ,5 <i>R</i>)-4,5-diallyl-1,3-bis(2,6-diisopropylphenyl)-4,5-dihydro-1 <i>H</i> -imidazol-3-ium chloride, 51.....	214
5.2.10 Second attempt to prepare (4 <i>S</i> ,5 <i>R</i>)-4,5-diallyl-1,3-bis(2,6-diisopropylphenyl)-4,5-dihydro-1 <i>H</i> -imidazol-3-ium chloride, 51.....	214
5.3 Catalytic tests with homogeneous [(NHC)Au] complexes and with silica-supported [(NHC)AuCl], M11	215
5.3.1 Rearrangement of allylic esters	215
5.3.1.1 Preparation of the substrates	215
Preparation of 1-phenylallyl acetate, 54.....	215
Preparation of 1-Phenylallyl benzoate, 60.....	216
General procedure for the preparation of substrates 56,57 and 62.	216
5.3.1.2 General procedures for catalytic tests	218
5.3.3 Cycloisomerization of γ -alkynoic acids	220
5.3.3.1 Preparation of the substrates	220
Preparation of dimethyl 2,2-di(prop-2-yn-1-yl)malonate, 75.....	220
Preparation of dimethyl 2,2-di(but-2-yn-1-yl)malonate, 76 and dimethyl 2-(but-2-yn-1-yl)malonate, 77.....	221
Preparation of dimethyl 2-(but-2-yn-1-yl)-2-(prop-2-yn-1-yl)malonate, 78..	222
General procedure for the monohydrolysis of dimethyl 2,2-disubstituted malonates (GP 3).....	223
5.3.3.2 General procedures for catalytic tests	224
GENERAL CONCLUSIONS	226
FORMULA INDEX	228

Abbreviations

ABBREVIATIONS

$[\alpha]_{\lambda}^T$:	Specific optical rotation	DMAP:	<i>N,N'</i> -dimethyl-4-aminopyridine
Ac ₂ O:	acetic anhydride	DMF:	dimethylformamide
AcOEt:	ethyl acetate	DMSO:	dimethylsulfoxide
AcOH:	acetic acid	<i>dr</i> :	diastereomeric ratio
anh.:	anhydrous	DSC:	Differential Scanning Calorimetry
aq.:	aqueous	EA:	elemental analysis
Ar:	aryl	EDX:	energy-dispersive X-ray spectroscopy
atm:	atmosphere	<i>ee</i> :	enantiomeric excess
ATR (for IR):	Attenuated Total Reflectance	<i>er</i> :	enantiomeric ratio
AzPTES:	(3-azidopropyl)triethoxysilane	equiv.:	equivalent
Bn:	benzyl	ESI:	Electrospray Ionization
BnCl:	benzyl chloride	Et ₃ N:	triethylamine
Boc ₂ O:	di- <i>tert</i> -butyl dicarbonate	EtO:	ethoxy
BET:	Brunauer-Emmett-Teller	Et ₂ O:	diethyl ether
BJH :	Barrett-Joyner-Halenda	EtOH:	ethanol
cat.:	catalyst	Exp.:	experiment
Cbz:	benzyloxycarbonyl	FAB:	Fast Atom Bombardment
CF:	chemical formula	GC:	Gas Chromatography
ChCl:	choline chloride	GC-MS:	Gas Chromatography with Mass spectrometry detector
¹³ C-NMR:	13-Carbon Nuclear Magnetic Resonance	H _{Ar} :	aromatic hydrogen
CP-MAS:	Cross-Polarization Magic Angle Spinning	HMPA:	hexamethylphosphoramide
CP-TOSS:	Cross-Polarization with Total Suppression of Spinning Sidebands	¹ H-NMR:	Proton Nuclear Magnetic Resonance
CuAAC:	copper-catalyzed azide alkyne cycloaddition	HOMO:	Highest-Occupied Molecular Orbital
Cy:	cyclohexyl	HR-MS:	High Resolution Mass Spectrometry
d (NMR):	doublet	G-H I:	1 st generation Hoveyda-Grubbs' catalyst
dd (NMR):	double doublet	ICP:	Inductively Coupled Plasma
δ (NMR):	chemical shift	IL:	Ionic Liquid
DBU:	1,8-diazabicyclo[5.4.0]undec-7-ene	IMes:	Imidazole Mesityl
DCC:	<i>N,N'</i> -dicyclohexylcarbodiimide	ⁱ Pr:	isopropyl
DCE:	dichloroethane	ⁱ PrOH:	isopropanol
DCM:	dichloromethane	<i>J</i> (NMR):	coupling constant
DES:	deep eutectic solvent		

KHDMS:	potassium bis(trimethylsilyl)amide	ROMP:	Ring-Opening Metathesis Polymerization
λ :	wavelength	r.t.:	room temperature
lit.:	literature	s (NMR):	singlet
LUMO :	Lowest-Occupied Molecular Orbital	S _{BET} :	surface area measured by BET
M:	molar	SEM:	scanning electron microscopy
m (NMR):	multiplet	SIMes:	Saturated Imidazole Mesityl
MCR:	multicomponent reaction	SIPr:	[1,3-bis-(2,6-diisopropylphenyl)imidazolin-ylidene]
Me:	methyl	SOMO:	Singly Occupied Molecular Orbital
MeO:	methoxy	SSNMR:	Solid State Nuclear Magnetic Resonance
MeOH:	methanol	t (NMR):	triplet
Mes:	Mesityl	TBAF:	tetrabutylammonium fluoride
Me ₂ S:	dimethylsulfide	^t Bu:	<i>tert</i> -butyl
min:	minutes	TBOS:	tetrabutoxysilane
mol%:	molar percentage	TBTA:	(tris(benzyltriazolylmethyl)-amine)
m.p.:	melting point	TEC:	thiol-ene coupling
MS:	Mass Spectrometry	TEM:	transmission electron microscopy
MW:	molecular weight	TEOS:	tetraethoxysilane
NHC:	<i>N</i> -heterocyclic carbene	TGA:	thermogravimetry
Np:	nanoparticles	tht:	tetrahydrothiophene
ν (IR):	frequency	TLC:	Thin Layer Chromatography
<i>o</i> :	<i>ortho</i>	TMEOS:	tetramethoxysilane
OAc:	acetate	TMS:	trimethylsilyl
OBz:	benzoate	TMSBr:	trimethylbromosilane
P123:	Pluronic®, poly(ethylene oxide)-poly(propylene oxide) triblock copolymer PEO ₂₀ PPO ₇₀ PEO ₂₀	TMSCl:	trimethylchlorosilane
<i>p</i> :	<i>para</i>	TOF:	turn over frequency
PMO:	periodic mesoporous organosilica	TON:	turn over number
PMP:	<i>p</i> -methoxyphenyl	TPOS:	tetrapropoxysilane
POP:	porous organic polymer	THF:	tetrahydrofuran
PSS:	polyhedral silesquioxane	μ W:	microwave
p-XRD:	Powder X-Ray Diffraction	VOC:	volatile organic compound
q (NMR):	quartet	w/w:	weight percentage
®:	registered brand		
R _f :	retention factor		

Preface

ABSTRACT

The search for organic reactions proceeding with efficiency, selectivity and atom economy has emerged as a major goal in synthetic chemistry. In addition to these increasing concerns on sustainable characteristics of chemical processes, the use of supported catalysts in synthetic chemistry has considerably increased in recent years. In this manner, the covalent immobilization of catalytic species offers important advantages. However, the catalytic activity of supported species is greatly determined by the accessibility of the catalytic site to the reactants. Therefore, the choice of the support is an essential issue because its structure and properties can have an important influence on the course of chemical reactions mediated by catalysts immobilized onto it.

Organic-inorganic hybrid silica materials are silica gels modified with some organic moieties, which have been applied as versatile supports for a great variety of catalytic systems. In the present work, several organosilicas derived from proline sulfonamides, imidazolium and imidazolinium salts and a [(NHC)AuCl] complex have been prepared by sol-gel procedures and a *grafting* method. These materials have been tested as supported catalysts in several organic processes. In particular, asymmetric organocatalysis has been approached by supported proline sulfonamides which have shown good performances in direct asymmetric aldol reactions under mild conditions (in water at room temperature) allowing its recycling up to 5 consecutive runs.

Silica-immobilization of imidazolium and imidazolinium salts has not enabled the generation of NHC species to catalyze the benzoin condensation or the annulation reaction of an enal with a vinyl ketone. However, a silica-supported imidazolium salt has been used as a recyclable organocatalyst for the chemoselective *N-tert*-butyloxycarbonylation of aromatic amines.

Finally, supported [(NHC)AuCl] complex represents the first example of an [(NHC)-Au] derived silica material which has been prepared by sol-gel process. It has been successfully applied as an [(NHC)Au]⁺ supported catalyst, facilitating transformations such as the rearrangement of allylic esters or the cycloisomerization of γ -alkynoic acids to 5-membered enol-lactones. It has been reused up to 6 consecutive cycles in the last reaction. Moreover, the hybrid silica material displays better catalytic performance than the corresponding homogeneous analogue.

RESUM

La recerca de reaccions orgàniques que procedeixin amb eficiència, selectivitat i economia atòmica s'ha convertit en un objectiu important per la química sintètica. A més de la conscienciació sobre la sostenibilitat dels processos químics, l'ús de catalitzadors suportats en la química sintètica ha augmentat considerablement en els últims anys. D'aquesta manera, la immobilització covalent d'espècies catalítiques ofereix avantatges importants. No obstant, l'activitat catalítica de les espècies suportades està fortament determinada per l'accessibilitat del reactiu al centre actiu. Per tant, l'elecció del suport és una qüestió essencial donat que la seva estructura i propietats poden influir de manera important en el curs de les reaccions químiques facilitades pels catalitzadors immobilitzats en aquest suport.

Els materials híbrids orgànico-inorgànics derivats de sílice són gels de sílice modificats amb components orgànics, que s'han aplicat com a suports versàtils per a una gran varietat de sistemes catalítics. En el present treball, diverses organosíliques derivades de prolinsulfonamides, de sals d'imidazoli i d'imidazolini i d'un complex [(NHC)AuCl] han estat preparades mitjançant procediments sol-gel, així com també pel mètode de *grafting*. Aquests materials han estat assajats com a catalitzadors suportats en diversos processos orgànics. Concretament, l'organocatàlisi asimètrica ha estat abordada per prolinsulfonamides suportades que han mostrat bons resultats en les reacció aldòlica asimètrica directa en condicions suaus (en aigua a temperatura ambient) i han permès el seu reciclatge fins a 5 cicles consecutius .

La immobilització de sals d'imidazoli i d'imidazolini no ha permès la generació d'espècies NHC per catalitzar la condensació benzoïnica o la reacció d'anelació d'un enal amb una vinil-cetona. No obstant això, una sal imidazoli suportada s'ha pogut utilitzar com a organocatalitzador reciclable per a la protecció quimioselectiva amb Boc d'amines aromàtiques .

Finalment, un complex suportat de tipus [(NHC)AuCl] representa el primer exemple de material de sílice derivat d'un complex de [(NHC)-Au(I)] que s'ha preparat mitjançant el procés sol-gel. S'ha aplicat amb èxit com a catalitzador suportat [(NHC)Au]⁺, facilitant transformacions com ara la transposició d'èsters al·lílics o la cicloisomerització d'àcids γ -alquinoics per donar lloc a enol-lactones de 5 membres, i permetent la seva reutilització fins a 6 cicles consecutius en l'última reacció. A més, aquest material híbrid de sílice mostra un millor comportament catalític que l'anàleg homogeni corresponent.

RESUMEN

La búsqueda de reacciones orgánicas que procedan con eficiencia, selectividad y economía atómica se ha convertido en un objetivo importante para la química sintética. Además de la concienciación sobre la sostenibilidad de los procesos químicos, el uso de catalizadores soportados en química sintética ha aumentado considerablemente en los últimos años. De esta manera, la inmovilización covalente de especies catalíticas ofrece ventajas importantes. Sin embargo, la actividad catalítica de las especies soportadas se encuentra fuertemente determinada por la accesibilidad de los reactivos al centro activo. Por lo tanto, la elección del soporte es una cuestión esencial debido a que su estructura y propiedades pueden influir de forma importante en el curso de las reacciones químicas mediadas por catalizadores inmovilizados en este soporte.

Los materiales híbridos orgánico-inorgánicos derivados de sílice son geles de sílice modificados con componentes orgánicos, que se han aplicado como soportes versátiles para una gran variedad de sistemas catalíticos. En el presente trabajo, varias organosílicas derivadas de prolinsulfonamidas, de sales de imidazolio y de imidazolinio y de un complejo [(NHC)AuCl] han sido preparados mediante el proceso sol-gel así como por el método de *grafting*. Estos materiales han sido ensayados como catalizadores soportados en diversos procesos orgánicos. Concretamente, la organocatálisis asimétrica ha sido abordada por prolinsulfonamidas soportadas, que han mostrado buenos resultados en la reacción aldólica asimétrica directa en condiciones suaves (en agua a temperatura ambiente) y han permitido su reciclaje hasta 5 ciclos consecutivos.

La inmovilización de sales de imidazolio y de imidazolinio no ha permitido la generación de especies NHC para catalizar la condensación benzoínica o la reacción de anelación de un enal con una vinil-cetona. Sin embargo, la sal de imidazolio soportada se ha utilizado como organocatalizador reciclable para la protección quimioselectiva con Boc de aminas aromáticas.

Por último, un complejo soportado de tipo [(NHC)AuCl] representa el primer ejemplo de material de sílice derivado de un complejo de [(NHC)-Au(I)] que ha sido preparado mediante el proceso sol-gel. Se ha aplicado con éxito como catalizador [(NHC)Au]⁺, facilitando transformaciones tales como la transposición de ésteres alílicos o la cicloisomerización de ácidos γ -alquinoicos para dar lugar a enol-lactonas de 5 miembros, permitiendo su reutilización hasta 6 ciclos consecutivos en la última reacción. Además, el material híbrido derivado de sílice muestra un mejor comportamiento catalítico que el análogo homogéneo correspondiente.

CHAPTER 1

**Introduction to organic-inorganic hybrid silica
materials**

CHAPTER 1.

INTRODUCTION TO ORGANIC-INORGANIC HYBRID SILICA MATERIALS

1. Hybrid silica materials

Technological advances generate a constantly demand for novel materials. Many of the well-established materials, such as metals, ceramics or plastics, cannot fulfill all technological desires for the various new applications. Mixtures of materials can show superior properties compared with their pure counterparts.¹ Research in functional hybrid materials is trying to exploit the chance for creating smart materials that benefit from the best of the individual components. The term hybrid material is used for many different systems spanning a wide area of different materials, such as crystalline highly ordered coordination polymers, amorphous sol-gel derived materials, with and without interactions between the inorganic and the organic units, etc.²

Organic-inorganic hybrid materials can be roughly defined as molecular or nano-composites with organic components intimately mixed with an inorganic skeleton (metal oxides and metal-oxo polymers) at the range from a few Å to several nanometers. The main advantage of organic-inorganic hybrids is that their properties are not only the sum of the individual contributions of both phases. Because of the many possible combinations of the components, this field is very creative, since it provides the opportunity to invent an almost unlimited set of new materials with a large spectrum of known and, as yet, unknown properties. Material properties of these hybrids can be tuned by modifications of the composition on the molecular scale. If, for example, more hydrophobicity of a material is desired, the amount of hydrophobic molecular components should be increased. Since the compositional variations are carried out on the molecular scale, a gradual fine tuning of the material properties is possible. Innumerable examples of these materials have been prepared over the past decades,³ offering an enormous variety of applications in diverse fields such as optics,⁴ electronics,⁵ membranes,⁶ protective coatings,⁷ sensors,⁸ controlled drug delivery⁹ and

¹ Hybrid Materials. Synthesis, Characterization, and Applications. ed. Kickelbick, G. WILEY-VCH. Weinheim, Germany, 2007.

² Judeinstein, P.; Sanchez, C. *J. Mater. Chem.* **1996**, *6*, 511.

³ Special issue on hybrid materials: Sanchez, C.; Shea, K. J.; Kitagawa, S. Guest Ed. *Chem. Soc. Rev.*, **2011**, *40*, 471.

⁴ (a) Carlos, L. D.; Ferreira, R. A. S.; Bermudez, V. R.; Ribeiro, S. J. L. *Adv. Mater.*, **2009**, *21*, 509.

(b) Tani, T.; Mizoshita, N.; Inagaki, S. *J. Mater. Chem.* **2009**, *19*, 4451.

⁵ (a) Zhang, Y.; Tang, Q.; Li, H.; Hu, W. *Appl. Phys. Lett.*, **2009**, *94*, 203304. (b) Lu, M.; Xie, B. H.; Kang, J. H.; Chen, F. C.; Yang, Y.; Peng, Z. H. *Chem. Mater.* **2005**, *17*, 402.

⁶ (a) Mistry, M. K.; Choudhury, N. R.; Dutta, N. K.; Knott, R.; Shi, Z. Q.; Holdcroft, S. *Chem. Mater.* **2008**, *20*, 6857. (b) Wang, B. Q.; Li, B.; Deng, Q.; Dong, S. J. *Anal. Chem.* **1998**, *70*, 3170.

⁷ Zheludkevich, M. L.; Salvado, I. M.; Ferreira, M. G. S. *J. Mater. Chem.* **2005**, *15*, 5099.

catalysis.¹⁰ Concerning the latter application, supported catalysts based on hybrid silica materials have been an intense research field as they can be easily separated from the reaction mixture and to be reused for further reaction runs offering eco-friendly advantages with less consumption of costly and/or toxic catalysts.

A more detailed definition distinguishes between the possible interactions connecting the inorganic and the organic species for silica-based hybrid materials.¹¹

- **Class I hybrid silica materials** are those that show weak interactions between the two phases, such as van der Waals, hydrogen bonding or weak electrostatic interactions (Figure 1.1).

- **Class II hybrid silica materials** are those that show strong chemical interactions between the components, mainly through covalent bonds (Figure 1.1).

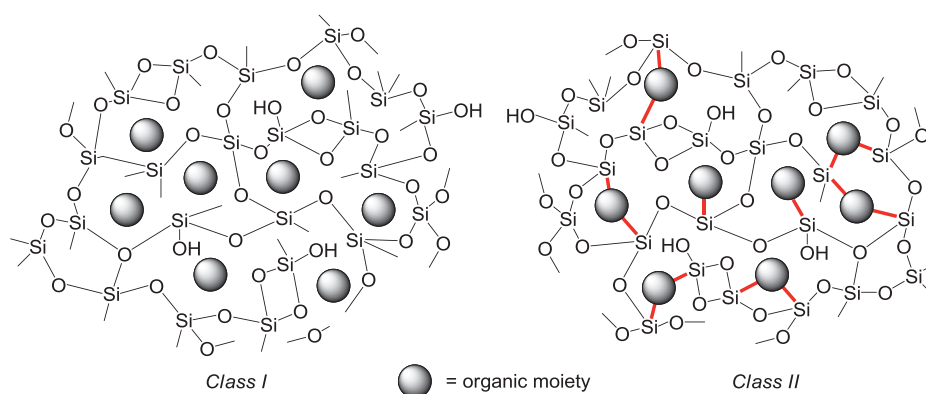


Figure 1.1. Hybrid silica material classification.

Blends are formed if no strong chemical interactions exist between the inorganic and organic building blocks, hence, *Class I* materials can be separated by classical techniques (e.g organic solvent extraction). *Class II* materials are more convenient to

⁸ (a) Coti, K. K.; Belowich, M. E.; Liong, M.; Ambrogio, M. W.; Lau, Y. A.; Khatib, H. A.; Zink, J. I.; Khashab, N. M.; Stoddard, J. F. *Nanoscale* **2009**, *1*, 16. (b) Grate, J. W.; Kaganove, S. N.; Patrash, S. J.; Craig, R.; Bliss, M. *Chem. Mater*, **1997**, *9*, 1201.

⁹ (a) Yang, P.; Gai, S.; Lin, J. *Chem. Soc. Rev.* **2012**, *41*, 3679. (b) Giret, S.; Théron, C.; Gallud, A.; Maynadier, M.; Gary-Bobo, M.; Garcia, M.; Wong Chi Man, M.; Carcel, C. *Chem. Eur. J.* **2013**, *19*, 12806. (c) Botella, P.; Corma, A.; Quesada, M. *J. Mat. Chem.* **2012**, *22*, 6394. (d) Zhang, H.; Pan, D. K.; Zou, K.; He, J.; Duan, X. *J. Mater. Chem.* **2009**, *19*, 3069. (e) Zhang, H.; Pan, D. K.; Zou, K.; He, J.; Duan, X. *J. Mater. Chem.* **2009**, *19*, 3069.

¹⁰ (a) Ciriminna, R.; Carà, P. D.; Sciortino, M.; Pagliaro, M. *Adv. Synth. Catal.* **2011**, *353*, 677. (b) Elias, X.; Pleixats, R.; Wong Chi Man, M. *Tetrahedron*, **2008**, *64*, 6770 (c) Yin, L.; Liebscher, J. *Chem. Rev.* **2007**, *107*, 133. (d) Corma, A.; García, H. *Adv. Synth. Catal.*, **2006**, *348*, 1391. (e) Hoffmann, F.; Cornelius, M.; Morell, J.; Fröba, M. *Angew. Chem. Int. Ed.*, **2006**, *45*, 3216. (f) Wight, A. P.; Davis, M. E. *Chem. Rev.* **2002**, *102*, 3589. (g) De Vos, D. E.; Dams, M.; Sels, B. F.; Jacobs, P. A. *Chem. Rev.* **2002**, *102*, 3615. (h) Lindner, E.; Schneller, T.; Auer, F.; Mayer, H. A. *Angew. Chem. Int. Ed.*, **1999**, *38*, 2155. (i) Ying, J. Y.; Mehnert, C. P.; Wong, M. S. *Angew. Chem. Int. Ed.*, **1999**, *38*, 56. (j) Moreau, J. J. E.; Wong Chi Man, M. *Coord. Chem. Rev.*, **1998**, *178-180*, 1073.

¹¹ Sanchez, C.; Ribot, F.; *New. J. Chem.* **1994**, *18*, 2007.

be used as supported catalysts as the catalytic units are covalently anchored to the matrix avoiding their leaching.¹²

2. Preparation of organic-inorganic hybrid silica materials

Synthetic strategies towards hybrid materials

In principle two different approaches can be used for the formation of hybrid materials:

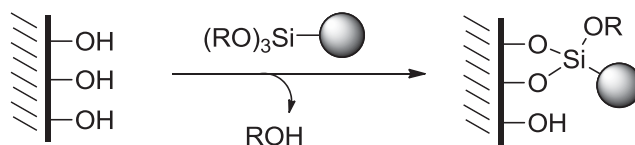
-Building block approach. One structural unit (the building block) is well-defined and it can also be found in the final material, as usually does not undergo significant structural changes during the material formation. Consequently, better structure-property predictions are possible.

-In situ formation of the components. Contrary to the building block approach, it is based on the chemical transformation of the precursors used throughout material's preparation. Well-defined discrete molecules are transformed to multidimensional structures which often show totally different properties from the original precursors.

2.1 Post-functionalization methods (*building block approach*)

In this method, the silica matrix is formed in a first step, applying well-established procedures, and the functionalization with organic groups is applied in a second step.

In the **grafting** process, surface free -OH groups (silanols) are reacted with the so-called *silane coupling agents* of the general composition $R_{4-n}SiX_n$ ($n= 1-3$; R= functional or nonfunctional organic group; X= OR' or halide), to form stable Si-O-Si covalent bonds (Scheme 1.1). Usually, molecules involved are organosilanes $RSi(OR')_3$, or less frequently chlorosilanes R_3SiCl or silazanes $HN(SiR_3)_2$.



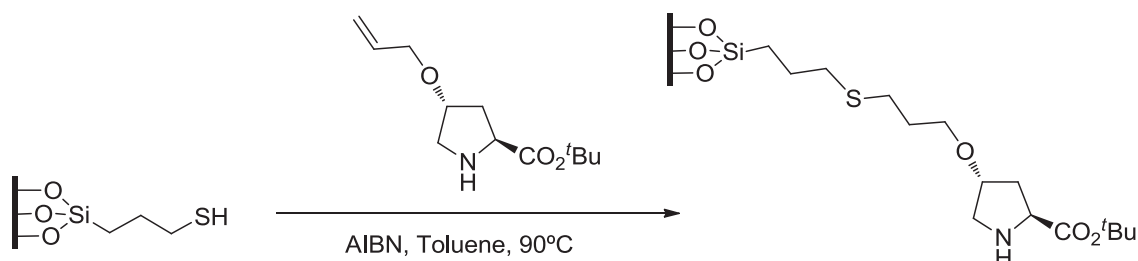
Scheme 1.1. Post-synthesis functionalization of a silica gel by *grafting*.

Alternatively, other surface reactions can also be applied, for example organosilicas bearing thiol, amine, chloride, azide or propargyl groups can be reacted with organocatalysts derivatized with an appropriate organic function. Furthermore,

¹² Zamboulis, A.; Moitra, N.; Moreau, J.J.E.; Cattoën, X.; Wong Chi Man, M. *J. Mater. Chem.* **2010**, *20*, 9322.

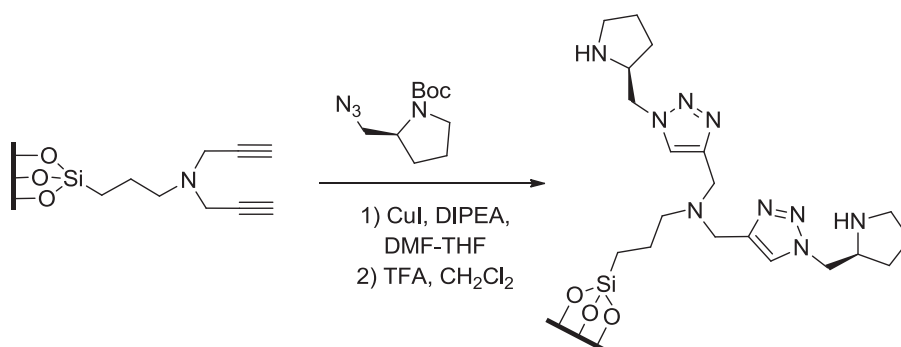
Chapter 1. Introduction to organic-inorganic hybrid materials

new methodologies derived from *click chemistry*¹³ represent a set of transformations that facilitate the preparation of such materials. Scheme 1.2 depicts an example of thiol-ene coupling (TEC) to afford a supported catalyst.¹⁴



Scheme 1.2. Immobilization of a proline derivative via thiol-ene coupling.

In the same manner, the copper-catalyzed azide-alkyne cycloaddition (CuAAC) represents another widely used methodology to functionalize a silica matrix.¹⁵ Homogeneous catalysts have been immobilized on silica supports.¹⁶ Scheme 1.3 shows an example of immobilization of a pyrrolidine organocatalyst by Ma and co-workers.¹⁷



Scheme 1.3. Immobilization of a pyrrolidine organocatalyst through CuAAC.

Equally important, *surface organometallic chemistry*¹⁸ can be used for the preparation of hybrid silica materials containing an organometallic moiety. This

¹³ Kolb, H. C.; Finn, M. G.; Sharpless, K. B. *Angew. Chem. Int. Ed.*, **2001**, *40*, 2004.

¹⁴ (a) Massi, A.; Cavazzini, A.; Del Zoppo, L.; Pandoli, O.; Costa, V.; Pasti, L.; Giovannini, P. P. *Tet. Lett.* **2011**, *52*, 619. (b) Boldolini, O.; Cacioll, L.; Cavazzini, A.; Costa, V.; Greco, R.; Massi, A.; Luisa, P. *Green Chem.* **2012**, *14*, 992.

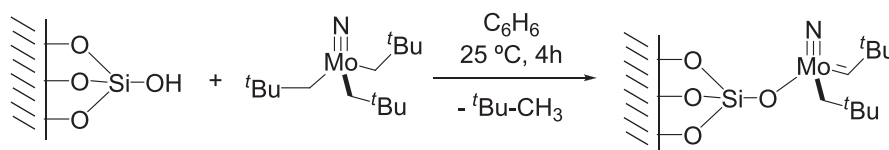
¹⁵ Cattoën, X.; Noureddine, A.; Croissant, J.; Moitra, N.; Bürglová, K.; Hodačová, J.; De los Cobos, O.; Lejeune, M.; Rossignol, F.; Toulemon, D.; Bégin-Colin, S.; Pichon, B.; Raehm, L.; Durand, J.-O.; Wong Chi Man, M. *J. Sol-Gel Sci. Technol.*, **2014**, *70*, 245.

¹⁶ Fernandes, A. E.; Jonas, A. M.; Riant, O. *Tetrahedron*, **2014**, *70*, 1709.

¹⁷ Zhao, Y.-B.; Zhang, L.-W.; Wu, L.-Y.; Li, R.; Ma, J.-T. *Tetrahedron: Asymmetry* **2008**, *19*, 1352.

¹⁸ (a) Copéret, C.; Basset, J.-M. *Adv. Synth. Catal.*, **2007**, *349*, 78. (b) Copéret, C.; Chabanas, M.; Petroff Saint-Arroman, R.; Basset, J.-M. *Angew. Chem. Int. Ed.*, **2003**, *42*, 156. (c) Yermakov, Y. I.; Kuznetsov, B. N.; Zakharov, V. A. *Stud. Surf. Sci. Catal.*, **1981**, *8*, 1.

methodology is based on the attachment of the complex to the oxide support. It should be taken into account that, in this case, the surface is directly involved in the coordination sphere of the metal (Scheme 1.4).¹⁹



Scheme 1.4. Immobilization of a molybdenum complex by *surface organometallic chemistry*.

2.2 The Sol-Gel process (*in situ formation of the components*)

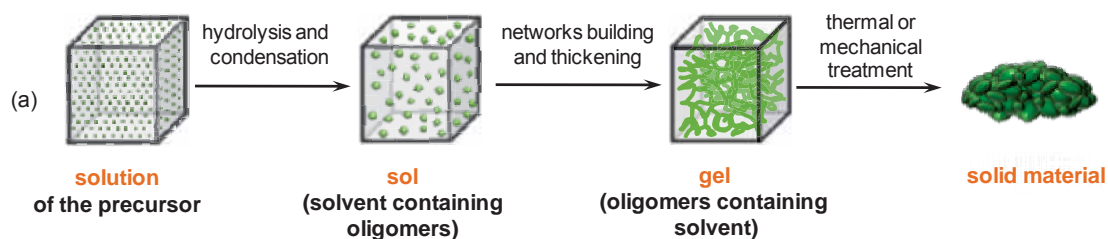
2.2.1 The Sol-Gel process

This methodology allows the preparation of homogeneous and pure inorganic materials in a reproducible way. It consists of the hydrolysis and polycondensation of a metal alkoxide or, occasionally, halides, nitrates or sulphates. The process occurs under very mild conditions (atmospheric pressure and low temperature <100°C). From the physical point of view, the process starts from a solution of molecular precursors and goes through a dispersion of colloidal particles (sol) which acts as the precursor for an integrated network.

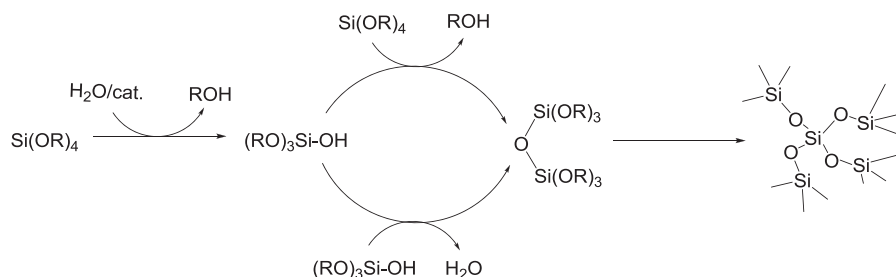
The process typically starts when a tetralkoxysilane such as tetraethoxysilane (TEOS) is catalytically hydrolyzed in a convenient solvent (ethanol, THF, DMF...) to give colloidal silanol and siloxane species, oligomers and other small clusters (*sol*, Scheme 1.5 (a)). These clusters condense to form more siloxane bridges, then small particles, and eventually tridimensional networks that entrap the solvent to form a *gel*. On the macroscopic scale, gelation is the thickening of the initial solution into an elastic solid (*gel*) which is not fluid. The gel point is not the end of the process. During the aging period of the gel, hydrolysis and condensation reactions continue (Scheme 1.5 (b)) and the network stiffens restraining the flow of the pores liquid. Although the system seems virtually unaffected, polymerization, coarsening and the phase transformation occur. Finally, the gel is dried and, after thermal or mechanical treatment, the hybrid material is obtained as a powder, called xerogel.

¹⁹ Blanc, F.; Chabanas, M.; Copéret, C.; Fenet, B.; Herdweck, E. *J. Organomet. Chem.*, **2005**, *690*, 5014.

Chapter 1. Introduction to organic- inorganic hybrid materials



(b) Hydrolysis and condensation reactions:



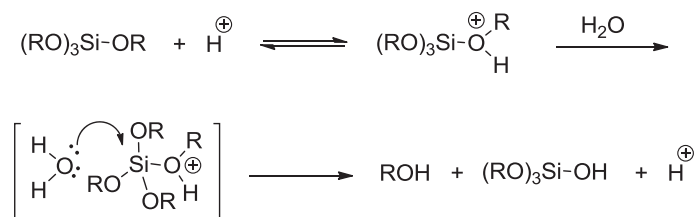
Scheme 1.5. a) Physics and b) Chemistry of the sol-gel process.

For tetraethoxysilanes, the nucleophilic attack of water to the silicon atom in the first step takes place through a different mechanism depending on the catalyst used,²⁰ acidic, basic or nucleophilic (F^- , N-methylimidazole, HMPA).

It is important to notice that the change of one parameter (temperature, solvent, concentration or catalyst) can often lead to two very different materials. For example, the change from base to acid catalysis would affect the internal structure. Hence, the final performance of the derived materials is strongly dependent on their processing and its optimization.

The mechanism of hydrolysis for each type of catalyst can be summarized as follows:

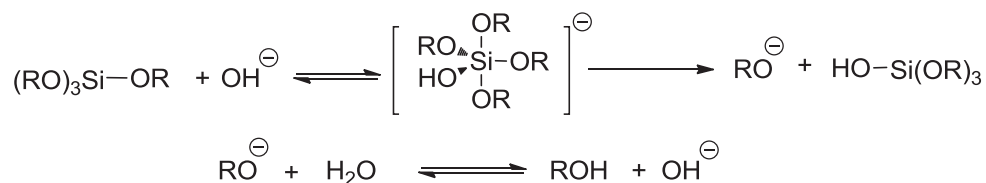
(a) *Acidic catalysis:* first, the reversible protonation of an alkoxy group gives better leaving character. Then a pentacoordinate intermediate is formed by the nucleophilic attack of water (or silanol) and an alcohol molecule is eliminated (Scheme 1.6).



Scheme 1.6. Hydrolysis of tetraalkoxysilane promoted by acidic catalysis.

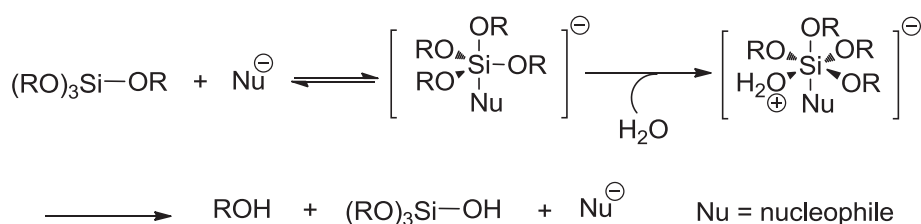
²⁰ Corriu, R.J.P.; Leclercq, D. *Angew. Chem. Int. Ed.* **1996**, 35, 1420.

(b) *Basic catalysis*: in the presence of hydroxide anions, a nucleophilic attack to the tetraalkoxysilane occurs through an anionic pentacoordinate intermediate, which is able to lose an alkoxide group (Scheme 1.7).



Scheme 1.7. Hydrolysis of tetraalkoxysilane promoted by basic catalysis.

(c) *Nucleophilic catalysis*: nucleophile coordination to the silicon centre of a tetraalkoxysilane generates an anionic pentacoordinate intermediate. This intermediate shows higher reactivity towards the nucleophilic substitution. Water or silanol coordinate this intermediate and form a hexacoordinated transition state which evolves to give an alcohol, a silanol and the regenerated catalyst. Many bases, even the hydroxide anion, can act as nucleophilic catalysts (Scheme 1.8).



Scheme 1.8. Hydrolysis of tetraalkoxysilane promoted by nucleophilic catalysis.

2.2.2 Co-condensation and bridged silesquioxanes

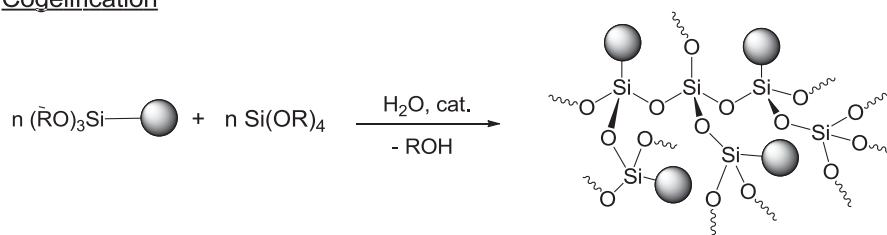
The organic fragment can be directly incorporated during the sol-gel process by co-gelification of an organotrialkoxysilane and a tetraalkoxysilane (Scheme 1.9 (a)). After hydrolysis and polycondensation, the final solid will contain organic groups dispersed in the silica matrix.²¹ On the other hand, if the organic compound bears two or more trialkoxysilyl groups, the sol-gel process can be performed without the addition

²¹ Baney, R.H.; Itoh, M.; Sakakibra, A.; Suzuki, T. *Chem. Rev.* **1995**, 95, 1409.

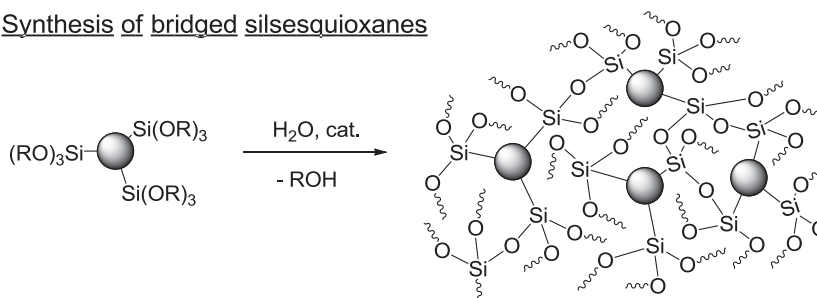
Chapter 1. Introduction to organic- inorganic hybrid materials

of tetralkoxysilane.²² These organosilicas are also called bridged silsesquioxanes, and are inherently homogeneous solids (Scheme 1.9 (b)).²³

(a) Cogelification



(b) Synthesis of bridged silsesquioxanes



Scheme 1.9. (a) Cogelification and (b) Synthesis of bridged silsesquioxanes.

2.2.3 Mesostructuring of organosilicas

According to IUPAC, materials can be classified according to their pore size in three categories:²⁴

- *Microporous* (pore size < 20 Å)
- *Mesoporous* (20-500 Å)
- *Macroporous* (> 500 Å)

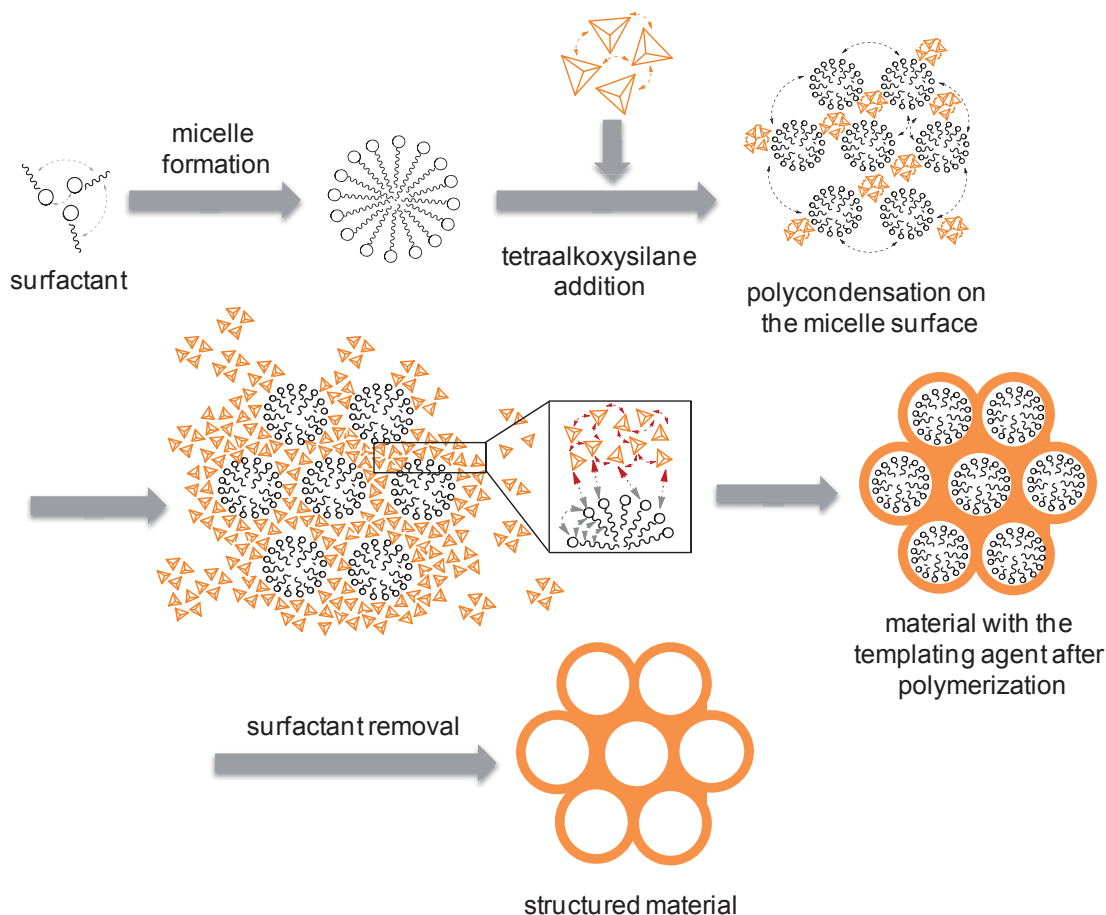
Materials prepared by simple co-condensation or polycondensation sol-gel processes in common organic solvents (ethanol, THF, DMF...) are usually amorphous with a wide pore distribution despite of their homogeneity. This lack of control on pore size, pore size distribution and other drawbacks can be overcome with the use of a *structure directing agent*. Surfactants are the most common molecules used to achieve pore organization in the final material. Due to their nature, in aqueous media, these molecules can organize in micelles. Initially, spherical micelles are formed in aqueous solution with the hydrophobic and non-polar chains at the inner side of the sphere and

²² Dieudonné, P.; Wong Chi Man, M.; Pichon, B.P.; Vellutini, L.; Bantignies, J.-L.; Blanc, C.; Creff, G.; Finet, S.; Sauvajol, J.-L.; Bied, C.; Moreau, J.J.E. *Small* **2009**, *5*, 503.

²³ (a) Corriu, R.J.P. *Eur. J. Inorg. Chem.* **2001**, 1109. (b) Loy, D.A.; Shea, K.J. *Chem. Mater.* **2001**, *13*, 3306. (c) Corriu, R.J.P. *Angew. Chem. Int. Ed.* **2000**, *39*, 1376. (d) Loy, D. A.; Shea, K.J. *Chem. Rev.* **1995**, *95*, 1431.

²⁴ Rouquerol, J.; Avnir, d.; Fairbridge, C.W.; Everett, D. H.; Haynes, J.H.; Pernicone, N.; Ramsay, J.D.F.; Sing, K.S.W.; Unger, K.K. *Pure & Appl. Chem.* **1994**, *66*, 1739.

the polar heads oriented towards the exterior. These micelles act as a template, with hydrolysis and condensation reactions occurring at their surface due to electrostatic interactions (Scheme 1.10). At the end of the process the surfactant can be removed by calcination, affording materials with high surface area ($>500 \text{ m}^2/\text{g}$), regular pore distribution and pore diameter in the mesoporous range (20-100 Å) (Scheme 1.10).



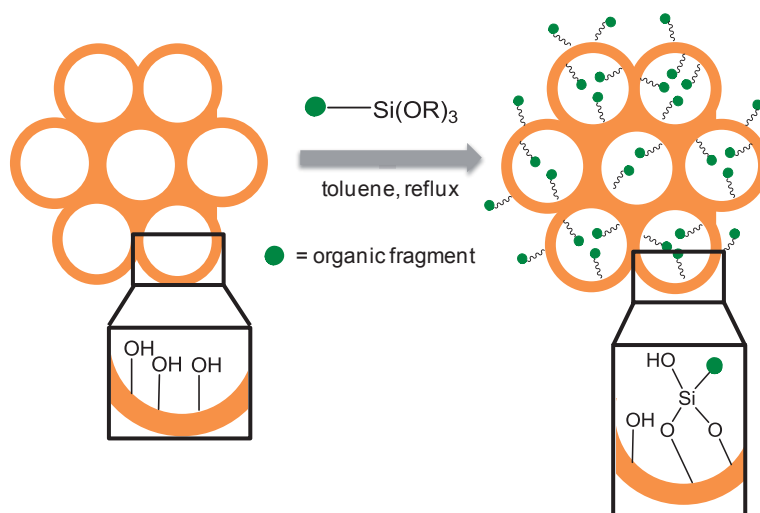
Scheme 1.10. Surfactant assisted formation of a mesoporous material.

Depending on their concentration, micelles interact with each other to form spherical, cylindrical, tubular or bilayer type structures, which can pack in tridimensional structures with different patterns (spherical, hexagonal, cubic, lamellar...) depending on the surfactant nature, its concentration and the temperature of the solution. Polymerization occurs at the micelle's surface because of the electrostatic interaction between surfactant or template (T) and charged silicon species (I). This interaction is strongly affected by the medium. Therefore, depending on the conditions used in the sol-gel process (basic, acidic or neutral medium) the selected surfactant will have to present the corresponding opposed charge to achieve the mentioned interaction (T^+I^- or T^-I^+). Neutral poly(ethylene oxide)-poly(propylene oxide) block copolymers such as $\text{PEO}_{20}\text{PPO}_{70}\text{PEO}_{20}$ (P123) are also used as templates in acidic

media. In this case electrostatic interactions occur between protonated surfactant and protonated silicon precursor through halide anion ($T^{\circ}H^+(X^{-})$).²⁵

Porosity and other textural parameters can be tuned by controlling the surfactant concentration or its alkyl chain length. After the removal of the structure-directing agent by calcination or by extraction with an organic solvent, the final material presents pores in the places previously occupied by the architectural assemblies of the surfactant. Taking into account the above-mentioned considerations, there are three synthetic approaches for the preparation of **mesostructured** organic-inorganic hybrid silica materials.²⁶ The properties of the final hybrid silica material considerably differ depending on the synthetic method used.

(a) The grafting method is based on a post-synthetic functionalization of a pre-formed mesostructured silica through anchoring the organic moiety (Scheme 1.11). This method has the advantage that, under the synthesis conditions used, the mesostructure of the starting phase is usually retained. However, the organosilanes react preferably at the external surface and at the pore openings, which leads to an irregular distribution of the organic groups in the material, reducing the porosity, or even blocking the pores (Scheme 1.11).

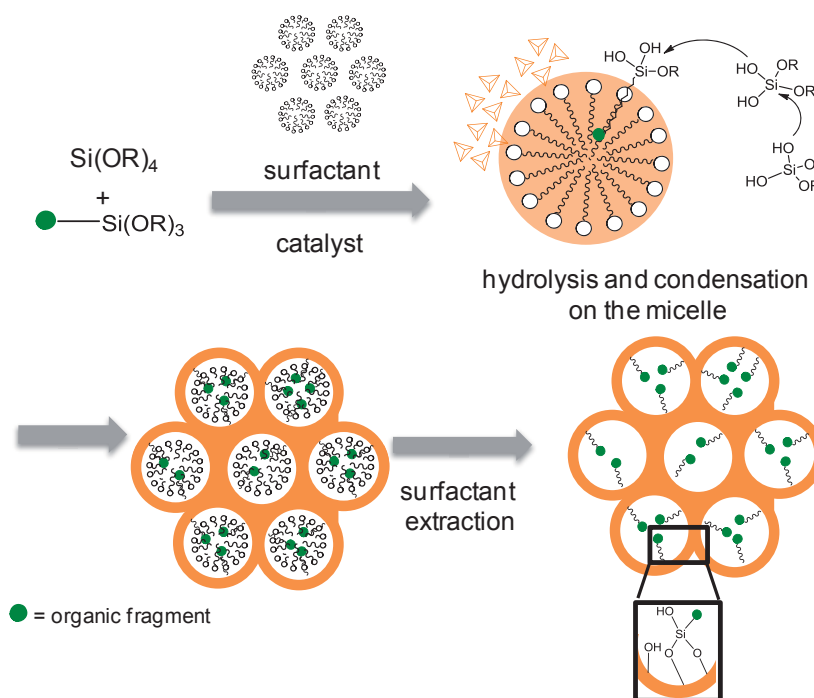


Scheme 1.11. Schematic pathway of the grafting method for the mesostructured organosilica.

²⁵ (a) Schmidt-Winkel, P.; Yang, P.; Margolese, D.I.; Chmelka, B.F.; Stucky, G.D. *Adv. Mater.* **1999**, *11*, 303. (b) Zhao, D.; Huo, Q.; Melosh, N.; Fredrickson, G.H.; Chmelka, B.F.; Stucky, G.D. *Science* **1998**, *179*, 548.

²⁶ Hoffman, F.; Fröba, M. *Chem. Soc. Rev.* **2011**, *40*, 608.

(b) The co-condensation approach (direct synthesis) consists in a co-gelification between a tetraalkoxysilane and an organotrialkoxysilane in the presence of a structure-directing agent. With this method, the organic functions are more homogeneously distributed and are mainly located at the surface of the pores (instead of being part of the pore wall) due to the incompatibility of the hydrophobic organic residue with the highly polar siloxane network (Scheme 1.12). The organotrialkoxysilane is oriented according to the micelle polarity, that is to say, the organic group towards the hydrophobic inner space and the polar silylated head group towards the surface. Moreover, the condensation rate of the organosilane component is lower than that of the pure tetraalkoxysilane, leading to a delayed participation in the polycondensation process and explaining the fact that organic groups remain on the pore surface. At the end of the process, the structure-directing agent is better removed by extraction with a solvent, as the calcination at high temperatures would destroy the organic fragment.



Scheme 1.12. Co-condensation method assisted by surfactant.

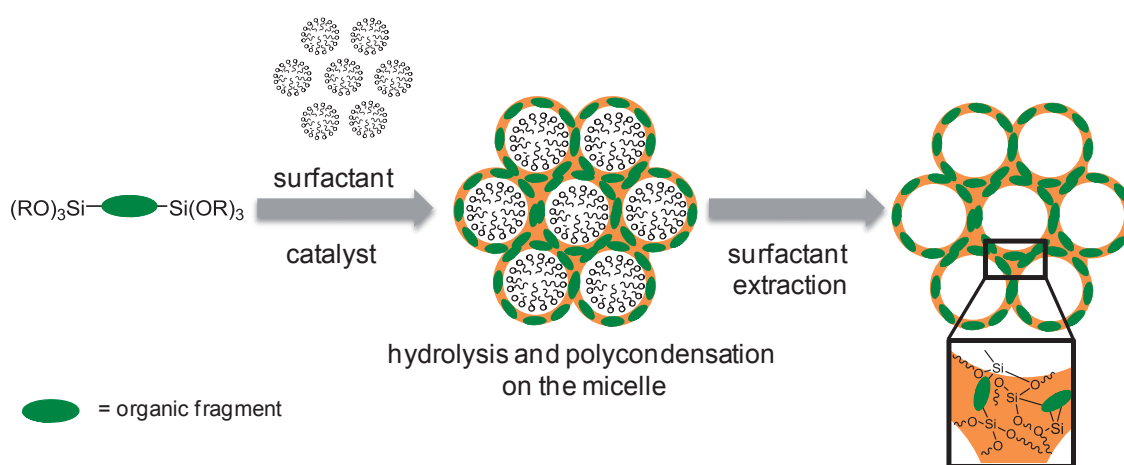
(c) Periodic mesoporous organosilicas (PMO).²⁷ In this case a structure-directing agent is also used, but instead of starting from tetraalkoxysilanes, bridged organosilanes of the type $(R'O)_3Si-R-Si(OR')_3$ are involved (Scheme 1.13). They are

²⁷ (a) Mizoshita, N.; Tani, T.; Inagaki, S. *Chem. Soc. Rev.*, **2011**, *40*, 789. (b) Gu, S.; Jaroniec, M. *J. Mater. Chem.*, **2011**, *21*, 6389. (c) Wang, W.; Lofgreen, J. E.; Ozin, G. A. *Small*, **2010**, *6*, 2634. (d) Yang, Q.; Liu, J.; Zhang, L. *J. Mater. Chem.*, **2009**, *19*, 1945. (e) Yuan, P.; Zhao, L.; Liu, N. *Chem. Eur. J.*, **2009**, *15*, 11319. (f) Mohanty, P.; Landskron, K. *Nanoscale Res. Lett.*, **2009**, *4*, 1524. (g) Tani, T.; Mizoshira, N.; Inagaki, S. *J. Mater. Chem.*, **2009**, *19*, 4451.

Chapter 1. Introduction to organic- inorganic hybrid materials

capable of undergoing cross-linking reactions carrying the organic functionality R on and leading to materials whose density of organic groups cannot be higher. In the final hybrid material, organic groups are an integral part of the pore walls, meaning that the framework itself is modified.

However, it is also possible to apply this approach starting with two or more bridged silsesquioxane precursors. Furthermore, this method can be combined with the co-condensation method employing mixtures of bridged bis(trialkoxysilyl)organosilanes with terminal organotrialkoxysilanes or tetraalkoxysilanes.



Scheme 1.13. General pathway to construct PMO from bis-silylated organic bridging units.

(d) Self-directed assembly.^{28,29} In this approach the organic precursor contains a self-assembling organic unit which confers the regular structure to the final material, acting as an internal templating agent. The self-structuring can result from weak intermolecular interactions such as π -stacking, hydrophobic interactions or hydrogen bonds. This kind of materials displays interesting properties, particularly for the nanostructure field, even though they are generally non-porous.³⁰ Nevertheless, self-

²⁸ (a) Díaz, U.; García, T.; Velty, A.; Corma, A. *J. Mater. Chem.* **2009**, *19*, 5970. (b) Pichon, B. P.; Wong Chi Man, M.; Dieudonné, P.; Bantignies, J.-L.; Bied, C.; Sauvajol, J.-L.; Moreau, J. J. E. *Adv. Funct. Mater.* **2007**, *17*, 2349. (c) Alauzun, J.; Mehdi, A.; Reyé, C.; Corriu, R. J. P. *J. Mater. Chem.* **2005**, *15*, 841. (d) Cerveau, G.; Chappellet, S.; Corriu, R. J. P. *J. Mater. Chem.* **2003**, *13*, 2885. (e) Boury, B.; Corriu, R. J. P. *Chem. Commun.* **2002**, 795. (f) Moreau, J. J. E.; Vellutini, L.; Wong Chi Man, M.; Bied, C. *J. Am. Chem. Soc.* **2001**, *123*, 1509. (g) Moreau, J. J. E.; Vellutini, L.; Wong Chi Man, M.; Bied, C.; Bantignies, J.-L.; Dieudonné, P.; Sauvajol, J.-L. *J. Am. Chem. Soc.* **2001**, *123*, 7957.

²⁹ Nobre, S. S.; Cattoën, X.; Ferreira, R. A. S.; Carcel, C.; de Zea Bermúdez, V.; Wong Chi Man, M.; Carlos, L. D. *Chem. Mater.* **2010**, *22*, 3599.

³⁰ Moreau, J. J. E.; Pichon, B. P.; Arrachart, G.; Wong Chi Man, M.; Bied, C. *New J. Chem.* **2005**, *29*, 653.

assembly is not restricted to non-porous materials, it has been described in the pore wall region of highly ordered mesoporous materials prepared using surfactants. In these cases, π -stacking, hydrophobic and hydrophilic interactions direct the self-assembly of phenyl or biphenylene bridged precursors with lamellar arrangement.³¹

3. Characterization of hybrid silica materials

The determination of the physical and chemical properties is of considerable importance for an improved understanding of interfacial phenomena in various fields, such as catalysis, electrochemistry, chromatography... As it has already been mentioned, the properties of the materials obtained by the sol-gel process strongly depend on the experimental conditions. Surface area or porosity are significantly affected by some polymerization parameters such as substrate concentration, catalyst, solvent, temperature, ageing time, presence or not of a templating agent, ... Consequently, there is an important need of different techniques, which provide their characterization in order to understand the activity of the prepared materials.³² Chemical analyses provide information about the amount of organic fragments loaded in the material. Physical parameters like surface area, pore size distribution, material morphology or texture are very important in catalysis, as they affect reagent and product diffusion or the accessibility of the catalytic centre. A brief summary of the different material characterization methods is presented here.

3.1 ²⁹Si and ¹³C Solid State Nuclear Magnetic Resonance (SSNMR)

Solid State Nuclear Magnetic Resonance (SS NMR) spectroscopy is a widely employed physical method, since it provides similar information to that obtained in solution. While molecular substances in solution give spectra characterized by sharp peaks, the spectra in the solid state, by contrast, are broad owing to various internal and external interactions.

The ²⁹Si-SSNMR confirms the existence of a covalent bond between silicon and the organic component and it provides information about the degree of condensation in the hybrid silica material. In fact, during the sol-gel process a great variety of silicon species is formed containing different numbers of Si-O-Si bonds. These species lead to structures giving signals with different chemical shifts in the ²⁹Si-SSNMR spectrum depending on the alkoxy groups bonded to the silicon atom (Figure 1.2).

³¹ (a) Kapoor, M. P.; Yang, Q.; Inagaki, S. *J. Am. Chem. Soc.* **2002**, 124, 15176. (b) Inagaki, S.; Guan, S.; Ohsuna, T.; Terasaki, O. *Nature* **2002**, 416, 304.

³² Corma, A. *Chem. Rev.*, **1995**, 95, 559.

Chapter 1. Introduction to organic-inorganic hybrid materials

According to this, signals are classified as Q, D, T and M. We can differentiate between *monofunctional silicon* (M) coming from monoalkoxysilanes; *difunctional* (D) from dialkoxysilanes; *trifunctional* (T) from trialkoxysilanes; and *quadrifunctional* (Q) from tetraalkoxysilanes. Furthermore, these signals are complemented with numeric superscripts (from 0 to 4) which are used to indicate the degree of condensation; 0 if condensation did not occur; 1 if only one alkoxy group has condensed; 2 if two alkoxy groups have condensed and so on (Figure 1.3). The nature of the organic moiety (alkyl, aryl,...) or of the catalyst used in the sol-gel process can also affect the chemical shift.

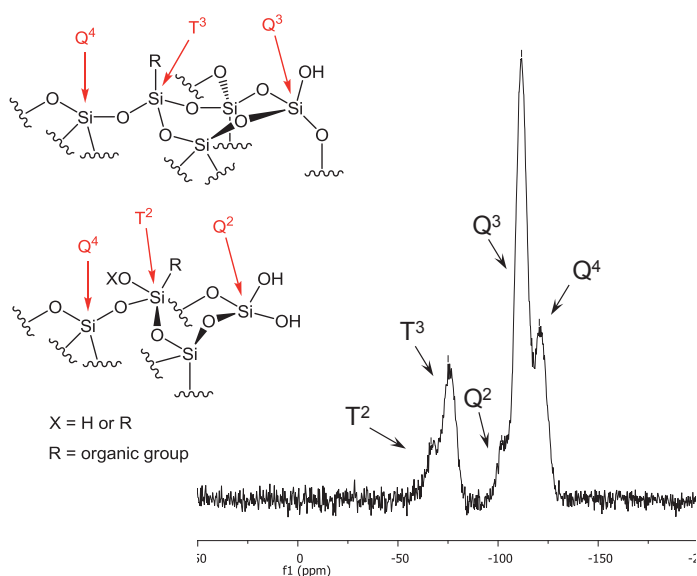


Figure 1.2. Example of ^{29}Si -SSNMR of material **M3** (See Chapter 2).

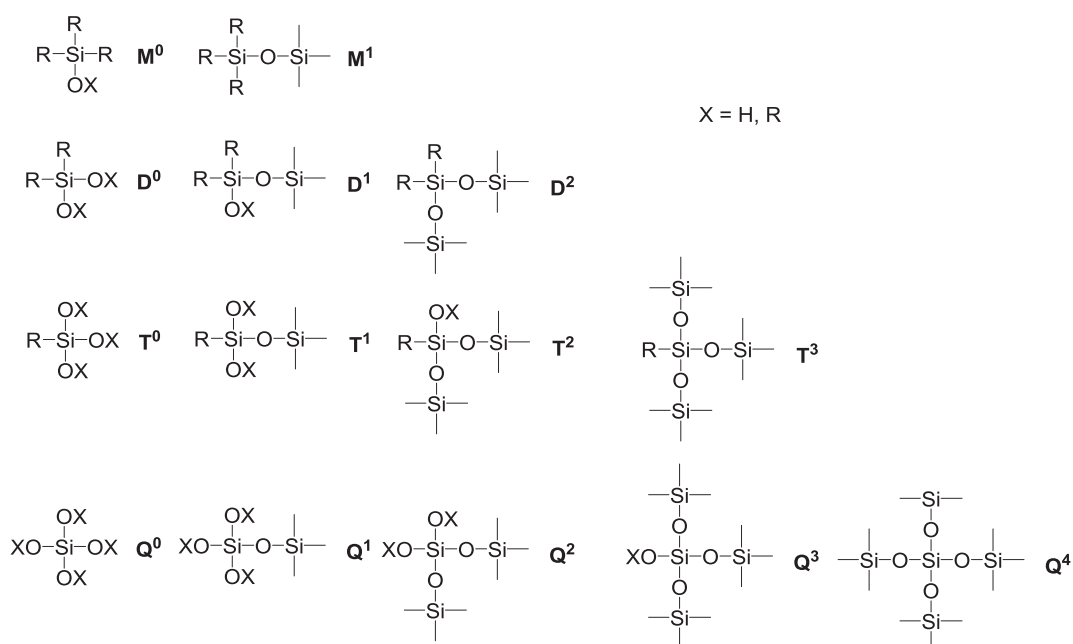


Figure 1.3. Silicon environments and their corresponding label in the ^{29}Si -SSNMR.

The ^{13}C -SSNMR is quite useful to check that the organic functionality has been loaded in the final material. It provides qualitative information for the identification of organic functional groups. The ^{13}C -SSNMR spectrum appears to be similar to the common ^{13}C -NMR in solution but with broader peaks (Figure 1.4). However, in solid state signals of different carbon atoms easily overlap.

Different acquisition modes have been developed for recording ^{13}C -SSNMR, among them Cross Polarized Magic Angle Spinning (CP-MAS) and Cross-Polarized with Total Suppression of Spinning Sidebands (CP-TOSS) are mainly used. The CP-MAS has higher sensitivity and better resolution but when the spinning rate is not fast enough undesired spinning bands appear in the spectrum. This phenomenon is overcome when using CP-TOSS.

It must be taken into account that solid state ^{13}C and ^{29}Si solid state NMR suffer from low sensitivity.³³ Actually, in many cases, functionalized silicon sites T^n are too diluted to be readily observed in the ^{29}Si -SSNMR. Generally, for high dilution of the organic component in the hybrid material (tetraalkoxysilane/organotrialkoxysilane ratio higher than 10), the spectrum provides mainly information about the Q^n and proton-rich sites (Si-OH). The ^{13}C -SSNMR suffers from similar drawback and, therefore, for high dilution of organic component, little evidence of the organic moiety incorporation is often obtained.

³³ Lelli, M.; Gajan, D.; Lesage, A.; Caporini, M. A.; Vitzthum, V.; Miéville, P.; Héroguel, F.; Rascón, F.; Roussey, A.; Thieleux, C.; Boualleg, M.; Veyre, L.; Bodenhouse, G.; Copéret, C.; Emsley, L. *J. Am. Chem. Soc.* **2011**, *133*, 2104.

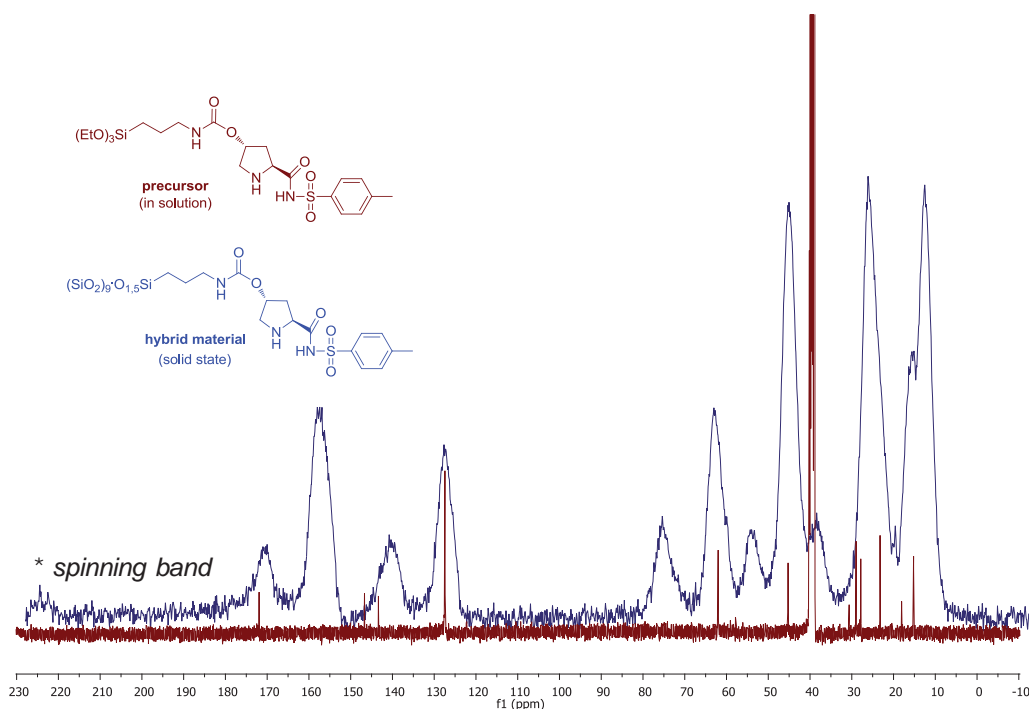


Figure 1.4. Comparison of ^{13}C -NMR of compound **2** in CDCl_3 solution (red) and ^{13}C -CP-MAS-NMR of material **M4** (blue, See Chapter 2).

3.2 Vibrational Spectroscopy (IR and Raman)

Infrared and Raman spectroscopy give complementary information. Infrared spectroscopy (IR) allows the qualitative identification of functional groups present in the material which have representative signals (*i.e.* carbonyl, nitrile, isonitrile, sulfonyl or azide). It is worth noting that the use of this technique is limited to hybrid materials with low organic fragment dilution in the inorganic framework, as when the ratio tetraalkoxysilane/organosilane is higher than 10, the IR spectrum shows mainly bands corresponding to Si-O-Si vibrations (around 1100 cm^{-1}), surface adsorbed water and silanol species ($3500 - 3200\text{ cm}^{-1}$).³⁴

Laser Raman spectroscopy can be used to observe some weak or inactive vibrations in the infrared range. Besides, some bands can be observed without the interference of intense bands such as Si-O-Si vibrations. However, some processes are difficult to detect (*i.e.* the protonation of Brønsted bases) in the Raman spectrum as the observed bands arise from changes in the polarizability associated with skeletal and stretching vibrations.^{32,34}

³⁴ Sassi, Z.; Bureau, J. C.; Bakkali, A. *Vibrational Spectroscopy*, **2002**, 28, 251.

3.3 Thermogravimetric analysis

This technique gives an idea of thermal stability of a given material, including structural decomposition, oxidation, corrosion or moisture adsorption/desorption. Specifically, it determines changes in the mass of the a material as a function of temperature.³⁵ In hybrid materials, is commonly used for the determination of the loading of inorganic and organic components.

The record is the thermogravimetric or TG curve, where the mass is plotted on the ordinate decreasing downwards and temperature (T) or time (t) on the abscissa increasing from left to right (Figure 1.5).

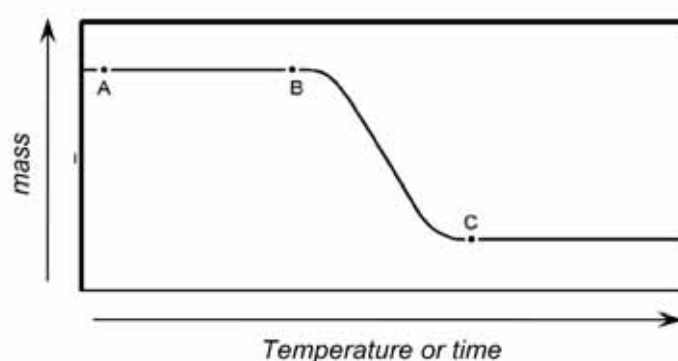


Figure 1.5. Thermogravimetric curve.

In the TG curve of hybrid materials the first region (A-B) presents a slightly negative slope (temperatures in the range of 20-200°C) and it corresponds to the thermodesorption of physically adsorbed water molecules from the silica surface.³⁶ The second weight loss region occurs between B and C; it can be divided in two parts, each one associated with a different process. The first part (normally in the range 200-400 °C) can be attributed to the condensation of silanol groups and the cross-linking of surface silanol with some organic functionalities. The second part between 400 and 600 °C can be attributed to the thermal decomposition of the chemically bonded organic groups. At temperatures exceeding 700°C (region after point C) the organic component of hybrid materials is destroyed completely and thus, from the residual mass the inorganic content of the hybrid material can be determined.

Simultaneous TGA-DSC (Differential Scanning Calorimetry) measures both heat flow and weight changes in a material as a function of temperature or time in a controlled atmosphere. The simultaneous measurement of these properties simplifies

³⁵ Mannsfield, E.; Kar, A.; Quinn, T.P.; Hooker, A. *Anal. Chem.* **2010**, *82*, 9977.

³⁶ Jaroniec, C.P.; Gilpin, R.K.; Jaroniec, M. *J. Phys. Chem. B.* **1997**, *101*, 6861.

the interpretation of the results as complementary information is obtained (for instance, if certain events are endothermic or exothermic).

3.4 Elemental Analysis

The chemical composition of hybrid materials (carbon, hydrogen, nitrogen, sulphur, chlorine, bromine or iodine) coming from the organic fragment can be analysed by combustion. The amount of other elements such as silicon or metals (gold) can be determined by inductively coupled plasma (ICP) analysis.

The theoretical and experimental contents can considerably differ and, generally, less organic functionality than expected is loaded in the hybrid silica material. This fact can be rationalized taking into account that the hydrolysis rate is lower for organotrialkoxysilanes with respect to tetraalkoxysilanes. Within the group of tetraalkoxysilanes, the hydrolysis rate decreases in the following order: tetramethoxysilane (TMOS) > tetraethoxysilane (TEOS) > tetrapropoxysilane (TPOS) > tetrabutoxysilane (TBOS). The degree of condensation also contributes to the difference between theoretical and experimental values, since some alkoxy groups are not hydrolyzed or some silanol groups do not condense. Discrepancy between the two values may also come from traces of surfactant or high-boiling point solvent remaining in the material after the processing.

3.5 Surface area analysis

Gas adsorption-desorption measurements allow the determination of surface area, the pore volume and the pore size distribution. This technique is one of the most powerful tools for the determination of porosity in solid materials. *Adsorption* is the process in which atoms or molecules are weakly bound to the surface of a solid, and form a layer at the interface. Its counterpart, *desorption*, denotes the reverse process, in which the amount of adsorbed atoms or molecules decreases.

The amount of gas (usually N₂) adsorbed to the material as a function of relative pressure is measured at a constant temperature (77 K) from thoroughly degassed samples. The adsorption isotherm is built by adding controlled doses of nitrogen gas on the cold sample, and monitoring the corresponding relative pressure in the surrounding environment (p/p^0). When p/p^0 reaches 1, spontaneous liquefaction of N₂ occurs. Under these conditions consecutive molecular layers of nitrogen can be adsorbed on the solid surface. In the *monolayer adsorption* all the adsorbed molecules are in contact with the surface layer of the sample, whereas in *multilayer adsorption*, the adsorption space accommodates more than one layer of molecules, so that not all adsorbed molecules

are in direct contact with the surface layer of the sample. The surface area of a given sample, for example a hybrid material, may be calculated from *monolayer adsorption*. Therefore, it is necessary to identify the amount of N₂ adsorbed in an unimolecular layer.

The graphic representing the relationship, at constant temperature, between the amount adsorbed and the equilibrium pressure of the gas is known as the *adsorption-desorption isotherm*.³⁷ The shape of the isotherm contains information about interactions between adsorbent and adsorptive. In some cases, a *hysteresis* loop is observed when adsorption and desorption curves do not coincide. In 1985 the *International Union of Pure and Applied Chemistry* (IUPAC) classified isotherms in six types,³⁸ types I, II and IV being the most frequently observed (Figure 1.6).

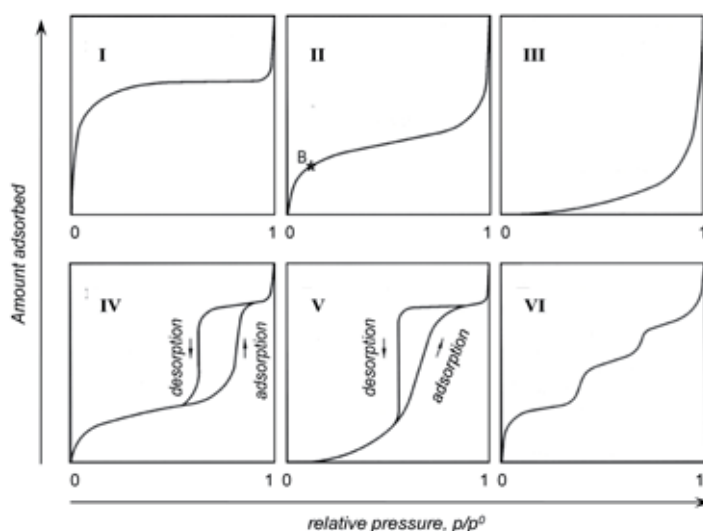


Figure 1.6. Types of isotherm according to the IUPAC rules (reference 38).

- (a) *Type I* isotherms are given by microporous solids having relatively small external surfaces, where adsorption takes place at low relative pressure.
- (b) *Type II* is the isotherm for non-porous or macroporous materials. Some mesoporous solids also give this adsorption curve, where a monolayer adsorption is observed at low relative pressure and saturation at high relative pressure, but without hysteresis loop. The interaction between adsorbate and adsorbent is strong. Point B represents the beginning of the almost linear

³⁷ *Gas adsorption equilibria. Experimental methods and adsorptive isotherms*. Ed. Keller, J. U. SPRINGER: Boston, 2005.

³⁸ Sing, K. S. W.; Everett, D. H.; Haul, R. A. W.; Moscou, L.; Pierotti, R. A.; Rouquérol, J.; Siemienińska, T. *Pure Appl. Chem.*, **1985**, *4*, 603.

middle section of the isotherm. It is often taken to indicate the stage at which monolayer coverage is complete and multilayer adsorption is about to begin.

- (c) *Type III* isotherms present a convex shape which indicates a relatively weak interaction between adsorbent and adsorbate. Type III is not common, but a number of systems (for example, nitrogen on polyethylene) show this profile. Because of its convex curvature over the entire range of pressure, these isotherms do not exhibit point B.
- (d) *Type IV* isotherms are generally given by mesoporous materials. They have a characteristic hysteresis loop, which is associated with capillary condensation taking place in mesopores, and the limiting uptake over a range of high relative pressure. In Type IV isotherms there is an important increase of the amount adsorbed at upper-intermediate relative pressure and the filling mechanism corresponds to a *monolayer-multilayer* adsorption.
- (e) *Type V* isotherms arise from a deviation of Type IV. Adsorption-desorption are observed at relative pressure $p/p^0 \approx 0.5$.
- (f) *Type VI* isotherms are obtained when stepwise multilayer adsorption on uniform non-porous surfaces occurs. The sharpness of the steps depends on the system and the temperature, whereas the step-height represents the monolayer capacity of each adsorbed layer. These isotherms are typically obtained with argon or krypton on graphitised carbon at liquid nitrogen temperature.

Many hybrid materials show adsorption isotherms which actually are a combination of types I-VI. Mesoporous materials can also contain a certain amount of micropores, which in a Type IV isotherm can be recognized because of a higher adsorption at low relative pressure.

The hysteresis appearing in the multilayer range of isotherms is usually associated with capillary condensation in mesoporous structures. This phenomenon occurs when the gas is firstly adsorbed in pores, where it can condense to the liquid state after enough gas supply. Although the effect of various factors on adsorption hysteresis is not fully understood, the shapes of hysteresis loops have often been identified with specific pore structures. The variety of shapes exhibited by the hysteresis loops have been classified by the IUPAC in four types, types H1 and H2 being the most frequent (Figure 1.7).

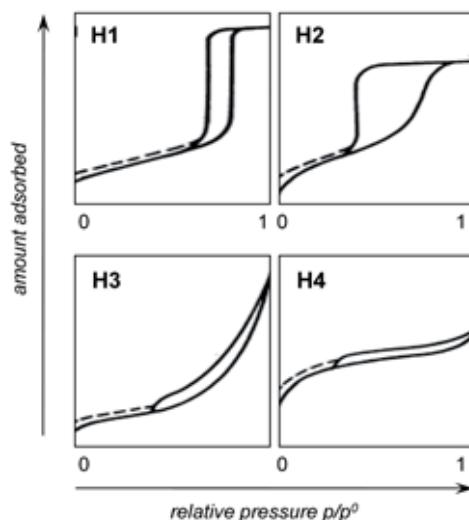


Figure 1.7. Types of hysteresis loops according to the IUPAC (reference 38).

- (a) *Type H1* has adsorption and desorption branches almost parallel and is often associated with specific pore structure. Mesoporous materials like SBA-15, MCM-41 or MCM-48 exhibit this type of hysteresis.
- (b) *Type H2* has a loop difficult to interpret. Normally the desorption branch presents a more pronounced slope with respect to the adsorption one. This hysteresis is representative for materials with higher disorder as inorganic oxide gels and porous glasses.
- (c) *Type H3* is observed in aggregates of plate-like particles giving rise to slit-shaped pores. An aggregate is an assembly of particles which are loosely coherent.
- (d) *Type IV* loop is associated with narrow slit-like pores.

The curve shape gives information about the pore size (p/p^0 from the hysteresis point); about the pore volume (the area limited by adsorption and desorption curves), and about the pore diameter distribution (related with the slope of the hysteresis).

Several mathematical transformations have been developed to transform the adsorption isotherm data into a calculated surface area, but the Brunauer-Emmett-Teller (BET)³⁹ method is the most widely used, though it is not suitable to measure the specific surface area of microporous materials. The Barrett-Joyner-Halenda (BJH)⁴⁰ method determines the pore size distribution from the $dV/d\log(D)$ function, while the t-

³⁹ Brunauer, S.; Emmett, P. H.; Teller, E. J. *J. Am. Chem. Soc.*, **1938**, 60, 309.

⁴⁰ Barrett, E. P.; Joyner, L. G.; Halenda, P. P. *J. Am. Chem. Soc.*, **1951**, 73, 373.

Plot calculation provides information about the contribution of micro- and mesopores in the material.

3.6 Powder X-Ray Diffraction

The powder X-Ray diffraction (PXRD) technique is useful to withdraw information about the organization of hybrid materials. The sample is irradiated by a beam of X-rays, which interacts with the repeating planes of the sample. Bragg's law describes the interaction with the following equation:

$$n \cdot \lambda = 2 d_{hkl} \sin \theta$$

Where θ stands for the angle between the incident beam and the plane, d_{hkl} represents the distance between two consecutive identical planes, and λ is the incident beam wavelength (Figure 1.8).

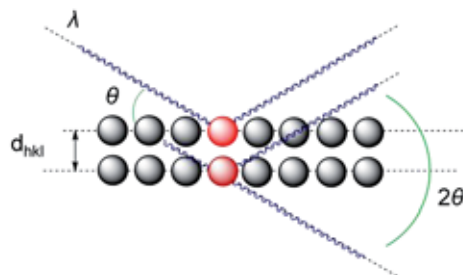


Figure 1.8. Schematic representation of Bragg's law.

The distance between planes can be determined from the incident beam and the measured dispersion angles. Normally, results are represented by PXRD plot, which reproduce the intensity I with respect to a parameter called q , which is calculated as follows $q = \frac{4\pi \sin \theta}{\lambda}$. The relationship between q and d is the following: $q = 2\pi / d$. If the material is organized, well-defined peaks can be observed in the plot and from their pattern (Figure 1.9) it is possible to know the type of organization (hexagonal, lamellar, cubic, worm-like, ...). On the other hand, amorphous materials do not allow obtaining clear signals.

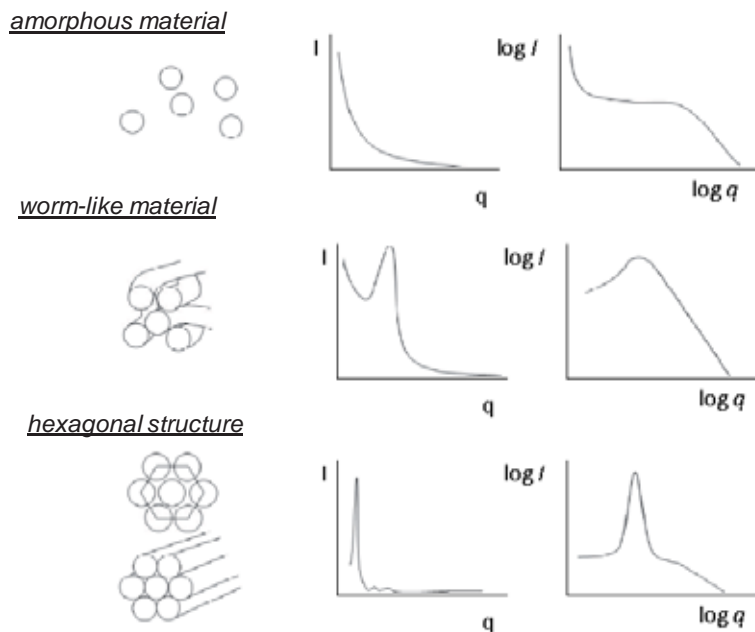


Figure 1.9. Examples of powder X-ray diffraction patterns.

Concerning the morphology of the sample, Small Angle X-ray Scattering (SAXS) gives information on the network microstructure.⁴¹ The single interference peak in the SAXS curve ($I(q)$ vs q , Figure 1.10) indicates the type of ordering (a small width stands for a well defined structure).^{41b} For instance, the presence of only a single scattering peak indicates short-range ordering.^{41c} Other structural information might be obtained from SAXS. In the case of lamellar organization, the interlamellar spacing (separation between siliceous domains) may be calculated using SAXS data,⁴² which can be compared with the results obtained by microscopy and BET analyses.

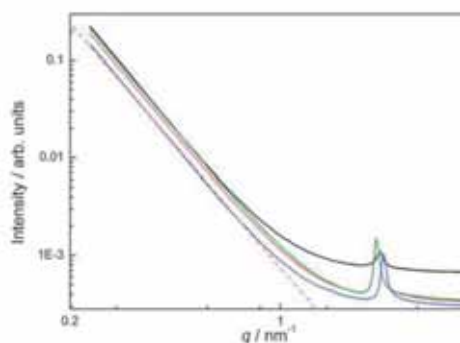


Figure 1.10. SAXS patterns of several hybrid materials doped with Eu^{3+} (according to reference 39).⁴²

⁴¹ (a) Sassi, Z.; Bureau, J. C.; Bakkali, A. *Vibrational Spectroscopy*, **2002**, *28*, 251. (b) van der Elskan, J.; Bras, W.; Dings, J.; Michielsen, J. C. F. *Phys. Rev. B*, **1996**, *54*, 3110. (c) Wen, S.; Wilkes, L. *Chem. Mater.* **1996**, *8*, 1667.

⁴² Nobre, S. S.; Brites, C. D. S.; Ferreira, R. A. S.; de Zea Bermudez, V.; Carcel, C.; Moreau, J. J. E.; Rocha, J.; Wong Chi Man, M.; Carlos, L. D. *J. Mater. Chem.*, **2008**, *18*, 4172.

3.7 Electron Microscopy

The morphology of the material can be studied by two different kinds of electron microscopies: Scanning Electron Microscopy (SEM) and Transmission Electron Microscopy (TEM).

Scanning Electron Microscopy provides information about the surface morphology, texture, particle shape and size of materials. The microscope only explores the sample surface, which is previously covered with a metallic thin layer. Electrons from the incident beam scanning the sample can be dispersed or they produce secondary electrons. Dispersed and secondary electrons are collected and evaluated by an electronic device, which converts this information into a pixel. With this technique, realistic tridimensional images of the hybrid surface are obtained (Figure 1.11).

Transmission Electron Microscopy allows the recording of images obtained when electrons are transmitted through an ultra thin specimen of the material. With this technique, mesoporous channels located inside the material can be seen in structured materials, as well as their structural organization (Figure 1.12). For mesoporous materials, the sum of pore diameter and wall width gives the parameter cell, which can be quantitatively (but not very precisely) determined by TEM, complementing BET and XRD analyses.

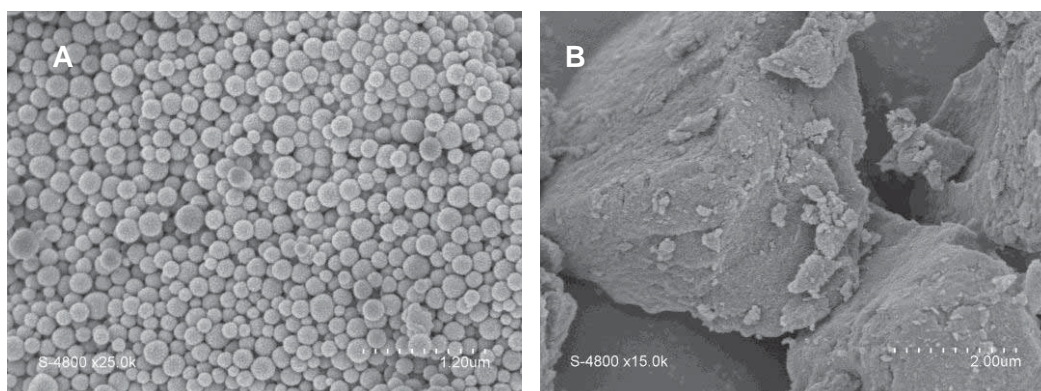


Figure 1.11. SEM Images of (a) silica nanospheres and (b) hybrid material **M11** (See Chapter 4).

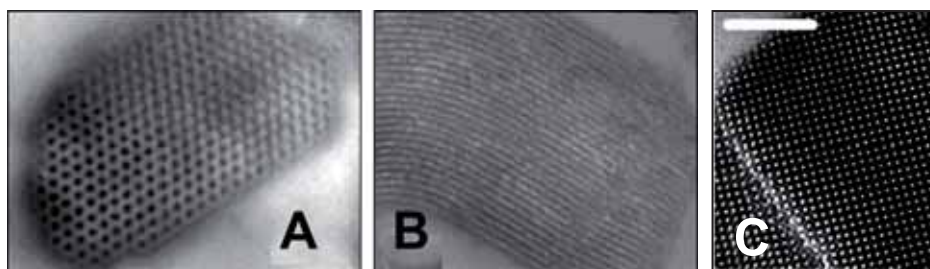


Figure 1.12. TEM images of ordered mesoporous materials:

- (a) perpendicular or (b) parallel to channels of hexagonal 2D silica (according to reference 40);⁴³
(c) along [100] direction in a cubic cage-like silica (according to reference 41).⁴⁴

To conclude, it should be mentioned that only the combination of several different techniques enable the fully characterization of an hybrid silica material. Usually the information brought by the different analyses is compared in order to better understand the effect of the structure and morphology on the properties of hybrid silica materials.

⁴³ Mehdi, A.; Reyé, C.; Corriu, R. J. P. *Chem. Soc. Rev.*, **2011**, *40*, 563.

⁴⁴ Boullanger, A.; Alauzun, J.; Mehdi, A.; Reyé, C.; Corriu, R. J. P. *New J. Chem.*, **2010**, *34*, 738.

CHAPTER 2

**Organosilicas derived from proline sulfonamides
and proline tetrazoles**

Applications in asymmetric organocatalysis

1. INTRODUCTION

1.1 Introduction to asymmetric organocatalysis

Until few years ago, enzymes and chiral transition metal complexes were generally considered as the two main pillars of efficient asymmetric catalysis. More recently, small chiral organic molecules have revealed as efficient catalysts, presenting remarkable enantioselectivities. This rediscovery has initiated an explosive growth of research activities in *organocatalysis*.⁴⁵ In 2007, List⁴⁶ included these compounds as the third pillar of modern asymmetric catalysis.

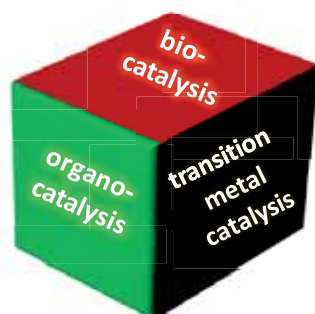


Figure 2.1. The tree main pillars in asymmetric catalysis.

In fact, molecules such as acetaldehyde had already been used as catalysts in ancient times (Liebig in 1859) and in 1912 a modestly enantioselective cyanohydrin synthesis catalyzed by natural quinine and quinidine alkaloids was reported.⁴⁷ However, the term organic catalysis was not introduced until 1928 by Langenbeck⁴⁸ and it first appeared in the literature in 1931 as “*organische katalyse*.”⁴⁹ In the 1960s, Pracejus⁵⁰ showed that significant enantioselectivities (up to 74 % enantiomeric excess) were obtained in the methanol addition to phenyl methyl ketene when using 1 mol% of *O*-acetylquinine. But the milestone of this period came from the pharmaceutical industry in the 1970s, when Hajos at Roche and Weichert at Schering published the first and highly enantioselective catalytic aldol reaction using the simple amino acid L-proline as catalyst in the preparation of the Wieland-Miescher

⁴⁵ Houk, K. N.; List, B. Guest Ed. *Acc. Chem. Res.*, **2004**, *37*, 487.

⁴⁶ *Organocatalysis*: ed. Reetz, M. T.; List, B.; Jaroch, S.; Weinmann, H.; SPRINGER: Berlin, 2007.

⁴⁷ (a) Bredig, G. *Chem-Ztg*, **1912**, *35*, 324. (b) Bredig, G; Fiske, W. S. *Biochem. Z.*, **1912**, *46*, 7.

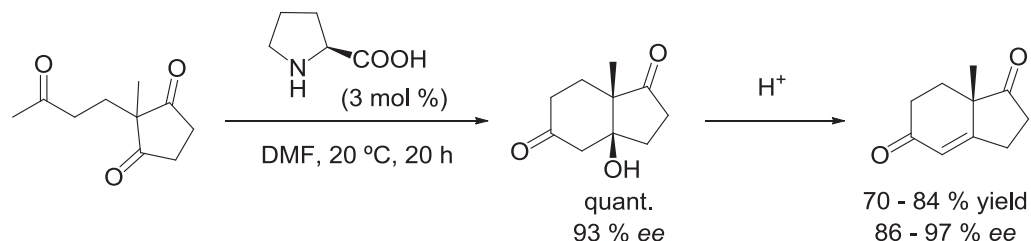
⁴⁸ Langenbeck, W. *Angew. Chem.*, **1928**, *41*, 740.

⁴⁹ Langenbeck, W. *Angew. Chem.*, **1931**, *45*, 97.

⁵⁰ (a) Pracejus, H.; Samtleben, R. *Tetrahedron Lett.*, **1970**, *25*, 2189. (b) Pracejus, H. *Fortschr. Chem. Forch.*, **1967**, *8*, 493. (c) Pracejus, H.; Kellner, U. *Z. Chem.*, **1964**, *4*, 226. (d) Pracejus, H.; Maetje, H. *J. Prak. Chem.*, **1964**, *24*, 195. (e) Pracejus, H. *Justus Liebigs Ann. Chem.*, **1960**, *634*, 9. (f) Pracejus, H. *Justus Liebigs Ann. Chem.*, **1956**, *601*, 61.

Chapter 2. 1.Introduction

unsaturated ketone, an intermediate in the synthesis of a great variety of steroid derivatives (Scheme 2.1).⁵¹



Scheme 2.1. L-proline catalyzed Hajos-Parrish-Eder-Sauer-Wiechert reaction.

Nevertheless, the interest of both industry and academia for organocatalysis did not significantly increase until 2000, when simultaneous reports of two different groups initiated a great deal of research activities on this field. The first work, described by List, Lerner and Barbas, dealt with intermolecular aldol reactions catalyzed by L-proline.⁵² In the second one, MacMillan reported several Diels-Alder reactions between α,β -unsaturated aldehydes and dienes, which were catalyzed by a chiral imidazolidinone.⁵³

The advent of organocatalysis brought several benefits with respect to the use of metal complexes, such as (i) easier experimental procedures under non-inert conditions, due to the stability of the organic molecules towards air and water; (ii) reduction in chemical waste and no metal contamination of final products, because organic molecules are considered typically environmentally friendly; (iii) availability of both catalyst enantiomers (in the case of aminoacids); and (iv) potential saving in costs, time and energy. These advantages have attracted the interest of researchers in this field and asymmetric organocatalysis has become a powerful tool for the stereoselective synthesis of highly valuable chiral building blocks.⁵⁴

⁵¹ (a) Hajos, Z. G.; Parrish, D. R. *J. Org. Chem.*, **1974**, *39*, 1615. (b) Ruppert, J.; Eder, U.; Wiechert, R. *Chemische Berichte*, **1973**, *106*, 3636. (c) Eder, U.; Sauer, G.; Wiechert, R. *Angew. Chem. Int. Ed. Eng.*, **1971**, *10*, 496. (d) Hajos, H.; Parrish, D. R. (F. Hoffmann-la Roche & Co. AG, German Patent) Germany DE 2102623 A, 1971. (e) Eder, U.; Sauer, G.; Wiechert, R. (Schering AG, German Patent) Germany DE 2014757 A, 1971.

⁵² List, B.; Lerner, R. A.; Barbas III, C. F. *J. Am. Chem. Soc.*, **2000**, *122*, 2395.

⁵³ Ahrendt, K. A.; Borths, C. J.; MacMillan, D. W. C. *J. Am. Chem. Soc.* **2000**, *122*, 4243.

⁵⁴ (a) MacMillan, D. W. C. *Nature*, **2008**, *455*, 304. (b) Guillena, G.; Nájera, C.; Ramón, D. J. *Tetrahedron: Asymmetry*, **2007**, *18*, 2249. (c) Pellissier, H. *Tetrahedron*, **2007**, *63*, 9267. (d) Bertelsen, S.; Jørgensen, K. A. *Chem. Soc. Rev.* **2009**, *38*, 2178. (e) Dondoni, A.; Massi, A. *Angew. Chem. Int. Ed.* **2008**, *47*, 4638. Special issues on organocatalysis: (f) List, B. Guest Ed. *Chem. Rev.*, **2007**, *107*, 5413. (g) Kocovsky, P.; Malkov, A. V. Guest Ed. *Tetrahedron*, **2006**, *62*, 243.

1.2 Organocatalysis classification. Activation modes.

According to the fact that in organocatalysis some mechanistic details still remain unknown, an specific criteria of classification has not been established. Consequently, different organocatalyst classifications have been proposed, one of them being dependent on the nature of organocatalyst-substrate interaction (covalent or non-covalent).⁵⁵

(a) Covalent Organocatalysis. Usually occurs through the formation of covalent catalyst-substrate adducts, which are the active catalytic species. Classical examples concerning this group are the amine based reactions. In this case amino acids, peptides, alkaloids or other *N*-containing molecules are used as chiral catalysts. Most of these reactions imply the so-called enamine cycle. Other examples involve chiral iminium salts (Morita-Baylis-Hillman reaction), carbenes (Stetter reaction) or oxidations of α,β -unsaturated systems and alkenes (epoxidation, cyclopropanation or asymmetric aziridination).

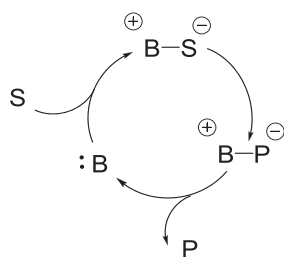
(b) Non-covalent Organocatalysis. Embraces neutral complexation or acid-base interaction between catalyst and substrate. The first case involves the “synenzymes”-catalyzed reactions, where a molecular catalyst operates in a similar way to enzymes, bringing reactants in the proximity of the active site without any covalent bond. In the second group, hydrogen bond catalysis or cation-anion association occurs, either in homogeneous or phase transfer conditions.

On the other hand, organocatalysts can also be classified depending on their nature. According to List, there are essentially four types of organocatalysts: Lewis bases, Lewis acids, Brønsted bases and Brønsted acids (Figure 2.2).⁵⁶

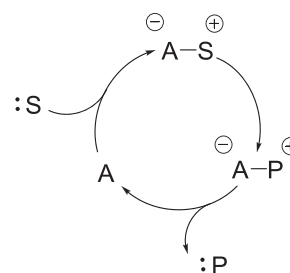
⁵⁵ *Enantioselective Organocatalysis, Reactions and Experimental Procedures*: ed. Dalko, P. I. WILEY-VCH: Weinheim, 2007.

⁵⁶ (a) Seayad, J.; List, B. *Org. Biomol.Chem.*, **2005**, *3*, 719. Example of Lewis base catalyst: (b) Shi, M.; Ma, G.-N.; Gao, J. *J. Org. Chem.*, **2007**, *72*, 9779. Examples of Lewis acid catalyst: (c) Yang, D. *Acc. Chem. Res.*, **2004**, *37*, 497. Examples of Brønsted acid catalyst: (d) Manabe, K.; Kobayashi, S. *Org. Lett.*, **1999**, *1*, 1965. (e) Schreiner, P. R. *Chem. Soc. Rev.*, **2003**, *32*, 289. Example of Brønsted base catalyst: (f) Tanaka, K.; Mori, A., Inoue, S. *J. Org. Chem.*, **1990**, *55*, 181.

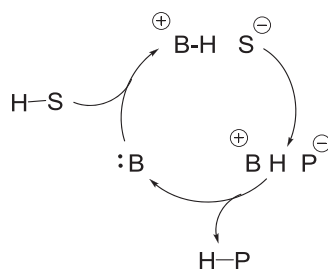
Chapter 2. 1.Introduction



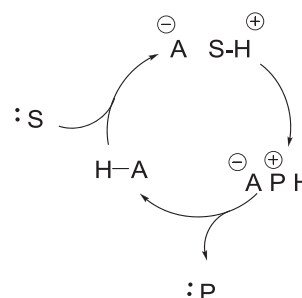
Lewis Base (B:) starts the catalytic cycle with the nucleophile addition to the substrate (S).^{56b}



Lewis Acid (A) activates the substrate (S) by forming the A⁻ - S⁺ adduct.⁵⁶



Brønsted Base (B) starts the catalytic cycle by partial deprotonation of the substrate.^{56f}



Brønsted Acid (A) starts the catalytic cycle by partial protonation of the substrate.^{56d,e}

Figure 2.2. Organocatalyst classification by List.

Importantly, the great success in organocatalysis can be attributed to the identification of several activation modes, which contributed to use them as a platform for the design of both new catalysts and new reactions.^{54a} These activation modes describe the interaction of a chiral organocatalyst with a functional group in an organized and predictable manner, leading to reactive species that can participate in many reaction types inducing asymmetry. The most common activation modes used in organocatalysis are the following:

(a) Enamine catalysis.⁵⁷ It is based in the interaction of an amine-containing catalyst (*i.e.* proline) with an enolizable carbonyl substrate to form an enamine intermediate (Scheme 2.2 a), which simultaneously engages with an electrophile through either hydrogen bond or electrostatic attraction. In this case, the energy of the highest-occupied molecular orbital (HOMO) of the nucleophile is increased. This activation mode was proposed in 2000 by Barbas, Lerner and List in the functionalization of carbonyl compounds at the α -carbon and it was first used as a generic mode of activation by MacMillan.⁵³ Some reaction variants comprise aldol

⁵⁷ For a review of enamine catalysis see: Mukherjee, S.; Yang, J.W.; Hoffmann, S.; List, B. *Chem. Rev.* **2007**, *107*, 5471.

reaction,⁵⁸ Mannich reaction,⁵⁹ α -amination,⁶⁰ α -oxygenation,⁶¹ α -halogenation⁶² and α -sulfenylation.⁶³

(b) *Hydrogen-bonding catalysis*. The substrate-catalyst interaction occurs through a well-defined hydrogen bond, which activates the lowest-occupied molecular orbital (LUMO) of the electrophile by decreasing its energy (Scheme 2.2 b). This activation mode was confirmed by the work of Jacobsen⁶⁴ and Corey⁶⁵ when activating imine electrophiles in asymmetric versions of the Strecker reaction. It has also been applied in Mannich reactions,⁶⁶ ketone cyanosilylation⁶⁷ or reductive amination,⁶⁸ among others.

(c) *Iminium catalysis*.⁶⁹ Contrary to the previous activation modes, it was designed rather than discovered. It is based on the concepts involved in the reactions catalyzed by Lewis acids and amines. In this case, the iminium ion formed from an α,β -unsaturated aldehyde and an amine organocatalyst emulates the Lewis acid activation, since the energy of the LUMO of the electrophile is lowered (Scheme 2.2 c).⁷⁰ Jørgensen and MacMillan have intensively developed this activation mode, which is currently applied in conjugate Friedel-Crafts⁷¹ and Diels-Alder reactions,⁷² cyclopropanation,⁷³ epoxidation,⁷⁴ aziridination⁷⁵ or Mukaiyama-Michael reaction.⁷⁶

⁵⁸ (a) Jia, Y.-N.; Wu, F.-C.; Zhu, G.-J.; Da, C.-S. *Tetrahedron Lett.*, **2009**, *50*, 3059. (b) Tanimori, S.; Naka, T.; Kirihata, M. *Synthetic Comm.*, **2004**, *34*, 4043.

⁵⁹ Ting, A.; Schaus, S. E. *Eur. J. Org. Chem.*, **2007**, 5797.

⁶⁰ (a) Sharma, A.; Sunoj, R. B. *Chem. Commun.*, **2011**, *47*, 5759. (b) Duthaler, R. O. *Angew. Chem. Int. Ed.*, **2003**, *42*, 975.

⁶¹ Takeuchi, N.; Handa, S.; Koyama, K.; Kamata, K.; Goto, K.; Tobinaga, S. *Chem. Pharmaceut. Bull.*, **1991**, *39*, 1655.

⁶² Marquez, C. A.; Fabbretti, F.; Metzger, J. O. *Angew. Chem. Int. Ed.*, **2007**, *46*, 6915.

⁶³ Marigo, Wabnitz, T. C.; Fielenbach, D.; Jørgensen, K. A. *Angew. Chem. Int. Ed.*, **2005**, *44*, 794.

⁶⁴ Sigman, M.; Jacobsen, E. N. *J. Am. Chem. Soc.*, **1998**, *120*, 4901.

⁶⁵ Corey, E. J.; Grogan, M. J. *Org. Lett.*, **1999**, *1*, 157.

⁶⁶ Tian, X.; Jiang, K.; Peng, J.; Du, W.; Chen, Y.-C. *Org. Lett.*, **2008**, *10*, 3583.

⁶⁷ Qin, B.; Liu, X.; Shi, J.; Zheng, K.; Zhao, H.; Feng, X. *J. Org. Chem.*, **2007**, *72*, 2374.

⁶⁸ Huang, Y.-B.; Cai, C. *J. Chem. Res.*, **2009**, *11*, 686.

⁶⁹ For a review of iminium catalysis see: Erkkilä, A.; Majander, I.; Pihko, P.M. *Chem. Rev.* **2007**, *107*, 5416.

⁷⁰ King, H. D. *Org. Lett.*, **2005**, *7*, 3437.

⁷¹ Chauder, B.; Feldman, P. L. *Chemtracts*, **2002**, *15*, 461.

⁷² (a) De Nino, A.; Bortolini, O.; Maiuolo, L.; Garofalo, A.; Russo, B.; Sindona, G. *Tetrahedron Lett.*, **2011**, *52*, 1415. (b) Iafe, R. G.; Houk, K. N. *J. Org. Chem.*, **2008**, *73*, 2679.

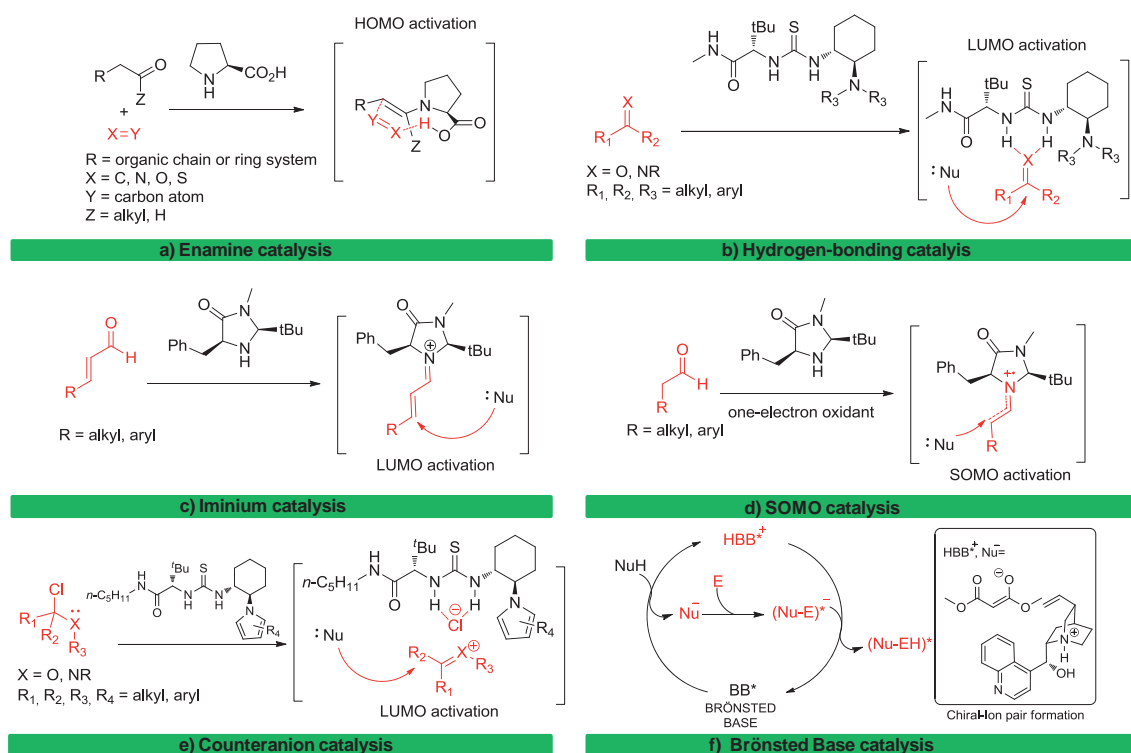
⁷³ (a) Terrasson, V.; van der Lee, A.; de Figueiredo, R. M.; Campagne, J. M. *Chem. Eur. J.*, **2010**, *16*, 7875. (b) Lakhdar, S.; Appel, R.; Mayr, H. *Angew. Chem. Int. Ed.*, **2009**, *48*, 5034.

⁷⁴ Novikov, R.; Lacour, J. *Tetrahedron: Asymmetry*, **2010**, *21*, 1611.

⁷⁵ Carter, C.; Fletcher, S.; Nelson, A. *Tetrahedron: Asymmetry*, **2003**, *14*, 1995.

⁷⁶ Brown, S. P.; Goodwin, N. C.; MacMillan, D. W. C. *J. Am. Chem. Soc.*, **2003**, *125*, 1192.

Chapter 2. 1. Introduction



Scheme 2.2. Several activation modes in organocatalysis.

(d) SOMO catalysis. Reactive radical cations with three π -electrons can be generated by one-electron oxidation of an electron-rich enamine (Scheme 2.2 d). The resulting electrophilic single-occupied molecular orbital (SOMO) enables the reaction of this intermediate with a variety of weak nucleophiles, resulting in formal alkylation products.⁷⁷ SOMO catalysis examples can be found on α -allylation,⁷⁸ α -enolation,⁷⁹ α -vinylation⁸⁰ or α -heteroarylation.⁸¹ Remarkably, it complements the enantioselective organocatalysis by enamine pathways.

(e) Counterion catalysis. Developed by Jacobsen, this activation mode directs enantioselective additions into transiently generated *N*-acyl-iminium ions and oxocarbenium ions.⁸² In this case, the approach of the nucleophiles is governed by an ion pair formed between the cationized substrate and the anionic catalyst-chloride complex, generated from chiral thiourea catalyst and halide ions (Scheme 2.2 e). Thioureas are known to electrostatically bind to carbon-chlorine bonds in chloroamides

⁷⁷ Narasaka, K.; Okauchi, T.; Tanaka, T; Murakami, M. *Chem. Lett.*, **1992**, 10, 2099.

⁷⁸ Anon. *Chemtracts*, **2007**, 20, 450.

⁷⁹ Jang, H.-Y.; Hong, J.-B.; MacMillan, D. W. C. *J. Am. Chem. Soc.*, **2007**, 129, 7004.

⁸⁰ Kim, H.; MacMillan, D. W. C. *J. Am. Chem. Soc.*, **2008**, 130, 398.

⁸¹ Beeson, T. D.; Mastracchio, A.; Hong, J.; Ashton, K; MacMillan, D. W. C. *Science*, **2007**, 316, 582.

⁸² (a) Reisman, S. E.; Doyle, A. G.; Jacobsen, E. N. *J. Am. Chem. Soc.*, **2008**, 130, 7198. (b) Raheem, I.; Thiara, P. S.; Peterson, E. A.; Jacobsen, E. N. *J. Am. Chem. Soc.*, **2007**, 129, 13404.

and chloroacetals. This activation mode seems to act more through the space rather than through bonds, but it is sufficient to transfer stereochemical information from the catalyst to the substrate.

(f) Brönsted Base catalysis. Over the past few years a considerable number of publications has arisen dealing with chiral Brönsted bases as catalytic promoters of asymmetric transformations involving the reaction between a relatively acidic pronucleophile and an electrophile. The mechanistic pathway generally adopted for a carbon pronucleophile is depicted in Scheme 2.2 f.⁸³ In the key step, a pro-nucleophile unit loses one proton to render a new species with enhanced nucleophilicity, which forms a chiral ion-pair with the protonated form of the base. Thus, ion pairing arises as the principal interaction between a substrate and a Brönsted base catalyst, which will be responsible for the stereo-induction. Various nitrogen-containing compounds have been used as chiral Brönsted bases, such as tertiary amines, guanidines, amidines and imidazoles. Alkaloids of the Cinchona family constitute a straightforward source of enantiopure base catalysts. To enhance both the activity and the asymmetric induction, ambifunctional catalysts have been designed, which combine the Brönsted basic site with another hydrogen-bonding site. Thus, Cinchona derivatives containing additional urea or thiourea functionalities can anchor both nucleophilic and electrophilic components in the transition state. In that way, concurrent activation of both substrates is achieved and a higher degree of stereochemical order in the transition state is obtained.

1.3 Enamine catalysis in α -functionalization of carbonyl compounds.

Organocatalysis is dominated by Lewis base catalysts such as amines and carbenes. Moreover, amino acids are simple, naturally abundant and low cost compounds capable of inducing chirality. Among them, L-proline has been established as one of the most efficient and simple asymmetric organocatalyst for the aldol reaction,^{84,85} as well as for other reactions where carbonyl compounds are functionalized at the α -carbon, such as Michael additions, Mannich reactions or formal aza-Diels Alder reactions.⁸⁶

⁸³ Palomo, C.; Oiarbide, M. Lopez, R. *Chem. Soc. Rev.*, **2009**, 38, 632.

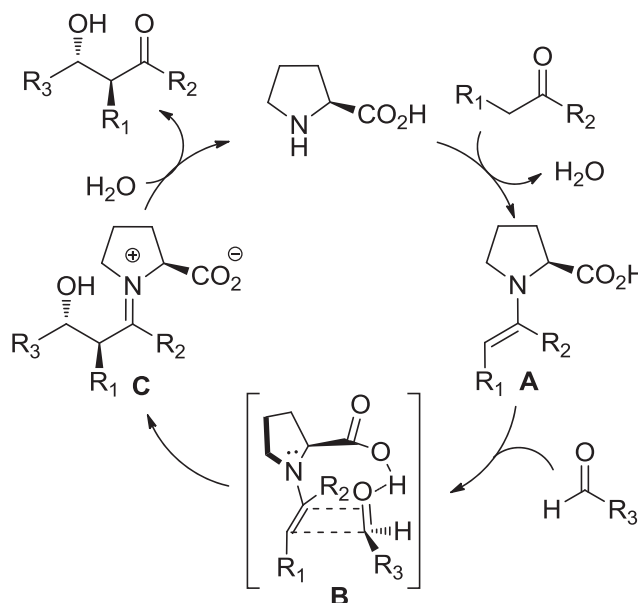
⁸⁴ Melchiorre, P.; Marigo, M.; Carlone, A.; Bartoli, G. *Angew. Chem. Int. Ed.* **2008**, 47, 6138.

⁸⁵ For aldol reaction: (a) Trost, B. M.; Brindle, C. S. *Chem. Soc. Rev.* **2010**, 39, 1600. (b) Mase, N.; Nakai, Y.; Ohara, N.; Yoda, H.; Takabe, K.; Tanaka, F.; Barbas III, C. F. *J. Am. Chem. Soc.*, **2006**, 128, 734.

⁸⁶ For Michael reaction: (c) List, B.; Pojarliev, P.; Martin, H. J. *Org. Lett.* **2001**, 3, 2423. For Mannich reaction: (d) Notz, W.; Sakthivel, K.; Bui, T.; Zhong, G.; Barbas III, C. F. *Tetrahedron*

Chapter 2. 1. Introduction

The generally accepted mechanism for an aldol reaction catalyzed by L-proline starts with the enamine formation (**A**). This step is followed by the addition of the enamine to the carbonyl group of the electrophile, which is activated by the carboxylic acid of proline through hydrogen-bond formation (**B**). Finally, the hydrolysis of the resulting iminium ion **C** affords the final product and regenerates the chiral catalyst (Scheme 2.3).^{54d,87}

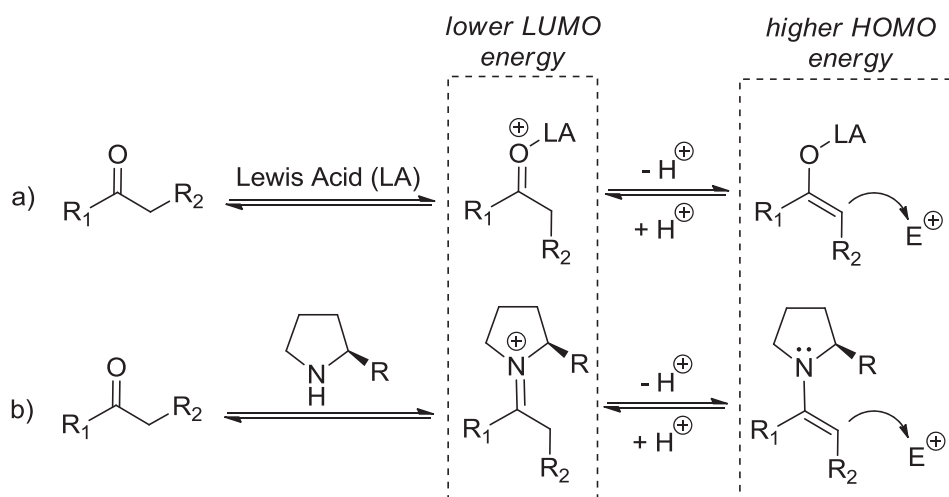


Scheme 2.3. List-Houk model mechanism of intermolecular proline-catalyzed aldol reaction.⁸⁷

Strikingly, the principle for proline activation is similar to the activation of carbonyl compounds by Lewis acids. In the reversible condensation of primary or secondary amines with the carbonyl compounds, the iminium intermediates show a similar electronic situation of their π orbitals than the Lewis acid-carbonyl adducts (Scheme 2.4). As a result, the LUMO energy lowers and the acidity of the α -proton increases, promoting a fast deprotonation and the enamine generation (HOMO activation).⁸⁴

Letts, **2001**, *42*, 199. For aza-Diels Alder reaction: Sundén, H.; Ibrahim, I.; Eriksson L.; Córdova, A. *Angew. Chem. Int. Ed.* **2005**, *44*, 4877.

⁸⁷ (a) Reisinger, C. M.; Pan, S. C.; List, B. "New Concepts for Catalysis" in *Systems Chemistry*: ed. Hicks, M. G.; Kettner, C. BELSTEIN-INSTITUT: Bozen, 2009. (b) Klussmann, M.; Iwamura, H.; Mathew, S. R.; Wells, D. H.; Pandya, U.; Armstrong, A.; Blackmond, D. G. *Nature*, **2006**, *441*, 621. (c) Marquez, C.; Metzger, J. O. *Chem. Commun.*, **2006**, 1539. (d) Bassan, A.; Zou, W. B.; Reyes, E.; Himo, F.; Córdova, A. *Angew. Chem. Int. Ed.*, **2005**, *44*, 7028. (e) List, B. *Acc. Chem. Res.*, **2004**, *37*, 548. (f) Bahmanyar, S.; Houk, K. N.; Martin, H. J.; List, B. *J. Am. Chem. Soc.*, **2003**, *125*, 2475. (g) Bahmanyar, S.; Houk, K. N. *J. Am. Chem. Soc.*, **2001**, *123*, 12911.



Scheme 2.4. Carbonyl activation by (a) Lewis acid; (b) enamine formation.⁸⁴

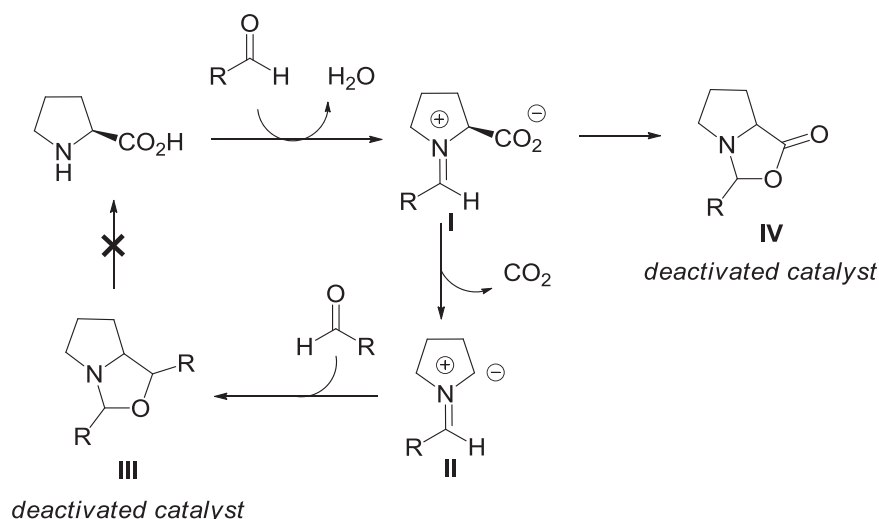
The addition step of the enamine to the electrophile has a similar energy barrier as the enamine formation and some recent computational studies showed that the rate determining step occurs before or during the new carbon-carbon bond formation, being either the enamine formation or the electrophile addition.⁸⁸ Consequently, the rate determining step is dependent on certain reaction conditions or substrates.

When the electrophile is an aldehyde, catalyst deactivation can occur through oxazolidinone formation (see compounds **III** or **IV** as deactivated forms of proline, Scheme 2.5).⁸⁹ In order to prevent the catalyst deactivation and the formation of by-products, the nucleophilic ketone can be used in large excess and the reaction can be performed in the presence of water.⁹⁰

⁸⁸ (a) Zhu, H.; Clemente, F. R.; Houk, K. N.; Meyer, M. P. *J. Am. Chem. Soc.*, **2009**, *131*, 1632. (b) Zotova, N.; Broadbelt, L. J.; Armstrong, A.; Blackmond D. G. *Bioorg. Med. Chem. Lett.*, **2009**, *19*, 3934.

⁸⁹ Trost, B. M.; Brindle, C. S. *Chem. Soc. Rev.* **2010**, *39*, 1600.

⁹⁰ (a) Pihko, P. M.; Laurikainen, K. M.; Nyberg, A. I.; Kaavi, J. A. *Tetrahedron*, **2006**, *62*, 317. (b) Nyberg, A. I.; Usano, A.; Pihko, P. M. *Synlett*, **2004**, 1891.



Scheme 2.5. Catalyst deactivation pathways.

Apart from the nucleophilic addition of enamine intermediate to electrophiles containing π -bonds such as aldehydes,⁹¹ imines⁹² or Michael acceptors,⁹³ enamine catalysis can also be applied in nucleophilic substitutions if the electrophile contains single bonds, α -chlorination⁹⁴ and α -sulfenylation⁹⁵ representing two examples among other α -functionalization reactions.

1.4 Organocatalysts based on proline derivatives

L-Proline is a bifunctional organocatalyst since it plays a dual role in the enamine cycle. The amino group acts as a Lewis base, while the carboxylic group acts as a Brønsted acid. This amino acid is known to catalyze a wide range of reactions with excellent results. Despite its high selectivity, L-proline still lacks efficiency in many cases. Indeed, L-proline-catalyzed reactions typically require high catalyst loadings (up to 30 mol %), excess of nucleophile and long reaction times, which is often attributed to its low solubility in organic media. Consequently, some modifications on the proline skeleton have been introduced not only to overcome these drawbacks but also to modulate its reactivity, improving its catalytic activity and the reaction conditions.⁹⁶

⁹¹ List, B.; Lerner, R. A.; Barbas III, C. F. *J. Am. Chem. Soc.*, **2000**, 122, 2395.

⁹² (a) Veverková, E.; Šebesta, R.; Toma, Š. *Tetrahedron: Asymmetry*, **2010**, 21, 58. (b) Sundén, H.; Ibrahem, I.; Eriksson L.; Córdova, A. *Angew. Chem. Int. Ed.* **2005**, 44, 4877.

⁹³ Andrey, O.; Alexakis, A.; Tomassini, A.; Berardinelli, G. *Adv. Synth. Catal.*, **2004**, 346, 1147.

⁹⁴ Brochu, M. P.; Brown, S. P.; MacMillan, D. W. C. *J. Am. Chem. Soc.*, **2004**, 126, 4108.

⁹⁵ Marigo, M.; Wabnitz, T. C.; Fielenbach, D.; Jørgensen, K. A. *Angew. Chem. Int. Ed.*, **2005**, 44, 794.

⁹⁶ Guillena, G.; Nájera, C.; Ramón, D. J. *Tetrahedron: Asymmetry*, **2007**, 18, 2249.

Since the discovery of 4-hydroxyproline by Fischer in 1902,⁹⁷ a wealth of proline derivatives have been synthesized. Proline based-organocatalysts can be classified into seven general categories (prolinols and protected prolinols, prolinamines, proline esters, proline tetrazoles, prolinamides and proline sulfonamides) (Figure 2.3).⁹⁸ Among them, proline tetrazole was first synthesized in 1971 by Grzonka and co-workers.⁹⁹ In contrast, proline sulfonamides represent one of the most recent additions to this large family of compounds.

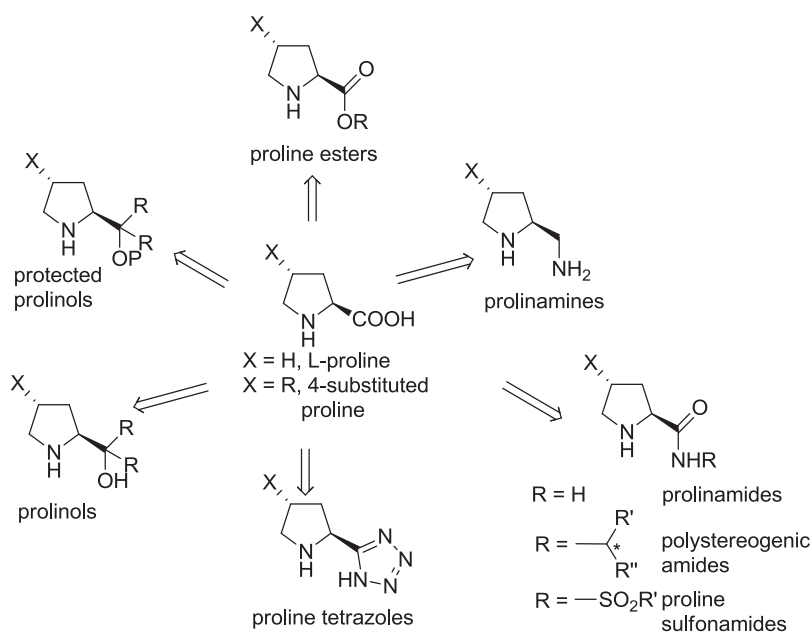


Figure 2.3. Classes of proline derivatives.

In proline-based catalysts the conformation of the enamine intermediate is responsible for the stereoselection in the electrophile approach. Two main factors influence the facial selectivity, depending on the pyrrolidine ring substituents.¹⁰⁰ On one hand, an H-bond interaction can take place if the electrophile contains an electronegative heteroatom acting as a H-bond acceptor. It happens in proline-catalyzed aldol, Mannich or amination reactions, where the attack occurs through the *re*-face at the β -C atom of the enamine intermediate (Figure 2.4, a). On the other hand, catalysts with bulky substituents in the 2-position of the pyrrolidine ring, like diarylprolinols, direct the attack through the *si*-face at the β -C atom of the enamine, *i.e.* in sulfenylation reactions or addition to electron deficient olefins (Figure 2.4, b). These

⁹⁷ Fischer, E. *Ber. Dtsch. Chem. Ges.* **1902**, 35, 2660.

⁹⁸ Yang, H.; Carter, R. G. *Synlett*, **2010**, 2827.

⁹⁹ (a) Grzonka, Z.; Liberek, B. *Roczniki Chemii* **1971**, 45, 967. (b) Hartikka, A.; Arvidsson, P.I. *Tetrahedron: Asymmetry* **2004**, 15, 1831.

¹⁰⁰ Bertelsen, S.; Jørgensen, K. A. *Chem. Soc. Rev.*, **2009**, 38, 2178

Chapter 2. 1.Introduction

two directing effects will lead to different enantiomers, even if both catalysts have the same absolute stereochemistry.¹⁰¹

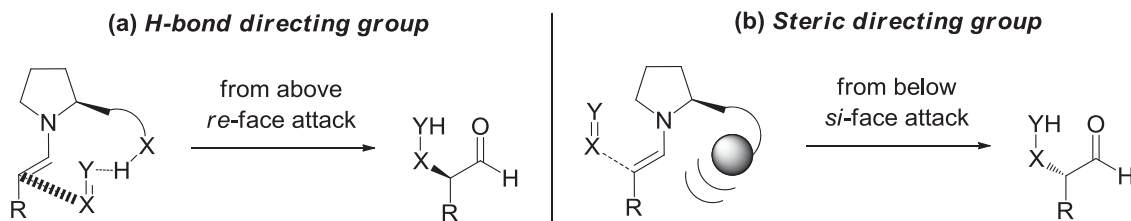


Figure 2.4. Stereinduction through (a) H-bond interaction and (b) steric effects.

1.4.1 Proline sulfonamides as asymmetric organocatalysts

Berkessel and co-workers¹⁰² reported the synthesis of the first catalysis-focused proline aryl sulfonamides **a-c** in 2004 (Figure 2.5). They disclosed their potential organocatalytic activity in the aldol reaction without using inert conditions. Compared to L-proline, the enantioselectivity could be improved to 98% ee while maintaining high activity at low catalyst loadings. The origin of the improved enantioselectivity observed with the arylsulfonamide catalysts may be explained by a better shielding of one of the enantiotopic faces of the aldehyde by the aryl ring (Figure 2.6). They also speculated that "tighter" hydrogen bonding in the transition state could account for the better stereoselection observed.

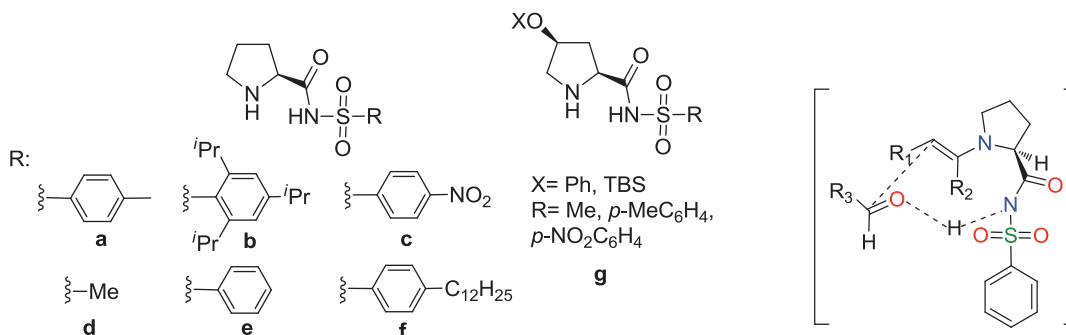


Figure 2.5. Examples of proline sulfonamides catalysts.

Figure 2.6. Proposed transition state for aldol reaction.

In the following year, Ley and co-workers¹⁰³ reported the synthesis of other two examples of the sulfonamide family **d-e** (Figure 2.5). These catalysts proved to be effective at facilitating both aldol reactions and Mannich reactions under inert

¹⁰¹ Franzén, J.; Marigo, M.; Fielenbach, D.; Wabnitz, T. C.; Kjærsgaard, A.; Jørgensen, K. A. *J. Am. Chem. Soc.*, **2005**, *127*, 18296.

¹⁰² Berkessel, A.; Koch, B.; Lex, J. *Adv. Synth. Catal.* **2004**, *346*, 1141.

¹⁰³ Cobb, A. J. A.; Shaw, D.M.; Longbottom, D.A.; Gold, J.B.; Ley, S.V. *Org. Biomol. Chem.* **2005**, *3*, 84.

conditions. It is important to note that the vast majority of organocatalyzed processes involving proline or proline surrogates employ polar solvents such as DMF and DMSO. For this reason, Carter¹⁰⁴ presented the introduction of a long hydrocarbon chain in the *para* position of the aromatic ring of the sulfonamide **f** (Figure 2.5) which improved its solubility properties in non-polar solvents and even allowed its use under neat conditions. Alternatively, Fu¹⁰⁵ introduced a bulky group to induce steric hindrance at the 4-position as hydrophobic group (Figure 2.5, **g**), which afforded excellent diastereo- and enantio-selectivities performing the reaction in water media. Authors hypothesized that phenoxy moiety may build a sort of *hydrophobic pocket* where the reaction took place favoring the formation of one enantiomer.

Other examples of prolinsulfonamides as organocatalysts for the aldol reaction¹⁰⁶ have been described in the literature, as well as for Michael addition,¹⁰⁷ Mannich reaction,¹⁰⁸ aza-Diels Alder,¹⁰⁹ Yamada-Otani type condensation,¹¹⁰ cyclopropanation¹¹¹ and α -oxidation of carbonyl compounds.¹¹² Remarkably, other more specific applications have been achieved, such as the synthesis of enantiomerically enriched secondary and tertiary phenylthio- and phenoxy-aldols via direct aldol reaction,¹¹³ enantioselective synthesis of (*R*)-Convolutamydine A, B and E through aldol reaction,¹¹⁴ 1,3- dipolar cycloaddition,¹¹⁵ enantioselective synthesis of

¹⁰⁴ (a) Yang, H.; Carter, R.G. *Org. Lett.* **2008**, *10*, 4649. (b) Yang, H.; Mahapatra, S.; Cheong, P.H.-Y.; Carter, R. G. *J. Org. Chem.* **2010**, *75*, 7279.

¹⁰⁵ (a) Zhang, S.-p.; Fu, X.-k.; Fu, S.-d.; Pan, J.-f. *Catal. Commun.* **2009**, *10*, 401. (b) Fu, S.-d.; Fu, X.-k.; Zhang, S.-p.; Zou, X.-c.; Wu, X.-j. *Tetrahedron Asym.* **2009**, *20*, 2390.

¹⁰⁶ (a) Silva, F.; Sawicki, M.; Gouverneur, V. *Org. Lett.* **2006**, *8*, 5417. (b) Wang, X.J.; Zhao, Y.; Liu, J.T. *Org. Lett.* **2007**, *9*, 1343. (c) Hara, N.; Tamura, R.; Funahashi, Y.; Nakamura S. *Org. Lett.* **2011**, *13*, 1662. (d) Tang, G.; Hu, X.; Altenbach, H.J. *Tet. Lett.* **2011**, *52*, 7034. (e) Aitken, D. J.; Bernard, A. M.; Capitta, F.; Frongia, A.; Guillot, R.; Ollivier, J.; Piras, P.P; Secci, F.; Spiga, M. *Org. Biomol. Chem*, **2012**, *10*, 5045.

¹⁰⁷ Tsandi, E.; Kokotos, C.G.; Kousidou, S.; Ragoussis, V.; Kokotos G. *Tetrahedron* **2009**, *65*, 1444.

¹⁰⁸ (a) Yang, H.; Carter, R. G. *J. Org. Chem.* **2009**, *74*, 2246. (b) Veverková, E.; Strasserová, J.; Sebesta, R.; Toma, S. *Tetrahedron Asym.* **2010**, *21*, 58. (c) Veverková, E.; Liptáková, L.; Veverka, M.; Sebesta, R.; *Tetrahedron Asym.* **2013**, *24*, 548.

¹⁰⁹ (a) Sundén, H.; Ibrahim, I.; Eriksson, L.; Córdova, A. *Angew. Chem. Int. Ed.* **2005**, *44*, 4877.

(b) Yang, H.; Carter, R. G. *J. Org. Chem.* **2009**, *74*, 5151.

¹¹⁰ (a) Yang, H.; Carter, R.G. *Tetrahedron*, **2010**, *66*, 4854. (b) Yang, H.; Carter, R. *Org. Lett.* **2010**, *12*, 3108. (c) Yang, H.; Banerjee, S.; Carter, R. *Org. Biomol. Chem.* **2012**, *10*, 4851.

¹¹¹ Hartikka, A.; Slósarczyk, A. T.; Arvidsson, P. I. *Tetrahedron. Asym.* **2007**, *18*, 1403.

¹¹² Sundén, H.; Dahlin, N.; Ibrahim, I.; Adolfsson, H.; Córdova, A. *Tetrahedron Lett.* **2005**, *46*, 3385.

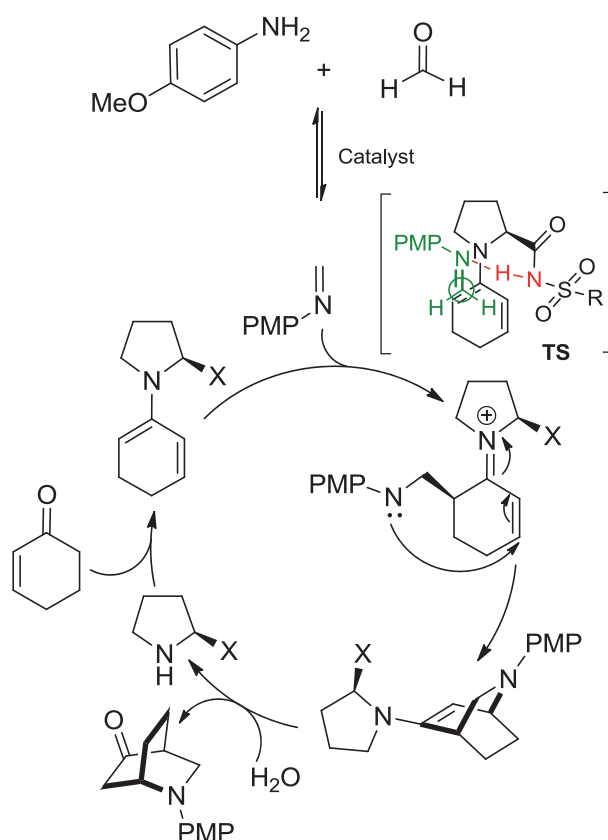
¹¹³ Bernard, A. M.; Frongia, A.; Piras, P. P.; Secci, F.; Spiga, M. *Tetrahedron Lett.* **2008**, *49*, 3037.

¹¹⁴ (a) Nakamura, S.; Hara, N.; Nakashima, H.; Kubo, K.; Shibata, N.; Toru, T. *Chem. Eur. J.* **2008**, *14*, 8079. (b) Hara, N.; Nakamura, S.; Shibata, N.; Toru, T. *Chem. Eur. J.* **2009**, *15*, 6790.

¹¹⁵ Xiao, J.-A.; Liu, Q.; Ren, J.-W.; Liu, J.; Carter, R.G.; Chen, X.-Q.; Yang, H. *Eur. J. Org. Chem.* **2014**, 5700.

Lycopodine via Michael addition,¹¹⁶ asymmetric synthesis of 2-aryl-2,3-dihydro-4-quinolones through an intramolecular Mannich reaction.¹¹⁷

Among all these reactions mentioned above, we would like to remark the aza-Diels Alder reaction as it has been of our interest in the catalytic tests and it is one of the most powerful C-C bond-forming reactions for the preparation of nitrogen-containing compounds such as piperidines and quinolidine derivatives.^{109a} Córdova proposed a mechanism to explain the stereochemical outcome of the reaction (Scheme 2.6). In the first step the proline derived catalyst forms a chiral enamine with the α,β -unsaturated ketone. Next, the in situ generated imine attacks the *si* face of the chiral diene *via* transition state **TS**, and an activated iminium salt is formed. The secondary amine of the chiral iminium salt performs a subsequent selective 6-*endo-trig* cyclization to furnish the corresponding chiral azabicyclic intermediate. Next, the amino acid derivative is released, the desired aza-Diels Alder adduct is obtained by hydrolysis and the catalytic cycle can be repeated. Thus, the reaction proceeds through a tandem one-pot three component Mannich/Michael reaction pathway.



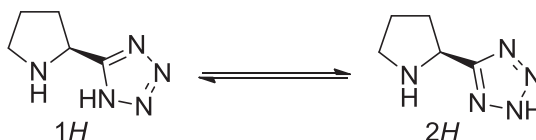
Scheme 2.6. aza-Diels Alder proposed mechanism by Córdova.

¹¹⁶ Yang, H.; Carter, R.G. *J. Org. Chem.* **2010**, *75*, 4929.

¹¹⁷ Zheng, H.; Liu, Q.; Wen, S.; Yang, H.; Luo, Y. *Tetrahedron Asym.* **2013**, *24*, 875.

1.4.2 Proline tetrazoles as asymmetric organocatalysts

As the acidity of the stereodirecting group plays a critical role in enhancing the reactivity, catalyst efficiency, and to an even great extent, enantioselectivity, proline tetrazole has been described as an excellent organocatalyst. Tetrazoles present similar aqueous pK_a values than carboxylic acids and show higher solubility,^{54b} being frequently used as their bioisosteres either in medicinal chemistry or in catalysis. Proline tetrazole exists as a mixture of two tautomers^{118a} (Scheme 2.7).



Scheme 2.7. 5-Pyrrolidine-2-yltetrazole. This compound exists as a mixture of tautomers 1H and 2H.

The first applications of this tetrazole derivative in asymmetric organocatalysis were performed for the aldol reaction. Saito and Yamamoto¹¹⁹ described the use of proline tetrazole for the direct aldol reaction between different ketones and chloral monohydrate in acetonitrile affording the expected products with high yields and enantioselectivities. At the same time, Arvidsson¹¹⁸ published its use for the direct aldol reaction between acetone and different aldehydes achieving the desired products with good yields and enantioselectivities in very short reaction times. The high solubility of the catalyst permitted its use in different solvents. The increased reactivity was more apparent when less reactive aldehydes were employed as aldol acceptors. Other examples of aldol reaction also show the great activity of the catalyst.¹²⁰ However, depending on the conditions, proline sulfonamides present better performances compared with the tetrazole derivative.^{104b,106b,e} Consequently, it seems that each catalyst structure may have reaction parameters which are favorable for its optimum performance.^{104b}

Ley also reported his work with proline tetrazole¹⁰³ as organocatalyst for the asymmetric Mannich and Michael reactions and commented that tetrazoles provided

¹¹⁸ (a) Hartikka, A.; Arvidsson, P.I. *Tetrahedron Asym.* **2004**, *15*, 1831. (b) Hartikka, A.; Arvidsson, P.I. *Eur. J. Org. Chem.* **2005**, 4287.

¹¹⁹ Torii, H.; Nakadai, M.; Ishihara, K.; Saito, S.; Yamamoto, H. *Angew. Chem. Int. Ed.* **2004**, *43*, 1983.

¹²⁰ (a) Enders, D.; Gasperi, T. *Chem. Commun.* **2007**, 88. (b) Tong, A.-T.; Harris, P.W.R.; Barker, D.; Brimble, M.A. *Eur. J. Org. Chem.* **2008**, 164. (c) Odedra, A.; Seeberger, P. H. *Angew. Chem. Int. Ed.* **2009**, *48*, 2699. (d) Xue, F.; Zhang, S.; Liu, L.; Duan, W.; Wang, W. *Chem. Asian. J.* **2009**, *4*, 1664. (e) Chercheja, S.; Nadakudity, S. K.; Eilbracht, P. *Adv. Synth. Catal.* **2010**, *352*, 637. (f) Funabiki, K.; Itoh, Y.; Kubota, Y.; Matsui, M. *J. Org. Chem.* **2011**, *76*, 3345. (g) Komatsu, Y.; Watanabe, R.; Ikishima, H.; Nakano, K.; Ichikawa, Y.; Kotsuki, H. *Org. Biomol. Chem.* **2012**, *10*, 293.

Chapter 2. 1.Introduction

"significant advantages" over sulfonamide catalysts through shorter reaction times and lower catalyst loadings. Mannich reactions could be performed in non-polar solvents whereas Michael additions were done in alcoholic solvents. Furthermore, tetrazole derivatives also provided unique reactivity as the sulfonamide catalysts were unable of generating the desired product such as in the Michael addition of cyclohexanone to α,β -unsaturated nitro compounds.

Subsequent work with proline tetrazole derivatives has shown its effective activity in a great variety of applications such as other Mannich reactions,¹²¹ addition of malonates to enones,¹²² addition of nitroalkanes to unsaturated ketones,¹²³ one-pot synthesis of chiral dihydro-1,2-oxazines,¹²⁴ α -aminoylation/aza-Michael reaction,¹²⁵ formal nitroso-Diels Alder,¹²⁶ Biginelli reaction,¹²⁷ functionalization of benzothiophene,¹²⁸ α -amination¹²⁹ and synthesis of 1-azabicyclo[3.3.1]nonanes via intramolecular Michael reaction.¹³⁰

1.5 Supported organocatalysts based on proline derivatives. Catalyst recovery and recycling.

Even though organocatalysis can be regarded as a green chemistry method due to high selectivity of organocatalytic reactions and their *atom economy*, there is a serious problem preventing active application of organocatalytic methods in chemical and pharmaceutical industries. As a rule, organocatalysts are less active than organometals and biocatalysts.¹³¹ They are needed in a significant amount (10-30 mol%), which imply tedious and time-consuming purification. To solve this problem,

¹²¹ (a) Chowdari, N. S.; Ahmad, M.; Albertshofer, K.; Tanaka, F.; Barbas III, C.F. *Org Lett.* **2006**, *8*, 13. (b) Hayashi, Y.; Urushima, T.; Aratake, S.; Okano, T.; Obi, K. *Org. Lett.* **2008**, *10*, 21. (c) Galzerano, P.; Agostino, D.; Benivenni, G.; Sambri, L.; Bartoli, G.; Melchiorre, P. *Chem. Eur. J.* **2010**, *16*, 6069.

¹²² (a) Knudsen, K. R.; Mitchell, C. E. T.; Ley, S. V. *Chem. Commun.* **2006**, 66. (b) Washolowski, V.; Knudsen, K. R.; Mitchell, C. E. T.; Ley, S. V. *Chem. Eur. J.* **2008**, *14*, 6155. (c) Pandey, G.; Adate, P. A.; Puranik, V.G. *Org. Biomol. Chem.* **2012**, *10*, 8260.

¹²³ Mitchell, C. E.T.; Brenner, S. E.; Garcia-Fontanet, J.; Ley, S. V. *Org. Biomol. Chem.* **2006**, *4*, 2039.

¹²⁴ (a) Kumarn, S.; Shaw, D. M.; Longbotton, D. A.; Ley, S. V. *Org. Lett.* **2005**, *7*, 4189. (b) Kumarn, S.; Oelke, A.J.; Shaw, D. M.; Longbotton, D. A.; Ley, S. V. *Org. Biomol. Chem.* **2007**, *5*, 2678.

¹²⁵ Lu, M.; Zhu, D.; Lu, Y.; Hou, Y.; Bin, T.; Zhong, G. *Angew. Chem. Int. Ed.* **2008**, *47*, 10187.

¹²⁶ Momiyama, N.; Yamamoto, Y.; Yamamoto, H. *J. Am. Chem. Soc.* **2007**, *129*, 1190.

¹²⁷ Wu, Y.-Y.; Chai, Z.; Liu, X.-Y.; Zhao, G.; Wang, S.-W. *Eur. J. Org. Chem.* **2009**, 904.

¹²⁸ Secci, F.; Cadoni, E.; Fattuoni, C.; Frongia, A.; Bruno, G.; Nicolò, F. *Tetrahedron*, **2012**, *68*, 4773.

¹²⁹ Msutu, A.; Hunter, R. *Tetrahedron Lett.* **2014**, *55*, 2295.

¹³⁰ Ngo, A. N.; El Kassimi, K. Amara, Z.; Drège, E.; Joseph, D. *Tetrahedron Lett.* **2012**, *53*, 3296.

¹³¹ Kucherenko, A.S.; Siyutkin, D.E.; Maltsev, O.V.; Kochetkov, S.V.; Zlotin, S.G. *Russ. Chem. Bull. Int. Ed.* **2012**, *61*, 1313.

recycling of the organocatalysts has been investigated by several research groups. One of the most widely applied strategies for this purpose consists in immobilizing the homogeneous catalyst on an insoluble support.¹³² This has the advantages of easy handling, clean separation of the products from the catalyst by filtration and facile recovery and reuse of the latter. Organocatalyst immobilization can be seen as an attempt to mimic enzymes, with proline derivatives playing the role of the enzyme's active site and the polymeric matrix that of a simplified peptide backbone, not directly involved in the catalytic activity.^{132f} Furthermore, it is known that some organic catalysts slowly decompose; in these cases, the immobilization would reduce the contamination of the final product, since decomposition products would remain linked to the support.

The choice of the support is quite relevant. On one hand, supported catalysts are often sterically hindered and hence less accessible than their non-supported counterpart. Actually, the immediate surroundings of the active site can strongly affect the stereochemical approach of the reagents. On the other hand, a higher density of catalytic sites can be translated into higher activity, but this is not a general rule.^{132g,133} Research on supported organocatalysts has been focused on two different general approaches, covalently supported and non-covalently supported catalysts.^{132c}

In the first approach, the support can be either soluble¹³⁴ or insoluble,¹³⁵ but in any case the solubility properties must allow an easy separation. Indeed, by changing some environmental conditions such as solvent polarity or reaction temperature, the advantages of homogeneous and heterogeneous systems can be coupled. Soluble

¹³² For immobilization of chiral organocatalysts on supports: (a) Zamboulis, A.; Moitra, N.; Moreau, J. J. E.; Cattoen, X.; Wong Chi Man, M. *J. Mater. Chem.*, **2010**, *20*, 9322. (b) Kristensen, T. E.; Hansen, T. *Eur. J. Org. Chem.*, **2010**, 3179. (c) Gruttadauria, M.; Giacalone, F.; Noto, R. *Chem. Soc. Rev.*, **2008**, *37*, 1666. (d) Corma, A.; García, H. *Adv. Synth. Catal.*, **2006**, *348*, 1391. (e) Benaglia, M. *New J. Chem.*, **2006**, *30*, 1525. (f) Cozzi, F. *Adv. Synth. Catal.*, **2006**, *348*, 1367. (g) Benaglia, M.; Pugliesi, A.; Cozzi, F. *Chem. Rev.*, **2003**, *103*, 3401. (h) *Chiral Catalyst Immobilization and Recycling*, ed. De Vos, D. E.; Vankelecom, I. F.; Jacobs, P. A., WILEY-VCH: Weinheim, 2000.

¹³³ Some examples of improved activity with higher density of active sites: (a) Trilla, M.; Pleixats, R.; Wong Chi Man, M.; Bied, C. *Green Chem.*, **2009**, *11*, 1815. (b) Limura, S.; Manabe, K.; Kobayashi, S. *Org. Biomol. Chem.*, **2003**, *1*, 2416. Example of how an increased loading of active sites does not necessarily correspond to increased catalytic activity: Anelli, P. L.; Montanari, F.; Quici, S. *J. Org. Chem.*, **1986**, *51*, 4910.

¹³⁴ Some examples of soluble supported proline catalysts: (a) Gu, L.; Wu, Y.; Zhang, Y.; Zhao, G. *J. Mol. Catal. A: Chem.*, **2007**, *263*, 186. (b) Benaglia, M.; Cinquini, M.; Cozzi, F.; Pugliesi, A.; Celentano, G. *J. Mol. Catal. A: Chem.*, **2003**, *204–205*, 157. (c) Benaglia, M.; Cinquini, M.; Cozzi, F.; Pugliesi, A.; Celentano, G. *Adv. Synth. Catal.*, **2002**, *344*, 533.

¹³⁵ Some examples of insoluble supported organocatalysts: (a) Kristensen, T. E.; Vestli, K.; Fredriksen, A.; Hansen, F. K. *Org. Lett.*, **2009**, *11*, 2968. (b) Prasetyanto, E. A.; Lee, S. C.; Park, S. E. *Chem. Commun.*, **2008**, 1995. (c) Gruttadauria, M.; Giacalone, F.; Mossuto Marculescu, A.; Noto, R. *Tetrahedron Lett.*, **2007**, *48*, 255. (d) Font, D.; Jimeno, C.; Pericàs, M. A. *Org. Lett.*, **2006**, *8*, 4653. (e) Kondo, K.; Yamano, T.; Takemoto, K. *Makromol. Chem.*, **1985**, *16*, 1781.

Chapter 2. 1. Introduction

polymeric supports such as polyethyleneglycol,^{134b-c,136} (Figure 2.7, Benaglia 2001) allow the recovery of the catalyst by precipitation in diethyl ether and filtration. The proline-supported catalyst could be recovered for 3 cycles in aldol (up to 96 % ee) and Mannich reactions (up to 94 % ee), although a high catalyst loading was required (30 mol %) and decreasing activity and selectivity were observed (81 % to 64 % ee) in the consecutive cycles. Promising results were obtained by supporting proline or proline sulfonamides on soluble dendrimers,¹³⁷ which offered similar yields and ee in much less time, when compared with *free* proline (2 h supported vs. 16 h non-supported). Recycling was achieved in some cases by precipitation and filtration.

Polymeric insoluble supports offer simpler procedures as they can be directly filtered. Catalyst heterogenization has as main drawback some diffusion problems and usually slower reactions. Gruttadauria¹³⁸ has done intense research on polystyrene supported prolinamides (Figure 2.7, Gruttadauria 2008), which were prepared through the thiol-alkene *click reaction*. In 2008, this group described a supported prolinamide with bulky groups, which required low catalyst loading (10 mol %). It offered good enantioselectivities (up to 94 % ee) as well as good recycling performance (6 cycles) without significant loss of activity in aqueous or solvent-free aldol reactions.

Pericàs¹³⁹ has recently reported the preparation of supported proline in vinyl addition polynorbornene (VA-PNB) resin through copper-catalyzed azide alkyne cycloaddition (CuAAC) reaction, which offered excellent selectivity (97% ee) in aldol reaction. Moreover, the supported catalyst could be recycled and reused for at least 7 runs without any appreciable loss in activity or in selectivity (Figure 2.7, Pericàs 2015).

Hairy polymeric particles¹⁴⁰ and inorganic solids such as zeolites (ITQ-2 and ITQ-6)¹⁴¹, zirconium phosphates¹⁴² and gold nanoparticles¹⁴³ (Figure 2.7, Mozumdar 2013) have also been successfully applied as catalysts supports for proline derivatives. The

¹³⁶ Benaglia, M.; Celentano, G.; Cozzi, F. *Adv. Synth. Catal.*, **2001**, *343*, 171.

¹³⁷ (a) Wu, Y.; Zhang, Y.; Zhao, G.; Wang, S. *Org. Lett.*, **2006**, *8*, 4417. (b) Bellis, E.; Kokotos, G. *J. Mol. Catal. A.: Chem.*, **2005**, *241*, 166.

¹³⁸ (a) Gruttadauria, M.; Salvo, A. M. P.; Giacalone, F.; Agrigento, P.; Noto, R. *Eur. J. Org. Chem.* **2009**, 5437. (b) Gruttadauria, M.; Giacalone, F.; Marculescu, A. M.; Salvo, A. M. P.; Noto, R. *ARKIVOC* **2009**, *8*, 5. (c) Gruttadauria, M.; Giacalone, F.; Marculescu, A. M.; Noto, R. *Adv. Synth. Catal.* **2008**, *350*, 1397.

¹³⁹ Sagamanova, I.K.; Sayalero, S.; Martínez-Arranz, S.; Albéniz, A.C.; Pericàs, M.A. *Catal. Sci. Technol.* **2015**, *5*, 754.

¹⁴⁰ Li, X.; Chen, M.; Yang, B.; Zhang, S.; Jia, X.; Hu, Z. *RSC Adv.* **2014**, *4*, 43278.

¹⁴¹ Calderón, F.; Fernández, R.; Sánchez, F.; Fernández-Mayoralas, A. *Adv. Synth. Catal.*, **2005**, *347*, 1395.

¹⁴² (a) Wu, C.; Long, X.; Fu, X.; Wang, G.; Mirza, Z. A. *RSC Adv.* **2015**, *5*, 3168. (b) Calogero, S.; Lanari, D.; Orrù, M.; Piermatti, O.; Pizzo, F.; Vaccaro, L. *J. Catal* **2011**, *282*, 112.

¹⁴³ Kumar, A.; Dewan, M.; De, A.; Saxena, A.; Aerry, S.; Mozumdar, S. *RSC Adv.* **2013**, *3*, 603.

catalyst recovery by easy separation by filtration was possible. Furthermore immobilization of proline in magnetite (Fe_3O_4) nanoparticles¹⁴⁴ offers the possibility of recovering the catalyst with a magnet (Figure 2.7, Heydari 2014).

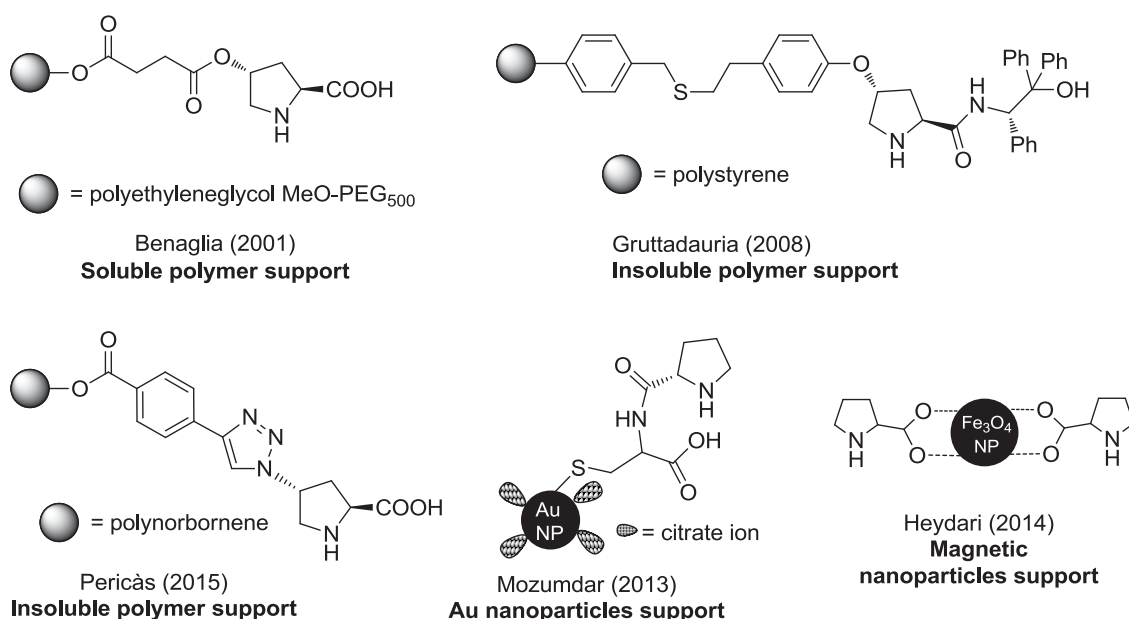


Figure 2.7. Some examples of supported proline-based organocatalysts.

Many efforts have been devoted by different groups to silica-immobilization of L-proline derivatives as recyclable organocatalysts for direct aldol reaction. In pioneering works, Fernández-Mayoralas¹⁴⁵ heterogenized proline on mesoporous support MCM-41 by grafting procedures (Figure 2.8, Fernández-Mayoralas 2005, 2007). Subsequent work by Wang's group led to the obtention of supported proline-based peptides¹⁴⁶ through post-synthesis functionalization of aminopropyl silica gel (Figure 2.8, Wang, 2009). Remarkably, a covalently proline-functionalized silica gel for continuous-flow aldol reaction has been described by Massi using a thiol-ene coupling.¹⁴⁷ Following a similar methodology, Massi and Cavazzini have recently prepared silica gel-immobilized proline mimetics, such as prolinamide, proline sulfonamide and pyrrolidiny

¹⁴⁴ (a) Azizi, K.; Heydari, A. *RSC Adv.* **2014**, *4*, 6508. (b) Gleeson, O.; Tekoriute, R.; Gun'ko, Y. K.; Connon, S. J. *Chem. Eur. J.*, **2009**, *15*, 5669.

¹⁴⁵ (a) Calderón, F.; Fernández, R.; Sánchez, F.; Fernández-Mayoralas, A. *Adv. Synth. Catal.*, **2005**, *347*, 1395. (b) Doyagüez, E. G.; Calderón, F.; Fernández-Mayoralas, A. *J. Org. Chem.*, **2007**, *72*, 9353.

¹⁴⁶ Yan, J.; Wang, L. *Chirality* **2009**, *21*, 413.

¹⁴⁷ Massi, A.; Cavazzini, A.; Zoppo, L. D.; Pandoli, O.; Costa, V.; Pasti, L.; Giovannini, P. P. *Tetrahedron Lett.*, **2011**, *52*, 619.

Chapter 2. 1. Introduction

tetrazole (Figure 2.8, Massi and Cavazzini, 2012)¹⁴⁸ with the aim to perform aldol reactions under continuous-flow conditions in packed-bed microreactors.

Recently, He¹⁴⁹ has also used the thiol-ene coupling approach to anchor a derivative of L-proline to mercaptopropyl-functionalized mesoporous silicas (Figure 2.8, He, 2014). The parent mesostructured silicas have been obtained under aqueous basic conditions in the presence of cetyltrimethylammonium bromide. By adjusting the molar ratios of 1,4-bis(triethoxysilyl)benzene, TEOS and (3-mercaptopropyl)trimethoxysilane, they achieved silica materials with alternating hydrophobic and hydrophilic blocks in the pore wall, with hydrophobic surface or with hydrophilic surface. These heterogeneous catalysts have been applied to the asymmetric aldol reaction and also to a more challenging Knoevenagel-Michael cascade reaction. *Trans*-4-hydroxy-L-proline has also been successfully grafted onto core-shell Fe₃O₄@SiO₂ magnetic microspheres¹⁵⁰ through a carbamate functionality (Figure 2.8, Ma, 2012).

Heterogenized silica-based organocatalysts for enantioselective aldol reaction have been prepared by Moreau and Wong Chi Man via the sol-gel process from two silylated derivatives of L-proline, featuring either a carbamate or an ether linker (example of carbamate in Figure 2.8, Wong Chi Man, 2009).¹⁵¹ Co-gelification of both monomers with variable amounts of TEOS was performed with and without dodecylamine as porogen, enabling the formation of materials with various organic loadings, pore sizes and surface areas.

In our research group, we have reported some organocatalytic materials for asymmetric aldol reaction based on prolinamide scaffolds developed by the group of Nájera.¹⁵² Thus, a non-porous bridged silsesquioxane was obtained from a bis-silylated aminoindane-derived prolinamide by sol-gel methodology in the absence of TEOS with a fluoride salt (TBAF) as catalyst. A similar procedure enabled the synthesis of the monosilylated aminoindane-derived prolinamide and permitted the preparation of different materials by sol-gel co-condensation of the organosilane with different amounts of TEOS (5 and 19 equivalents, respectively) under nucleophilic catalysis

¹⁴⁸ Bortolini, O.; Caciolli, L.; Cavazzini, A.; Costa, V.; Greco, R.; Massi, A.; Pasti, L. *Green Chem.*, **2012**, *14*, 992.

¹⁴⁹ An, Z.; Guo, Y.; Zhao, L.; Li, Z.; He, J. *ACS Catal.*, **2014**, *4*, 2566.

¹⁵⁰ Yang, H.; Li, S.; Wang, X.; Zhang, F.; Zhong, X.; Dong, Z.; Ma, J. *J. Mol. Catal. A: Chem.*, **2012**, *363–364*, 404.

¹⁵¹ Zamboulis, A.; Rahier, N. J.; Gehringer, M.; Cattoën, X.; Niel, G.; Bied, C.; Moreau, J. J. E.; Wong Chi Man, M. *Tetrahedron: Asymmetry*, **2009**, *20*, 2880.

¹⁵² (a) Monge-Marcet, A.; Cattoën, X.; Alonso, D. A.; Nájera, C.; Wong Chi Man, M.; Pleixats, R. *Green Chem.*, **2012**, *14*, 1601. (b) Monge-Marcet, A.; Pleixats, R.; Cattoën, X.; Wong Chi Man, M.; Alonso, D. A.; Almasi, D.; Nájera, C. *New J. Chem.*, **2011**, *35*, 2766.

(TBAF). Despite using the typical conditions for SBA-15 type materials in one of them, it was not possible to obtain such a structured porosity, most probably due to the bulky organic part of the precursor. Finally, the same monosilylated precursor was grafted onto SBA-15 type mesostructured silica. All these materials efficiently catalyzed the aldol reaction under green conditions (water, room temperature, absence of co-catalyst) (Figure 2.8, Pleixats, 2011, 2012).

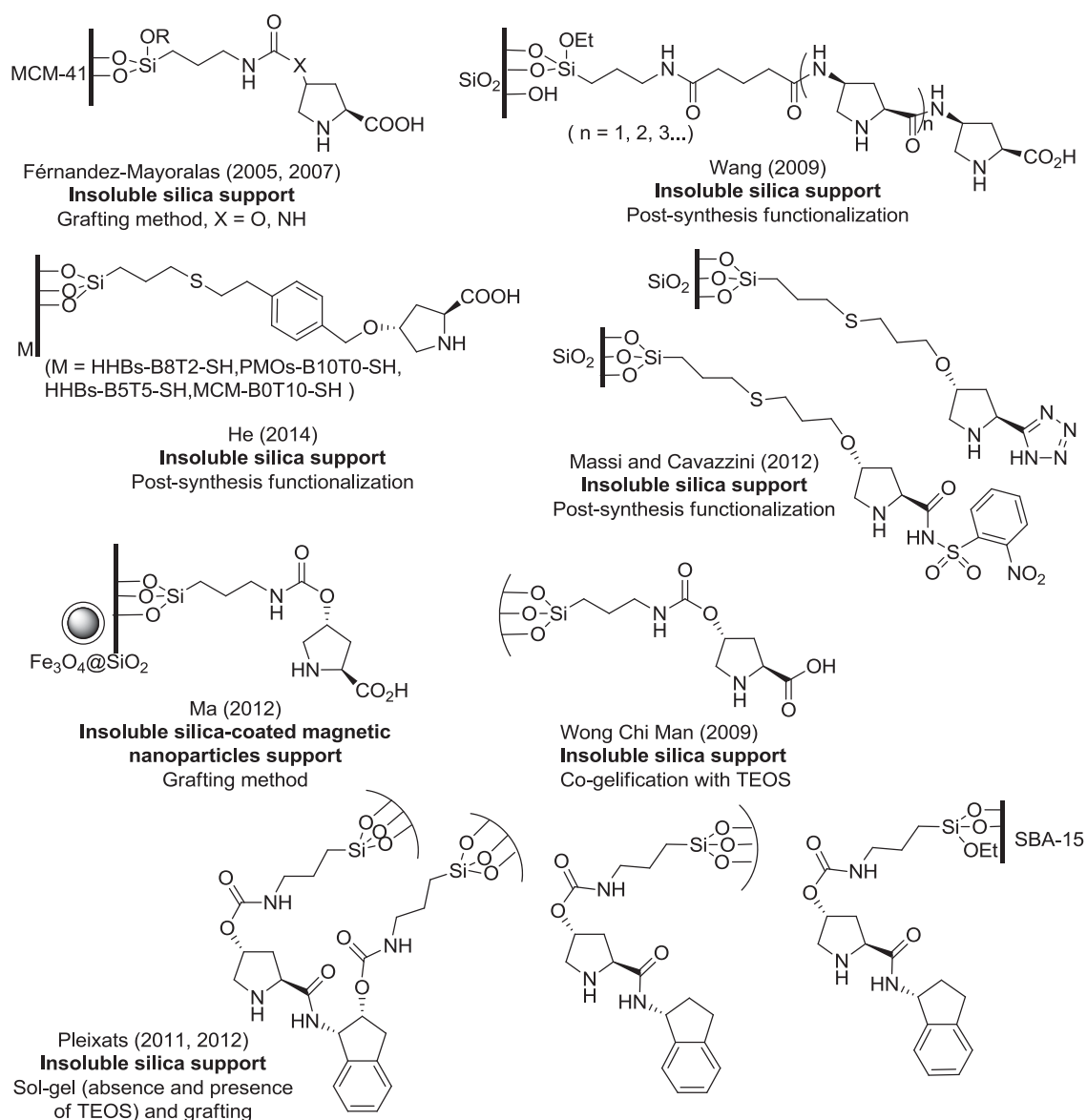


Figure 2.8. Some examples of silica-supported proline derivatives for organocatalysis.

On the other hand, supported organocatalysts with good recycling profiles can be obtained without a covalent linkage between the support and the organic catalyst. For instance, a layered clay material (montmorillonite) containing prolinium ions has also

Chapter 2. 1.Introduction

been prepared for enantioselective aldol reaction (Figure 2.9, Vaultier, 2009).¹⁵³ Similarly, Nakamura *et. al.*¹⁵⁴ reported a montmorillonite-entrapped sulfonylprolinamide as efficient organocatalyst in several organic transformations such as aldol reaction.

Non-covalently anchored proline-based materials were prepared by Gruttadauria's group by adsorption of L-proline onto the surface of imidazolium-modified silica gels bearing three different linkers (see Figure 2.9, Gruttadauria, 2007, for one example).¹⁵⁵ Later on, the same group prepared another organocatalyst following a similar methodology. In this case a *cis*-ion-tagged proline derivative with a robust amide linkage between the catalytic active site and the imidazolium tag was chosen for adsorption on multilayered covalently bonded supported ionic liquid phases (mlc-SILP).¹⁵⁶ In the same manner, a tripeptide (H-Pro-Pro-Asp-NH₂) has been adsorbed on the surface of modified silica gels functionalized with a monolayer of covalently attached imidazolium salts (Figure 2.9, Gruttadauria, 2007).¹⁵⁵

Recycling of organocatalysts is also possible under supercritical CO₂,¹⁵⁷ ionic liquids,¹⁵⁸ hydrogels,¹⁵⁹ sugars,¹⁶⁰ cyclodextrins,¹⁶¹ or fluorinated-derived catalysts used in biphasic systems.¹⁶²

¹⁵³ Srivastava, V.; Gaubert, K.; Pucheault, M.; Vaultier, M. *ChemCatChem*, **2009**, *1*, 94.

¹⁵⁴ Hara, N.; Nakamura, S.; Shibata, N.; Toru, T. *Adv. Synth. Catal.*, **2010**, *352*, 1621.

¹⁵⁵ Aprile, C.; Giacalone, F.; Gruttadauria, M.; Marculescu, A. M.; Noto, R.; Revell, J. D.; Wennemers, H. *Green Chem.*, **2007**, *9*, 1328.

¹⁵⁶ Montroni, E.; Lombardo, M.; Quintavalla, A.; Trombini, C.; Gruttadauria, M.; Giacalone, F. *ChemCatChem*, **2012**, *4*, 1000.

¹⁵⁷ Lee, S.-G.; Zhang, Y. J. Chapter 7. Enantioselective Catalysis in Ionic Liquids and Supercritical CO₂, in *Handbook of Asymmetric Heterogeneous Catalysis*, ed. Ding, D.; Uozumi, Y. WILEY-VCH: Weinheim, 2008.

¹⁵⁸ (a) Luo, S.; Mi, X.; Zhang, L.; Liu, S.; Xu, H.; Cheng, J.-P. *Tetrahedron*, **2007**, *63*, 1923. (b) Mečiarová, M.; Toma, Š.; Berkessel, A.; Koch, B. *Lett. Org. Chem.*, **2006**, *3*, 437. (c) Luo, S.; Mi, X.; Zhang, L.; Liu, S.; Xu, S.; Cheng, J.-P. *Angew. Chem., Int. Ed.*, **2006**, *45*, 3093.

¹⁵⁹ Rodríguez-Llansola, F.; Miravet, J. F.; Escuder, B. *Chem. Commun.*, **2009**, 7303.

¹⁶⁰ Ricci, A.; Bernardi, L.; Gioia, C.; Vierucci, S.; Robitzer, M.; Quignard, F. *Chem. Commun.*, **2010**, *46*, 6288.

¹⁶¹ Shen, Z.; Liu, Y.; Jiao, C.; Ma, J.; Li, M.; Zhang, Y. *Chirality*, **2005**, *17*, 556.

¹⁶² Fache, F.; Piva, O. *Tetrahedron: Asymmetry*, **2003**, *14*, 139.

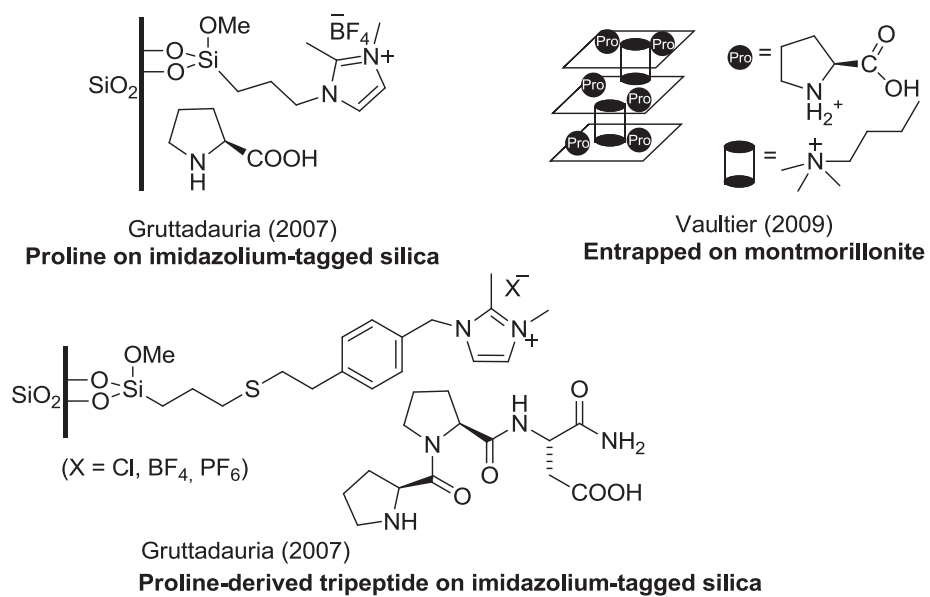
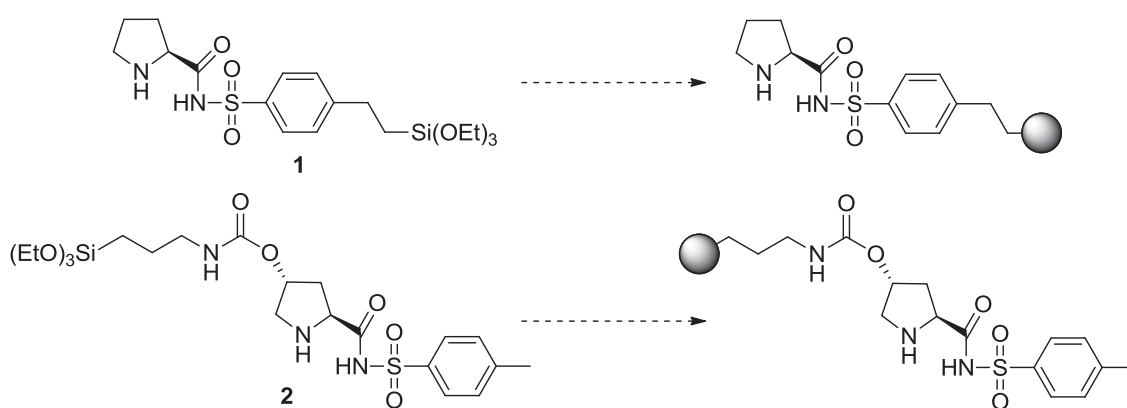


Figure 2.9. Some examples of recyclable proline-based organocatalysts without covalent linkage to the support.

2. OBJECTIVES

Following our interest on recyclable chiral supported organocatalysts derived from proline mimics we aimed at:

a) The preparation of hybrid silica materials from proline sulfonamide precursors. For this purpose, the synthesis of two different monosilylated monomers was planned (Scheme 2.8). Firstly, monosilylated precursor **1** was designed to afford an organosilica by co-condensation with TEOS. However, after preliminary catalytic tests with this material, a second and different precursor **2** was envisaged to enable the formation of several organosilicas by co-condensation with TEOS and by grafting method.



Scheme 2.8. Silylated proline sulfonamides and their corresponding derived organosilicas.

b) The preparation of organosilicas derived from the monosilylated proline tetrazole **3** by sol-gel procedures. This monomer would be obtained by using the CuAAC methodology to introduce the triethoxysilyl moiety (Scheme 2.9).



Scheme 2.9. Silylated proline tetrazole and its corresponding derived organosilica.

c) The assay of all these new hybrid silica materials as recyclable chiral organocatalysts in asymmetric reactions such as inter- and intramolecular direct aldol reactions and other commonly described reactions for each proline derivative.

3. RESULTS AND DISCUSSION

3.1. Preparation and catalytic applications of hybrid silica materials **M1** and **M2** derived from a silylated proline sulfonamide

As proposed by several authors,¹⁶³ proline sulfonamides offer excellent stereoselectivities in reactions based on enamine activation pathway due to the unusual strength of hydrogen bonds formed between the enamine derived from sulfonamide and the electrophile. For this reason, we decided to prepare a supported proline sulfonamide organocatalyst to compare its activity and selectivity with the homogeneous analogues described in the literature, and to test its recyclability.

3.1.1 Preparation of hybrid silica material **M1**

One of the earliest publications about proline sulfonamides organocatalysts, proposed the use of the arylsulfonamide moiety as a linker for the immobilization on a solid support.^{163a} Furthermore, Yang and Carter functionalized this sulfonamide group with a long aliphatic chain to improve the solubility of the catalyst.¹⁰⁴ This prompted us to synthesize a hybrid silica material derived from a monosilylated precursor which would present the silylated moiety attached to the aryl group of the sulfonamide. Thus, organosilica **M1** might be obtained from the silylated proline sulfonamide **1** (Scheme 2.10) by co-gelification with TEOS through the sol-gel process.

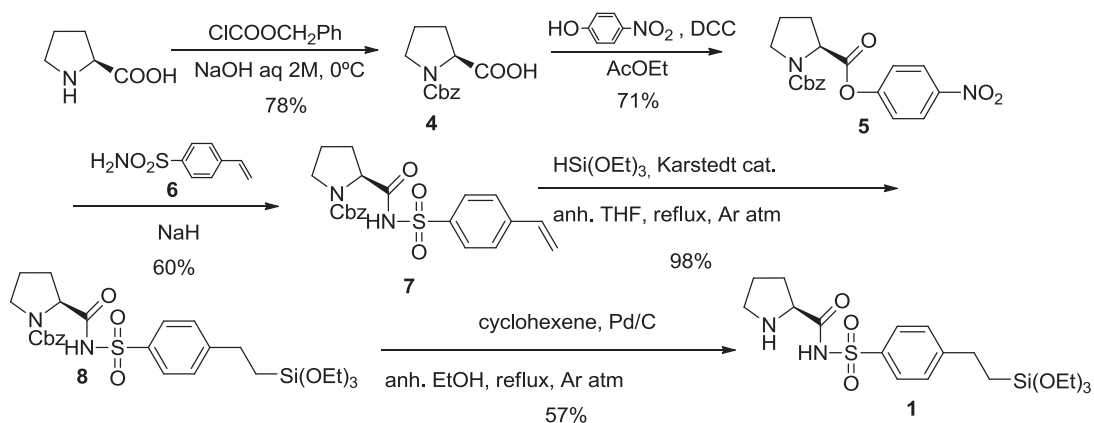


Scheme 2.10. Preparation of organosilica **M1** from its silylated precursor **1**.

The synthesis of the precursor **1** was envisaged and performed as depicted in Scheme 2.11. Commercial L-proline was protected with a Cbz group affording proline derivative **4**. Its subsequent coupling with *p*-nitrophenol in the presence of DCC yielded 4-nitrophenyl ester **5**, which reacted with the sodium salt of *p*-vinylphenylsulfonamide **6** to afford vinyl proline sulfonamide **7**. The hydrosilylation of **7** with $\text{HSi}(\text{OEt})_3$ in the presence of Pt Karstedt catalyst allowed the introduction of the triethoxysilyl group. Corresponding deprotection of N-Cbz group of derivative **8** yielded the monosilylated precursor **1**.

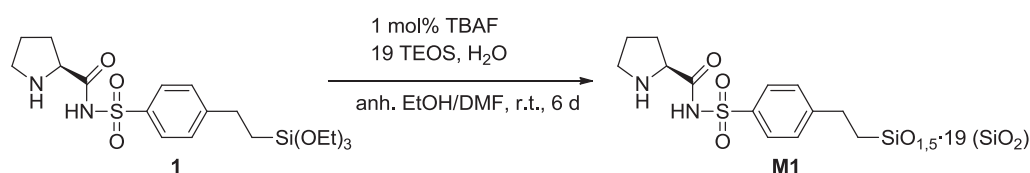
¹⁶³ (a) Berkessel, A.; Koch, B.; Lex, J. *Adv. Synth. Catal.* **2004**, *346*, 1141. (b) Yang, H.; Mahapatra, S.; Cheon, P.H.-Y.; Carter, R.G. *J. Org. Chem.* **2010**, *75*, 7579.

Chapter 2. 3. Results and Discussion



Scheme 2.11. Synthesis of the silylated precursor **1**.

Then, organosilica **M1** was prepared by sol-gel co-condensation of **1** with TEOS (molar ratio 1:19) under nucleophilic conditions using TBAF as catalyst (1 mol% with respect to Si), an stoichiometric amount of water (with respect to the ethoxy groups) and a mixture of anhydrous EtOH/DMF as solvent (Scheme 2.12).



Scheme 2.12. Preparation of hybrid silica material **M1**.

The solution gelled after 5 min and a yellow compact gel was obtained (Figure 2.10). After 5 days of ageing at room temperature, the gel was pulverized, washed successively with water, EtOH and acetone and finally dried overnight under vacuum at 50°C to yield **M1** as a white powder. Finally, **M1** was washed with CHCl₃ in a Soxhlet apparatus for 48 h in order to remove the residual DMF entrapped in the material.



Figure 2.10. Image obtained for the gel corresponding to **M1**.

Organosilica **M1** was characterized by elemental analysis, ²⁹Si-SSNMR and N₂-sorption measurements. This last technique revealed the mesoporous nature of the

material, presenting a *type IV* isotherm (Figure 2.11, left), showing a hysteresis loop and a sharp distribution of pores; the pore diameter distribution (Figure 2.11, right) was centered mainly around 35 Å with a total pore volume of 0.43 cm³/g and a BET surface area of 450 m²/g.

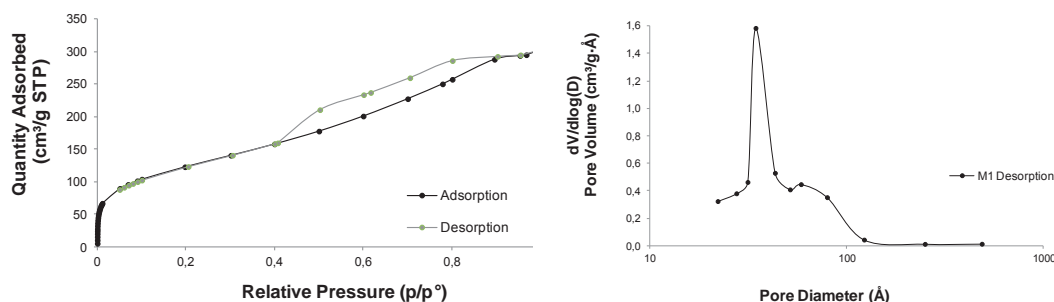


Figure 2.11. N₂-sorption isotherm (left) and pore size distribution (right) of **M1**.

The hybrid silica **M1** was found to contain 0.89 mmol of proline sulfonamide/g of material according to the nitrogen elemental analysis. The solid state ²⁹Si NMR spectrum (Figure 2.12) confirmed the covalent bonding of the organic moiety to the silica matrix by the presence of chemical shifts corresponding to T² and T³ signals at -62.64 and -72.07 ppm, respectively, in addition to the characteristic Q², Q³, Q⁴ signals corresponding to the condensed TEOS at -96.50, -105.22 and -113.45 ppm. The high dilution of the organic moiety in the inorganic matrix precluded the observation of the corresponding signals in the solid state ¹³C NMR. In contrast, the recorded IR spectra showed the typical adsorption at 1654 cm⁻¹ due to the carbonyl group of the proline sulfonamide.

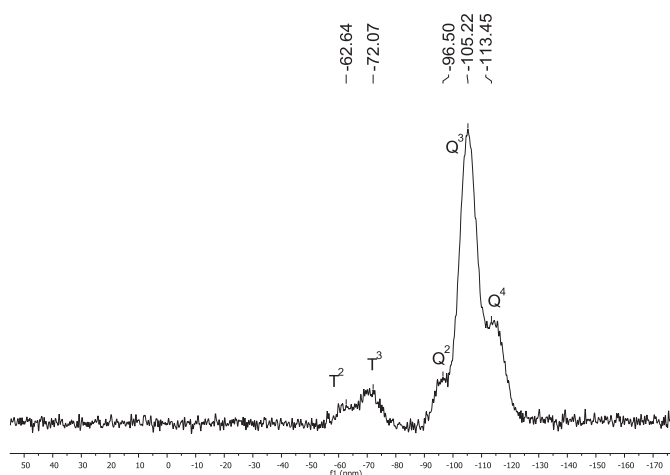
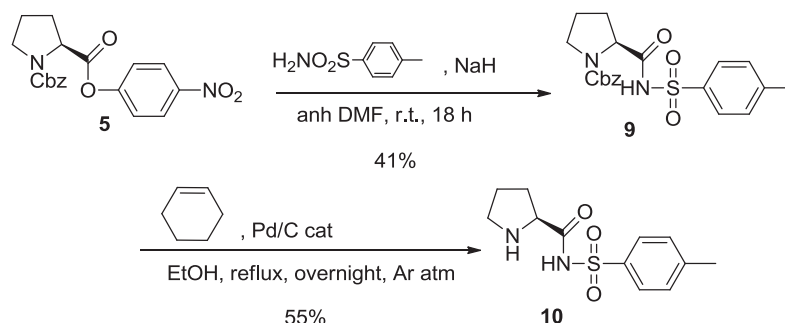


Figure 2.12. ²⁹Si SS NMR of material **M1**.

Chapter 2. 3. Results and Discussion

For comparative purposes, we prepared an homogeneous organocatalyst analogue, whose preparation is summarized in Scheme 2.13. Compound **9** was synthesized by reaction of **5** with the sodium salt of *p*-toluenesulfonamide, similarly to **7**, and after a deprotection step, the desired proline sulfonamide **10** was achieved.

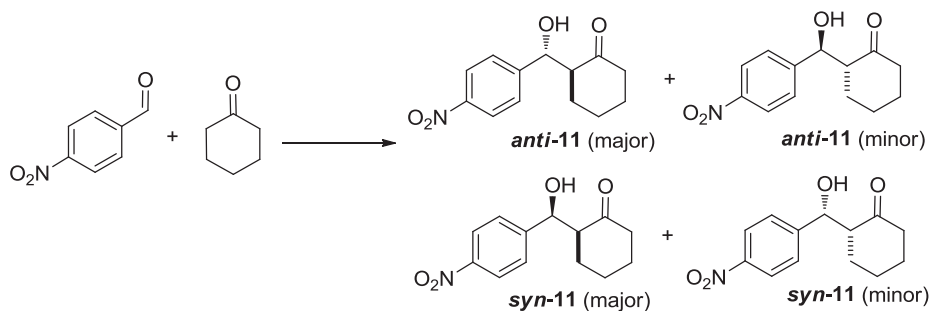


Scheme 2.13. Synthesis of homogeneous organocatalyst **8**.

3.1.2 Assay of **M1** in asymmetric organocatalysis

3.1.2.1 Catalytic tests of **M1** in the direct aldol reaction

The activity of the new supported organocatalyst **M1** was then evaluated in a typically used benchmark reaction, which is the direct asymmetric aldol reaction between *p*-nitrobenzaldehyde and cyclohexanone to afford the corresponding aldol products **11** (Scheme 2.14).



Scheme 2.14. Model reaction for direct asymmetric aldolisation.

Catalytic tests were performed using water as solvent, different catalyst loadings and at room temperature (Table 2.1). Additionally, the homogeneous analogue **10** was also tested in the same reaction and conditions in order to compare the results.

Processes using water as a reaction medium have attracted a great deal of attention because water is safe, inexpensive, environmental friendly and in some cases

endows unique properties to the reaction.¹⁶⁴ The use of water as a reaction medium needs further discussion,¹⁶⁵ since we can distinguish between reactions performed *on water*, *in water* and *in the presence of water*. Reaction *on water*^{165c} stands for a reaction on the surface of water, this happens when an emulsion is formed. It is generally said that reactions *in water*^{165c} imply the solution of reactants in this solvent. In contrast, processes carried out *in the presence of water*^{165c} are known as those occurring in a concentrated organic phase with water acting as a secondary phase. *On water* conditions often result in an acceleration of the reaction rate, whereas *in the presence of water* an increase in enantioselectivity may be observed.

Recently, Barbas and Hayashi independently reported that high enantioselectivities could be obtained in proline-catalyzed aldol reaction in the presence of large excess of water.¹⁶⁶ Later studies showed that a chiral catalyst in an emulsion formed from water and cyclohexanone significantly enhanced the reactivity and stereoselectivity of the direct asymmetric aldol reaction.^{164a}

In our case, the whole process takes place in heterogeneous fashion, probably at the interface between the hybrid silica material and the aqueous phase. Indeed, the initial mixture of substrates (cyclohexanone and *p*-nitrobenzaldehyde) was not soluble in water and formed a pale yellow heterogeneous suspension together with the insoluble material **M1**. At the end of the reaction a white homogeneous milky suspension containing **M1** was observed.

Following a very simple procedure consisting in the filtration and evaporation of the volatiles, compounds **11** were isolated in excellent yields as a diastereomeric mixture. It is noteworthy to point out that **M1** proceeds without the use of any co-catalyst.

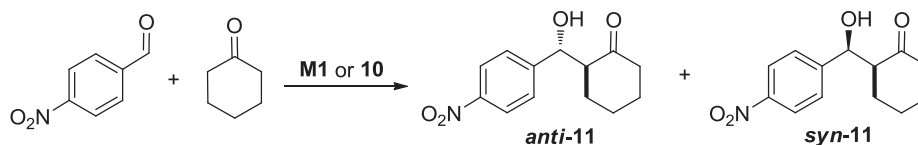
¹⁶⁴ a) Gao, J.; Liu, J.; Bai, S.; Wang, P.; Zhong, H.; Yang, Q.; Li, C. *J. Mater. Chem.*, **2009**, *19*, 8580. b) Nakadai, M.; Saito, S.; Yamamoto, H. *Tetrahedron*, **2002**, *58*, 8167.

¹⁶⁵ For a discussion on this topic see: a) Brogan, A. P.; Dickerson, T. J.; Janda, K. D. *Angew. Chem. Int. Ed.*, **2006**, *45*, 8100. b) Hayashi, Y. *Angew. Chem. Int. Ed.*, **2006**, *45*, 8103. c) Narayan, S.; Muldoon, J.; Finn, M. G.; Fokin, V. V.; Kolb, C.; Sharpless, K. B. *Angew. Chem. Int. Ed.*, **2005**, *44*, 3275.

¹⁶⁶ a) Mase, N.; Y. Nakai; Ohara, N.; Yoda, H.; Takabe, F.; Tanaka, F.; Barbas III, C.F. *J. Am. Chem. Soc.* **2006**, *128*, 734. b) Hayashi, Y.; Sumiya, T.; Takahashi, J.; Gotoh, H.; Urushima, T.; Shoji, M. *Angew. Chem. Int. Ed.* **2006**, *45*, 958.

Chapter 2. 3. Results and Discussion

Table 2.1. Catalytic performance^[a] of **M1** in the direct asymmetric aldol reaction of cyclohexanone with *p*-nitrobenzaldehyde.



Entry	Catalyst (mol%)	t (h)	Conv. (%) ^[b]	dr _(anti/syn) ^[b]	er _{anti} ^[c]	er _{syn} ^[c]
1	M1 (10) ^[d]	96	76 ^[g]	88/12	73/27	66/34
2	M1 (10) ^[e]	96	29 ^[h]	86/14	56/44	77/23
3	M1 (20) ^[d]	48	100	85/15	96/4	63/37
4	M1 (20) ^[e]	48	90	88/12	82/18	62/38
5	10 (20)	20	93	97/3	97/3	63/37
6	10 (10)	96	99	96/4	98/2	57/43

^[a] Reaction conditions: aldehyde (1 equiv.), cyclohexanone (5 equiv.), water (0.5 mL/mmol aldehyde) and the indicated amount of the corresponding catalyst at room temperature.

^[b] Determined by ¹H-NMR spectroscopy.

^[c] Determined by chiral Daicel Chiralpak AD-H column.

^[d] Fresh

^[e] 2nd run

^[g] 17% of this conv. corresponded to the undesired side product **12**, determined by ¹H-NMR spectroscopy.

^[h] 35% of this conv. corresponded to the undesired side product **12**, determined by ¹H-NMR spectroscopy.

Good diastereoselectivity was achieved with organosilica **M1** at 10% mol of catalyst loading, however the conversion and enantioselectivity obtained was lower than those obtained with its homogeneous analogue **10** (compare entries 1 and 6, Table 2.1). In addition, formation of a by-product with **M1** was observed, which deserves especial attention. The crotonization product (Figure 2.13) coming from a dehydration process is the most usual by-product of the direct aldol reaction between cyclohexanone and *p*-nitrobenzaldehyde. This product should present a characteristic signal for the olefinic proton at 7.47 ppm in the ¹H-NMR spectrum. This undesired side reaction often occurs during chromatography on silica gel of diastereomeric aldol mixtures. It is worth noting that we never performed such purification for **11** in our experimental procedure; this is actually one of the main advantages of our catalytic protocol. Besides, the undesired signals observed in our ¹H-NMR spectrum (Figure 2.14) did not match those reported for the crotonization product.¹⁶⁷ Other previous experience in the group¹⁶⁸ allowed us to identify the by-product obtained with **M1** as the

¹⁶⁷ Das, U.; Das, S.; Bandy, B.; Balzarini, J.; De Clercq, E.; Dimmock, J.R. *Bioorg. Med. Chem.*, **2008**, *16*, 6261.

¹⁶⁸ Monge, A. PhD Dissertation. Universitat Autònoma de Barcelona, 2011.

hemiacetal **12** (Figure 2.13). Such compound was detected by Giacomini¹⁶⁹ as a side product in the aldol reaction. The signals present in the ¹H-NMR spectrum of our reaction crude were consistent with those reported by Giacomini.

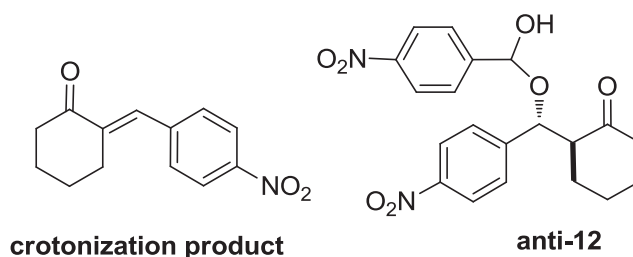


Figure 2.13. Undesired crotonization and hemiacetal (**12**) side products.

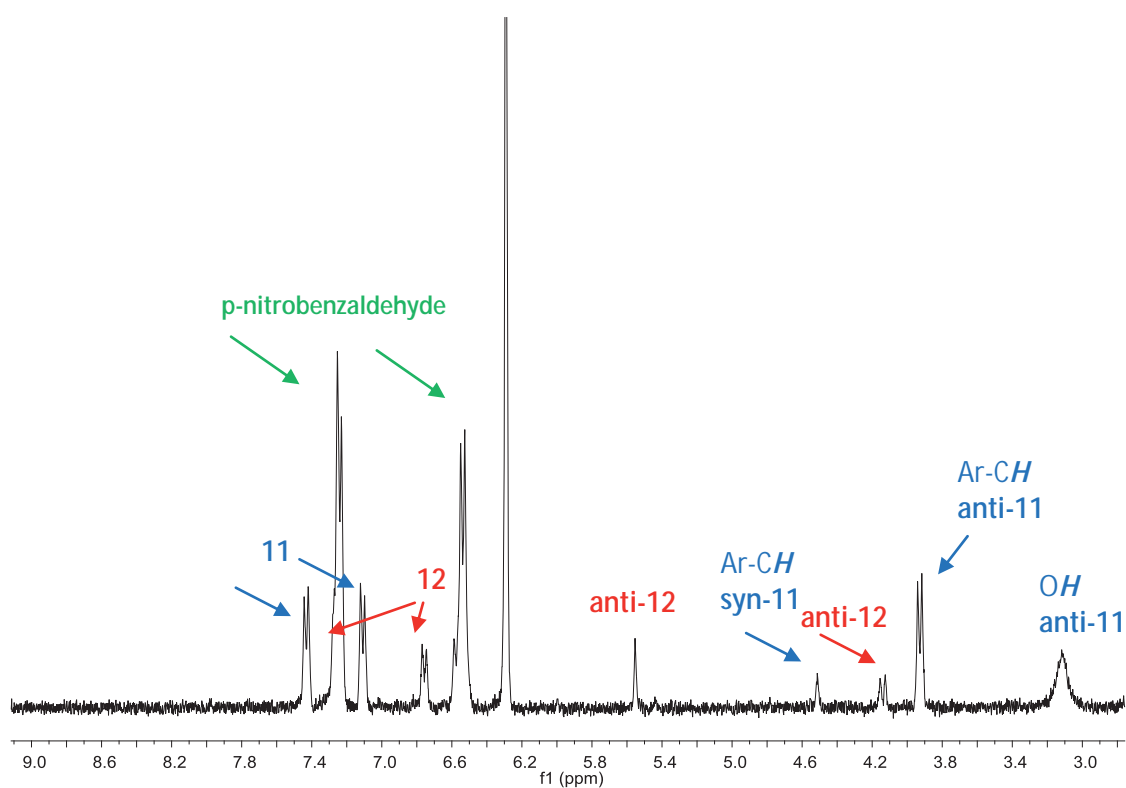


Figure 2.14. Zoom of the 3-9 ppm region of a ¹H-NMR spectrum.

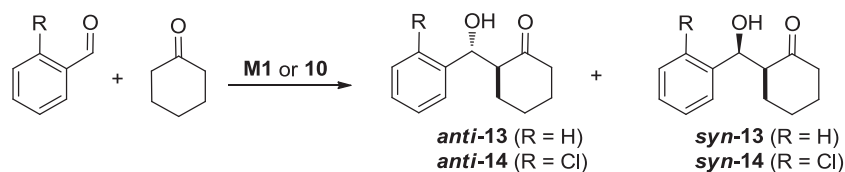
Material **M1** was then recovered and reused for a next cycle (Table 2.1, entry 2). The conversion decreased for the same reaction time in the second run and the formation of the same by-product **12** increased. Taking into account that in many publications the use of homogeneous proline sulfonamide can reach up to 30 mol%, we repeated the experiment by using a higher catalyst loading (20 mol%) (Table 2.1, entry 3). In this case, conversion was higher at lower reaction time and no formation of

¹⁶⁹ Emer, E.; Galletti, P.; Giacomini, D. *Eur. J. Org. Chem.*; **2009**, 3155.

side products was detected. Then the supported organocatalyst **M1** was recycled affording a slightly lower conversion and lower enantioselectivity (Table 2.1, entry 4). Homogeneous catalyst **10** gave better activity and selectivity than supported **M1** (higher reaction rate, diastereomeric and enantiomeric ratios) (Table 2.1, entries 5 and 6).

Even though these initial assays were not as encouraging as we expected, we applied our experimental protocol to other aromatic aldehydes as acceptors (Table 2.2) and to cyclopentanone as nucleophile (Table 2.3). Moreover, an intramolecular aldol reaction was also tested (Table 2.4). In all these cases the reactions afforded the desired aldol product and **M1** could be recycled.

Table 2.2 Catalytic performance^[a] of **M1** in the direct asymmetric aldol reaction of cyclohexanone with other aromatic aldehydes.



Entry	Catalyst (mol%)	Cycle	R	t (h)	Conv. (%) ^[b]	dr _(anti/syn) ^[b]	er _{anti} ^[c]
1	M1 (10)	1	H	96	100	82/18	78/22
2	M1 (10)	2	H	96	77	79/21	90/10
3	M1 (20)	1	H	96	85	87/13	81/19
4	M1 (20)	2	H	96	90	86/14	83/17
5	10 (20)	-	H	48	80	98/2	88/12
6	M1 (10)	1	Cl	96	42	90/10	75/25
7	M1 (10)	2	Cl	96	14	86/14	63/37
8	M1 (20)	1	Cl	96	92	91/9	77/23
9	M1 (20)	2	Cl	96	82	92/8	69/31
10	10 (20)	-	Cl	48	99	97/3	99/1

^[a] Reaction conditions: aldehyde (1 equiv.), cyclohexanone (5 equiv.), water (0.5 mL/mmol aldehyde) and the indicated amount of the corresponding catalyst (**M1** or **10**) at room temperature.

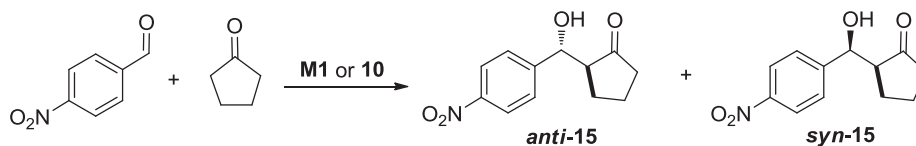
^[b] Determined by ¹H-NMR spectroscopy.

^[c] Determined by chiral Daicel Chiralcel OD column for **13** and Daicel Chiralpak AD-H column for **14**.

In the reaction of cyclohexanone with benzaldehyde and 2-chlorobenzaldehyde as acceptors, a clear asymmetric induction was observed, and similar diastereo- and enantioselectivities as in the previous case were achieved. Once more, the homogeneous catalyst **10** afforded faster reactions and better diastereo- and enantioselectivity than the supported organocatalyst **M1**.

Cyclopentanone was also tested as nucleophile in the aldol reaction with *p*-nitrobenzaldehyde (Table 2.3).

Table 2.3. Catalytic performance^[a] of **M1** in the direct asymmetric aldol reaction of cyclopentanone with *p*-nitrobenzaldehyde.



Entry	Catalyst (mol%)	Cycle	t (h)	Conv. (%) ^[b]	<i>dr</i> _(anti/syn) ^[b]	<i>er</i> _{anti} ^[c]	<i>er</i> _{syn} ^[c]
1	M1 (10)	1	48	96	56/44	71/29	54/46
2	M1 (10)	2	48	98	57/43	70/30	52/48
3	M1 (20)	1	24	96	46/54	65/35	nd
4	M1 (20)	2	24	98	40/60	59/41	nd
5	10 (20)	-	24	>99%	83/17	98/2	67/33

^[a] Reaction conditions: aldehyde (1 equiv.), cyclopentanone (5 equiv.), water (0.5 mL/mmol aldehyde) and the indicated amount of the corresponding catalyst (**M1** or **10**) at room temperature.

^[b] Determined by ¹H-NMR spectroscopy.

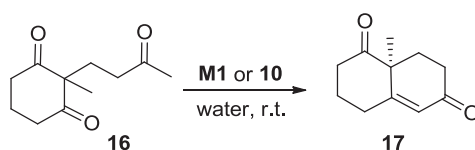
^[c] Determined by chiral Daicel Chiralpak AD-H column.

The decrease in the ring size of the ketone implied a clear reduction of the diastereoselectivity.¹⁷⁰ Depending on the amount of catalyst loading, the formation of a different diastereomer was slightly favoured (compare entries 1 and 3 in Table 2.3). The immobilization involves again a notable loss of stereoselectivity (compare *dr* and *er* values of entries 3 and 5 of Table 2.3).

The catalytic performance of organosilica **M1** was then evaluated in an intramolecular reaction, namely the Robinson annulation of triketone **16** to obtain the corresponding Wieland-Miescher ketone **17** (Table 2.4).

The experiments were performed in water, at room temperature and in presence of *p*-nitrobenzoic acid as a co-catalyst. The reaction did almost not occur in the absence of acid co-catalyst (compare entries 1 and 2 in Table 2.4). The crude mixtures obtained after filtration needed, in this case, to be purified by column chromatography on silica gel to reach pure **17**. Owing to the low reaction rate, the use of higher catalyst loading was highly desirable (compare 20 mol% of **M1** in entry 3 with 10 mol% in entry 1 of Table 2.4). As in all the previous tests, homogeneous catalyst **10** presented higher activity and selectivity than the heterogeneous **M1**.

¹⁷⁰ a) Almași, D.; Alonso, D.A.; Nájera, C. *Adv. Synth. Catal.* **2008**, 350, 2467. b) Almași, D.; Alonso, D.; Balaguer, A.-N.; Nájera, C. *Adv. Synth. Catal.* **2009**, 351, 1123.

Table 2.4. Catalytic performance^[a] of **M1** in the Robinson annulation.

Entry	Catalyst (mol%)	co-catalyst	Cycle	t (h)	Yield (%) ^[b]	er ^[c]
1	M1 (10)	<i>p</i> -NO ₂ C ₆ H ₄ CO ₂ H	1	144	47	55/45
2	M1 (10)	-	1	288	8	-
3	M1 (20)	<i>p</i> -NO ₂ C ₆ H ₄ CO ₂ H	1	168	76	68/32
4	10 (20)	<i>p</i> -NO ₂ C ₆ H ₄ CO ₂ H	-	96	89	86/14

^[a] Reaction conditions unless otherwise stated: triketone **16** (1 equiv.), water (0.5 mL/mmol triketone) and the indicated amount of the corresponding catalyst (**M1** or **10**) and *p*-nitrobenzoic acid as co-catalyst (20% mol).

^[b] Isolated yield by column chromatography.

^[c] Determined by chiral Daicel Chiralpak IC column.

3.1.2.2 Catalytic tests of **M1** in the aza-Diels Alder reaction

The hybrid silica material **M1** was also evaluated in the aza-Diels Alder reaction between 2-cyclohexenone and imine **18** (Scheme 2.15). Carter had reported the efficiency and selectivity of proline sulfonamides towards this type of reactions which also present an enamine catalytic pathway.¹⁷¹



Scheme 2.15. Aza-Diels Alder reaction of cyclohex-2-en-1-one and imine **18** for the formation of azabicyclo[2.2.2]octane **19**

For comparative purposes, we applied the same conditions described by Carter: 30 mol% of catalyst, in the absence of solvent, at room temperature and using 10 equivalents of commercially available 2-cyclohexen-1-one and freshly prepared imine **18**¹⁷² (Table 2.5).

¹⁷¹ Yang, H.; Carter, R.G. *J. Org. Chem.* **2009**, *74*, 5151-5156.

¹⁷² Anderson, J.C.; Howell, G. P.; Lawrence, R. M.; Wilson, C. S. *J. Org. Chem.* **2005**, *70*, 5665-5670.

Table 2.5. Catalytic performance^[a] of **M1** in the aza-Diels Alder reaction.

Entry	Catalyst (mol%)	Cycle	t (h)	Yield. (%) ^[b]	<i>dr</i> _{exo/endo} ^[d]
1	10 (30)	-	144	51	100/0 ^[e]
2	M1 (30)	1	240	24	46/54
3	M1 (30)	2	264	25 ^[c]	42/58

^[a] Reaction conditions: 2-cyclohexen-1-one (120 μ L, 10 equiv.), imine (1 equiv.) and the indicated amount of the corresponding catalyst were stirred together at room temperature.

^[b] Isolated yield.

^[c] Conversion. Determined by ¹H-NMR.

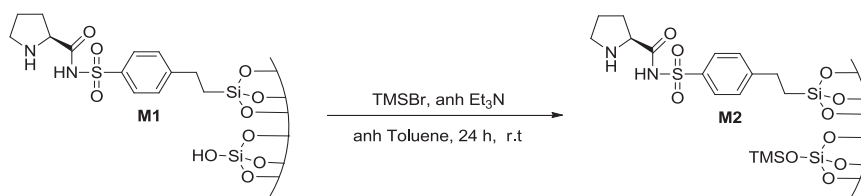
^[d] Determined by ¹H-NMR.

^[e] er: 99/1 (Determined by chiral Daicel Chiralcel OD column).

The reaction performed with the homogeneous catalyst **10** afforded 51% of isolated yield and complete diastereoselectivity for the *exo* diastereomer **19** (the er for this *exo* isomer was 99:1). However, the reaction performed with the supported catalyst **M1** led to the formation of a mixture of *endo* and *exo* diastereomers which were very difficult to separate (the *dr* was determined by ¹H NMR). The low yield and diastereoselectivity did not prompted us to perform more than one recycling experiment and we did not determine the enantioselectivity of the process.

3.1.3 Preparation of organosilica **M2**

Taking into account the possible deleterious effect of the acidic neighboring silanol groups in the selectivity of the asymmetric reactions with **M1**, we decided to perform the capping of these groups in order to improve the diastereo- and enantioselectivities. Organosilica **M2** was prepared by reaction of hybrid silica material **M1** with trimethylsilyl bromide in the presence of anhydrous triethylamine in toluene for 24 hours, following a methodology described by Copéret¹⁷³ (Scheme 2.16). Then, the solid was washed successively with toluene, methanol, diethyl ether and acetone, and finally dried overnight under vacuum at 50°C to yield **M2** as a white powder.

**Scheme 2.16.** Preparation of organosilica **M2**.

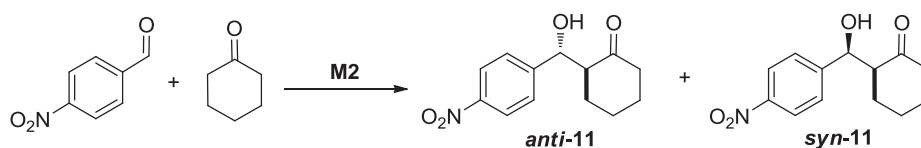
Organosilica **M2** was analyzed (elemental analysis) to determine the organocatalyst loading in the material (0.34 mmol proline sulfonamide / g material).

¹⁷³ Copéret, C.; Corriu, R. J.P. ; *et al. Chem. Eur. J* **2009**, *15*, 11820-11823.

3.1.4 Assay of **M2** in asymmetric organocatalysis3.1.4.1 Catalytic tests of **M2** in the direct aldol reaction

As we did with **M1**, the activity of the new organosilica **M2** was first evaluated in the direct asymmetric aldol reaction between cyclohexanone and *p*-nitrobenzaldehyde to give the aldol **11** (Table 2.6). Catalytic tests were conducted in water at room temperature using 5 equivalents of ketone with respect to the aldehyde.

Table 2.6. Catalytic performance^[a] of **M2** in the direct asymmetric aldol reaction of cyclohexanone with *p*-nitrobenzaldehyde.



Entry	Catalyst (mol%)	Cycle	t (h)	Conv. (%) ^[b]	<i>dr</i> (<i>anti/syn</i>) ^[b]	<i>er</i> _{<i>anti</i>} ^[c]	<i>er</i> _{<i>syn</i>} ^[c]
1	10	1	96	>99	91/9	75/25	71/29
2	10	2	96	>99	89/11	85/15	70/30
3	10	3	144	>99	88/12	77/23	54/45
4	10	4	168	>99	90/10	79/21	63/37
5	10	5	216	97	88/12	65/35	73/27
6	20	1	96	>99	92/8	85/15	66/34
7	20	2	96	>99	90/10	87/13	54/56

^[a] Reaction conditions unless otherwise stated: aldehyde (1 equiv.), cyclohexanone (5 equiv.), water (0.5 mL/mmol aldehyde) and the indicated amount of catalyst **M2** at room temperature.

^[b] Determined by ¹H-NMR spectroscopy.

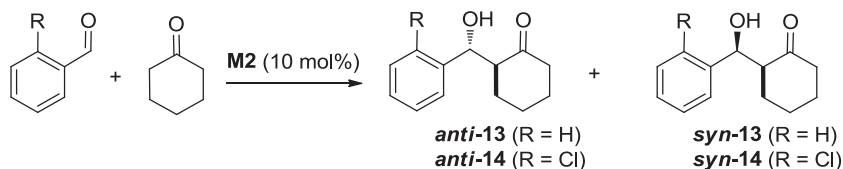
^[c] Determined by chiral Daicel Chiralpak AD-H column.

Contrary to the case of **M1**, supported catalyst **M2** could perform the reaction at 10 mol% loading avoiding the formation of the acetal by-product. This is consistent with the loss of the acidic character of the matrix, required for the acetalization process leading to **anti-12**. Furthermore, catalyst **M2** could be recycled up to 5 cycles without significant loss of selectivity, requiring increasing reaction times for complete conversion upon recycling. Similar to **M1**, the formation of the *anti* diastereomer was favoured. The increase of the catalyst loading (20 mol%, Table 2.6, Entries 6, 7) did not affect the diastereoselectivity but slightly enhanced the enantioselectivity.

After having obtained improved results with the new hybrid silica material **M2** in the mentioned benchmark reaction, we decided to test it in the other aldol reactions assayed with **M1**. Thus, **M2** was used as supported catalyst to perform the aldol

reaction between cyclohexanone and other aromatic aldehydes (benzaldehyde and 2-chlorobenzaldehyde) (Table 2.7).

Table 2.7. Catalytic performance^[a] of **M2** in the direct asymmetric aldol reaction of cyclohexanone with other aromatic aldehydes.



Entry	Cycle	R	t (h)	Conv. (%) ^[b]	dr _(anti/syn) ^[b]	er _{anti} ^[c]
1	1	H	144	>99	74/26	76/24
2	2	H	144	>99	65/35	74/26
3	3	H	144	73	54/46	51/49
4	1	Cl	168	96	87/13	76/24

^[a] Reaction conditions: aldehyde (1 equiv.), cyclohexanone (5 equiv.), water (0.5 mL/mmol aldehyde) and 10 mol% of catalyst **M2** at room temperature.

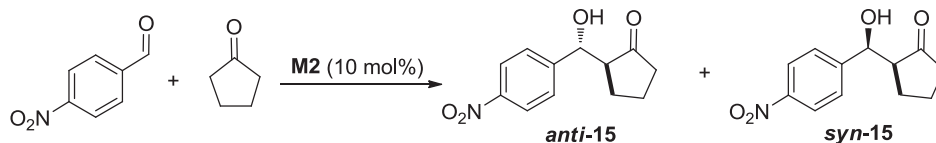
^[b] Determined by ¹H-NMR spectroscopy.

^[c] Determined by chiral Daicel Chiralcel OD column for **13** and Daicel Chiralpak AD-H column for **14**.

Although, unfortunately, the capping of silanols did not enhance the selectivity in the aldol reaction with these aldehydes, **M2** could be reused up to 3 cycles in the case of benzaldehyde. The long reaction times discouraged us to perform recycling experiments for **M2** using 2-chlorobenzaldehyde.

However, in the case of the aldol reaction of cyclopentanone with *p*-nitrobenzaldehyde (Table 2.8), the diastereoselectivity increased significantly with respect to **M1**, at only 10 mol% of catalyst loading, and **M2** clearly favoured the formation of the *anti* isomer.

Table 2.8. Catalytic performance^[a] of **M2** in the direct asymmetric aldol reaction of cyclopentanone with *p*-nitrobenzaldehyde.



Entry	Cycle	t (h)	Conv. (%) ^[b]	<i>dr</i> _(anti/syn) ^[b]	<i>er</i> _{anti} ^[c]	<i>er</i> _{syn} ^[c]
1	1	96	>99	74/26	67/33	--
2	2	96	>99	76/24	76/24	50/50

^[a] Reaction conditions: aldehyde (1 equiv.), cyclopentanone (5 equiv.), water (0.5 mL/mmol aldehyde) and the indicated amount of catalyst **M2** at room temperature.

^[b] Determined by ¹H-NMR spectroscopy.

^[c] Determined by chiral Daicel Chiralpak AD-H column.

3.1.5 Immobilization effect on the supported catalysts

After the analysis of the results obtained in aldol reactions with homogeneous **10**, and supported **M1** and **M2**, we reasoned that the characteristics of the matrix, the length of the linker and the site of immobilization to the inorganic matrix within the catalytic moiety can affect the catalytic performance of the material. To explain the loss of stereoselectivity in going from homogeneous to heterogeneous catalysts, we propose that the positioning of the point of attachment to the matrix close to the sulfonamide moiety in **M1** and **M2** might have induced an excess of rigidity in the active site which would have been deleterious for asymmetric induction. At the same time, this would have caused a deleterious effect of the matrix (steric hindrance, proximal acidic Si-OH groups competing with the acidic sulfonamide in the case of **M1**). For this reason, we decided to prepare a different supported proline sulfonamide-based organocatalyst with another point of attachment of the organic moiety to the silica matrix offering more flexibility to the catalyst functionality (Figure 2.15).

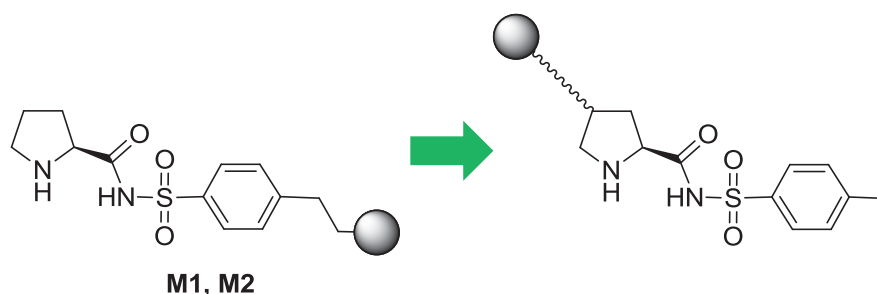


Figure 2.15. New strategy of immobilization

3.2 Preparation and catalytic applications of hybrid silica materials M3, M4, and M6 derived from monosilylated *trans*-4-hydroxyproline sulfonamide

With the aim of preparing a new supported proline sulfonamide catalyst bearing the linker to the silica matrix in the pyrrolidine ring instead of in the aryl ring, a different monosilylated precursor **2** was designed (Figure 2.16) starting from *trans*-4-hydroxy-L-proline. The introduction of the trialkoxysilyl moiety would be performed through the formation of a carbamate group.

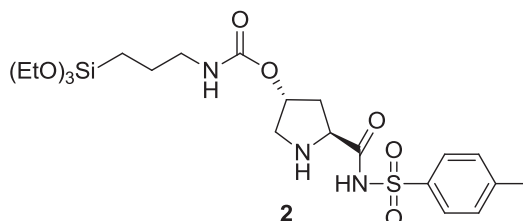
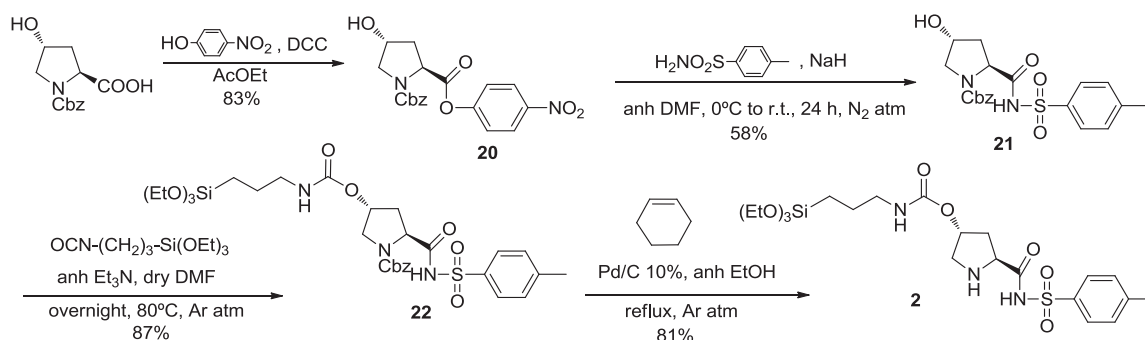


Figure 2.16. New silylated precursor **2**.

3.2.1 Preparation of the organosilicas M3, M4 and M6

The target monosilylated proline sulfonamide **2**, was prepared in 4 steps (35% overall yield) (Scheme 2.17) from commercially available *trans*-N-Cbz-4-hydroxy-L-proline. This starting material was converted to the 4-nitrophenyl ester **20** by a coupling reaction with *p*-nitrophenol. Further treatment of this ester with the sodium salt of *p*-toluenesulfonamide afforded compound **21**. The introduction of the silylated chain was achieved through the formation of a carbamate group by reaction of **21** with commercial (3-isocyanatopropyl)triethoxysilane to give the N-protected sulfonamide **22**. Subsequent removal of the Cbz group yielded the monosilylated precursor **2**.

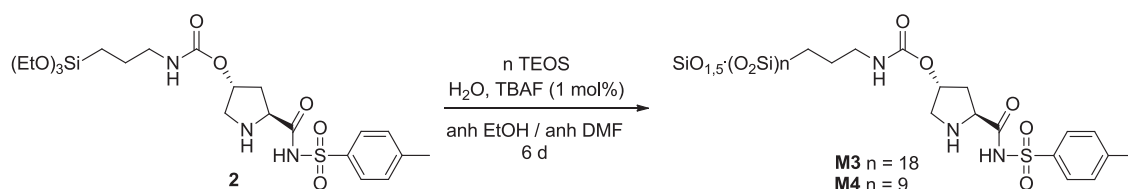


Scheme 2.17. Preparation of the silylated precursor **2**.

Chapter 2. 3. Results and Discussion

Three different hybrid silica materials were synthesized starting from precursor **2** using sol-gel methodologies (co-condensation with TEOS at different molar ratios) and also the grafting method.

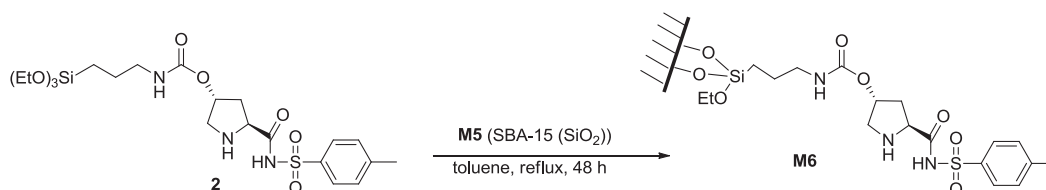
Organosilicas **M3** and **M4** were prepared by the hydrolytic co-condensation of **2** with TEOS (molar ratios 1:18, 1:9) under nucleophilic conditions (TBAF as catalyst) in a mixture of anhydrous DMF/EtOH as solvent (Scheme 2.18).



Scheme 2.18. Preparation of hybrid silica materials **M3** and **M4**.

The initial solutions gellified in 5 min and clear colourless gels were formed. After 6 days of ageing at room temperature, the gels were pulverized, washed with water, EtOH and acetone and finally dried overnight under vacuum at 50°C to yield **M3** and **M4** as white powders. Materials **M3-M4** were then washed with CHCl_3 in a Soxhlet apparatus for 48 h in order to remove the residual DMF entrapped in the solids.

Finally, a hybrid silica material **M6** was prepared by grafting **2** on a previously prepared mesostructured silica (SBA-15) **M5**. Organosilica **M6** was obtained as a white powder after refluxing **2** and **M5** in dry toluene for 24 h (Scheme 2.19). The SBA-15 type silica **M5** was obtained by hydrolytic polycondensation of tetraethoxysilane assisted by P123 under acidic conditions.¹⁷⁴



Scheme 2.19. Preparation of hybrid silica material **M6** by grafting.

The hybrid silica materials **M3**, **M4** and **M6** derived from **2** were characterized by elemental analysis, ^{29}Si -SSNMR, ^{13}C -SS NMR, N_2 -sorption measurements, and p-XRD for the case of **M6**. Some physical and spectroscopic data of **M3-M6** are presented in Table 2.9.

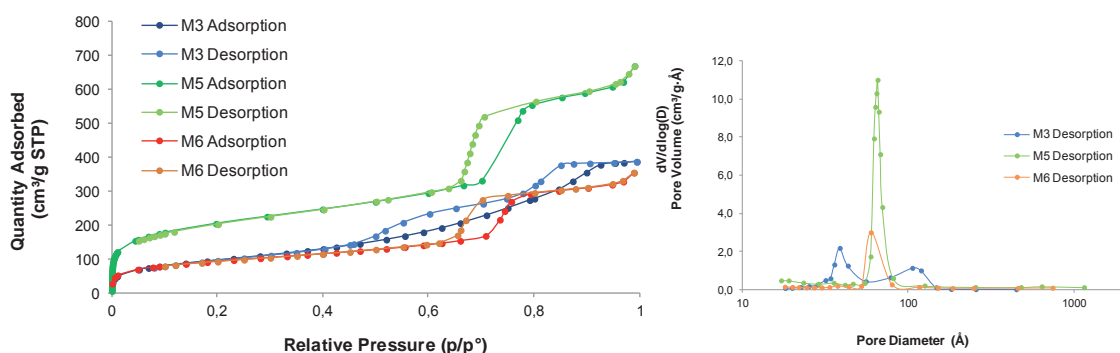
¹⁷⁴ Lettow, J.S.; Han, Y.J.; Schmidt-Winkel, P.; Yang, P.; Zhao, D.; Stucky, G.D.; Ying, J.Y. *Langmuir*, **2000**, *15*, 8291.

Table 2.9. Physical and spectroscopic data of materials **M3-M6**.

Mat	²⁹ Si-SSNMR (ppm)				N ₂ -sorption measurements		N/Si ratio		Cat. loading [mmol/g]
	T ³	Q ²	Q ³	Q ⁴	S _{BET} [m ² /g]	V _{pore} [cm ³ /g]	calc.	exp.	
M3	-75.05	-101.81	-111.73	-120.60	353	0.60	0.16	0.11	0.45
M4	-76.21	-102.26	-112.30	-121.39	<5	-	0.30	0.24	0.84
M5	-	-	-	-	732	1.03	-	-	-
M6	-77.27	-100.73	-110.87	-119.98	328	0.55	0.30	0.15	0.52

As it can be seen in Table 2.9 the ²⁹Si-SSNMR of all materials showed the characteristic T³ peaks, confirming that the integrity of the Si-C covalent bond was maintained during the formation of the hybrid silica material. Furthermore, they presented the corresponding Q peaks as they had been prepared with tetraethoxysilane. However, the condensation is not complete for these materials and, consequently, the experimental values of elemental analysis do not match the calculated ones. The IR spectra were recorded for all materials and a weak characteristic signal of (C=O) group was observed. The ¹³C-SSNMR was only recorded for **M4** since in the other two cases (**M3** and **M6**) the dilution of the organic moiety in the silica matrix was too high and none of the typical signals for proline sulfonamide could be observed.

N₂-sorption measurements revealed that **M4** was non-porous (the amount of nitrogen adsorbed was below the detection limit of the instrument used). This might be due to the relatively high amount of a bulky organic fragment (TEOS:2 molar ratio is 9:1 in this case). In Figure 2.17, the N₂-sorption isotherms and the pore size distributions of porous materials **M3**, **M5** and **M6** are compared.

**Figure 2.17.** Comparison of the N₂-sorption isotherms of materials **M3**, **M5** and **M6** (left) and pore size distribution (right) of **M3**, **M5** and **M6**.

The mesoporous sol-gel material **M3** had a characteristic *type IV* isotherm, showing a hysteresis loop. As expected, after a grafting process the BET specific surface area of **M6** was reduced with respect to the parent silica **M5** (from 732 to 328

m²/g) and also the pore volume (from 1.03 to 0.55 cm³/g), indicating that some space in the pores had been occupied by the precursor. However, the profile of the isotherms of these two materials was maintained (Figure 2.18), which suggests that the original mesostructure of **M5** was not affected by the grafting process.

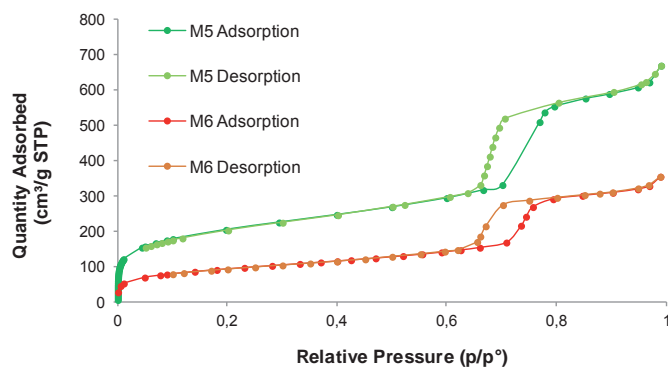


Figure 2.18. Comparison of the N₂-sorption isotherms of materials **M5** and **M6**.

M3 presented a bimodal distribution of pores (Figure 2.17, right), centered at 40 Å and at 110 Å, whereas **M5** and **M6** maintained the sharp distribution around 60 Å.

The p-XRD diffractogram of organosilica **M6** (Figure 2.19) shows a clear hexagonal 2D structure typical of SBA-15 type materials.

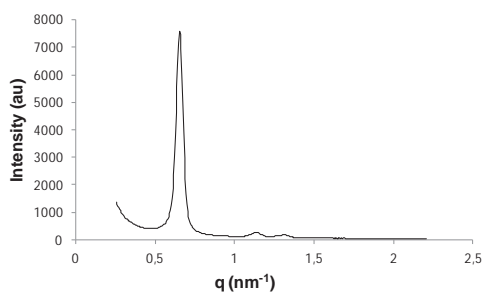


Figure 2.19. p-XRD diffractogram of **M6**.

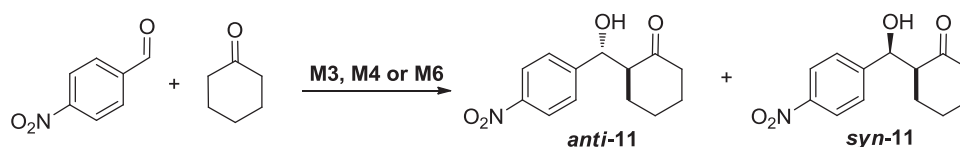
3.2.2 Assay of **M3**, **M4** and **M6** in asymmetric organocatalysis

3.2.2.1 Catalytic tests of **M3**, **M4** and **M6** in the direct aldol reaction

As we did with **M1** and **M2**, the activity of the new hybrid silica materials **M3**, **M4** and **M6** was first evaluated in the direct asymmetric aldol reaction between cyclohexanone and *p*-nitrobenzaldehyde to give the aldol **11** (Table 2.10). As in the previous tests, reactions were carried out in water at room temperature using 5 equivalents of ketone with respect to the aldehyde.

All the organosilicas derived from monosilylated precursor **2** showed higher enantioselectivity for the major *anti* diastereoisomer than materials **M1** and **M2**, even at 10 mol% of catalyst loading. In the case of the non-porous material **M4**, the catalytic events should take place only at the external surface of the particles, and therefore the whole process should be fast; however only a small part of the catalyst is accessible by the substrates and this may produce a decrease in the reaction rate. On the other hand, for porous organosilicas (**M3** and **M6**) the catalytic sites located inside the pores should all be accessible at a fast or slow rate. For this last situation, diffusion-controlled processes can occur lowering the reaction rate, because it is necessary not only to get the substrate close to the catalyst, but also to remove the product from the catalytic site once the catalytic reaction has occurred.

Table 2.10. Catalytic performance^[a] of **M3**, **M4** and **M6** in the direct asymmetric aldol reaction of cyclohexanone with *p*-nitrobenzaldehyde.



	M3 (10 mol%)				M4 (10 mol%)				M6 (10 mol%)			
	t [h]	Yield ^[b] [%]	<i>dr</i> ^[b]	<i>er</i> ^[c]	t [h]	Yield ^[b] [%]	<i>dr</i> ^[b]	<i>er</i> ^[c]	t [h]	Yield ^[b] [%]	<i>dr</i> ^[b]	<i>er</i> ^[c]
1	96	>99	84/16	90/10	144	85	90/10	84/16	96	>99	90/10	94/6
2	96	>99	75/25	95/5	144	>99	83/17	96/4	96	>99	88/12	97/3
3	144	>99	85/15	96/4	144	83	88/12	87/13	144	>99	92/8	90/10
4	168	>99	84/16	90/10	168	>99	84/16	87/13	168	>99	90/10	89/11
5	216	95	89/11	65/35	240	96	90/10	68/32	216	99	92/8	88/12

	M3 (20 mol%)				M4 (20 mol%)				M6 (20 mol%)			
	t [h]	Yield ^[b] [%]	<i>dr</i> ^[b]	<i>er</i> ^[c]	t [h]	Yield ^[b] [%]	<i>dr</i> ^[b]	<i>er</i> ^[c]	t [h]	Yield ^[b] [%]	<i>dr</i> ^[b]	<i>er</i> ^[c]
6	96	>99	79/21	97/3	144	98	87/13	98/2	96	>99	90/10	97/3
7	96	>99	79/21	88/12	144	>99	80/20	90/10	96	>99	86/14	88/12

^[a] Reaction conditions: aldehyde (1 equiv.), cyclohexanone (5 equiv.), water (0.5 mL/mmol aldehyde) and the indicated amount of the corresponding catalyst (**M3**, **M4** or **M6**) at room temperature. Entries 1 to 5 correspond to five consecutive cycles with 10 mol% of each material; entries 6 and 7 correspond to two consecutive cycles with 20 mol% of each material.

^[b] Determined by ¹H-NMR spectroscopy.

^[c] Determined by chiral Daicel Chiralpak AD-H column.

The effect of catalyst loading was evaluated (compare entries 1 and 6, Table 2.10). It slightly influenced the diastereoselectivity, the enantioselectivity and the reaction time (faster reaction with higher amount of catalyst, in the case of **M4**). The

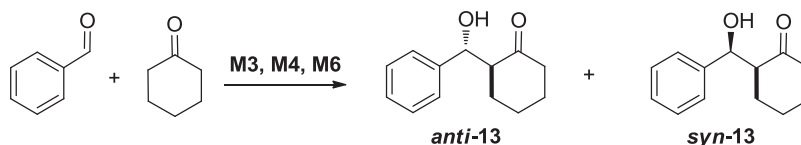
enantioselectivity achieved with **M3** and **M6** was superior to the one that presented **M4** at 10 mol% loading. This effect may be explained in terms of a confined environment, which can trigger chemical discrimination and, in some cases, increase selectivity. Confinement may also efficiently direct the stereochemical outcome through space constriction and molecular close contact.¹⁷⁵ Indeed, mimicking enzyme pockets with hybrid silica materials seems possible, although it would need the precise localization of the organic fragment within the material, which cannot be achieved by simple sol-gel co-condensation. In the case of dense material **M4**, the confinement effect cannot be observed due to the lack of porosity. If we compare the enantioselectivity between **M3** and **M6**, it seems that the presence of a regular mesoporous structure does not bring a very significant advantage in selectivity with respect to a simple sol-gel co-condensation.

Encouraged by the activity and selectivity exhibited by **M3**, **M4** and **M6** in the initial catalytic assays, we decided to perform recycling experiments for the mentioned aldol reaction. Recycling of all the materials was possible for 5 consecutive runs (entries 1 to 5 in Table 2.10), although a slight decrease in activity was observed upon recycling since longer times were needed to reach completion in the third or fourth run. While diastereoselectivity was more or less maintained throughout all cycles, a significant decrease in enantioselectivity was observed in the 5th run for **M3** and **M4** whereas it was maintained for **M6**. Considering these results obtained in the recycling experiments it seems that there is a positive influence of a regular mesoporous structure.

As in the previous cases, the new materials were tested in the aldol reaction with other substrates for comparative purposes. We first tested materials **M3**, **M4** and **M6** in the aldol reaction between cyclohexanone and benzaldehyde to give the aldol **13** (Table 2.11).

Similarly to the previous reaction, all the organosilicas derived from monosilylated precursor **2** showed higher enantioselectivity for the major *anti* diastereoisomer than materials **M1** and **M2** at 10 mol% of catalyst loading. We did not recycle them more than 3 consecutive cycles, because at the 3rd run both the rate and the enantioselectivity decreased considerably.

¹⁷⁵ Brunet, E. *Chirality*, **2002**, *14*, 135.

Table 2.11. Catalytic performance^[a] of **M3**, **M4** and **M6** in the direct asymmetric aldol reaction between cyclohexanone and benzaldehyde.

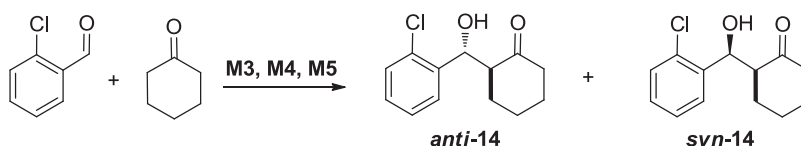
Run	M3 (10 mol%)				M4 (10 mol%)				M6 (10 mol%)			
	t [h]	Yield ^[b] [%]	<i>dr</i> ^[b]	<i>er</i> ^[c]	t [h]	Yield ^[b] [%]	<i>dr</i> ^[b]	<i>er</i> ^[c]	t [h]	Yield ^[b] [%]	<i>dr</i> ^[b]	<i>er</i> ^[c]
1	144	90	85/15	92/8	144	>99	85/15	92/8	144	79	89/11	90/10
2	144	>99	80/20	85/15	144	>99	73/27	81/19	144	>99	71/29	85/15
3	216	94	82/18	51/49	216	85	79/21	56/44	216	69	86/14	57/43

^[a] Reaction conditions: benzaldehyde (1 equiv.), cyclohexanone (5 equiv.), water (0.5 mL/mmol aldehyde) and the indicated amount of the corresponding catalyst (**M3**, **M4** or **M6**) at room temperature.

^[b] Determined by ¹H-NMR spectroscopy.

^[c] Determined by chiral Daicel Chiralcel OD column.

Aldol reaction between 2-chlorobenzaldehyde and cyclohexanone performed by catalysts **M3**, **M4** and **M6** afforded notable diastereoselectivities and enantioselectivities (Table 2.12).

Table 2.12. Catalytic performance^[a] of **M3**, **M4** and **M6** in the direct asymmetric aldol reaction of cyclohexanone with 2-chlorobenzaldehyde.

Entry	Catalyst (10 mol%)	t (h)	Conv. (%) ^[b]	<i>dr</i> _(anti/syn) ^[b]	<i>er</i> _{anti} ^[c]
1	M3	168	98	93/7	95/5
2	M4	168	94	89/11	94/6
3	M6	168	98	89/11	89/11

^[a] Reaction conditions: aldehyde (1 equiv.), cyclohexanone (5 equiv.), water (0.5 mL/mmol aldehyde) and the indicated amount of the corresponding catalyst (**M3**, **M4** or **M6**) at room temperature.

^[b] Determined by ¹H-NMR spectroscopy.

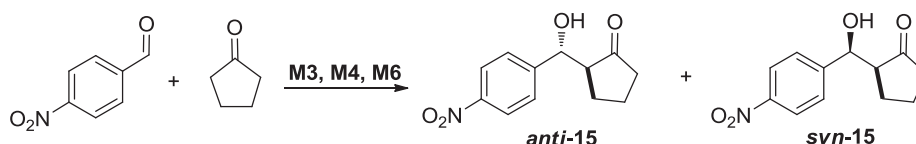
^[c] Determined by chiral Daicel Chiralpak AD-H column.

Similarly to what has been observed with **M1** and **M2**, the aldol reaction between cyclopentanone and *p*-nitrobenzaldehyde catalysed by **M3**, **M4** or **M6** gave lower diastereoselectivities than with cyclohexanone (Table 2.13). The enantioselectivities achieved with **M3** and **M6** were higher with respect to the other catalysts (**M1**, **M2** and

Chapter 2. 3. Results and Discussion

M4). Due to the low diastereoselectivities obtained, supported catalysts **M3**, **M4** and **M6** were not reused for more than two cycles. Unexpectedly, the major diastereoisomer changed from the first to the second run in the case of **M3** and **M6**.

Table 2.13. Catalytic performance^[a] of **M3**, **M4** and **M6** in the direct asymmetric aldol reaction of cyclopentanone with *p*-nitrobenzaldehyde.



Run	M3 (10 mol%)				M4 (10 mol%)				M6 (10 mol%)			
	t [h]	Yield ^[b] [%]	<i>dr</i> ^[b]	<i>er</i> ^[c]	t [h]	Yield ^[b] [%]	<i>dr</i> ^[b]	<i>er</i> ^[c]	t [h]	Yield ^[b] [%]	<i>dr</i> ^[b]	<i>er</i> ^[c]
1	96	>99	37/63	97/3	96	>99	54/46	69/31	96	>99	43/57	88/12
2	96	>99	57/43	80/20	96	>99	55/45	72/28	96	>99	62/38	81/19

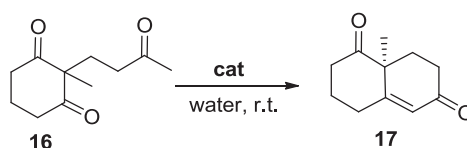
^[a] Reaction conditions: aldehyde (1 equiv.), cyclopentanone (5 equiv.), water (0.5 mL/mmol aldehyde) and the indicated amount of the catalyst (**M3**, **M4** or **M6**) at room temperature.

^[b] Determined by ¹H-NMR spectroscopy.

^[c] Determined by chiral Daicel Chiralpak AD-H column.

The catalytic performance of organosilicas **M3**, **M4** and **M6** was then evaluated in the intramolecular Robinson annulation of triketone **16** to obtain the corresponding Wieland-Miescher ketone **17** (Table 2.14).

Table 2.14. Catalytic performance^[a] of **M3**, **M4** and **M6** in the intramolecular aldol reaction with triketone **16**.



Entry	Catalyst (mol%)	co-catalyst	Cycle	t (h)	Yield. (%) ^[b]	<i>er</i> ^[c]
1	M3 (20)	<i>p</i> -NO ₂ C ₆ H ₄ CO ₂ H	1	288	44	68/32
2	M3 (20)	<i>p</i> -NO ₂ C ₆ H ₄ CO ₂ H	2	288	60	69/31
3	M4 (20)	<i>p</i> -NO ₂ C ₆ H ₄ CO ₂ H	1	288	71	69/31
4	M4 (20)	<i>p</i> -NO ₂ C ₆ H ₄ CO ₂ H	2	288	82	70/30
5	M6 (20)	<i>p</i> -NO ₂ C ₆ H ₄ CO ₂ H	1	288	63	68/32
6	M6 (20)	<i>p</i> -NO ₂ C ₆ H ₄ CO ₂ H	2	288	31	69/31

^[a] Reaction conditions: triketone **16** (1 equiv.), water (0.5 mL/mmol triketone) and the indicated amount of the corresponding catalyst (**M3**, **M4** or **M6**) and *p*-nitrobenzoic acid as co-catalyst (20% mol).

^[b] Isolated yield.

^[c] Determined by chiral Daicel Chiralpak IC column.

As in the case of **M1**, the experiments were performed in water, at room temperature and in the presence of *p*-nitrobenzoic acid as co-catalyst. In the absence of this acid, the isolated yields of diketone **17** were considerably lower at the same reaction time. The crude mixtures obtained after filtration needed to be purified by column chromatography on silica gel to reach pure **17**. Owing to the low reaction rate, tests were performed at 20 mol% of catalyst. Contrary to the results of the previous aldol tests, **M4** presented the highest activity, compared with **M3** and **M6**. However, the activities of the supported catalysts derived from **2** were lower than the activity found for **M1**.

3.2.2.2 Catalytic tests of **M3** and **M6** in the aza-Diels Alder reaction

The aza-Diels Alder reaction between cyclohex-2-en-1-one and imine **18** was tested with the organosilicas **M3** and **M6** derived from monomer **2** under the same conditions previously used for **M1** (excess of cyclohexenone, 30 mol% of catalyst, neat, rt) (Table 2.15).

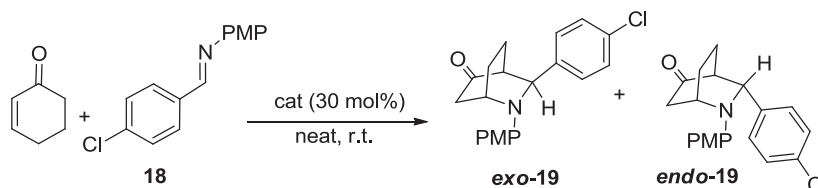


Table 2.15. Catalytic performance^[a] of **M3** and **M6** in the aza-Diels Alder reaction.

Entry	Catalyst (mol%)	Cycle	t (h)	Yield (%) ^[b]	<i>dr</i> _{<i>exo/endo</i>} ^[d]
1	10 (30)	-	144	51	100/0
2	M3 (30)	1	240	24	84/16
3	M3 (30)	2	264	24 ^[c]	31/69
4	M6 (30)	1	240	39	100/0
5	M6 (30)	2	264	71 ^[c]	55/45

^[a] Reaction conditions: 2-cyclohexen-1-one (120 μ L, 10 equiv.), imine (1 equiv.) and the indicated amount of the corresponding catalyst were stirred together at room temperature.

^[b] Isolated yield.

^[c] Conversion. Determined by ¹H-NMR.

^[d] Determined by ¹H-NMR.

Low or moderate yields or conversions were achieved. The organosilica **M6** showed the highest activity with a 39% isolated yield in the first cycle (entry 4 of table 2.15). Whereas with homogeneous proline sulfonamide **10**, a complete diastereoselectivity for the *exo* adduct was observed (entry 1 in Table 2.15, 51 % of isolated yield) this was not the case for the supported catalysts. For **M3**, a mixture of *exo/endo* adducts (84/16) was obtained in the first cycle, but the selectivity changed in favour of the *endo* adduct

in the second cycle (31/69) (entries 2 and 3 of table 2.15). In the case of **M6** the complete diastereoselectivity for the *exo* adduct in the first cycle was lost in the second run (ratio *exo/endo* of 55/45) (entries 4 and 5 of table 2.15). Due to the low activity and diastereoselectivity, the enantioselectivity of the process (*er* of the major diastereoisomer) was not determined. Silica-supported proline sulfonamides did not behave as efficient and selective recyclable catalysts in this reaction.

3.3 Attempts to prepare an organosilica derived from a proline tetrazole

As a second objective of this part of the thesis, we planned the preparation of an organosilica derived from a silylated proline tetrazole **3** (Figure 2.20) by sol-gel procedures in order to evaluate it as a recyclable chiral organocatalyst in aldol and other asymmetric reactions.

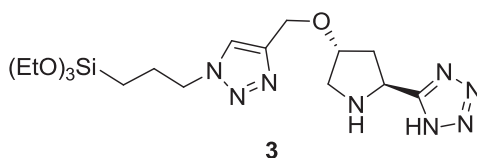


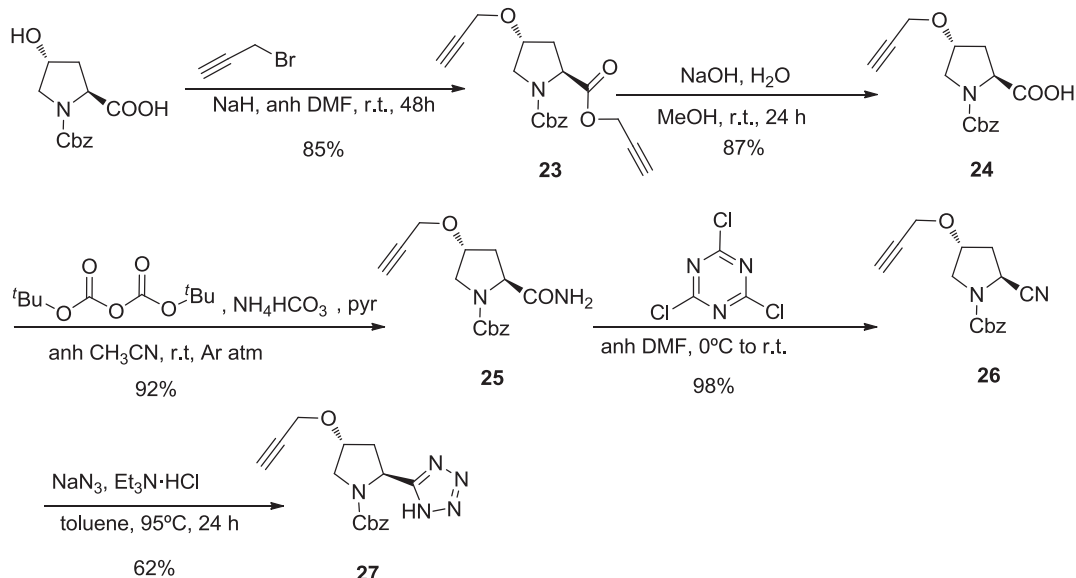
Figure 2.20. New silylated proline tetrazole-based precursor **3**.

Jonathan Ruiz had begun in our group the preparation of this precursor but he could not finish the synthetic route.¹⁷⁶ In this thesis we have repeated the first steps of the envisaged synthesis (Scheme 2.20) and we have tried to solve the problems encountered in the final steps towards the silylated monomer **3**.

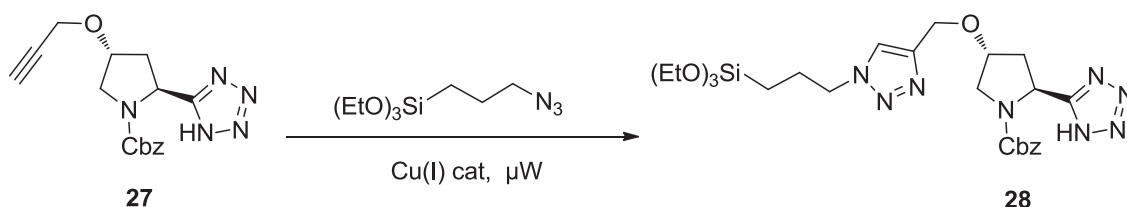
Double alkylation of commercially available *trans*-*N*-Cbz-4-hydroxy-L-proline with propargyl bromide afforded **23**. Mild saponification of the ester group of **23** enabled the obtention of the acid **24**, which was transformed to the amide **25** by treatment with di-*tert*-butyl dicarbonate and ammonium bicarbonate as a source of nitrogen. Amide **25** was reacted with cyanuric chloride in dimethylformamide to afford the nitrile derivative **26**. The proline tetrazole derivative **27** was obtained through a 1,3-dipolar cycloaddition between the cyano group of **26** and sodium azide in the presence of a source of protons (Et₃N.HCl).¹⁷⁷ The five-step synthesis of **27** took place with a 41% overall yield.

¹⁷⁶ Ruiz, J. *Master en Experimentació Química*. Universitat Autònoma de Barcelona, 2013.

¹⁷⁷ (a) Bortolini, O.; Caciolli, L.; Cavazzini, A.; Costa, V.; Greco, R.; Massi, A.; Pasti, L. *Green Chem.* **2012**, *14*, 992. (b) Himo, F.; Demko, Z.P.; Noodelman, L.; Sharpless, K.B. *J. Am. Chem. Soc.* **2002**, *124*, 12210.



Once compound **27** was obtained, we envisaged the use of the copper-catalyzed azide alkyne cycloaddition (CuAAC) reaction under anhydrous conditions, following the methodology developed by Cattoën-Wong Chi Man,¹⁷⁸ in order to introduce the silylated moiety. The first assay consisted on the reaction of the alkyne **27** with (3-azidopropyl)triethoxysilane in the presence of a Cu^I catalyst under microwave heating to afford **28** (Scheme 2.21).



Within our collaboration with the group of Wong Chi Man at the *École Nationale Supérieure de Chimie de Montpellier (ENSCM)* several conditions were used to perform this cycloaddition reaction (Table 2.16). The first attempt was performed in the presence of the complex [CuBr(PPh₃)₃] as a Cu^I catalyst in a 1:1 (v/v) mixture of anhydrous THF and dry NEt₃ as solvent (entry 1). The solution was submitted to microwave heating at 100°C for 5 min as the described methodology indicates for other substrates. The ¹HNMR spectrum showed no evidence of the formation of a new triazole group (Figure 2.21), which can be followed by the shift of the signal (CH₂-N)

¹⁷⁸ Moitra, N.; Moreau, J.J.E.; Cattoën, X.; Wong Chi Man, M. *Chem. Commun.* **2010**, 46, 8416.

Chapter 2. 3. Results and Discussion

from 3.2 ppm in the starting azide to approximately 4.3 ppm for the CH₂ next to the triazole ring.

Table 2.16. Attempts for the CuAAC^[a] between **27** and silylated azide to afford **28**.

Entry	Cu ^I catalyst	Ligand	Solvent	T (°C)	Time (min)	Conversion (%)
1	CuBr(PPh ₃) ₃	-	anh THF/NEt ₃	100 (μW)	5	-
2	CuBr(PPh ₃) ₃	TBTA ^[b]	anh DMF/NEt ₃	100 (μW)	10	-

^[a] Reaction conditions: alkyne **27** (2 mmol), azide (2 mmol), CuBr(PPh₃)₃ (0.01 mmol), THF/NEt₃ 1:1 (1 mL), microwaves 100°C for the time indicated under Ar atm.

^[b] TBTA ligand (0.01 mmol) was added to the reaction mixture before microwave heating.

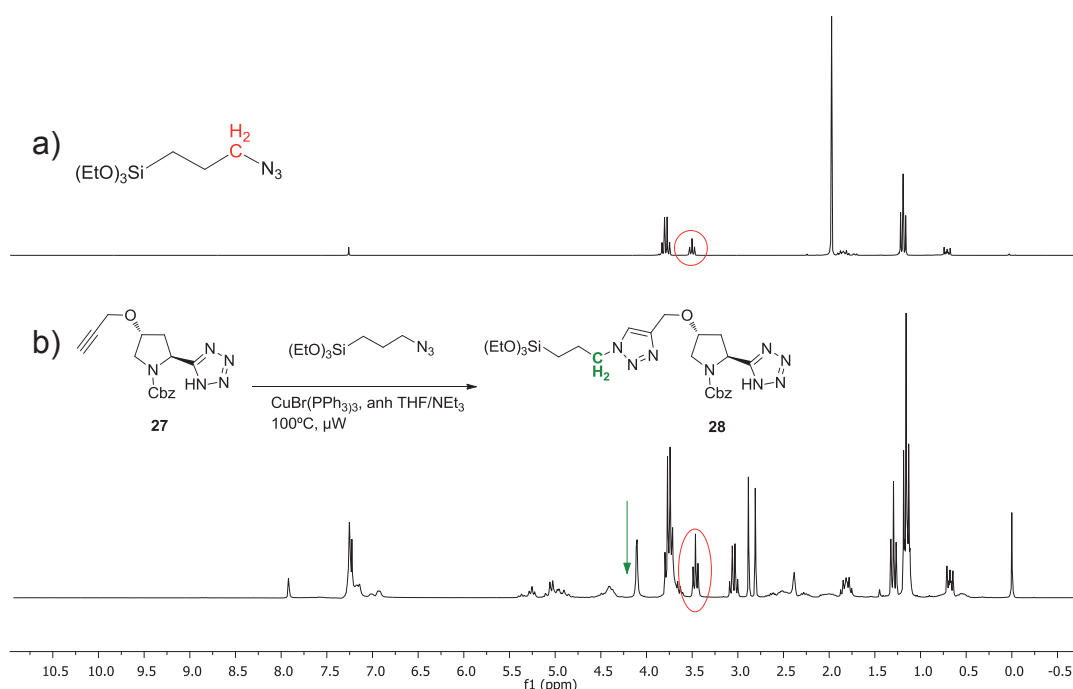
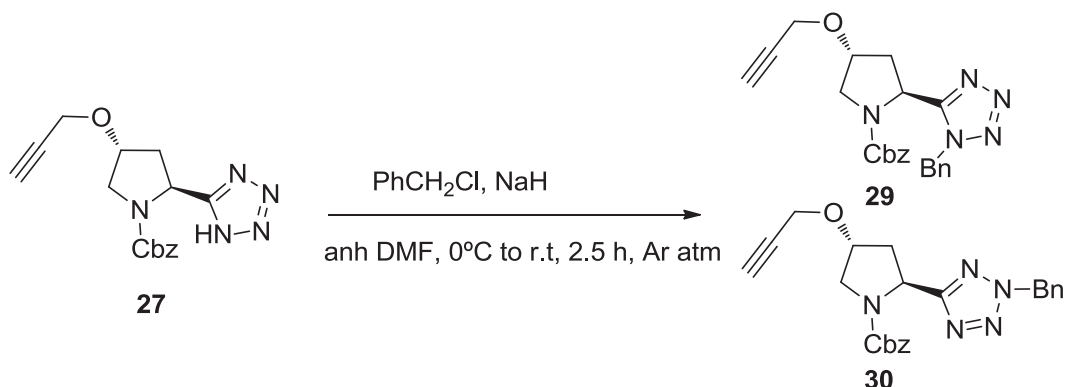


Figure 2.21. ¹H NMR spectrum comparison of starting silylated azide and aliquot of CuAAC reaction.

Then the reaction was carried out with the addition of TBTA ligand (tris(benzyltriazolylmethyl)amine) to stabilize the Cu^I catalyst (CuBr(PPh₃)₃:TBTA (1:1)) and THF was substituted by DMF (entry 2 in Table 2.16). However, those changes did not improve the performance of the reaction and the desired final compound **28** was not obtained.

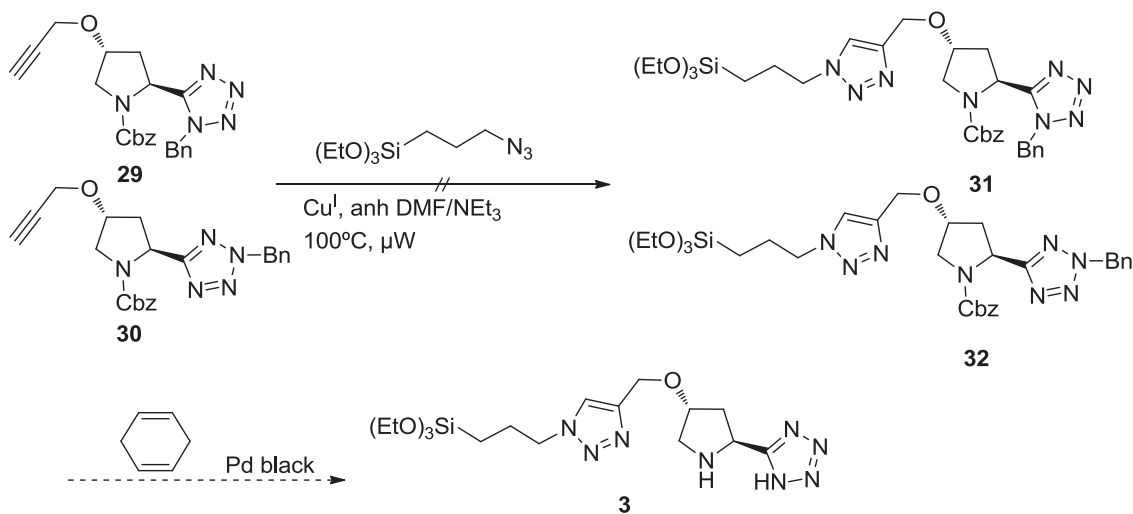
Taking into account that compound **27** presented a free NH acidic group in the tetrazole ring, we supposed that it could bring some incompatibility with the catalyst. At this point, we decided to protect the NH group by reaction of **27** with benzyl chloride to afford a mixture of alkylated regioisomers **29** and **30** due to the existence of different

tautomers of **27** (the same bidentate anion arising from both tautomers) (Scheme 2.22).



Scheme 2.22. Protection of tetrazole NH of compound **27**

The benzylated compounds **29** and **30** were very difficult to separate, for this reason we decided to react the mixture with (3-azidopropyl)triethoxysilane to obtain the mixture of silylated compounds **31** and **32**. Finally, the treatment with 1,4-cyclohexadiene and Pd black¹⁷⁹ would allow the removal of Cbz and Bn protecting groups to achieve the desired silylated monomer **3** (Scheme 2.23).



Scheme 2.23. Attempted of monosilylated compound **3**.

Several conditions were used to perform the 1,3-dipolar cycloaddition reaction (CuAAC) with the mixture of compounds **29+30** (Table 2.17). First, the reaction was performed with $[\text{CuBr}(\text{PPh}_3)_3]$ as catalyst under microwave heating at 100°C for 10 min in a mixture of DMF/ Et_3N (entry 1 of Table 2.17). No conversion was observed.

¹⁷⁹ Felix, A.M.; Heimer, E.P.; Lambros, T.J.; Tzougraki, C.; Meienhofer, J. *J.Org.Chem.*, **1978**, *43*, 4194.

Chapter 2. 3. Results and Discussion

Thinking that the problem could be a low reaction rate, the reaction was tried again under the same conditions but heating the mixture during 75 min (Table 2.17, Entry 2). However, the ^1H NMR spectrum after this time did not show any evidence of the formation of the triazole ring. Then, another attempt was tried by adding the ligand TBTA to the mixture of reagents, in order to improve the stability of Cu^{I} species and favour the reaction (Entry 3 of Table 2.17). Again, no evident changes were observed in the ^1H NMR spectrum. Finally, freshly prepared CuI was used as catalyst together with TBTA ligand (Table 2.17, entry 4) to ensure that the source of Cu^{I} was not the factor which determined the failure of the reaction.

Table 2.17. Different conditions used in the CuAAC^[a] between **29+30** and silylated azide to afford **31+32**.

Entry	Cu^{I} catalyst	Ligand	Solvent	T (°C)	Time	Conversion
1	$\text{CuBr}(\text{PPh}_3)_3$	-	$^{\text{anh}}\text{DMF}/\text{NEt}_3$	100 (μw)	10 min	-
2	$\text{CuBr}(\text{PPh}_3)_3$	-	$^{\text{anh}}\text{DMF}/\text{NEt}_3$	100 (μw)	75 min	-
3	$\text{CuBr}(\text{PPh}_3)_3$	TBTA ^[b]	$^{\text{anh}}\text{DMF}/\text{NEt}_3$	100 (μw)	30 min	-
4	CuI	TBTA ^[b]	$^{\text{anh}}\text{DMF}/\text{NEt}_3$	100 (μw)	30 min	-

^[a] Reaction conditions: alkyne **29+30** (2 mmol), azide (2 mmol), Cu^{I} (0.01 mmol), DMF/NEt_3 1:1 (1 mL), microwaves 100°C for the time indicated under Ar atm.

^[b] TBTA ligand (0.01 mmol) was added to the reaction mixture before microwave heating.

All the protocols tried were unsuccessful and compounds **31+32** could not be achieved through a CuAAC reaction. Consequently, the preparation of the desired monosilylated product **3** could not be completed and, unfortunately, the corresponding hybrid silica materials could not be prepared.

Finally, I would like to remark that in the final months of the thesis work I have participated in the preparation of a manuscript for a review article (by invitation of Green Chemistry) which is related with the subject of this chapter, entitled *Recyclable organocatalysts based on hybrid silicas*.

4. CONCLUSIONS

Several organosilicas derived from chiral monosilylated proline sulfonamides **1** and **2** have been prepared by the sol-gel co-gelification with tetraethyl orthosilicate (TEOS) under nucleophilic catalysis, which represents a versatile methodology for the obtention of silica-immobilized organocatalysts. Another material was also prepared by grafting the monomer **2** to a mesostructured SBA-15 type silica support. All the materials have been characterized by the usual techniques,

These organosilicas have been tested as chiral recyclable organocatalysts in direct asymmetric aldol reactions under mild conditions (in water at room temperature), no acid additives being necessary in most cases. For these reasons, we have developed a simple, efficient and environmentally friendly procedure. The experimental protocol avoids the formation of undesired crotonization by-products when using chromatography to separate the aldol compounds, since the supported catalysts are separated and recovered by simple filtration of the crude mixtures. However, the efficiencies and selectivities achieved were lower than those of the homogeneous proline sulfonamide analogue and of some silica-supported aminoindane-derived proline amides previously developed in the group.

The characteristics of the matrix, the nature and length of the linker, and the site of immobilization to the inorganic matrix within the catalytic organic moiety affects the catalytic performance of the material. Thus, materials **M3**, **M4** and **M6** derived from monomer **2** showed better enantioselectivities in aldol reaction than **M1** and **M2** derived from monomer **1**. Thus, the positioning of the point of attachment to the matrix close to the sulfonamide moiety in **M1** and **M2** might have induced an excess of rigidity in the active site, which would have caused a deleterious effect for asymmetric induction. Moreover, free Si-OH present in the material are not simple spectators and, if they are close to the active site, can also contribute to the catalysis due to its acidic character, entering in competition with acidic NH of the sulfonamide and leading to a decrease in the selectivity. This effect has been observed when comparing **M1** with the silanol-capped material **M2**.

All the silica-supported proline sulfonamides promoted the direct intermolecular asymmetric aldol reaction between ketones and aromatic aldehydes. In the case of cyclohexanone and *p*-nitrobenzaldehyde all materials exhibited good recycling profiles with good *er* for the major *anti*-diastereomer. The best results were obtained with the mesoporous organosilicas **M3** and **M6** derived from precursor **2**. Silica-supported

Chapter 2. 4. Conclusions

organocatalysts **M2**, **M3**, **M4** and **M6** were recycled up to 4 runs in this benchmark reaction without a significant loss of selectivity. For other aldehydes (benzaldehyde, 2-chlorobenzaldehyde), higher reaction times were required but the selectivities were notable. Furthermore, a Robinson annulation was tested with diketone **14** to prepare a Wieland-Miescher ketone **15**. In this case, the efficiency and the enantioselectivity decreased and the use of an acid co-catalyst was needed.

Materials **M1**, **M3** and **M6** were also assayed in aza-Diels Alder reaction between cyclohexenone and imine **16**. Low yields and diastereoselectivities were obtained (mixtures of *exo* and *endo* products in the first or in the second cycle), indicating that these supported catalysts are not good recyclable catalysts for this reaction.

We successfully performed the first five steps of the envisaged synthetic route for the obtention of the monosilylated proline tetrazole monomer **3** with the aim to prepare silica-supported organocatalysts by the sol-gel process. However we failed in the final steps by using CuAAC methodology under anhydrous conditions to introduce a triazole linker and the triethoxysilyl moiety.

5. EXPERIMENTAL SECTION

5.1. General remarks

Nuclear Magnetic Resonance (NMR) spectra were recorded at the *Servei de Ressonància Magnètica Nuclear* of the *Universitat Autònoma de Barcelona*. ^1H -NMR, ^{13}C -NMR, ^1H - ^1H COSY, ^1H - ^1H NOESY, ^1H - ^{13}C HSQC, ^1H - ^{13}C HMBC and SELTOCSY spectra were recorded using Bruker instruments (DRX-250, DPX-360 and AVANCE-III 400). Chemical shifts (δ) are given in ppm using the residual non-deuterated solvent as internal reference.

The ^{29}Si and ^{13}C CP-MAS solid state NMR spectra were obtained in the NMR service of UAB from a Bruker AV400WB; the repetition time was 5 seconds with contact times of 5 milliseconds.

Infrared spectroscopy (IR) spectra were recorded with a Bruker Tensor 27 spectrometer using a Golden Gate ATR module with a diamond window. When necessary, IR spectra were recorded using KBr pellets using a Thermo Nicolet IR2000 spectrometer.

Polarimetry. Specific rotation ($[\alpha]_{\lambda}^T$, ORD) values were obtained at 25°C and 589.6 nm using a JASCO J-175 polarimeter of *Servei d'Anàlisi Química* (SAQ) in UAB. They are given in $10^{-1}\text{deg cm}^2 \text{g}^{-1}$.

Elemental Analysis (EA) of C, N, H and Si were performed by the *Serveis Científico-Tècnics* of the *Universitat de Barcelona (SCT-UB)*. The percentages of C, N and H were determined by combustion in a EA-1108 C.E. elemental analyser of Thermo Scientific using BBOT as internal standard. The content of Si was determined by Inductively Coupled Plasma (ICP) in a multichannel Perkin-Elmer Optima 3200 L instrument.

Thin-Layer Chromatography (TLC) was performed using 0.25 mm plates (Alugram Sil G/UV₂₅₄).

Flash Chromatography was performed under compressed air pressure on a *Macherey-Nagel GmbH & Co KG* silica gel which had a particle size of 230 – 400 mesh and pore volume of 0.9 mL/g.

Chiral HPLC Chromatography. Enantiomeric excesses (ee) or ratios (er) were determined by chiral stationary phase HPLC (Daicel Chiralpack AD-H, Daicel Chiralcel

Chapter 2. 5. Experimental Part

OD and Daicel Chiralpack IC) with a Waters 2960 instrument using an UV photodiode array detector.

Surface areas were determined by the Brunauer-Emmet-Teller (BET) method from N₂ adsorption–desorption isotherms obtained with a *Micromeritics ASAP2020* analyzer after degassing samples for 30h at 55°C under vacuum. The total pore volumes were evaluated by converting the volume adsorbed at p/p^0 0.98 to the volume of liquid adsorbed (single point adsorption total pore volume of pores less than 4000 Å at $p/p^0 \approx 0.98$). The pore size distributions for the materials were determined from the desorption branch using the Barrett-Joyner-Halenda (BJH) method¹⁸⁰ which relies on the Kelvin equation to relate the width of the pores to the condensation pressure.

Powder X-Ray Diffraction (*p*-XRD) experiments were performed by Philippe Dieudonné (Laboratoire Charles Coulomb) at the *Université Montpellier II* using an instrument with a X-Ray source produced by a copper anode, which also had an *Osmic*-type monochromator to modulate the incident beam intensity (10⁸ photons/s). A 2D *image plate* detector was used. Powder samples were placed in 1.5 mm diameter glass capillaries.

Microwave assisted reactions were performed using a CEM Discover® Microwave instrument in *Institut Charles Gerhardt de Montpellier*, which operates between 0 and 300 W. The reactions were conducted in a 10 mL sealed reactor.

Other:

When required, experiments were carried out with standard high vacuum and Schlenk techniques under N₂ or Ar atmosphere using dry solvents and in some cases degassed by the freeze-and-thaw method and cannula or syringe-transferred.

Commercial reagents were directly used as received except the (3-isocyanatopropyl)triethoxysilane, benzaldehyde and 2-chlorobenzaldehyde which were distilled prior to use. Na₂SO₄ and MgSO₄ used to adsorb water of organic layers were anhydrous. Karstedt catalyst was used as received and purchased as Platinum(0)-1,3-divinyl-1,1,3,3-tetramethyldisiloxane complex solution in xylene (~2% Pt).

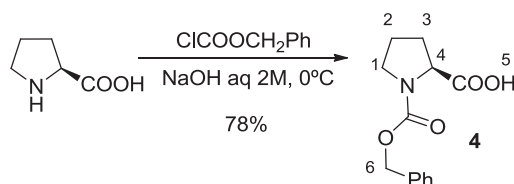
Dry solvents were obtained from two instruments: *PureSolv* (Innovative Technologies: THF, CH₂Cl₂ and pentane) and in some experiments from *MBraun SPS-800* (MBraun:

¹⁸⁰ Barrett, E. P.; Joyner, L. G.; Halenda, P. P. *J. Am. Chem. Soc.*, **1951**, 73, 373.

THF). Other dry solvents were prepared using standard methods: NEt_3 and DMF were distilled over CaH_2 . Toluene was refluxed over Na/benzophenone whereas ethanol was distilled on Mg/I_2 . When needed, deuterated NMR solvents such as CDCl_3 were dried by distillation over CaH_2 . For the preparation of hybrid silica materials, distilled and deionized water was used (*MilliQ H₂O*).

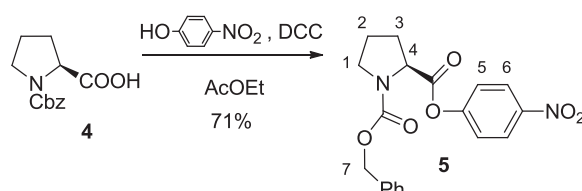
5.2 Preparation of hybrid silica materials derived from proline sulfonamides

5.2.1 Synthesis of (S)-1-((benzyloxy)carbonyl)pyrrolidine-2-carboxylic acid, **4**.¹⁸¹



In a 250 mL three necked round bottom flask benzyl chloroformate (3.3 mL, 1.20 g/mL, 23.2 mmol) and aqueous sodium hydroxide (2 M, 15 mL, 30 mmol) were added simultaneously over 15 min with vigorous stirring to an ice-cooled solution of L-proline (2.345 g, 20.2 mmol) in aqueous sodium hydroxide (2 M, 10 mL, 20 mmol). The solution was then extracted with diethyl ether (2 x 25 mL) and the aqueous layer retained and acidified to approximately pH 4 with 6 M HCl. The resulting acid solution was extracted with ethyl acetate (2 x 50 mL) and the organic layer washed with water (2 x 50 mL), dried over anhydrous sodium sulfate and filtered, yielding **4**,¹⁸¹ as a colourless oil (3.978 g, Yield: 78%). **CF**: $\text{C}_{13}\text{H}_{15}\text{NO}_4$. **MW**: 249.26 g/mol. **¹HRMN (DMSO-*d*⁶, 250 MHz) δ (ppm)**: (rotamer mixture, aprox. 50/50) 7.36-7.28 (m, 5H, H_{ar}), 5.06 (m, 2H, H_6), 4.22 (m, 1H, H_4), 3.42 (m, 2H, H_1), 2.27-2.13 (m, 1H, H_{3a}), 1.98-1.78 (m, 3H, $H_{3b}+H_2$).

5.2.2. Synthesis of (S)-1-benzyl 2-(4-nitrophenyl) pyrrolidine-1,2-dicarboxylate, **5**.¹⁸²



In a 100 mL round bottom flask (S)-1-((benzyloxy)carbonyl)pyrrolidine-2-carboxylic acid **4** (4.09 g, 16.4 mmol) was dissolved in ethyl acetate (30 mL) and *p*-nitrophenol (2.689 g, 16.5 mmol) was added. The solution was cooled to 0°C with an ice bath and then

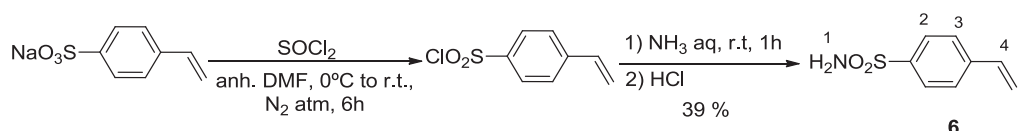
¹⁸¹ Berger, A.; Kurta, J.; Katchalski, E. *J. Am. Chem. Soc.* **1954**, *76*, 5552–5554.

¹⁸² Diakos, C.I.; Zhang, M.; Beale, J.P.; Fenton, R.R.; Hambley, T.W. *Eur. J. Med. Chem.* **2009**, *44*, 2807.

Chapter 2. 5. Experimental Part

N,N'-dicyclohexylcarbodiimide (DCC) (3.48 g, 16.4 mmol) was added. The mixture was stirred for 30 minutes at this temperature and then it was allowed to rise to room temperature and stirred for a further hour. The solid *N,N'*-dicyclohexylurea formed during the reaction was removed by filtration and washed with ethyl acetate. The combined washings and filtrate were taken to dryness by rotary evaporation. The resulting yellow solid was redissolved in chloroform (30 mL) to precipitate further urea derivative that was again removed by filtration. The solution of the filtrate was washed with aqueous Na₂CO₃ (5%, 5 x 20 mL) until the aqueous phase did not present yellow color. The organic layer was washed with water (2 x 25 mL), dried with anhydrous Na₂SO₄ and concentrated under vacuum to afford **5**¹⁸² as a pale yellow solid (4.31 g, Yield: 71%). **CF**: C₁₉H₁₈N₂O₆. **MW**: 370,36 g/mol. **[α]_D²⁰**: -34.7 (DMF, c:0.95). **IR (ATR) (cm⁻¹)**: 2980, 2985, 1765, 1696, 1518, 1423, 1346, 1133, 860, 753, 696. **¹HRMN (DMSO-d⁶, 120°C, 360 MHz) δ (ppm)**: 8.25 (d, J = 9.1 Hz, 2H, H₆), 7.36 – 7.30 (m, 7H, H₅ + H_{ar}), 5.16 (m, 2H, H₇), 4.60 (m, 1H, H₄), 3.56 (apparent t, J = 6.8 Hz, 2H, H₁), 2.45-2.39 (s, 2H, H_{3a}), 2.26-2.17 (m, 1H, H_{3b}), 2.01 (m, 2H, H₂). **¹HRMN (DMSO-d⁶, 25°C, 360 MHz) δ (ppm)**: rotamer mixture (50:50). 8.29 (m, 2H, H₆), 7.36 (m, 7H, H₅ + H_{ar}), 7.16 (d, 2H, J= 7.2 Hz, H₅), 5.20-5.02 (m, 2H, H₇), 4.65-4.54 (m, 1H, H₄), 3.57-3.43 (m, 2H, H₁), 2.44-2.35 (m, 1H, H_{3a}), 2.27-2.15 (m, 1H, H_{3b}), 1.96 (m, 2H, H₂). **¹³CRMN (DMSO-d⁶, 25°C, 90 MHz) δ (ppm)**: 171.57, 171.30, 155.75, 155.47, 154.92, 154.08, 145.86, 137.34, 137.11, 129.02, 128.96, 128.57, 128.43, 128.31, 128.09, 125.92, 125.81, 123.45, 123.27, 66.60, 66.46, 59.23, 58.48, 30.28, 29.20, 24.11, 23.13.

5.2.3 Synthesis of 4-vinylbenzenesulfonamide, **6**.¹⁸³

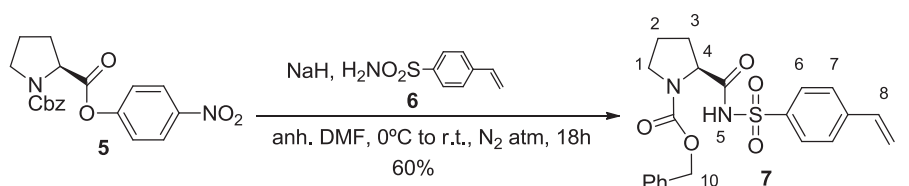


Sodium 4-vinylbenzenesulfonate (5.009 g, 24.3 mmol) was added, under stirring and nitrogen atmosphere, to ice-cooled thionyl chloride (15 mL, 1.64 g/cm³, 207 mmol) keeping the temperature below 10°C. Then, anhydrous DMF (15 mL) was added and the mixture was stirred at room temperature for 6 h and slowly poured into ice-water (100 mL). Extractions with diethyl ether (2 x 40 mL) and dichloromethane (1 x 30 mL) were performed and the organic layers were washed with water and dried with anhydrous Na₂SO₄. The combined organic solution containing 4-vinylsulfonyl chloride was reduced to a third of volume and poured into aqueous ammonia (32%, 15 mL). The mixture was stirred for 1 hour at room temperature. After this time, the residue was neutralized with HCl 10% and extracted with dichloromethane (4 x 50 mL). Organic

¹⁸³ Blanco, B. *PhD Dissertation*. Universitat Autònoma de Barcelona, **2004**.

layer was dried with and concentrated under vacuum to afford 4-vinylbenzenesulfonamide, **6**¹⁸⁴ (1.742 g, Yield: 39%). **CF**: C₈H₉NO₂S. **MW**: 183,23 g/mol. **m.p.**: 135-137 °C (lit.¹⁸⁴138-139°C). ¹HRMN (CDCl₃, 250 MHz) δ (ppm): 7.88 (d, 2H, J = 8.4 Hz, H₂), 7.53 (d, 2H, J = 8.4 Hz, H₃), 6.76 (dd, 1H, J=17.5 Hz and J= 10.9 Hz, H₄), 5.89 (d, 1H, J = 17.5 Hz, H_{5b}), 5.44 (d, 1H, J = 10.9 Hz, H_{5a}), 4.90 (s, 2H, H₁). ¹³CRMN (CDCl₃, 100.6 MHz) δ (ppm): 142.41, 141.43, 135.40, 127.11, 127.06, 111.70. IR (ATR) cm⁻¹: 3341, 3256, 3064, 1866, 1541, 1396, 1302, 1158, 1102, 995, 932, 908, 843, 655.

5.2.4 Synthesis of (S)-benzyl 2-(((4-vinylphenyl)sulfonyl)carbamoyl)pyrrolidine-1-carboxylate, **7**.



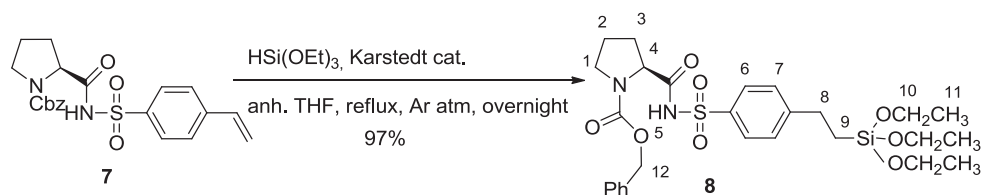
To a solution of *p*-vinylbenzenesulfonamide **6** (1.73 g, 9.45 mmol) in 30 mL of anhydrous DMF was added sodium hydride (0.514 g, 60% dispersion in mineral oil, 12.84 mmol, washed previously with anh. pentane 2 x 5mL) at 0°C. After stirring for 0.5 h allowing to rise to room temperature, *N*-Cbz-L-proline (4-nitrophenyl) ester **5**, (3.191 g, 8.62 mmol), dissolved in 10 mL of anhydrous DMF, was added. The yellow solution was stirred overnight at room temperature and then poured onto crushed ice (200 g). The pH was adjusted to 3 by addition of citric acid. The aqueous layer was extracted with ethyl acetate (3 x 100 mL). The organic layer was washed with water (2 x 100 mL), dried over anhydrous sodium sulfate and concentrated under vacuum. The yellow oil residue was purified by flash chromatography on silica gel using mixtures of hexane/AcOEt (70:30 to AcOEt) to afford **7** as a colourless powder (2.151 g Yield: 60%). **CF**.: C₂₁H₂₂N₂O₅S. **MW**: 414,47 g/mol. **m.p.**: 155-156°C. [α]_D²⁵: -31.7 (CHCl₃, c: 1.04). ¹HRMN (DMSO-d₆, 130°C, 360 MHz) δ (ppm): 7.87 (d, J = 8.4 Hz, 2H, H₆), 7.60 (d, J = 8.4 Hz, 2H, H₇), 7.28 (m, 5H, H_{ar}), 6.82 (dd, 1H, J = 17.6 Hz, J = 10.8 Hz, H₈), 5.93 (d, 1H, J = 17.6 Hz, H_{9a}), 5.44 (d, 1H, J = 10.8 Hz, H_{9b}), 5.03 (d, J= 12.9 Hz, 1H, H_{10a}), 4.90 (d, J=12.9 Hz, H_{10b}), 4.30 (m, 1H, H₄), 3.41 (apparent t, J = 7.2 Hz, 2H, H₁), 2.16 (m, 1H, H_{3a}), 2.01 (m, 3H, H_{3b} + H₂). ¹HRMN (DMSO-d₆, 25°C, 360 MHz) δ (ppm): rotamer mixture (50:50). 12.35 (br, 1H, H₅), 7.86 (d, 2H, J=8.4 Hz, H₆), 7.82 (d, 2H, J=8.4 Hz, H₆), 7.70 (d, J= 8.4 Hz, 2H, H₇), 7.62 (d, J= 8.4 Hz, 2H, H₇), 7.35-7.27 (m, 8H, H_{ar}), 7.13 (m, 2H, H_{ar}), 6.82 (m, 2H, H_{8+8'}), 6.04 (d, 1H, J=17.8 Hz, H_{9a}), 5.99 (d, 1H, J=17.8 Hz, H_{9a'}), 5.49 (d, J=7.7 Hz, 1H, H_{9b}), 5.46 (d, J=7.7 Hz, 1H, H_{9b'}), 5.02-4.65 (m, 4H, H₁₀+H_{10'}), 4.25 (dd, 1H, J= 8.5 Hz, J= 3.3 Hz, H₄), 4.20 (dd, 1H, J= 8.5 Hz, J=

¹⁸⁴ Wiley, R.H.; Schmitt, J.M. *J. Am. Chem. Soc.* **1956**, *10*, 2169.

Chapter 2. 5. Experimental Part

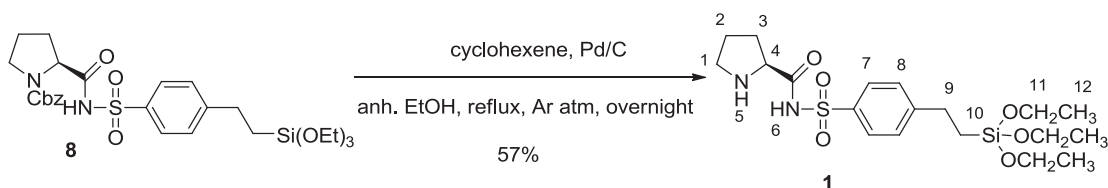
3.3 Hz, H₄), 3.33 (masked by H₂O peak, 4H, H₁+H₁'), 2.15 (m, 2H, H_{3a}+H_{3a}), 1.77-1.66 (m, 6H, H_{3b}+H_{3b}+H₂+H₂). ¹³CRMN (DMSO-d⁶, 25°C, 62.5 MHz) δ (ppm): 173.16, 172.89, 155.50, 154.90, 143.52, 139.47, 138.16, 137.95, 136.57, 129.48, 128.99, 128.16, 127.78, 119.38, 66.28, 60.95, 59.55, 47.00, 46.39, 30.37, 29.27, 23.48, 22.58. IR (ATR) cm⁻¹: 3028, 2367, 2091, 1986, 1680, 1450, 1425, 1351, 1197, 1175, 1140, 1121, 1087, 930, 901, 872, 854, 834, 767, 741, 698, 654. HRMS (ESI): calculated for [¹²C₂₁H₂₂N₂O₅S+Na]⁺: 437.1142 ; found: 437.1133.

5.2.5 Synthesis of (S)-benzyl 2-(((4-(2-(triethoxysilyl)ethyl)phenyl)sulfonyl)carbamoyl)pyrrolidine-1-carboxylate, **8**.



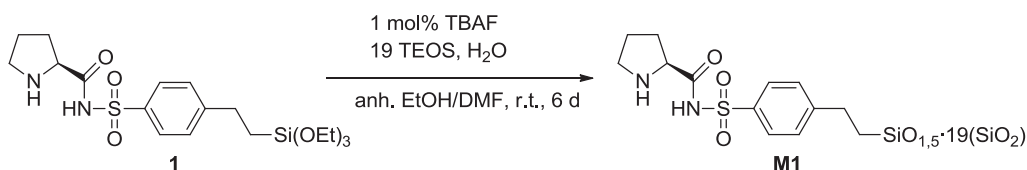
In a 25 mL Schlenk tube under nitrogen atmosphere, compound **7** (2.592 g, 6.25 mmol) was dissolved in dry THF (10 mL) and HSi(OEt)₃ (1.4 mL, 0.89 g/cm³, 7.58 mmol) and Karstedt's catalyst (0.7 mL of a solution containing 2% Pt, 0.06 mmol) were added. The mixture was stirred overnight at reflux under inert atmosphere of Ar. After this time, the volatiles were removed under vacuum and the excess of triethoxysilane was distilled off. The residue was washed with dry pentane (3 x 2 mL) and **8** was obtained as a brown oil (3.590 g, Yield: 97%). **CF**: C₂₈H₄₁N₂O₈SSi. **MW**: 593,78 g/mol. [α]_D²⁵: -33.6 (CHCl₃, c: 0.98). ¹HRMN (DMSO-d⁶, 140°C, 400 MHz) δ (ppm): rotamer mixture (50:50) 7.83 (d, J = 8.2 Hz, 1H, H₆), 7.81 (d, J = 8.2 Hz, 1H, H₆'), 7.38 (d, J = 8.2 Hz, 2H, H₇), 7.28 (m, 5H, H_{ar}), 5.04 -4.99 (m, 2H, H₁₂), 4.31 (m, 1H, H₄), 3.81-3.70 (m, 3H, H₁₀) 3.51 (q, J = 6.9 Hz, 3H, H₁₀'), 3.42 (m, 2H, H₁), 2.73 (m, 2H, H₈), 2.15 (m, 1 H, H_{3a}) 1.78 (m, 3H, H_{3b} + H₂), 1.42-1.28 (m, 1H, H₉), 1.25-1.15 (m, 4.5 H, H₁₁), 1.12 (t, 4.5 H, J = 6.9 Hz, H₁₁'), 0.96-0.74 (m, 1H, H₉'). ¹HRMN (DMSO-d⁶, 25°C, 400 MHz) δ (ppm): rotamer mixture (65:35). 12.31 (br, 1H, H₅), 7.82-7.73 (m, 2H, H₆), 7.47 (m, 1H, H₇), 7.38-7.28 (m, 5H, H_{ar}+H₇'), 7.13 (m, 1H, H_{ar}), 5.02 (apparent s, 1H, H₁₂), 4.79 (d, 0.5 H, J= 12.9 Hz, H₁₂'), 4.79 (d, 0.5 H, J= 12.9 Hz, H₁₂), 4.25-4.19 (m, 1H, H₄), 3.77-3.65 (m, 6H, H₁₀) 3.38 (masked by H₂O peak, 2H, H₁), 2.74-2.60 (m, 2H, H₈), 2.18-2.13 (m, 1 H, H_{3a}) 1.79-1.66 (m, 3H, H_{3b} + H₂), 1.36-1.18 (m, 1H, H₉), 1.18-1.06 (m, 9H, J = 8 Hz, H₁₁'), 0.96-0.82 (m, 1H, H₉'). ¹³CRMN (DMSO-d⁶, 25°C, 100.6 MHz) δ (ppm): 172.10, 154.51, 153.89, 150.91, 150.58, 137.44, 137.21, 128.91, 128.84, 128.75, 128.73, 128.34, 128.03, 127.91, 127.37, 66.18, 66.04, 60.00, 59.44, 58.58, 58.42, 57.87, 56.10, 46.94, 46.40, 30.47, 29.31, 28.33, 28.25, 27.92, 23.58, 22.75, 18.41, 18.04, 14.59, 11.49. IR (ATR) cm⁻¹: 2973, 1673, 1415, 1351, 1078, 768.

5.2.6 Synthesis of (S)-N-((4-(2-(triethoxysilyl)ethyl)phenyl)sulfonyl)pyrrolidine-2-carboxamide, 1.



In a 250mL Schlenk tube under nitrogen, compound **8** (3.590 g, 6.20 mmol) was dissolved in dry EtOH (110mL) and some few drops of dry DMF until a homogeneous solution was obtained. Cyclohexene (3.1 mL, 0.814 g/cm³, 30.7 mmol) and Pd/C 10% (0.422 g, 10% Pd, 0.04 mmol) were added and the mixture was stirred overnight at reflux under atmosphere of Ar. After this time, the reaction was cooled to room temperature and filtered through cannula. The filtrates were concentrated under vacuum affording a yellow solid, which was washed with dry THF (3x 20 mL) giving **1** as a white solid (1.687 g, Yield: 57%). **CF**: C₁₉H₃₂N₂O₆SSi. **MW**: 444.62 g/mol. **m.p.**: 189-193°C. **[α]_D^T**: -31.9 (CHCl₃, c:1.04). **¹HRMN (DMSO-d₆, 25°C, 400 MHz) δ (ppm)**: 8.89 (br, 1H, H₆), 8.18 (br, 1H, H₅), 7.68 (d, 2H, J = 8Hz, H₇), 7.24 (d, 2H, J = 8Hz, H₈), 3.82-3.66 (m, 1H, H₄), 3.76 (q, J = 8 Hz, 6H, H₁₁) 3.19-3.13 (m, 1H, H₁), 3.07-3.01 (m, 1H, H₁), 2.66-2.59 (m, 2H, H₉), 2.12-2.09 (m, 1 H, H_{3a}), 1.84-1.76 (m, 2H, H₂), 1.74-1.69 (m, 1H, H_{3b}), 1.32 (m, 1H, H₁₀), 1.15 (t+m, 9H, J=8 Hz, H₁₂), 0.92-0.87 (m, 1H, H₁₀). **¹³CRMN (DMSO-d₆, 25°C, 100.6 MHz) δ (ppm)**: 172.12, 147.13, 146.73, 143.41, 127.42, 62.00, 57.87, 45.31, 28.99, 28.12, 27.86, 23.24, 17.88, 15.20, 11.73. **HRMS (ESI)**: calculated for [¹²C₁₉H₃₂N₂O₆SSi+Na]⁺: 467.1643; found: 467.1637. **IR (ATR) cm⁻¹**: 2972, 1585, 1254, 1077, 830.

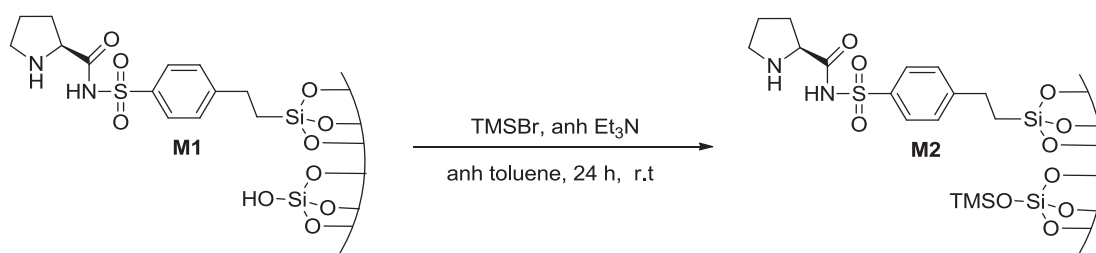
5.2.7 Preparation of the hybrid silica material M1.



To a stirred solution of **1** (1.68 g, 3.79 mmol) and TEOS (16.3 mL, 0.940 g/cm³, 71.9 mmol) in a mixture of anhydrous EtOH (66 mL) and dry DMF (11 mL) at room temperature was added a mixture of MilliQ water (5.4 mL, 300 mmol, H₂O/EtO=1) and a commercial solution of 1M TBAF in anhydrous THF (760 μL, 0.76 mmol, 1 mol% F with respect to Si). The resulting solution was stirred for 1 minute and after this time a gel was formed which was left to age at room temperature for 6 days. At that time, the gel was crushed, filtered off and washed with water (3 x 20 mL), ethanol (3x 20 mL) and acetone (3 x 20 mL). The solid obtained was extracted with chloroform in a soxhlet

apparatus in order to remove residual DMF. The final solid was dried overnight at 50°C under vacuum (1.0 mbar) and finally **M1** (5.867 g) was obtained as a white solid. ^{29}Si -CP-MAS NMR (79.5 MHz) δ : -62.64 (T^2), -72.07 (T^3), -96.50 (Q^2), -105.22 (Q^3), -113.45 (Q^4). EA calculated for $\text{C}_{13}\text{H}_{17}\text{N}_2\text{O}_3\text{SSiO}_{1.5}\cdot 19\text{SiO}_2$ (considering complete conversion): 10.66 %C, 1.17%H, 1.91 %N, 2.18 %S, 38.20 %Si; found: 12.04 %C, 2.41%H, 2.49 %N, 1.37 %S, 35.64 %Si (0.89 mmol proline sulfonamide/ g material). Some DMF remaining entrapped in the material despite the overnight drying under vacuum at 50°C, which would explain the fact that the N content in **M1** was higher than expected. BET S_{BET} : 450 m^2/g ; pore diameter: pore diameter distribution centered around 35 Å; average pore diameter (4V/A, BET): 41 Å; pore volume: 0.43 cm^3/g . IR (ATR) ν (cm^{-1}): 1652, 1058, 801.

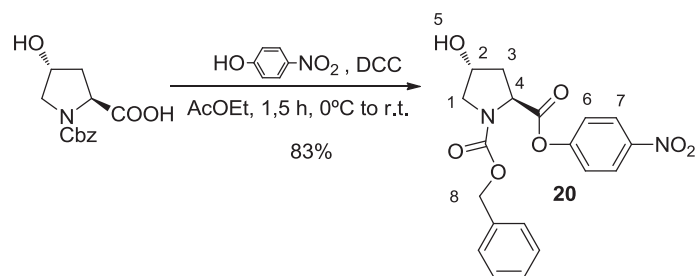
5.2.8 Preparation of hybrid silica material M2



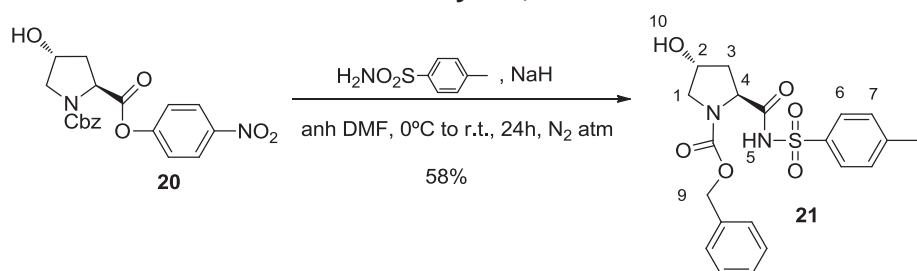
In a 50 mL Schlenk tube under nitrogen material **M1** (0.257 g) was added and degassed for 30 min. After this time, anhydrous toluene (15 mL), TMSBr (0.5 mL, 1.16 g/cm^3 , 3.79 mmol, 1 mol TMS respect to 1 mol $-\text{OH}^{185}$) and anhydrous Et₃N (0.5 mL, 0.727 g/cm^3 , 3.49 mmol) were added and stirred at r.t. under Ar atmosphere for 24 h. Then, the material was filtered and washed with toluene (3 x 15 mL), methanol (3 x 15 mL), Et₂O (3 x 15 mL) and acetone (3 x 10 mL) to afford **M2** as a white powder (0.249 g). EA found: 11.97 %C, 2.30%H, 0.96 %N, 1.31 %S, 35.64 %Si (0.34 mmol proline sulfonamide/ g material). IR (ATR) ν (cm^{-1}): 2963, 1621, 1052, 844, 799, 757.

¹⁸⁵ To calculate the maximum number of silanols to be protected, we supposed that all trialkoxy and tetraalkoxy groups present in the reactants had been hydrolyzed to silanols but not condensed, then each triethoxysilane moiety would give 3 silanols and each equivalent of TEOS would give 4 more Si-OH.

5.2.9 Synthesis of (2S,4R)-1-benzyl 2-(4-nitrophenyl) 4-hydroxypyrrolidine-1,2-dicarboxylate, **20**.

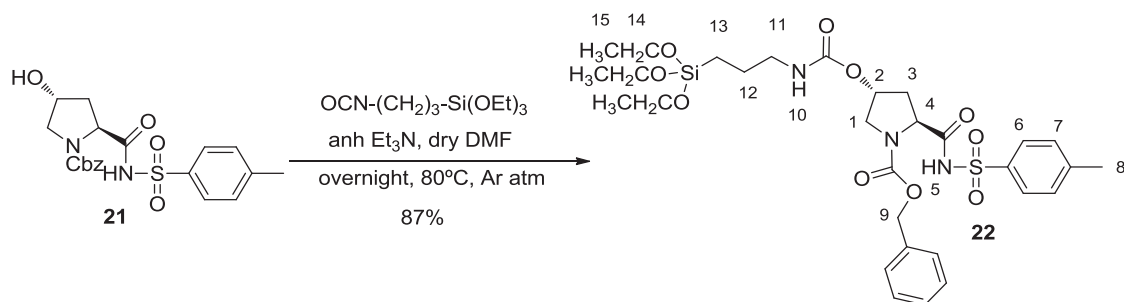


In a 50 mL round bottom flask commercial *N*-Cbz-*trans*-4-hydroxy-L-proline (0.558 g, 2.1 mmol) was dissolved in ethyl acetate (5 mL) and few drops of DMF. To this solution *p*-nitrophenol (0.330 g, 2.4 mmol) was added. The solution was cooled to 0°C with an ice bath and then *N,N'*-dicyclohexylcarbodiimide (DCC) (0.461 g, 2.2 mmol) was added. The mixture was stirred for 30 minutes at this temperature and then it was allowed to rise to room temperature and stirred for a further hour. The solid *N,N'*-dicyclohexylurea formed during the reaction was removed by filtration and washed with ethyl acetate. The combined washings and filtrate were taken to dryness by rotary evaporation. The resulting yellow solid was redissolved in chloroform (30 mL) to precipitate further urea derivative that was again removed by filtration. The solution of the filtrate was washed with Na₂CO₃ (5%, 5 x 20 mL) until the aqueous phase did not present yellow color. The organic layer was washed with water (2 x 25 mL), dried with anhydrous Na₂SO₄ and concentrated under vacuum to afford **20** as a pale yellow solid (0.670 g, Yield: 83%). **CF**: C₁₉H₁₈N₂O₇. **MW**: 386,36 g/mol. **[α]_D^T**: -85.9 (CHCl₃, c:1.2). **¹HRMN (CDCl₃, 400 MHz) δ (ppm)**: (mixture of rotamers 50:50) 8.17 (d, 2H, J = 9.1 Hz, H₇), 8.03 (d, 2H, J = 9.1 Hz, H₇), 7.28-7.18 (m + d, J= 9.1 Hz, 14 H, H_{ar}+H₆, masked by CDCl₃ signal), 6.72 (d, J = 9.1 Hz, 2H, H₆), 5.23 (d, 1H, J= 11.8 Hz, H_{8a}), 5.10 (apparent s, 2H, H₈), 4.94 (d, 1H, J= 11.8 Hz, H_{8b}), 4.66 (q, 2H, J = 8 Hz, H₄+H_{4'}), 4.53 (br, 2H, H₅+H_{5'}), 3.70-3.66 (m, 2H, H₂+H_{2'}), 2.46-2.37 (m, 2H, H_{3a}+H_{3a'}), 2.22-2.14 (m, 2H, H_{3b}+H_{3b'}), 1.86-1.70 (m, 4H, H₁+H_{1'}). **¹³CRMN (CDCl₃, 25°C, 100.6 MHz) δ (ppm)**: 171.00, 170.96, 155.76, 155.59, 155.29, 154.82, 145.90, 145.81, 136.57, 136.23, 128.97, 128.83, 128.80, 128.49, 128.22, 128.13, 125.49, 125.38, 122.67, 122.33, 70.25, 69.36, 67.72, 67.46, 58.15, 57.70, 55.37, 54.71, 39.08, 38.18, 33.50, 25.19, 24.52. **IR (ATR) cm⁻¹**: 3326, 2931, 1689, 1616, 1591, 1522, 1498, 1416, 1345, 1206, 1177, 1127, 1082, 967, 918, 862, 738, 697.

5.2.10 Synthesis of (2*S*,4*R*)-benzyl 4-hydroxy-2-(tosylcarbamoyl)pyrrolidine-1-carboxylate, **21**.

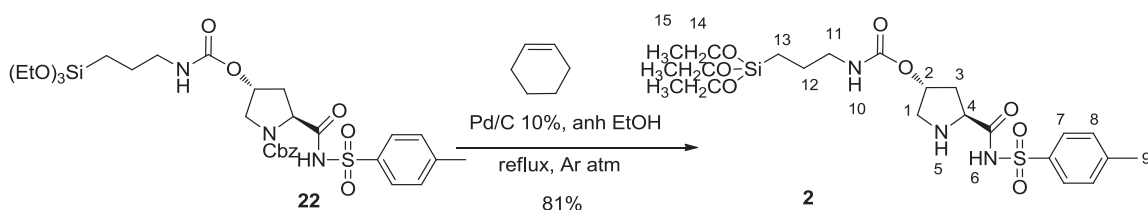
To a solution of *p*-toluenesulfonamide (3.135 g, 18.3 mmol) in 40 mL of dry DMF was added sodium hydride (0.734 g, 60% dispersion in mineral oil, 18.3 mmol) at 0°C. After stirring for 30 minutes allowing to rise to room temperature, compound **20**, (5.108 g, 13.2 mmol), dissolved in 25 mL of dry DMF and 10 mL of dry CH₂Cl₂, was added to the reaction mixture. The yellow solution was stirred overnight at room temperature and then poured onto crushed ice (200 g). The pH was adjusted to 3 by addition of citric acid. The aqueous layer was extracted with ethyl acetate (3 x 100 mL). The organic layer was washed with water (2 x 100 mL), dried over anhydrous sodium sulfate and concentrated under vacuum. The yellow oil residue was purified by flash chromatography on silica gel using hexane/AcOEt (70:30 to AcOEt) to afford the corresponding proline sulfonamide **21** as a colourless powder (3.20 g Yield: 58%). **CF**:C₂₀H₂₂N₂O₆S. **MW**: 418,46 g/mol. **mp.**: 86-88°C. **[α]_D²⁰**: -91.7 (CHCl₃, c: 1.15). **¹H NMR (DMSO-*d*⁶, 400 MHz) δ (ppm)**: (mixture of rotamers 50:50) 12.30 (br, 2H, H₅ + H_{5'}), 7.78 (d, 2H, J = 8.2 Hz, H₇), 7.74 (d, 2H, J = 8.2 Hz, H_{7'}), 7.41 (d, 2H, J = 8.2 Hz, H₆), 7.36-7.28 (m, 10H, H_{ar} + H_{ar'} + H_{6'}), 7.13 (m, 2H, H_{ar} + H_{ar'}), 5.11 (br, 2H, H₁₀ + H_{10'}), 5.02 (m, 2H, H₉), 4.95 (d, 1H, J=13.0 Hz, H_{9a'}), 4.64 (d, 1H, J=13.0 Hz, H_{9b'}), 4.32 (ap t, 1H, J=8.0 Hz, H₄), 4.26 (ap t, 1H, J=8.0 Hz, H_{4'}), 4.18 (m, 2H, H₂ + H_{2'}), 3.42-3.33 (masked by H₂O peak, m, 4H, H₃ + H_{3'}), 2.40 (s, 3 H, H₈), 2.32 (s, 3 H, H_{8'}), 2.15-2.04 (m, 2H, H₁), 1.76-1.69 (m, 1H, H_{1a'}), 1.67-1.60 (m, 1H, H_{1b'}). **¹³C NMR (DMSO-*d*⁶, 25°C, 100.6 MHz) δ (ppm)**: 172.07, 171.65, 154.88, 154.17, 144.84, 137.32, 137.15, 136.96, 136.86, 130.06, 130.03, 128.93, 128.73, 128.39, 128.07, 128.04, 127.89, 127.35, 68.67, 67.91, 58.97, 58.48, 55.45, 54.95, 37.91, 20.88. **IR (ATR) cm⁻¹**: 2880, 1672, 1596, 1419, 1347, 1171, 1129, 966, 915, 867, 814, 769, 739, 697, 658. **HRMS (ESI)**: calculated for [¹²C₂₀H₂₂N₂O₆S+Na]⁺: 441.1091; found: 441.1095.

5.2.11 Synthesis of (2*S*,4*R*)-benzyl 2-(tosylcarbamoyl)-4-(((3-(triethoxysilyl)propyl)carbamoyl)oxy)pyrrolidine-1-carboxylate, **22**.



In a 25 mL Schlenk tube under argon atmosphere, compound **21** (1.498 g, 3.58 mmol), dry and degassed NEt_3 (0.5 mL, 0.727 g/cm³, 3.59 mmol) and freshly distilled (3-isocyanatopropyl)triethoxysilane (1.8 mL, 0.999 g/cm³, 7.26 mmol) were dissolved in dry DMF (8 mL). The mixture was stirred overnight under argon atmosphere at 80°C. After this time, DMF and excess of silane were distilled off, and **22** was obtained as a pale brown paste (2.075 g, Yield: 87%). **CF**: $\text{C}_{30}\text{H}_{43}\text{N}_3\text{O}_{10}\text{SSi}$. **MW**: 665,83 g/mol. $[\alpha]_D^{25}$: -79.9 (CHCl_3 , c:1.3). **¹HRMN (DMSO-*d*⁶, 400 MHz) δ (ppm)**: (mixture of rotamers 50:50) 12.11 (br, 1H, H₅), 7.76 (m, 2H, H₆), 7.26 (m, 6H, H_{ar} + H₇), 7.10 (m, 1H, H_{ar}), 5.74 (br, 1H, H₁₀), 5.00 (m, 1.5H, H₉ + H₄), 4.63 (m, 1H, H₉), 4.49 (m, 0.5H, H₄), 4.32 (m, 1H, H₂), 3.98-3.71 (m, 6H, H₁₄), 3.50 (m, 2H, H₁), 2.96 (m, 2H, H₁₁), 2.37 (s, 1.5H, H₈), 2.30 (s, 1.5H, H₈), 2.37-1.63 (m, 2H, H₃), 1.46 (m, 2H, H₁₂), 1.13 (m, 9H, H₁₅), 0.49 (m, 2H, H₁₃). **¹³CRMN (DMSO-*d*⁶, 25°C, 100.6 MHz) δ (ppm)**: 171.52, 156.96, 155.84, 154.41, 153.90, 144.33, 136.86, 129.44, 128.51, 128.44, 127.76, 78.40, 71.35, 69.27, 66.29, 58.44, 57.72, 52.77, 42.93, 36.37, 35.21, 22.57, 20.94, 17.77, 6.92. **IR (ATR) cm⁻¹**: 3345, 2974, 2978, 2883, 2359, 1697, 1537, 1417, 1350, 1254, 1191, 1167, 1072, 955, 875, 767, 696, 658. **HRMS (ESI)**: calculated for $[\text{C}_{30}\text{H}_{43}\text{N}_3\text{O}_{10}\text{SSi}+\text{Na}]^+$: 688.2331; found: 688.2330.

5.2.12 Synthesis of (3*R*,5*S*)-5-(tosylcarbamoyl)pyrrolidin-3-yl (3-(triethoxysilyl)propyl)carbamate, **2**

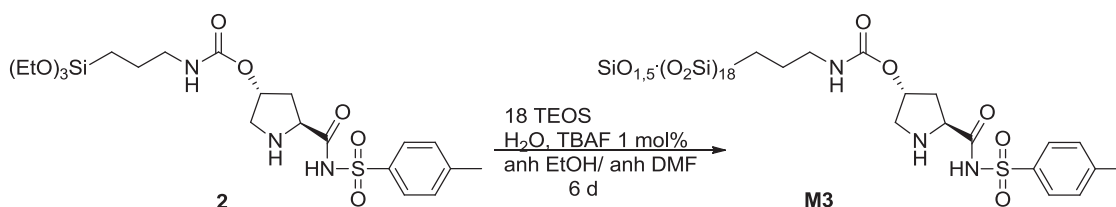


In a 10mL Schlenk tube under nitrogen, **22** (0.226 g, 0.34 mmol) was dissolved in dry EtOH (3 mL). Cyclohexene (150 μL , 0.814 g/cm³, 1.48 mmol) and Pd/C 10% (0.079 g, 10% Pd, 0.075 mmol) were added and the mixture was stirred overnight at reflux under

Chapter 2. 5. Experimental Part

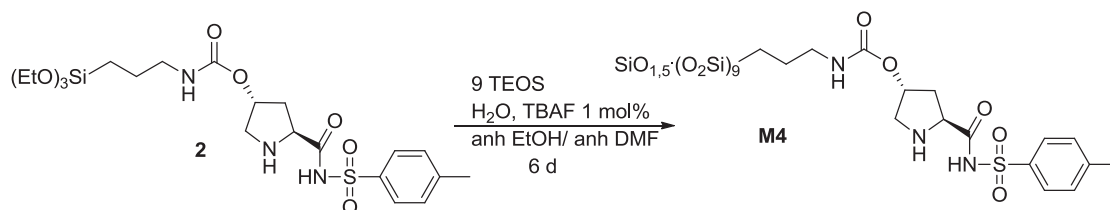
atmosphere of Ar. After this time, the reaction was cooled to room temperature and filtered through cannula. The filtrates were concentrated under vacuum affording **2** as a yellow solid (0.181 g, Yield: 81%). **CF:** C₂₂H₃₇N₃O₈SSi. **MW:** 531.69 g/mol. **mp.:** >270°C. $[\alpha]_D^{25}$: -67.0 (CHCl₃, c:1.57). **¹HRMN (DMSO-d⁶, 250 MHz) δ (ppm):** 7.67 (d, 2H, J = 7.5 Hz, H₇), 7.20 (d, 2H, J = 7.5 Hz, H₈), 3.99-3.69 (m, 6H, H₁₄), 3.12-3.03 (m, 2H, H₄ + H₂), 2.94 (m, 2H, H₁₁), 2.50 (masked by DMSO-d⁶ peak, 2H, H₁), 2.31 (s, 3H, H₉), 2.23-1.95 (m, 2H, H₃), 1.45 (m, 2H, H₁₂), 1.20-0.96 (m, 9H, H₁₅), 0.50 (m, 2H, H₁₃). **¹³CRMN (DMSO-d⁶, 25°C, 100.6 MHz) δ (ppm):** 171.93, 146.69, 146.35, 127.51, 127.44, 62.00, 45.25, 30.63, 28.96, 27.85, 23.23, 18.07, 15.20. **IR (ATR) cm⁻¹:** 3312, 2928, 1697, 1548, 1443, 1252, 1198, 1130, 1076, 957, 837, 813, 775, 663. **HRMS (ESI):** calculated for [¹²C₂₂H₃₇N₃O₈SSi+Na]⁺: 554.1963; found: 554.1974.

5.2.13 Preparation of hybrid silica material M3

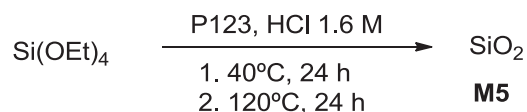


To a stirred solution of **2** (0.519 g, 1.01 mmol) and TEOS (4.1 mL, 0.940 g/cm³, 18 mmol) in anhydrous EtOH (19 mL) and a few drops of anhydrous DMF (1.5 mL) were added MilliQ water (1.4 mL, 77.8 mmol, H₂O/EtO = 1) and a commercial solution of 1M TBAF in anhydrous THF (0.2 mL, 0.2 mmol, 1 mol% F respect to Si). The resulting solution was stirred for 5 min at room temperature. After this time a gel was formed which was left to age at room temperature for 6 days. At that time, the gel was crushed, filtered off and washed with water (3 x 15 mL), ethanol (3 x 15 mL) and acetone (3 x 15 mL). After this time the solid was washed with CHCl₃ with a Soxhlet apparatus for 48 h in order to remove the residual DMF entrapped in the material. The solid was dried overnight at 50°C under vacuum affording **M3** (1.419 g) as a white solid. **²⁹Si-CP-MAS NMR (79.5 MHz) δ:** -66.53 (T²), -75.05 (T³), -101.81 (Q²), -111.73 (Q³), -120.60 (Q⁴). **IR (ATR) (cm⁻¹):** 2359, 2019, 1999, 1969, 1083, 203, 672, 633. **BET** S_{BET}: 353 m²/g; pore diameter distribution centered around 40 Å; average pore diameter (4V/A, BET): 53 Å; pore volume: 0.60 cm³/g. **EA calculated for C₁₆H₂₂N₃O₅SSiO_{1.5}·18SiO₂** (considering complete conversion): 12.88 %C, 1.49%H, 2.82 %N, 2.14 %S, 35.64 %Si; **found:** 9.02 %C, 2.41%H, 1.90%N, 0.42 %S, 33.06%Si (0.45 mmol proline sulfonamide / g material).

5.2.14 Preparation of hybrid silica material M4



To a stirred solution of **2** (0.836g, 1.57 mmol) and TEOS (3.2 mL, 0.940 g/cm³, 14.1 mmol) in anh EtOH (19 mL) and a few drops of anh DMF (1.5 mL) were added MilliQ water (1.1 mL, 61.1 mmol, H₂O/EtO = 1) and a commercial solution of 1M TBAF in anhydrous THF (157 μL, 0.16 mmol, 1 mol% F respect to Si). The resulting solution was stirred for 5 min at room temperature. After this time a gel was formed which was left to age at room temperature for 6 days. At that time, the gel was crushed, filtered off and washed with water (3 x 15 mL), ethanol (3 x 15 mL) and acetone (3 x 15 mL). After this time the solid was washed with CHCl₃ with a Soxhlet apparatus for 48 h in order to remove the residual DMF entrapped in the material. The solid was dried overnight at 50°C under vacuum affording **M4** (1.560 g) as a white solid. **¹³C-CP-MAS NMR (100.6 MHz) δ:** 166.03, 152.93, 134.26, 121.62, 68.19, 54.71, 45.68, 35.71, 29.41, 16.64, 4.87, 1.80. **²⁹Si-CP-MAS NMR (79.5 MHz) δ:** -68.48 (T²), -76.21 (T³), -102.26 (Q²), -112.30(Q³), -121.39 (Q⁴). **IR (ATR) (cm⁻¹):** 3404, 2091, 2031, 1563, 1080, 954, 795, 665. **BET** S_{BET}: <5 m²/g; non porous material. **EA calculated for C₁₆H₂₂N₃O₅SSiO_{1.5}·9SiO₂** (considering complete conversion): 20.19 %C, 2.33%H, 4.41 %N, 3.36 %S, 29.39 %Si; **found:** 14.19 %C, 2.67%H, 3.52%N, 0.87 %S, 29.33%Si (0.84 mmol proline sulfonamide/ g material).

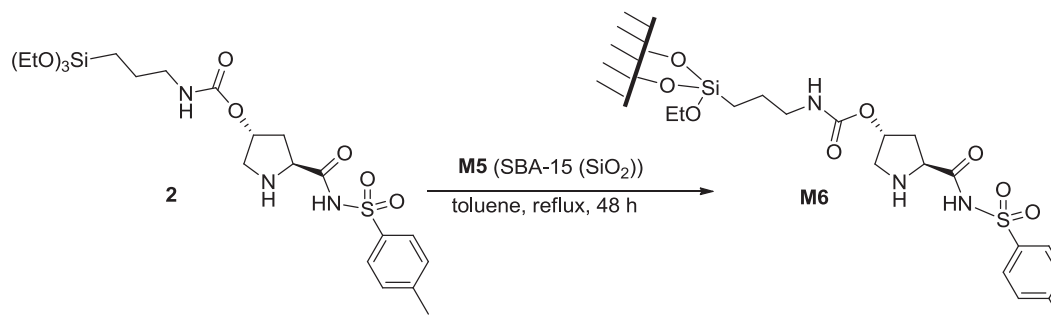
5.2.15 Preparation of mesostructured silica of SBA-15 type, M5.¹⁷⁴

Under stirring P123 (12.3 g, 2.12 mmol) was dissolved in aqueous HCl (450 mL, 1.6 M, 720 mmol) at 40°C in a 1L round bottomed flask. When this solution was completely homogeneous (2h aprox), TEOS 98% (27mL, 0.94 g/cm³, 122 mmol) was added and the mixture was stirred for 24 h at 40°C. Then a reflux condenser was placed onto the flask, the stirring was stopped and the suspension heated at 120°C for 24 h more. The mixture was cooled down to room temperature, filtered off and the solid washed with water (2 x 100 mL) and dried under air overnight. To eliminate P123, this solid was calcined (ramp 5 min, 10°C/min, then 6 h at 500°C and finally cooled down to r.t.). Mesostructured silica **M4** was obtained as a white solid (7.78 g, 130 mmol). **IR (ATR) (cm⁻¹):** 3389, 1036, 809. **BET** S_{BET}: 732 m²/g; pore diameter: pore diameter distribution

Chapter 2. 5. Experimental Part

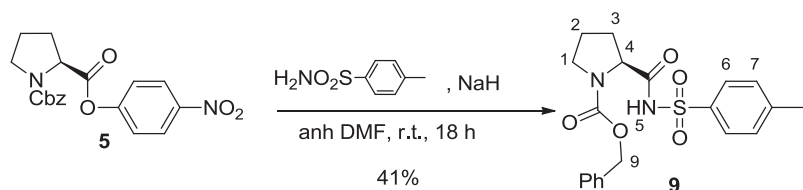
centered around 70 Å; average pore diameter (4V/A, BET): 59 Å; pore volume: 1.03 cm³/g. **pXRD**: (2D hexagonal) (see Annex).

5.2.16 Preparation of hybrid silica material M6



In a 250 mL round bottom flask equipped with a Dean-Stark apparatus, compound **2** (0.806 g, 1.60 mmol) and SBA-15 type silica **M5** (1.521 g, 25.4 mmol) were refluxed in dry toluene (80 mL) for 24 h. After this time the suspension was filtered. The solid was washed with ethanol (3 x 25 mL), acetone (3 x 25 mL) and diethyl ether (3 x 25 mL) then dried overnight at 50°C under vacuum and finally crushed to give the grafted material **M6** as a white solid (2.067 g). **²⁹Si-CP-MAS NMR (79.5 MHz) δ**: -68.17 (T²), -77.27 (T³), -100.73 (Q²), -110.87 (Q³), -119.98 (Q⁴). **IR (ATR) (cm⁻¹)**: 2360, 2029, 1079, 953, 805, 615. **BET** S_{BET}: 328 m²/g; pore diameter: pore diameter distribution centered around 60 Å; average pore diameter (4V/A, BET): 63 Å; pore volume: 0.55 cm³/g. **pXRD**: q = 0.653 nm⁻¹, 1.138 nm⁻¹, 1.304 nm⁻¹; (2D hexagonal). **EA calculated**: 20.19 %C, 2.33 %H, 4.41 %N, 3.36 %S, 29.39 %Si; **found**: 10.36 %C, 2.0.6 %H, 2.20 %N, 0.58 %S, 30.09 %Si (0.52 mmol proline sulfonamide/ g material).

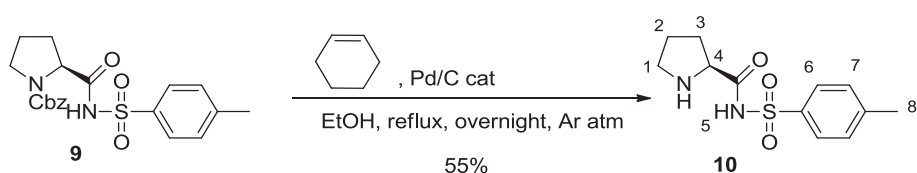
5.2.17 Preparation of (S)-benzyl 2-(tosylcarbamoyl)pyrrolidine-1-carboxylate, 9.



To a solution of *p*-toluenesulfonamide (0.893 g, 5.22 mmol) in 20 mL of dry DMF was added sodium hydride (0.216 g, 60% dispersion in mineral oil, 5.40 mmol). After stirring for 30 minutes at room temperature, *N*-Cbz-L-proline (4-nitrophenyl) ester **5**, (1.496 g, 3.94 mmol) dissolved in 5 mL of dry DMF was added to the reaction. The yellow solution was stirred overnight at room temperature and then poured onto crushed ice (50 g). The pH was adjusted to 3 by addition of citric acid. The aqueous layer was extracted with ethyl acetate (3 x 50 mL). The organic layer was washed with water (2 x 50 mL), dried over anhydrous sodium sulfate and concentrated under vacuum. The

yellow oil residue was purified by flash chromatography on silica gel using hexane/AcOEt mixtures (70:30 to AcOEt) to afford the corresponding proline sulfonamide **9** as a pale brown powder (0.645 g Yield: 41%). **CF**: C₂₀H₂₂N₂O₅S. **MW**: 402.46 g/mol. **m.p.**: 129-132°C. $[\alpha]_D^{25}$: -31.5 (DMF, c:1.04). **¹HRMN (CDCl₃, 400 MHz) δ (ppm)**: 10.39 (br, 1H, H₅), 7.90 (d, 2H, J = 7.0 Hz, H₆), 7.38-7.9 (m, 5H, H_{ar}), 7.29 (d, 2H, J = 7.0 Hz, H₇), 5.19 (m, 2H, H₉), 4.27 (m, 1H, H₄), 3.43 (m, 2H, H₁), 2.41 (s, 3H, H₈), 1.85 (m, 3H, H₃+H_{2a}), 1.25 (m, 1H, H_{2b}). **¹³CRMN (CDCl₃, 100.6 MHz) δ (ppm)**: 175.18, 157.49, 149.60, 141.19, 136.28, 129.76, 128.93, 128.70, 128.63, 128.49, 68.12, 60.64, 46.99, 23.99, 23.09, 21.31.

5.2.18 Preparation of (S)-N-tosylpyrrolidine-2-carboxamide, **10**.

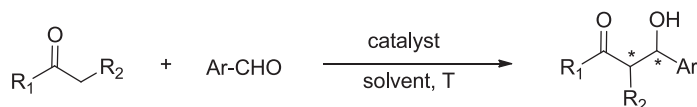


In a round bottom flask, *N*-Cbz protected proline sulfonamide **9** (2.252 g, 8.39 mmol) was dissolved in EtOH (11 mL). Cyclohexene (280 μL, 0.814 g/cm³, 27.6 mmol) and Pd/C 10% (1.293 g, 10% Pd, 0.135 mmol) were added and the mixture was stirred overnight at reflux. After this time, the reaction was cooled to room temperature and filtered through cannula. The precipitate was washed with warm MeOH (2 x 50 mL). The filtrates were concentrated under vacuum affording a solid which recrystallized from MeOH to give **10**¹⁸⁶ as a white solid (0.671 g, Yield: 55%). **CF**: C₁₂H₁₆N₂O₃S. **MW**: 268.33 g/mol. **m.p.**: 189-191°C. $[\alpha]_D^{25}$: -33.7 (DMF, c:0.97). **¹HRMN (DMSO-d₆, 400 MHz) δ (ppm)**: 8.47 (br, 1H, H₅), 7.66 (d, 2H, J = 8Hz, H₆), 7.19 (d, 2H, J = 8Hz, H₇), 3.79 (apparent t, 1H, J = 6Hz, H₄), 3.16-3.12 (m, 1H, H_{1a}), 3.06-2.99 (m, 1H, H_{1b}), 2.32 (s, 3H, H₈), 2.12-2.08 (m, 1H, H_{3a}), 1.84-1.76 (m, 2H, H_{3b} + H_{2a}), 1.74-1.70 (m, 1H, H_{2b}). **¹³CRMN (DMSO-d₆, 100.6 MHz) δ (ppm)**: 171.99, 143.08, 140.53, 128.67, 127.38, 61.98, 45.29, 29.01, 23.25, 20.74.

¹⁸⁶ Berkessel, A.; Koch, B.; Lex, B. *Adv. Synth. Catal.* **2004**, 346, 1141.

5.3 Catalytic tests with proline sulfonamide derived organosilicas

5.3.1 Intermolecular aldol reactions

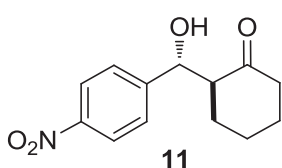


General procedure for homogeneous catalyst. In a vial, cyclohexanone (110 μL , 0.947 g/mL, 1.07 mmol), milliQ water (106 μL , 0.5 mL/mmol aldehyde) and homogeneous catalyst¹⁸⁷ were stirred together for 20 min at room temperature. After this time, the corresponding aldehyde (0.21 mmol) was added and the mixture was stirred until ¹H-NMR showed complete consumption of the aldehyde. Then the crude mixture was diluted with AcOEt (2 mL) and anhydrous Na₂SO₄ was added. The organic layer was then filtered and concentrated under vacuum to give a solid or an oil. From this residue, the conversion, the anti/syn ratio of the diastereomeric mixtures and *er* were determined.

General procedure for silica-supported catalysts. In a vial, cyclohexanone (5 eq), milliQ water (0.5 mL/mmol aldehyde) and the supported catalyst¹⁸⁷ were stirred together for 20 min at room temperature. After this time, the corresponding aldehyde (1 equiv.) was added and the mixture was stirred until ¹H-NMR showed complete consumption of the aldehyde. Then the crude mixture was diluted with AcOEt (2 mL) and filtered. The insoluble catalytic material was washed several times with AcOEt (3 x 1.5 mL) and the combined filtrates were concentrated under vacuum. From this residue, the conversion, the anti/syn ratio of the diastereomeric mixture and *er* were determined. The catalytic material was dried under vacuum and directly used in the next cycle.

Compounds **11-15** have been previously described and their spectral and analytical data were consistent with literature values.

(S)-2-((R)-hydroxy(4-nitrophenyl)methyl)cyclohexanone, 11.¹⁸⁸ **CF:** C₁₃H₁₅NO₄.



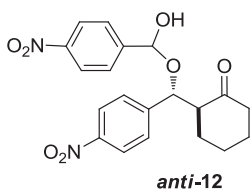
MW: 249.26 g/mol. The diastereomeric ratio, as determined by ¹H-NMR analysis of the final solid, was found to be between 75/25-97/3, favoring the *anti* isomer. ¹H-NMR

¹⁸⁷ Check the amount of catalyst in the corresponding tables in section section 2:3 Results and Discussion.

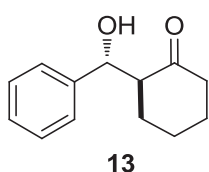
¹⁸⁸ Almaši, D.; Alonso, D.A.; Nájera, C. *Adv. Synth. Catal.* **2008**, 350, 2467.

(CDCl₃, 250 MHz): (diastereomeric mixture *anti/syn* 85/15) 8.21 (d, J = 7.6 Hz, 2H_{anti}, 2H_{syn}), 7.51 (d, J = 7.6 Hz, 2H_{anti}, 2H_{syn}), 5.48 (br, 1H_{syn}), 4.90 (d, J = 7.6 Hz, 1H_{anti}), 4.08 (m, 1H_{anti}), 3.18 (d, J = 4.2 Hz, 1H_{syn}), 2.64-2.32 (m, 2H_{anti}, 2H_{syn}), 2.16-2.04 (m, 1H_{anti}, 1H_{syn}), 1.84-1.25 (m, 6H_{anti}, 6H_{syn}). **HPLC**: Daicel Chiralpack AD-H column, flow 1 mL/min, 254 nm, *n*-hexane/*i*-PrOH 95/5, *anti* isomer: t_{maj}: 71.70 min, t_{min}: 52.76 min; *syn* isomer t_{maj}: 46.92 min, t_{min}: 38.51 min.

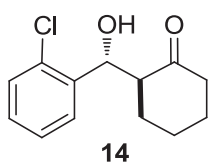
2-[[hydroxy(4-nitrophenyl)methoxy](4-nitrophenyl)methyl]cyclohexanone,



12.¹⁸⁹ **CF**: C₂₀H₂₀N₂O₇ **MW**: 400.4 g/mol. The presence of diastereomer *anti-12* was observed in some aldol reaction tests to obtain **11**. Its spectroscopic data matched those previously described. **¹H-NMR (CDCl₃, 250 MHz)**: (some of the characteristic signals) 8.21 (d, J = 8.4 Hz, 2H, H_{ar}), 7.73 (d, J = 8.9 Hz, 2H, H_{ar}), 7.55 (m, 2H, H_{ar}), 6.53 (s, 1H), 5.11 (d, J = 10.3 Hz, 1H). The rest of the signals for **12** were masked by **11**. **HPLC**: a peak at 90.00 min for *anti-12* was observed when using Daicel Chiralpack AD-H column, flow 1 mL/min, 254 nm, *n*-hexane/*i*-PrOH 95/5.



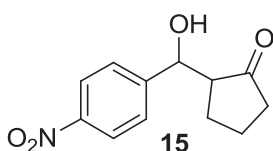
(S)-2-((R)-hydroxy(phenyl)methyl)cyclohexanone, 13.¹⁸⁸ **CF**: C₁₃H₁₆O₂. **MW**: 204.26 g/mol. The diastereomeric ratio, as determined by ¹H-NMR analysis of the final solid, was found to be between 54/46-98/2, favoring the *anti* isomer. **¹H-NMR (CDCl₃, 250 MHz)**: (diastereomeric mixture *anti/syn* 86/14), 7.49-7.28 (m, 5H_{anti}, 5H_{syn}), 5.39 (br, 1H_{syn}), 4.79 (d, J = 9.1 Hz, 1H_{anti}), 4.09 (br, 1H_{anti}), 2.66-2.32 (m, 3H_{anti}, 3H_{syn}), 2.21-2.05 (m, 1H_{anti}, 1H_{syn}), 1.76-1.52 (m, 4H_{anti}, 4H_{syn}), 1.45-1.25 (m, 1H_{anti}, 1H_{syn}). **HPLC**: Daicel Chiralpack OD-H column, flow 0.5 mL/min, 254 nm, *n*-hexane/*i*-PrOH 95/5, *anti* isomer: t_{maj}: 24.17 min, t_{min}: 29.33 min; *syn* isomer t_{maj}: 20.42 min, t_{min}: 19.79 min.



(S)-2-((R)-(2-chlorophenyl)(hydroxy)methyl)cyclohexanone, 14.¹⁸⁸ **CF**: C₁₃H₁₅ClO₂. **MW**: 238.71 g/mol. The diastereomeric ratio, as determined by ¹H-NMR analysis of the final solid, was found to be between 86/14-97/3, favoring the *anti* isomer. **¹H-NMR (CDCl₃, 250 MHz)**: (diastereomeric mixture *anti/syn* 91/9) 7.58-7.56 (m, 1H_{anti}, 1H_{syn}), 7.48-7.29 (m, 2H_{anti}, 2H_{syn}), 5.73 (br, 1H_{syn}), 5.38 (d, J = 8.6 Hz, 1H_{anti}), 4.10

¹⁸⁹ Ermer, E.; Galletti, P.; Giacomini, D. *Eur. J. Org. Chem.* **2009**, 3155.

(br, 1H_{anti}), 2.69 (m, 1H_{anti}, 1H_{syn}), 2.51-2.36 (m, 2H_{anti}, 2H_{syn}), 2.16-2.09 (m, 1H_{anti}, 1H_{syn}), 1.88-1.41 (m, 5H_{anti}, 5H_{syn}). **HPLC:** Daicel Chiralpack AD-H column, flow 1 mL/min, 254 nm, *n*-hexane/*i*-PrOH 95/5, *anti* isomer: t_{maj}: 17.31 min, t_{min}: 20.37 min; *syn* isomer t_{maj}: 9.59 min, t_{min}: 10.34 min.

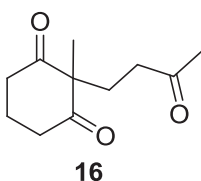


2-(hydroxy(4-nitrophenyl)methyl)cyclopentanone, 15.¹⁸⁸

CF: C₁₂H₁₃NO₄. **MW:** 235.24 g/mol. The diastereomeric ratio, as determined by ¹H-NMR analysis of the final solid, was found to be between 37/63-83/17. **¹H-NMR (CDCl₃, 250**

MHz): (diastereomeric mixture *anti/syn* 46/54) 8.21 (d, J = 8.3 Hz, 2H_{anti}, 2H_{syn}), 7.53 (m, 2H_{anti}, 2H_{syn}), 5.42 (br, 1H_{syn}), 4.84 (d, J = 8.9 Hz, 1H_{anti}), 4.75 (s, 1H_{anti}), 2.53-2.34 (m, 2H_{anti}, 2H_{syn}), 2.20-1.95 (m, 2H_{anti}, 2H_{syn}), 1.88-1.72 (2H_{anti}, 2H_{syn}). **HPLC:** Daicel Chiralpack AD-H column, flow 1.2 mL/min, 254 nm, *n*-hexane/*i*-PrOH 95/5, *anti* isomer: t_{maj}: 41.10 min, t_{min}: 31.01min.; *syn* isomer t_{maj}: 22.99 min, t_{min}: 21.48 min.

5.3.2 Intramolecular aldol condensation (Robinson annulation)



2-methyl-2-(3-oxobutyl)cyclohexane-1,3-dione, 16.¹⁹⁰ this compound had been already prepared by Dra. Amàlia Monge. Clear brown oil. **CF:** C₁₁H₁₆O₃ **MW:** 196.24 g/mol. **¹H-NMR (CDCl₃, 250 MHz):** 2.73-2.51 (m, 4H), 2.29 (t, J = 7.3 Hz, 2H),

2.05-1.84 (m, 7H), 1.18 (s, 3H). **¹³CRMN (CDCl₃, 62.5 MHz).** 211.9, 209.4, 64.1, 37.7, 37.1, 29.2, 28.8, 19.2, 16.7.

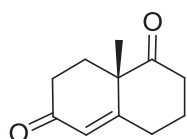
General procedure for homogeneous catalyst. In a vial, triketone **16** (1 equiv.), milliQ water (0.5 mL/mmol triketone), *p*-nitrobenzoic acid and homogeneous catalyst¹⁹¹ (0.021 mmol, 10%) were stirred together for 20 min at room temperature until ¹H-NMR showed complete conversion of triketone. Then the crude mixture was diluted with AcOEt (2 mL) and anhydrous Na₂SO₄ was added. The organic layer was then filtered and concentrated under vacuum and the residue purified by flash chromatography on silica gel using hexane/AcOEt mixtures as eluent to afford **17** as a pale brown oil.

¹⁹⁰ Bradshaw, B.; Etxebarria-Jardi, G.; Bonjoch, J.; Vióquez, S.F.; Guillena, G.; Nájera, C. *Adv. Synth. Catal.* **2009**, *351*, 2482.

¹⁹¹ Check the amount of catalyst and co-catalyst in the corresponding tables in section section 2:3 Results and Discussion.

General procedure for silica-supported organocatalysts. In a vial, triketone **16** (5 eq), milliQ water (0.5 mL/mmol aldehyde) *p*-nitrobenzoic acid and the corresponding supported organocatalyst¹⁹¹ were stirred together at room temperature until ¹H-NMR showed complete conversion of triketone. Then the crude mixture was diluted with AcOEt (2 mL) and filtered. The insoluble catalytic material was washed several times with AcOEt (3 x 1.5 mL) and the combined filtrates were concentrated under vacuum. The residue was purified by flash chromatography on silica gel using hexane/AcOEt mixtures as eluent to afford **17** as a pale brown oil. The catalytic material was dried under vacuum and directly used in the next cycle.

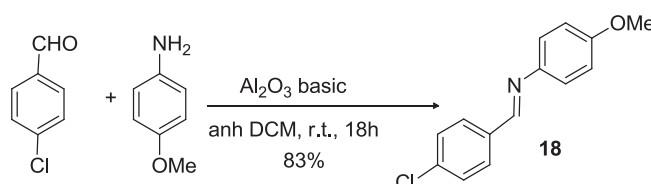
Compound **16** has been previously described and their spectral and analytical data were consistent with literature values.

**17**

(S)-8a-methyl-3,4,8,8a-tetrahydronaphthalene-1,6(2H,7H)-dione, 17.¹⁸⁸ Purified by flash chromatography using hexane/AcOEt 100/0 to 90/10 as eluent to afford **17** as a clear brown oil. **CF:** C₁₁H₁₄O₂. **MW:** 178,23 g/mol. **¹H-NMR (CDCl₃, 360 MHz):** 5.86 (d, J = 1.7 Hz, 1H), 2.77-2.67 (m, 2H), 2.53-2.43 (m, 4H), 2.19-2.11 (m, 3H), 1.78-1.64 (m, 1H), 1.45 (s, 3H). **HPLC:** Daicel Chiralpack IC column, flow 1.0 mL/min, 254 nm, *n*-hexane/*i*-PrOH 80/20, t_R: 31.8 min, t_S: 35.9 min.

5.3.3 Aza-Diels Alder reaction

5.3.3.1 Preparation of *N*-(4-chlorobenzylidene)-4-methoxyaniline, **18**.¹⁹²

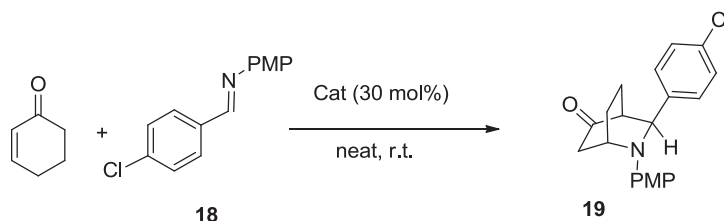


In a 100 mL Schlenk tube under nitrogen, basic Al₂O₃ (8.022 g, 1.0 g per mmol amine) was added to a solution of *p*-anisidine (1.016 g, 8.25 mmol) (purified by dissolution in Et₂O, followed by treatment with activated charcoal, filtration, and evaporation; stored in a darkened container at <0 °C) in anhydrous DCM (40 mL) at room temperature and after a period of 5 min, 4-chlorobenzaldehyde (1.204 g, 8.56 mmol) was added. The mixture was left to stir for 14 h at room temperature before filtration through Celite and removal of solvents *in vacuo*, to yield the crude imine **18** (1.691 g, Yield: 83%). **CF:** C₁₄H₁₂ClNO. **MW:** 245,70 g/mol. **¹H-NMR (CDCl₃, 360 MHz):** 8.45 (s, 1H), 7.83 (d, J =

¹⁹² Anderson, J.C.; Howell, G.P.; Lawrence, R.M.; Wilson, C.S. *J. Org. Chem.* **2005**, *70*, 5665.

8.1Hz, 2H), 7.43 (d, J = 8.3 Hz, 2H), 7.24 (d, J = 8.3 Hz, 2H), 6.94 (d, J = 9.3 Hz, 2H), 3.84 (s, 3H). ¹³C-NMR (CDCl₃, 90 MHz): 157.2, 155.0, 143.2, 129.9, 129.23, 127.0, 122.4, 118.8, 114.50, 55.4.

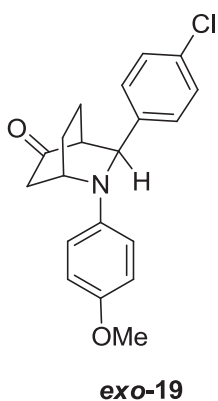
5.3.3.2 Catalytic tests



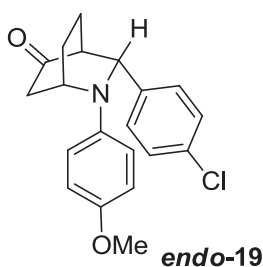
General procedure for homogeneous catalyst. In a vial, cyclohexenone (120 μ L, 0.993 g/mL, 1.24 mmol, 10 equiv), imine **18** (0.125 mmol) and homogeneous catalyst **10**¹⁹³ (0.038 mmol, 30 mol%) were stirred together at room temperature until TLC showed complete consumption of the imine. Volatiles were evaporated under vacuum and the crude mixture was purified by silica gel chromatography with hexane/AcOEt mixtures as eluent (100:0 to 90:10). Product **19** was obtained as a yellow oil.

General procedure for silica-supported organocatalysts. In a vial, cyclohexenone (120 μ L, 0.993 g/mL, 1.24 mmol, 10 equiv), imine **18** (0.125 mmol) and the corresponding supported organocatalyst¹⁹³ (0.038 mmol, 30 mol%) were stirred together at room temperature until TLC showed complete consumption of the imine. Then the crude mixture was diluted with AcOEt (2 mL) and filtered. The insoluble catalytic material was washed several times with AcOEt (3 x 1.5 mL) and the combined filtrates were concentrated under vacuum. and the crude mixture was purified by column chromatography on silica gel with hexane/AcOEt mixtures as eluent (100:0 to 90:10). Product **19** was obtained as a yellow oil. The catalytic material was dried under vacuum and directly used in the next cycle.

¹⁹³ Check the amount of catalyst in the corresponding tables in section section 2:3 Results and Discussion.



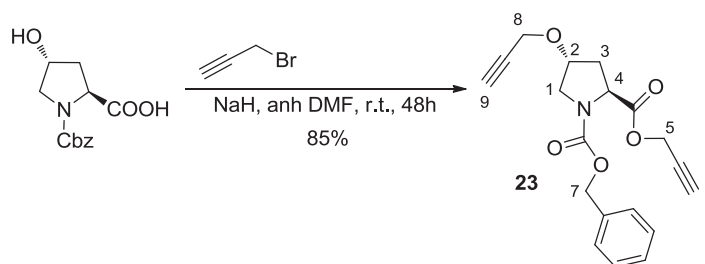
3-(4-chlorophenyl)-2-(4-methoxyphenyl)-2-azabicyclo[2.2.2]octan-5-one, exo-19.¹⁹⁴ **CF:** C₂₀H₂₀ClNO₂. **MW:** 341,83 g/mol. **¹H-NMR (CDCl₃, 250 MHz):** 7.36 (m, 4H), 6.75 (d, J = 8.9 Hz, 2H), 6.53 (d, J = 8.9 Hz, 2H), 4.68 (m, 1H), 4.42 (m, 1H), 3.71 (s, 3H), 2.79-2.72 (m, 1H), 2.62 (m, 1H), 2.42-2.34 (m, 1H), 2.29-2.14 (m, 1H), 1.98-1.81 (m, 1H), 1.76-1.50 (m, 2H). **¹³C-NMR (CDCl₃, 62.5 MHz):** 214.2, 152.7, 142.7, 139.4, 133.4, 129.3, 128.0, 115.1, 114.6, 62.0, 55.5, 50.7, 48.8, 41.7, 26.0, 15.9.



3-(4-chlorophenyl)-2-(4-methoxyphenyl)-2-azabicyclo[2.2.2]octan-5-one, endo-19.^{194b} **CF:** C₂₀H₂₀ClNO₂. **MW:** 341,83 g/mol. Observed as a minor product in catalytic tests. **¹H-NMR (CDCl₃, 250 MHz):** 7.33-7.27 (m, 4H), 6.78-6.76 (m, 2H), 6.61-6.58 (m, 2H), 4.55 (m, 1H), 4.42 (m, 1H), 3.72 (s, 3H), 2.76-2.69 (m, 2H), 2.49-2.44 (m, 1H), 2.24 (m, 1H), 2.18 (m, 1H), 2.03 (m, 1H), 1.75 (m, 1H).

5.4 Attempt to prepare a monosilylated proline tetrazole 3

5.4.1 Preparation of (2*S*,4*R*)-1-benzyl 2-(prop-2-yn-1-yl) 4-(prop-2-yn-1-oxo)pyrrolidine-1,2-dicarboxylate, 23.



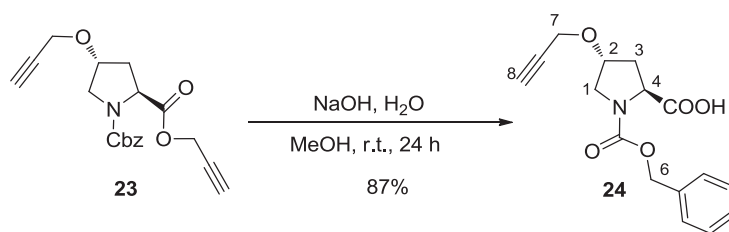
In a 100 mL Schlenk tube under inert atmosphere *N*-Cbz-*trans*-4-hydroxy-L-proline (3.998 g, 15.1 mmol) was dissolved in anhydrous DMF (36 mL). The solution was cooled to 0°C and NaH (1.761 g, 60% dispersion in mineral oil, 44.0 mmol) was added. The mixture was stirred for 30 min at 0°C and then propargyl bromide was added (2.8 mL, 1.335 g/cm³, 31.4 mmol). The solution was stirred for 48 h allowing to reach the room temperature. After this time, water (25 mL) was added to the reaction mixture and the pH was adjusted to 2 with HCl 5M. The organic layer containing the product was separated and the aqueous layer further extracted with Et₂O (3 x 50 mL). The

¹⁹⁴ (a) Yang, H.; Carter, R.G. *J. Org. Chem.* **2009**, *74*, 5151. (b) Constantino, U.; Fringuelli, F.; Orrù, M.; Nocchetti, M.; Piermatti, O.; Pizzo, F. *Eur. J. Org. Chem.* **2009**, 1214.

Chapter 2. 5. Experimental Part

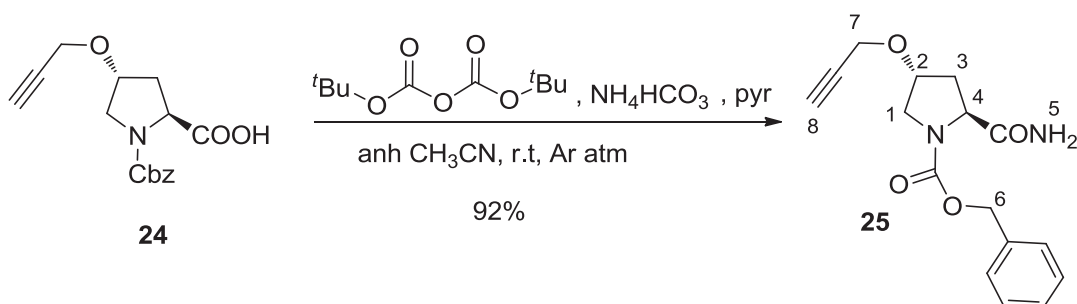
combined organic layers were dried over anhydrous Na_2SO_4 and concentrated under reduced pressure. A brown oil was obtained which was purified by column chromatography on silica gel (hexane:AcOEt 90:10 to 70:30) giving **23** as a yellow oil (4.375 g, Yield: 85%). **CF**: $\text{C}_{19}\text{H}_{19}\text{NO}_5$ **MW**: 341.36 g/mol. $[\alpha]_D^{25}$: -43.5 (CHCl_3 , c:1.26). **^1H NMR (CDCl_3 , 400 MHz) δ (ppm)**: (rotamers mixture 50:50): 7.35 (m, 10 H, $\text{H}_{\text{ar}}+\text{H}_{\text{ar}}$), 5.24-5.04 (m, 4H, H_7+H_7), 4.78 (m, 2H, H_5), 4.61-4.46 (m, 4H, $\text{H}_4+\text{H}_4+\text{H}_5$), 4.38 (br, 2H, H_2+H_2), 4.26-4.10 (m, 4H, H_8+H_8), 3.83-3.78 (m, 1H, $\text{H}_{1\text{a}}$), 3.72-3.66 (m, 3H, $\text{H}_{1\text{b}}+\text{H}_{1'}$), 2.52-2.41 (m, 6H, $\text{H}_6+\text{H}_9+\text{H}_6+\text{H}_9+\text{H}_3$), 2.21-2.11 (m, 2H, H_3). **^{13}C NMR (CDCl_3 , 100.6 MHz) δ (ppm)**: 171.73, 171.54, 154.75, 154, 13, 136.34, 136.20, 128.42, 128.37, 127.99, 127.95, 127.85, 127.79, 79.03, 77.14, 76.29, 75.54, 75.19, 74.93, 67.23, 57.76, 57.51, 56.36, 52.65, 52.43, 51.62, 51.48, 36.40, 35.16.

5.4.2 Preparation of (2S,4R)-1-((benzyloxy)carbonyl)-4-(prop-2-yn-1-yloxy)pyrrolidine-2-carboxylic acid, **24**.



A solution of NaOH_{aq} (1.860 g in 12 mL H_2O) was added dropwise to a solution of **23** (4.375 g, 12.8 mmol) in MeOH (18 mL) at room temperature. The mixture was stirred until TLC showed complete conversion of **23**. The reaction mixture was diluted with H_2O (10 mL), acidified to pH 10 with HCl 5M and extracted with Et_2O (3 x 15 mL). The aqueous layer was acidified to pH 4 and extracted with AcOEt (3 x 50 mL). The combined organic layers (AcOEt) were dried with Na_2SO_4 and concentrated under vacuum. The crude was purified by column chromatography on silica gel ($\text{CH}_2\text{Cl}_2/\text{MeOH}$ 100:0 to 95:5) yielding **24** as a yellow oil (3.366 g, 87%). **CF**: $\text{C}_{16}\text{H}_{17}\text{NO}_5$. **MW**: 303.31 g/mol. $[\alpha]_D^{25}$: -40.6 (CHCl_3 , c:1.36). **^1H NMR (CDCl_3 , 400 MHz) δ (ppm)**: 7.39-7.30 (m, 5H, H_{ar}), 5.23-5.10 (m, 2H, H_6), 4.55-4.47 (m, 1H, H_4), 4.36 (m, 1H, H_2), 4.22-4.12 (m, 2H, H_7), 3.82-3.62 (m, 2H, H_1), 2.53-2.39 (m, 2H, $\text{H}_{3\text{a}}+\text{H}_8$), 2.37-2.30 (m, 0.5H, $\text{H}_{3\text{b}}$), 2.24 (m, 0.5H, $\text{H}_{3\text{b}}$). **^{13}C NMR (CDCl_3 , 100.6 MHz) δ (ppm)**: 177.46, 175.10, 156.15, 154.31, 136.17, 135.89, 128.50, 128.35, 128.29, 128.20, 127.94, 127.87, 127.58, 79.02, 76.09, 75.53, 74.98, 67.82, 67.28, 58.06, 57.41, 56.42, 51.60, 36.54, 34.60.

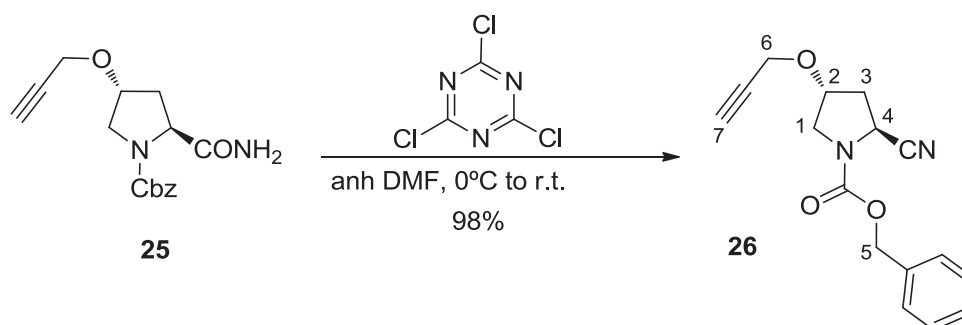
5.4.3 Preparation of (2*S*,4*R*)-benzyl 2-carbamoyl-4-(prop-2-yn-1-yloxy)pyrrolidine-1-carboxylate, **25**.



In a 250 mL Schlenk tube under inert atmosphere, product **24** (6.484 g, 21.4 mmol), di-*tert*-butyl-dicarbonate (7 mL, 1.02 g/cm³, 32.7 mmol), NH₄HCO₃ (2.537 g, 32.1 mmol) were dissolved in anhydrous CH₃CN (66 mL). Then pyridine (1.3 mL, 0.978 g/cm³, 16.1 mmol) was added and the reaction mixture was stirred at room temperature overnight (monitored by TLC). After this time, the solution was concentrated under vacuum until 10 mL. Then, H₂O (50 mL) and AcOEt (50 mL) were added and the organic layer was separated. The aqueous layer was extracted with further AcOEt (3 x 50 mL). The combined organic layers were dried with anhydrous Na₂SO₄ and concentrated under vacuum yielding **25** as an orange solid (5.922 g, Yield: 92%).

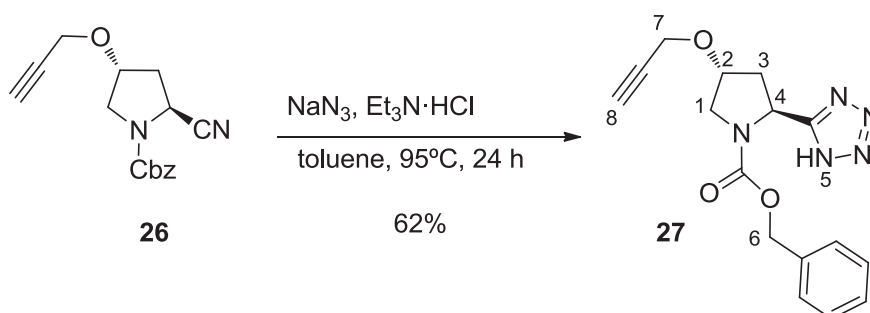
CF: C₁₆H₁₈N₂O₄ **MW:** 302.33 g/mol. **[α]_D²⁰:** -51.9 (CHCl₃, c: 0.99). **¹H NMR (CDCl₃, 400 MHz) δ (ppm):** (rotamers mixture): 7.36 (m, 10 H, H_{ar}+H_{ar'}), 6.70 (m, 1H, H₅), 5.83 (m, 1H, H₅), 5.44 (m, 2H, H₅'), 5.18 (m, 4H, H₆+H_{6'}), 4.47 (m, 2H, H₄+H_{4'}), 4.36 (m, 2H, H₂+H_{2'}), 4.15 (m, 4H, H₇+H_{7'}), 3.91-3.56 (m, 2H, H₁), 2.52 (m, 2H, H₃), 2.44 (m, 2H, H₈+H_{8'}), 2.20 (m, 2H, H₃'). **¹³C NMR (CDCl₃, 100.6 MHz) δ (ppm):** 173.86, 156.67, 136.50, 128.87, 128.51, 128.23, 128.16, 79.26, 77.20, 75.70, 74.83, 67.53, 59.09, 58.54, 56.42, 51.93, 51.41, 36.59, 33.48.

5.4.4 Preparation of (2*S*,4*R*)-benzyl 2-cyano-4-(prop-2-yn-1-yloxy)pyrrolidine-1-carboxylate, **26**.



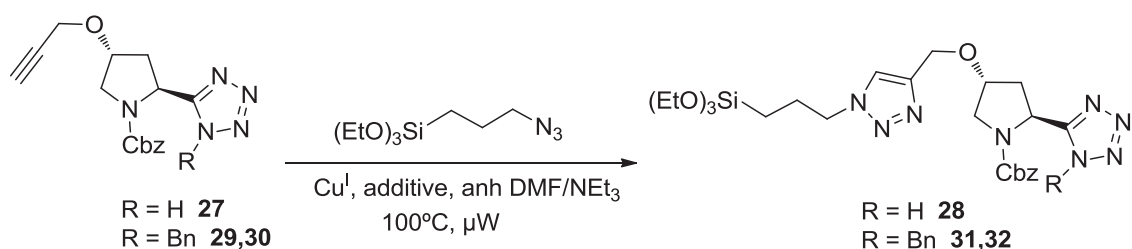
In a 250 mL Schlenk tube under inert atmosphere, product **25** (5.753 g, 19 mmol) was dissolved in dry DMF (65 mL). The solution was cooled to 0°C and cyanuric chloride (3.87 g, 21 mmol) was added. The reaction mixture was stirred at 0°C for 1 h and then allowed to rise to the room temperature for 72 h (TLC monitoring). After this time, the solution was cooled to 0°C, diluted with H₂O (40 mL) and extracted with AcOEt (4 x 100 mL). The combined organic layers were dried with anhydrous Na₂SO₄ and concentrated under vacuum. The crude was purified by column chromatography on silica gel (hexane/AcOEt 70:30) yielding **26** (5.33 g, Yield: 98%) as a pale yellow solid. **CF**: C₁₆H₁₆N₂O₃ **MW**: 284.31 g/mol. $[\alpha]_D^{25}$: -46.3 (CHCl₃, c:1.19). **¹HNMR (CDCl₃, 400 MHz) δ (ppm)**: (rotamers mixture) 7.46-7.35 (m, 10 H, H_{ar}+H_{ar'}), 5.24-5.21 (m, 4 H, H₅+H_{5'}), 4.67 (ap t, J=7.5 Hz, 1H, H₄), 4.62 (ap t, J=7.5 Hz, 1H, H_{4'}), 4.42 (m, 2 H, H₂+H_{2'}), 4.23-4.12 (m, 4 H, H₆+H_{6'}), 3.83-3.80 (m, 1H, H_{1a}), 3.71-3.68 (m, 1H, H_{1b}), 3.63-3.57 (m, 2H, H₁), 2.59-2.41 (m, 6H, H₃+H₃' +H₇+H_{7'}). **¹³CNMR (CDCl₃, 100.6 MHz) δ (ppm)**: 154.44, 153.92, 135.84, 135.68, 128.58, 128.19, 128.14, 118.60, 118.25, 78.73, 77.22, 75.81, 75.42, 74.95, 68.14, 67.91, 56.64, 51.12, 50.99, 45.82, 45.42, 37.50, 36.20.

5.4.5 Preparation of (2*S*,4*R*)-benzyl 4-(prop-2-yn-1-yloxy)-2-(1*H*-tetrazol-5-yl)pyrrolidine-1-carboxylate, **27**.



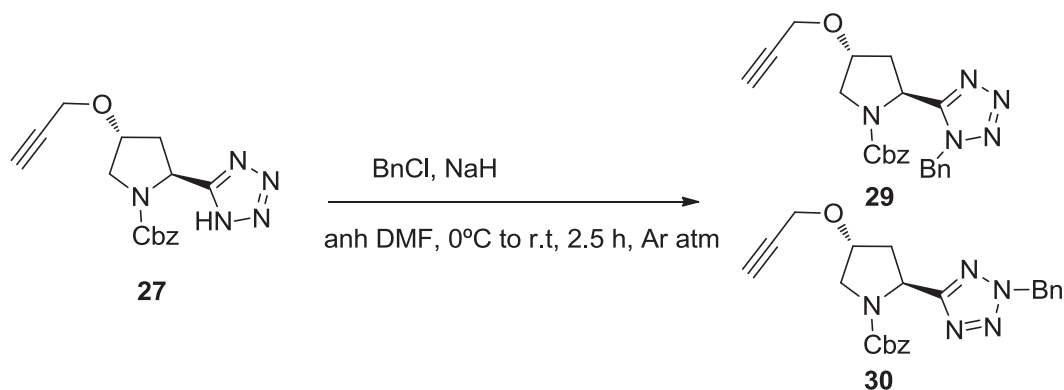
In a 100 mL Schlenk tube equipped with a reflux condenser under inert atmosphere, product **26** (5.33 g, 19 mmol), NaN₃ (1.87 g, 29 mmol) and Et₃N·HCl

5.4.7 General procedure for click reactions under microwave heating.

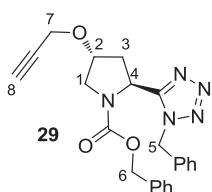


Under inert atmosphere, a microwave tube was charged with the corresponding proline tetrazole (1 mmol), Az-PTES (0.25 mL, 1g/mL, 1 mmol), Cu catalyst ($5 \cdot 10^{-3}$ mmol), TBTA ($5 \cdot 10^{-3}$ mmol) when indicated and a 1:1 solution of anh NEt_3 / anh DMF (0.5 mL). The tube was closed and heated under microwave activation (100°C , 200W) for the time indicated in the table. After this time, volatiles were removed under vacuum and the crude mixture was analyzed by $^1\text{H-NMR}$ without further purification.

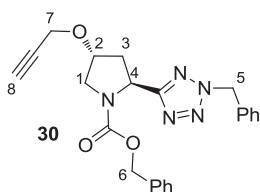
5.4.8 Procedure for Bn protection of NH groups of proline tetrazole 27.



A solution of proline tetrazole **27** (1.013 g, 2.89 mmol) in anh DMF (5 mL) was added to a solution of NaH (0.0765 g, 60% dispersion in mineral oil, 3.12 mmol) in anhydrous DMF (3.5 mL) cooled at 0°C under inert atmosphere. The reaction mixture was stirred 30 min. After this time, benzyl chloride (0.33 mL, 1.10 g/cm^3 , 2.87 mmol) was added and the solution was stirred at room temperature for 2 hours. Then the reaction mixture was poured into iced water (20 g) and extracted with AcOEt (3 x 40 mL). The combined organic layers were washed with HCl 10% (3 x 30 mL), NaHCO_3 (aq) (3 x 30 mL) and brine (3 x 30 mL), dried with anhydrous Na_2SO_4 and concentrated under vacuum. The crude was purified by column chromatography on silica gel (hexane:AcOEt 50:50) yielding a mixture of two regioisomers **29** and **30**.



(2S,4R)-benzyl 2-(1-benzyl-1H-tetrazol-5-yl)-4-(prop-2-yn-1-yloxy)pyrrolidine-1-carboxylate, 29. CF: C₂₃H₂₃N₅O₃. MW: 417.46 g/mol. ¹HNMR (CDCl₃, 400 MHz) δ (ppm): ¹³CNMR (CDCl₃, 100.6 MHz) δ (ppm): 7.37-7.25 (m, 9H, H_{ar}), 7.05 (m, 1H, H_{ar}), 5.74 (m, 1H, H_{6a}), 5.59 (m 1H, H_{6b}), 5.34 (m, 1H, H₄), 5.21-4.91 (m, 2H, H₅), 4.53-4.35 (m, 1H, H₂), 4.23-4.10 (m, 2H, H₇), 3.87-3.67 (m, 2H, H₁), 2.49-2.28 (m, 2H, H₃), 2.17-2.11 (m, 1H, H₈). ¹³CNMR (CDCl₃, 100.6 MHz) δ (ppm): (rotamers mixture) 168.63, 168.19, 155.25, 154.99, 136.86, 136.52, 133.51, 129.27, 128.72, 128.63, 128.50, 128.19, 127.83, 79.23, 77.20, 76.30, 75.59, 74.84, 67.11, 66.98, 66.76, 61.19, 61.08, 57.87, 57.62, 56.57, 56.49, 56.35, 56.31, 56.24, 38.83, 37.64.



(2S,4R)-benzyl 2-(2-benzyl-2H-tetrazol-5-yl)-4-(prop-2-yn-1-yloxy)pyrrolidine-1-carboxylate, 30. CF: C₂₃H₂₃N₅O₃. MW: 417.46 g/mol. ¹HNMR (CDCl₃, 400 MHz) δ (ppm): 7.39-7.28 (m, 7H, H_{ar}), 7.24-7.20 (m, 1H, H_{ar}), 7.07 (m, 1H, H_{ar}), 6.92 (m, 1H, H_{ar}), 5.90-5.57 (m, 1H, H_{6a}), 5.36-5.28 (m, 0.5H, H_{6b}), 5.12-4.86 (m, 3H, H₄+H₅), 4.79-4.75 (m, 0.5H, H_{6b}), 4.53-4.40 (m, 1H, H₂), 4.18-4.05 (m, 2H, H₇), 3.91-3.72 (m, 2H, H₁), 2.41 (m, 1H, H_{3a}), 2.14-2.06 (m, 1H, H_{3b}), 1.66 (m, 1H, H₈). ¹³CNMR (CDCl₃, 100.6 MHz) δ (ppm): (rotamers mixture) 157.88, 156.72, 156.21, 155.58, 154.10, 136.24, 135.57, 134.63, 133.98, 129.50, 129.26, 129.14, 129.05, 128.84, 128.52, 128.14, 127.69, 127.28, 79.05, 78.96, 77.20, 75.60, 75.06, 74.99, 74.85, 60.27, 56.33, 56.17, 51.63, 51.24, 50.81, 50.04, 48.88, 38.56, 37.02.

CHAPTER 3

**Organosilicas derived from imidazolium and
imidazolinium salts.**

Applications in catalysis

1. INTRODUCTION

1.1 Introduction to NHC carbenes as organocatalysts

Among the plethora of methods developed over the years for carbon-carbon bond formation, a large number of them take advantage of those who make organic molecules react in an inverse manner compared to their innate polarity-driven reactivity. Usually, a carbonyl group reacts as an electrophile at carbon, however, this polarity can be reversed when the carbonyl group is converted to an acyl anion by reaction with dithianes,¹⁹⁶ cyanohydrins¹⁹⁷ or N-heterocyclic carbenes, becoming a nucleophile. In the same manner, the activation of methyl/methylene group imparted by the electron withdrawing effect of an adjacent carbonyl group provides a similar effect. In other words, the reaction occurring at the carbon adjacent to the carbonyl group of aldehyde, ketone, carboxyl surrogates *etc.*, proceeds *via* the intermediacy of an enamine or an enol/enolate. Just as a carbonyl would facilitate the reaction of an electrophile at the α -carbon *via* enol/enolate, the reaction at the β carbon *via* a potentially reactive intermediate, an homoenolate, is conceptually feasible.¹⁹⁸ In this context, N-heterocyclic carbenes have been offering plenty of catalytic developments to the chemistry of this synthon equivalents.

Although the term **Nucleophilic Heterocyclic Carbene (NHC)** came into usage only recently, the existence of such species was clearly established half a century ago.¹⁹⁹ Historically, it was known that coenzyme thiamine catalyses decarboxylation and a number of other important reactions in biological systems, but no mechanistic guidance was available. In 1958, Breslow postulated that the thiazolium moiety in thiamine is acidic enough to be deprotonated under mildly basic conditions to generate a thiazolylidene species, capable of addition to an activated carbonyl group, leading to a polarity reversal of the latter (*umpolung*), and thus sets in motion a sequence of events culminating in decarboxylation of pyruvic acid, acetoin condensation, etc.

Because of their pronounced reactivity, carbenes could not be isolated until recently and were regarded as reactive intermediates.²⁰⁰ Bertrand and co-workers and Arduengo *et. al.* in the late 1980s and early 1990s, reported the obtention of stable nucleophilic carbenes and, since then, the broad application of N-heterocyclic carbenes

¹⁹⁶ (a) Corey, E.J.; Seebach, D. *Angew. Chem. Int. Ed. Engl.* **1965**, *4*, 1075. (b) Corey, E.J.; Seebach, D. *Angew. Chem. Int. Ed. Engl.* **1965**, *4*, 1077.

¹⁹⁷ Stork, G.; Maldonado, L. *J. Am. Chem. Soc.* **1971**, *93*, 5286.

¹⁹⁸ Nair, V.; Vellalath, S.; Pattooradi, B. *Chem. Soc. Rev.* **2008**, *37*, 2691.

¹⁹⁹ Enders, D.; Niemeier, O.; Henseler, A. *Chem. Rev.* **2007**, *107*, 5606.

²⁰⁰ Rice, F.O.; Glaserbrook, A.L. *J. Am. Chem. Soc.* **1934**, *56*, 2381.

Chapter 3.1. Introduction

(NHCs) in organic synthesis has been impressively demonstrated. Beside their role as excellent ligands in metal-based catalytic reactions, carbene-based organocatalysis has emerged as an exceptionally fruitful research area in synthetic organic chemistry.²⁰¹

There are four main types of NHC carbenes which are classified as: thiazol- (A), triazol- (B), imidazol- (C), and imidazolin-2-ylidenes (D) (Figure 3.1). As typical structural features, all carbenes are neutral and possess a bivalent carbon atom with an electron sextet. Although the most of the work is devoted to the design and development of the azolium cationic scaffold to impart specific chemical properties in organocatalysis, the contribution of the anionic counterpart should not be ignored. In this regard, You and Ren reported the influence of counteranions of these salts on the catalytic activity of the NHCs generated in situ.²⁰² Nucleophilicity and basicity of the carbene species could be tuned by changing the counteranion.

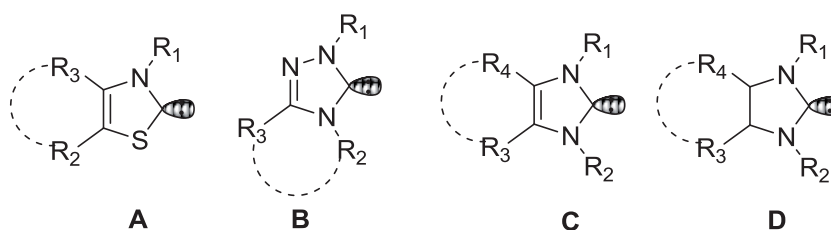


Figure 3.1. General types of N-heterocyclic carbenes.

1.2 NHC-catalyzed transformations

A rational way to classify organocatalytic NHC reactions is based on the catalytic activation modes of the substrates.²⁰³ Since these catalysts undergo a covalent bond formation reaction with the substrate, NHC-substrate adducts are present in all cases. Theoretically, such an intermediate can be traced back to a synthon as was introduced by Corey.²⁰⁴ According to the present state of NHC organocatalysis we will use eight synthons. Furthermore, these synthons can be divided into three groups according to the three major attributes of *N*-heterocyclic carbenes (Figure 3.2): a) ambiphilicity, which is the result of the σ -donor and π -acceptor character of *N*-heterocyclic carbenes (Figure 3.3), b) moderate nucleophilicity and c) strong basicity.

²⁰¹ Reviews: (a) Enders, D.; Balensiefer, T. *Acc. Chem. Res.* **2004**, *37*, 534. (b) Zeitler, K. *Angew. Chem., Int. Ed.* **2005**, *44*, 7506. (d) Marion, N.; Díez -González, S.; Nolan, S. P. *Angew. Chem., Int. Ed.* **2007**, *46*, 2988.

²⁰² Wei, S.; Wei, X-G.; Su, X.; You, J.; Ren, Y. *Chem. Eur. J.* **2011**, *17*, 5965.

²⁰³ Grossmann, A.; Enders, D. *Angew. Chem. Int. Ed.* **2012**, *51*, 314.

²⁰⁴ Corey, E.J. *Pure Appl. Chem.* **1967**, *14*, 19.

NHC Attribute	Synthon	Typical Reactions	NHC Attribute	Synthon	Typical Reactions
Ambiphilicity (σ -donor and π -acceptor)		a¹-d¹-Umpolung: - Benzin condensation - Stetter Reaction - Hydroacylation a³-d³-Umpolung: - Homoenolate Reaction - "Michael Umpolung" Extended Umpolung: - Ring Opening - Redox Esterification - Redox Amidation	Nucleophilicity (σ -donor)		Transesterification Morita-Baylis-Hillman-Reaction "Claisen Rearrangement"
Basicity		Enolate reactions: - Aldol Reaction - Michael Addition			Formal Cycloadditions - [2+2], [4+2], Cycloadditions

Figure 3.2. Synthon classification of NHC-catalyzed reactions according to ref 203.

1.2.1 Ambiphilicity or Umpolung

Pioneered by Seebach, the concept of "umpolung" (polarity reversal) triggered a novel way of thinking beyond the traditional reactivity patterns in the retrosynthetic analysis of target molecules.²⁰⁵ The term *umpolung* now refers to a powerful strategy in organic synthesis that consists of the inversion of the innate reactivity of a functional group.²⁰⁶ Indeed, the presence of lone pairs on heteroatoms, such as nitrogen and oxygen, offers them the possibility of donating electrons (Figure 3.3 A). As a consequence, the successive atoms of the skeleton of the molecule are alternatively defined as being donor (d^{2n}) and acceptor (a^{2n+1}) positions (Figure 3.3 B). Any process that enables the interchange of this normal reactivity falls under the definition of reactivity umpolung.^{205,207}

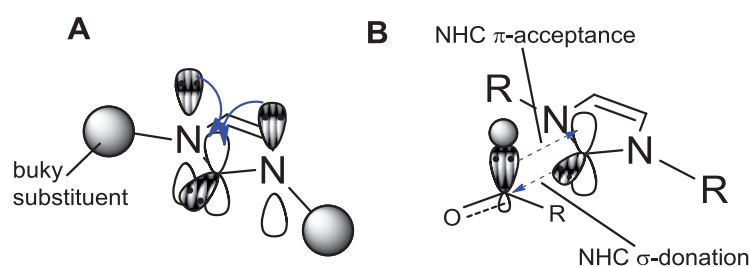


Figure 3.3. Electronic ambiphilicity of *N*-heterocyclic carbenes. A) stabilization of the singlet carbene by electron donation of the N atoms; B) formation of the Breslow intermediate by σ -donation and π -acceptance.

The vast majority of organocatalyzed transformations that are proceeding through umpolung are mediated by *N*-heterocyclic carbenes. NHCs possess several modes of action (Figure 3.4), which are represented in detail in numerous comprehensive reviews along with more focused ones.

²⁰⁵ Seebach, D. *Angew. Chem. Int. Ed.* **1979**, *18*, 239.

²⁰⁶ Bugaut, X.; Glorius, F. *Chem. Soc. Rev.* **2012**, *41*, 3511.

²⁰⁷ Gröbel, B.T.; Seebach, D. *Synthesis*, **1977**, 357.

Chapter 3.1. Introduction

Nowadays three types of umpolung are associated with NHC catalysis: a) umpolung of aldehydes to acyl nucleophiles (a^1-d^1 umpolung) first reported by Ugai *et al.* in 1943 in the thiazol-2-ylidene-catalyzed benzoin reaction,²⁰⁸ b) the "conjugate umpolung"²⁰⁹ (a^3-d^3 umpolung) independently developed by Glorius and Burstein^{210a} and by Bode and He,^{210b} and c) the "extended umpolung" (sometimes referred as an "internal redox reaction")²¹¹ independently demonstrated by Bode and co-workers^{212a} and Rovis and co-workers.^{212b} Although the mechanisms of these reactions have not been completely verified yet,²⁰³ similar mechanisms can be postulated for all three kinds of umpolung.

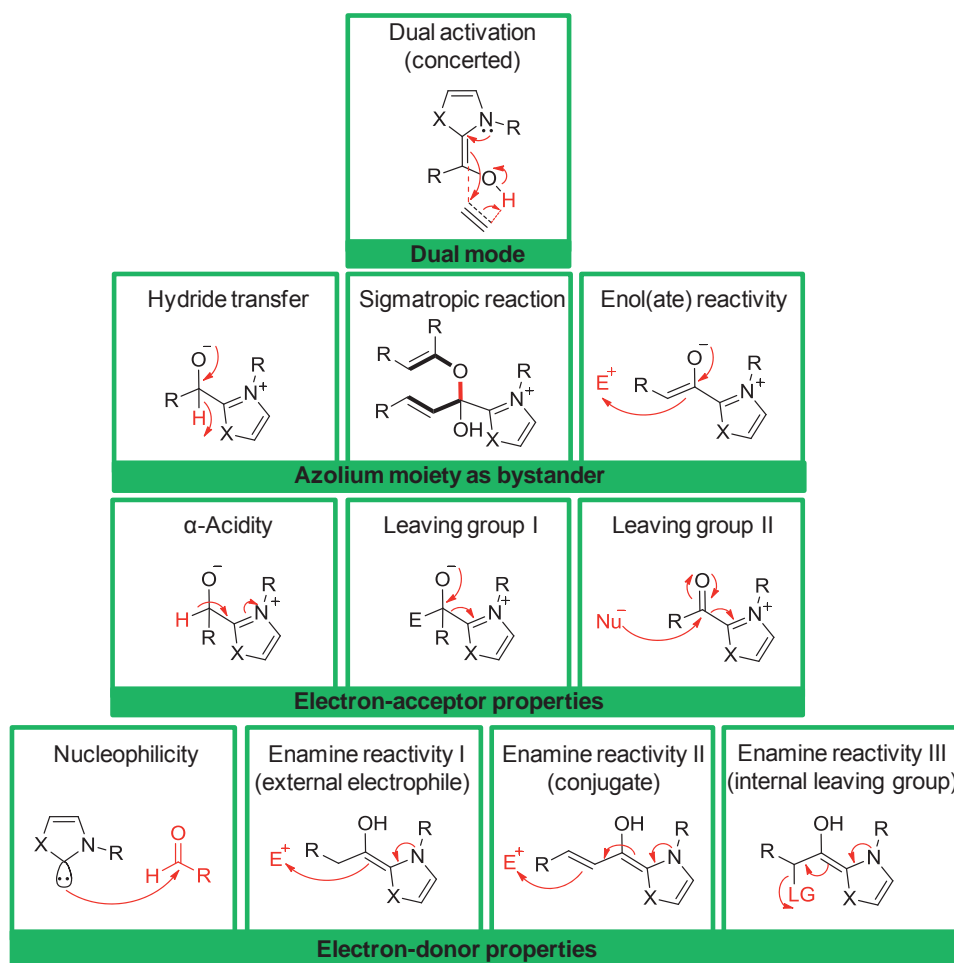


Figure 3.4. Modes of action in NHC organocatalysis according to ref 206.

²⁰⁸ Ugai, T., Tanaka, S.; Dokawa, S. *J. Pharm. Soc. Jpn.* **1943**, 63, 296.

²⁰⁹ For reviews on conjugate umpolung with NHCs see: a) Nair, V.; Babu, B.P. *Chem. Soc. Rev.* **2008**, 37, 2691. b) Nair, V.; Menon, R.S.; Biju, A.T.; Sinu, C.R.; Paul, R.R.; Jose, A.; Sreekumar, V. *Chem. Soc. Rev.* **2011**, 40, 5336.

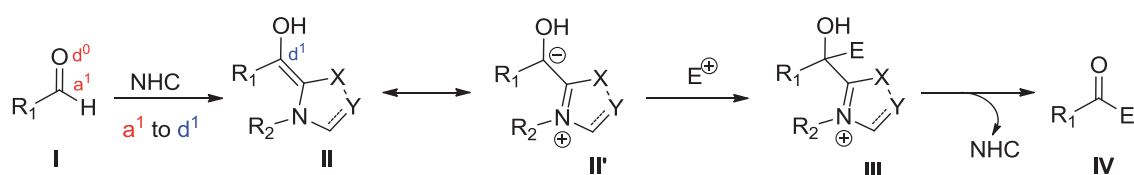
²¹⁰ For the first works on conjugate umpolung see: (a) Burstein, C.; Glorius, F. *Angew. Chem. Int. Ed.* **2004**, 43, 6205. (b) He, M.; Bode, J.W. *Org. Lett.* **2005**, 7, 3131.

²¹¹ For extended umpolung with NHCs see: Vora, H.U.; Rovis, T. *Aldrichimica Acta* **2011**, 44, 3.

²¹² For the first extended umpolung reactions with NHCs see: (a) Chow, K.Y.; Bode, J.W.; *J. Am. Chem. Soc.* **2004**, 126, 8126. (b) Reynolds, N.T.; Read de Alaniz, J.; Rovis, T. *J. Am. Chem. Soc.* **2004**, 126, 9518.

1.2.1.1 Classical Umpolung (a^1 to d^1)

For a^1 - d^1 umpolung, the catalytic cycle starts with the nucleophilic attack of the σ -donor lone pair of the carbene on the carbonyl group of an aldehyde **I**. Breslow intermediate **II** is generated through deprotonation of the carbene-aldehyde adduct by the external base (Scheme 3.1). Subsequently, this intermediate **II** (also drawn as its mesomeric zwitterionic form **II'**) can react with different electrophiles, such as another carbonyl compounds in the benzoin reaction, or with Michael acceptors in the Stetter reaction, or with activated or unactivated double and triple bonds without electron-withdrawing groups, or with alkyl halides. After the reaction, the carbene is liberated and can re-enter in the catalytic cycle.



Scheme 3.1. Formal mechanism of NHC reactions attributed to a^1 - d^1 umpolung.

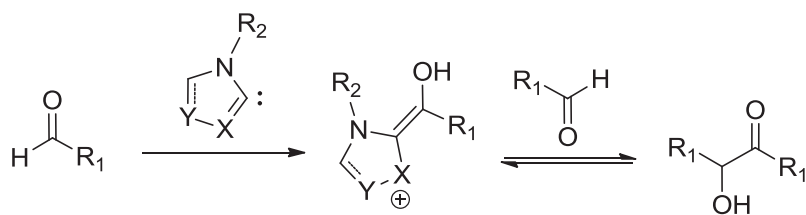
One of the most known and ancient reactions in which an umpolung mechanism is operating is the **benzoin condensation**. In 1832, Wöhler and Liebig described that cyanide anions could dimerize aldehydes in an atom-economical fashion to afford α -hydroxyketones (benzoin).²¹³ More than 100 years after this discovery, Ukai and co-workers showed that a catalytic amount of thiazolium salts could achieve the same transformation.²¹⁴ Later on, Breslow made a mechanistic proposal for this process, which has since then provided the guideline for most developments in NHC-catalyzed reactions (Scheme 3.2).²¹⁵ The formation of such 1,2 (or 1,4)-functionalized products, as opposed to the 1,3 (or 1,5)-substitution pattern afforded by normal polarity reactions (aldol reaction, Michael addition), is typical of umpolung reactivity. The use of azolium-derived NHCs in place of cyanide anions to catalyze the benzoin condensation represents a lower toxicity of the reaction.

²¹³ Wöhler, F.; Liebig, J. *Ann. Pharm.*, **1832**, 3, 249.

²¹⁴ Ukai, T.; Tanaka, R.; Dokawa, T. *J. Pharm. Soc. Jpn.*, **1943**, 63, 296.

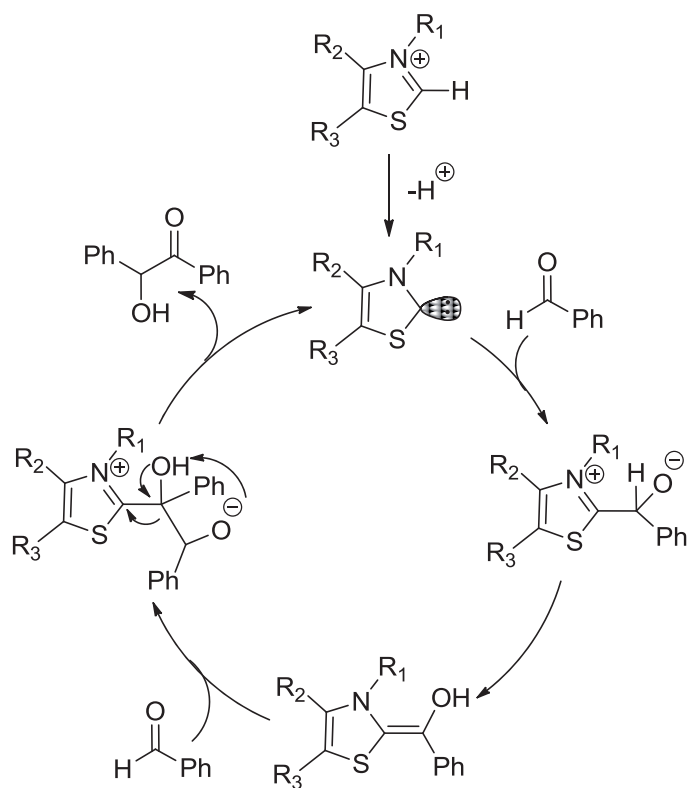
²¹⁵ Breslow, R. *J. Am. Chem. Soc.* **1958**, 80, 3719.

Chapter 3.1. Introduction



Scheme 3.2. NHC-catalyzed α^1 to δ^1 umpolung of aldehydes: benzoin condensation.

In this mechanism, the catalytically active species is a thiazolin-2-ylidene, which is formed *in situ* by deprotonation of the thiazolium salt (Scheme 3.3). Then the nucleophilic attack to the carbonyl function of an aldehyde generates a thiazolium salt-aldehyde adduct. A subsequent proton transfer affords an enamine type intermediate, the Breslow intermediate, in which the originally electrophilic carbon atom of the aldehyde has gained nucleophilic character. This nucleophilic acylation reagent (equivalent to a δ^1 -synthon in the terminology of Seebach) reacts again with an electrophilic substrate such as the carbonyl group of a second aldehyde molecule. The formed intermediate eliminates benzoin, and the original carbene catalyst is regenerated (Scheme 3.3).

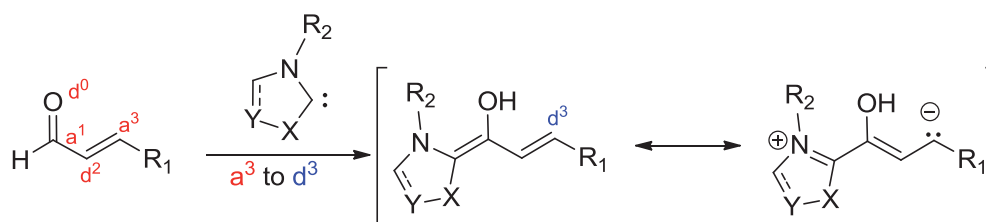


Scheme 3.3. Catalytic cycle of benzoin condensation as proposed by Breslow.

The reversibility of the benzoin condensation offers the possibility to react the Breslow intermediate with a second electrophile, thereby considerably increasing the usefulness of NHC-catalyzed transformations. In the middle of the 1970's, Stetter reported for the first time the reaction of the Breslow intermediate with Michael acceptors, giving access to valuable 1,4-dicarbonyl compounds.²¹⁶ Different Michael acceptors, including α,β -unsaturated ketones, esters, nitriles, sulfones, have then been used in this transformation. This **Stetter reaction** enables a new catalytic pathway for the synthesis of 1,4-diketones, 4-ketoesters, and 4-ketonitriles^{217,218} and is commonly catalyzed by thiazolium salts.¹⁹⁹

1.2.1.2 Conjugate umpolung (a^3 to d^3)

When an α,β -unsaturated aldehyde and a NHC are combined, the conjugation of the system allows the transfer of the nucleophilic properties of the Breslow intermediate to the β -position, which represents a d^3 -nucleophile and thus, constitute an a^3 - d^3 umpolung (Scheme 3.4).



Scheme 3.4. NHC-catalyzed a^3 to d^3 umpolung of α,β -unsaturated aldehydes.

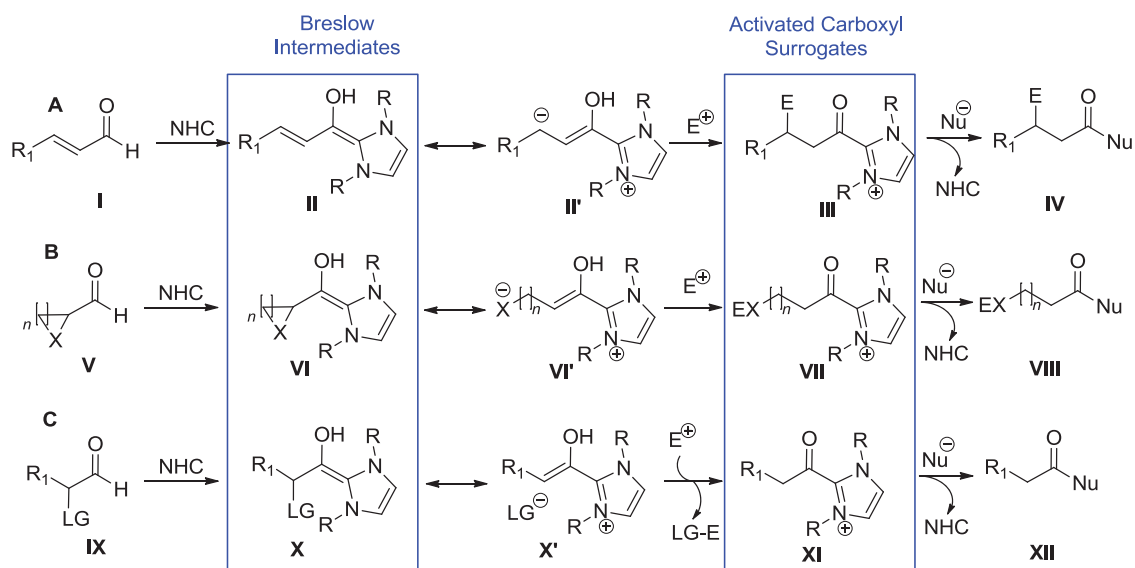
The difference between the conjugate or the extended umpolung with respect to the classical umpolung is that, in the former cases, after the formation of the Breslow intermediates **II**, **VI** and **X**, the position of the formal negative charge can be transferred by the double bond and, therefore, the electrophile is trapped in a different place (Scheme 3.5). Furthermore, the conjugate and the extended umpolung are followed by the formation of the activated carboxyl surrogates **III**, **VII** and **XI**. To close the catalytic cycle an stoichiometric amount of another nucleophile, that is, an alcohol or an amine, is needed.

²¹⁶ Stetter, H. *Angew. Chem. Int. Ed.* **1976**, *15*, 639.

²¹⁷ Hachisu, Y.; Bode, J. W.; Suzuki, K. *J. Am. Chem. Soc.* **2003**, *125*, 8432.

²¹⁸ Stetter, H.; Kuhlmann, H. *Org. React.* **1991**, *40*, 407.

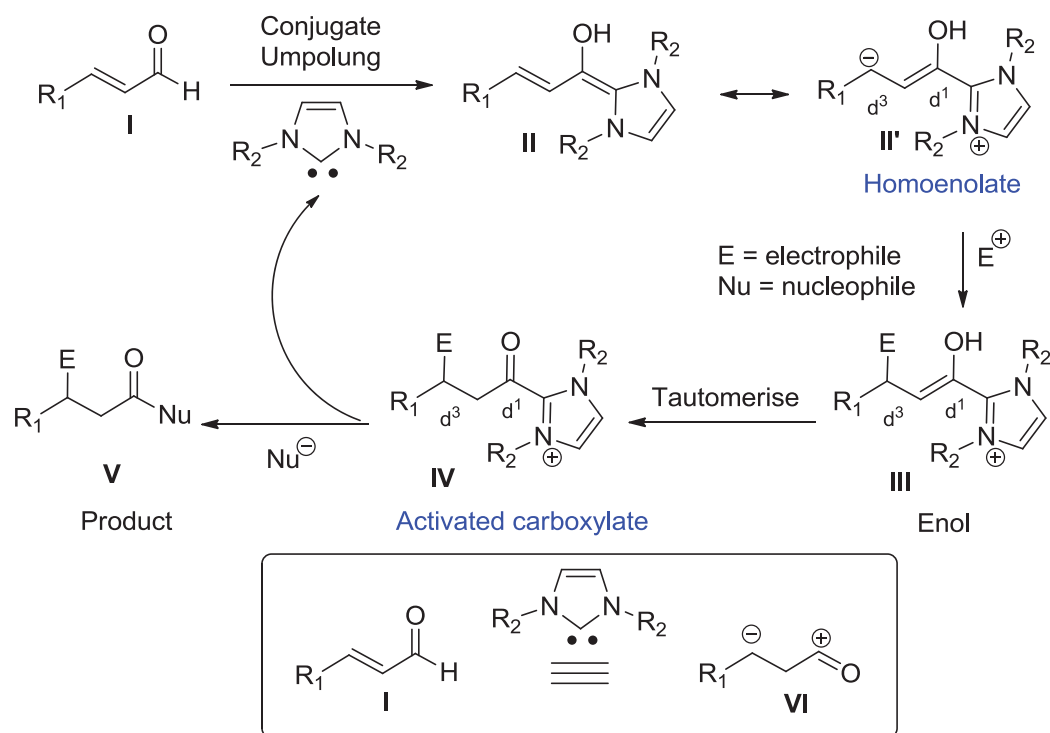
Chapter 3.1. Introduction



Scheme 3.5. Comparison of formal mechanisms of NHC reactions attributed to: A) α^3 - δ^3 umpolung, B) extended umpolung by ring opening or C) extended umpolung by elimination of the leaving group.

If the addition of an NHC to an aldehyde generates an enol/enaminol (Breslow intermediate), the addition of an NHC to an α,β -unsaturated aldehyde generates a conjugated acyl anion, more appropriately called an *homoenolate*, an species containing anionic carbon β to a carbonyl group.

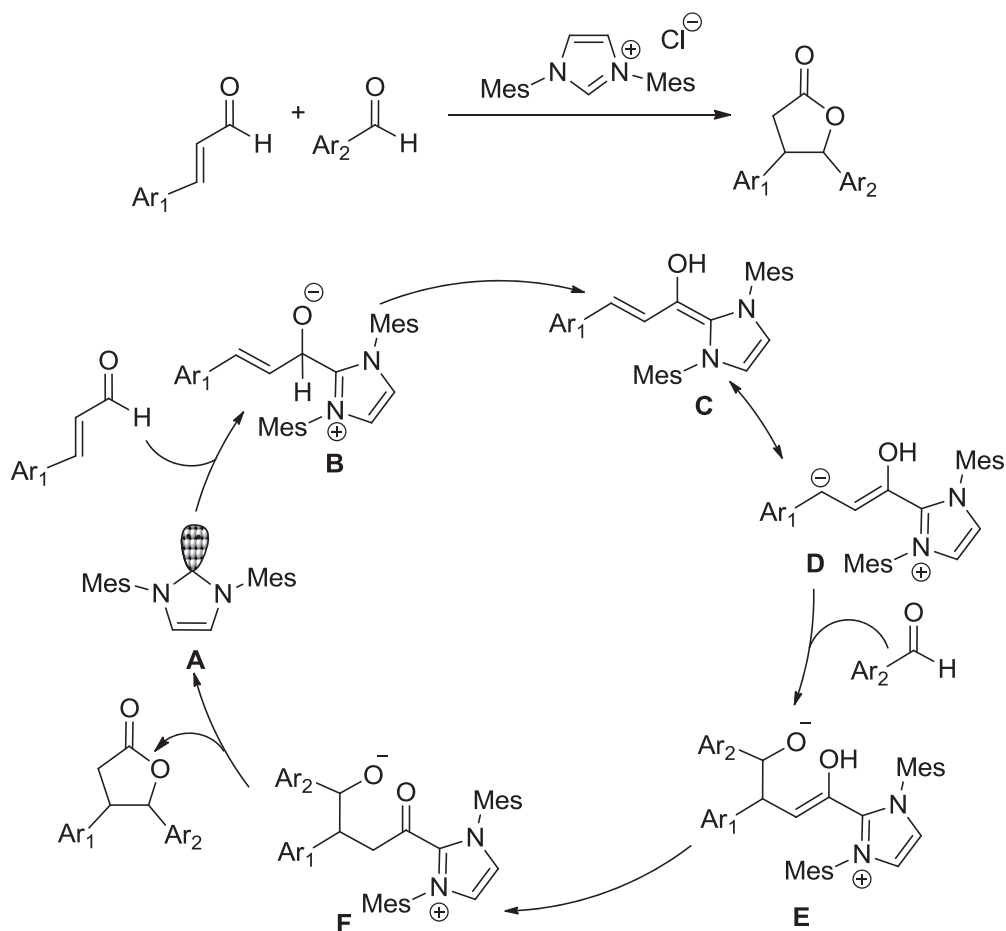
If we have a look into the homoenolate (**II'**) reactivity (Scheme 3.6), we can conclude that due to the extended conjugation, it exhibits significant nucleophilic reactivity at the β -position. Formation of a new bond with an electrophile at the β -position affords an enol (**III**) which tautomerises to the activated carboxylate equivalent (**IV**). The latter can react with a nucleophile to regenerate the catalyst and furnish the final product **V** of the reaction. If the electrophile (**E**) and the nucleophile (**Nu**) are part of a single molecule, the above-described sequence of events will result in an annulation reaction. Thus, enals (**I**) can be considered as synthetic equivalents of the 1,3-dipole **VI** under conditions of NHC catalysis.



Scheme 3.6. NHC-catalyzed generation of homoenolates and subsequent reaction profile.

The concept of NHC-catalyzed generation of homoenolate equivalents was first implemented by the groups of Bode and Glorius.²¹⁹ Both reported the same transformation, namely the selective annulation of enals and aromatic aldehydes to afford γ -butirolactones (Scheme 3.7). In the postulated catalytic cycle, the α,β -unsaturated aldehyde is attacked by the *in situ* formed carbene **A**. The resulting zwitterionic intermediate **B** deprotonates to give the homoenolate intermediate (resonance forms **C** and **D**). This, in turn, attacks the aromatic aldehyde as a d^3 -nucleophile under formation of the alcoholate **E**. The tautomerization of **E** to the acylimidazolium intermediate **F** is followed by an intramolecular attack of the alcoholate oxygen atom at the carbonyl function to afford the γ -butirolactone and the regeneration of the catalyst (Scheme 3.7).

²¹⁹ (a) Sohn, S. S.; Rosen, E.L.; Bode, J.W. *J. Am. Chem.Soc.* **2004**, 126, 14370. (b) Burstein, C.; Glorius, F. *Angew. Chem. Int. Ed.* **2004**, 43, 6205. (c) Burstein, C.; Tschan, S.; Xie, X.; Glorius, F. *Synthesis* **2006**, 2418.



Scheme 3.7. Formation of γ -butyrolactones by NHC-catalyzed conjugate umpolung of enals.

Glorius and co-workers observed that a sterically demanding precatalyst is the key to success for the generation of a homoenolate species within this methodology.²²⁰ Thus, the use of a sterically-demanding carbene avoided the formation of products arising from classical umpolung (benzoin condensation and Stetter reaction) by an efficient shielding of the nucleophilic center of the resulting Breslow intermediate (Figure 3.5). Moreover, the same effect is responsible for the favored formation of the homoenolate species as the use of thiazolium salts as precatalysts only afforded the formation of the benzoin product in poor yields. Furthermore, it was then shown that the strength and the amount of the base used to generate the NHC was also crucial to prevent the protonation of the homoenolate intermediate.²²¹

²²⁰ Burstein, C.; Tschan, S.; Xie, X.; Glorius, F. *Synthesis* **2006**, 2418.

²²¹ (a) Chan, A.; Scheidt, K.A. *Org. Lett.* **2005**, *7*, 905. (b) Sohn, S. S.; Bode, J.W. *Org. Lett.* **2005**, *7*, 3873.

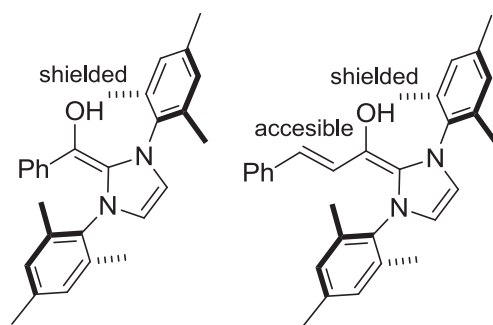


Figure 3.5. Possible sterical influence of the catalyst on the nucleophilicity.

Similarly, the group of Bode published a study of the influence of the aromatic substituent at N₁ of the triazolium salts.²²² They could rationalize the often observed superiority of mesityl-substituted NHCs²²³ in homoenolate chemistry by their ability to render the initial addition of the catalyst to the enal irreversible.

Subsequent work to the synthesis of γ -lactones has evolved into a multitude of NHC catalyzed homoenolate reactions.²⁰⁹ For example, the synthesis of lactams,²²⁴ γ -spirolactones,²²⁵ pyrazolidinones,²²⁶ pyridazinones,²²⁷ spirocyclopentanones²²⁸ and cyclopentanols²²⁹ are noteworthy. Homoenolates have also been shown to add efficiently to nitrostyrenes²³⁰ and sulfoimines leading to the precursors for novel γ -aminobutyric acid derivatives.²³¹

Another interesting reaction is the NHC mediated annulation of enals with vinyl ketones which leads to the synthesis of [2H]-pyranones.²³² The unravelling of the mechanism was the key for understanding the unexpected formation of [2H]-pyranones instead of a cyclopentene derivative. The authors theorized that the use of a weak amine such as DMAP for the deprotonation of the NHC precatalyst generates a stronger conjugate acid (DMAPH⁺) (Scheme 3.8). The homoenolate equivalent **C**

²²² Mahatthananchai, J.; Bode, J.W. *Chem. Sci.* **2012**, *3*, 192.

²²³ Chiang, P.C.; Bode, J.W. *TCl Mail*, **2011**, *149*, 2.

²²⁴ (a) He, M.; Bode, J.W. *Org. Lett.* **2005**, *7*, 3131. (b) He, M.; Bode, J.W. *J. Am. Chem. Soc.* **2008**, *130*, 418.

²²⁵ (a) Nair, V.; Vellalath, S.; Poonoth, M.; Mohan, R.; Suresh, E. *Org. Lett.* **2006**, *8*, 507. (b) Nair, V.; Vellalath, S.; Poonoth, M.; Suresh, E.; Viji, S. *Synthesis* **2007**, 3195.

²²⁶ Chan, A.; Scheidt, K. A. *J. Am. Chem. Soc.* **2008**, *130*, 2741.

²²⁷ Chan, A.; Scheidt, K. A. *J. Am. Chem. Soc.* **2008**, *129*, 5334.

²²⁸ Nair, V.; Babu, B. P.; Vellalath, S.; Suresh, E. *Chem. Commun.* **2008**, 747.

²²⁹ Nair, V.; Babu, B. P.; Vellalath, S.; Varghese, V.; Raveendran, A. E.; Suresh, E. *Org. Lett.* **2009**, *11*, 2507.

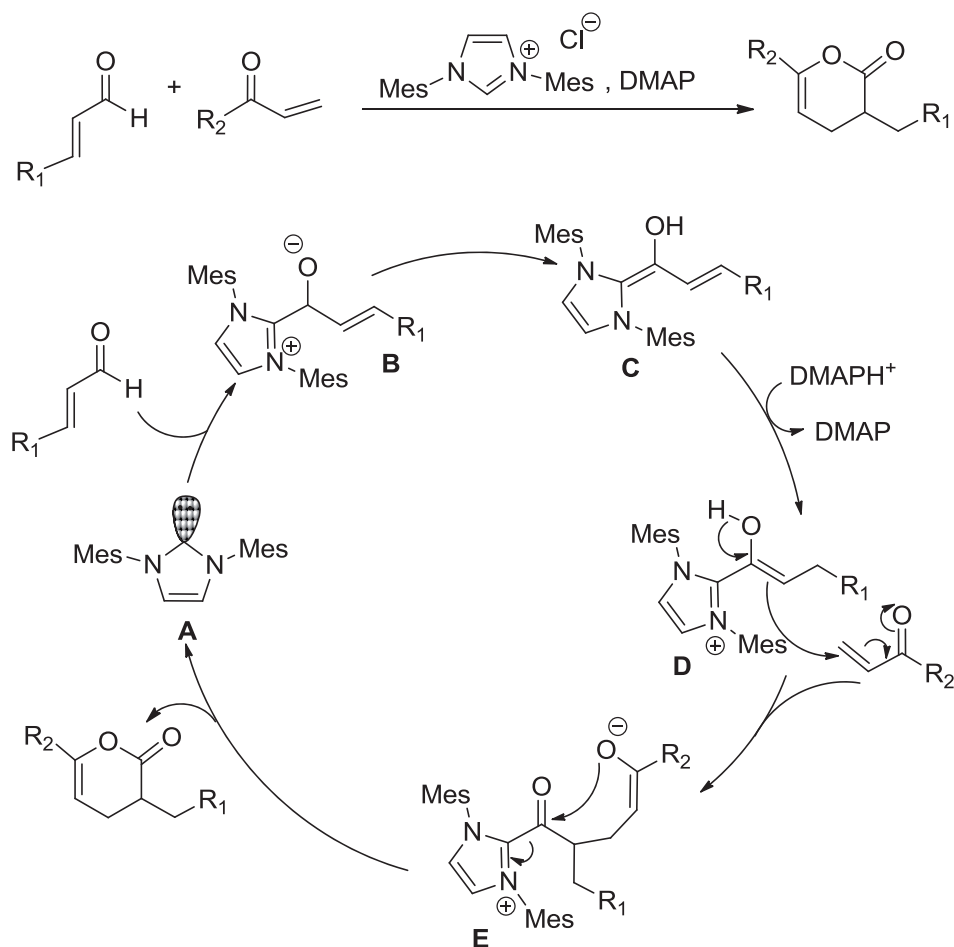
²³⁰ Nair, V.; Sinu, C. R.; Babu, B. P.; Varghese, V.; Jose, A.; Suresh, E. *Org. Lett.* **2009**, *11*, 5570.

²³¹ Nair, V.; Varghese, V.; Babu, B. P.; Sinu, C. R.; Suresh, E. *Org. Biomol. Chem.* **2010**, *8*, 761.

²³² Nair, V.; Paul, R.P.; Lakshmi, K.C.S.; Menon, R.S.; Jose, A.; Sinu, C.R. *Tetrahedron Lett.* **2011**, *52*, 5992.

Chapter 3.1. Introduction

formed initially from the enal and NHC undergoes a β -protonation presumably by DMAPH^+ to afford enol **D**. The subsequent Michael addition to the vinyl ketone affords species **E**, which upon intramolecular O-acylation reaction delivers the [2H]-pyranone.



Scheme 3.8. Mechanistic proposal for annulation reaction of enals and vinyl ketones according to ref 232.

1.2.2 Basicity

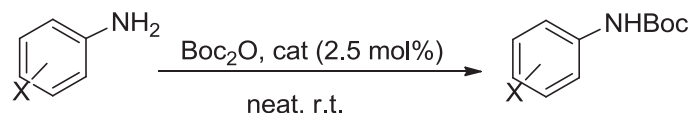
Another attribute of *N*-heterocyclic carbenes is their basicity. There are several theoretical and experimental reports on this topic where pK_a values between 21 and 25 were reported for the corresponding conjugate acids in DMSO and in water.²³³ The largest effects on pK_a were observed by varying *N*-substituent or ring size, while the effects of C4-C5 saturation were small.^{233b} As expected, due to their strong basicity, there are some reports on aldol²³⁴ and Michael reactions²³⁵ catalyzed by NHCs.

²³³ (a) Kim, Y.-J.; Streitwieser, A. *J. Am. Chem. Soc.* **2002**, *124*, 5757. (b) Magill, A. M.; Cavell, K. J.; Yates, B. F. *J. Am. Chem. Soc.* **2004**, *126*, 8717. (c) Amyes, T. L.; Diver, S. T.; Richard, J. P.; Rivas, F. M.; Toth, K. *J. Am. Chem. Soc.* **2004**, *126*, 4366. (d) Chu, Y.; Deng, H.; Cheng, J.-P. *J. Org. Chem.* **2007**, *72*, 7790. (e) Higgins, E. M.; Sherwood, J. A.; Lindsay, A.G.; Armstrong, J.; Massey, R. S.; Alder, R.W.; O'Donoghue, A. *Chem. Commun.* **2011**, *47*, 1559.

²³⁴ Du, G.-F.; He, L.; Gu, C.-Z.; Dai, B. *Synlett* **2010**, 2513.

1.3 Organocatalysis by 1-alkyl-3-methylimidazolium cation

Recently, Chakraborti has reported a nonsolvent application for imidazolium-based Ionic Liquids (ILs) as its environmentally friendly image as alternative solvents seems now to be under scrutiny²³⁶ on several issues such as combustibility,²³⁷ toxicity²³⁸ and bio-degradability.²³⁹ Thus, they have been described as organocatalysts for chemoselective *N-tert*-butyloxycarbonylation of amines (Scheme 3.9).²⁴⁰ The catalytic activity is based on the 1-alkyl-3-methylimidazolium cation.



Scheme 3.9. Imidazolium-based Ionic Liquid catalyzed *N*-*tert*-butyloxycarbonylation of amines.

The C-2 hydrogen of imidazolium ion exhibits acidic character²⁴¹ and possesses hydrogen bond donor (HBD) ability.²⁴² The hydrogen bond (H-B) formation ability of the C-2 H in 1-butyl-3-methylimidazolium (bmim) based ionic liquids (ILs) plays a crucial role in their catalytic activity.²⁴³ The IL acts as an inducer of "electrophilic activation" of Boc_2O through bifurcated hydrogen bond²⁴⁴ formation between the C-2 hydrogen of the bmim moiety and the carbonyl oxygen atoms of $(\text{Boc})_2\text{O}$ (Scheme 3.10). The anions of bmim-based ILs are hydrogen bond acceptors.²⁴⁵

²³⁵ (a) Phillips, E. M.; Riedrich, M.; Scheidt, K. A. *J. Am. Chem. Soc.* **2010**, *132*, 13179. (b) Truong, T.-K.-T.; Giang, V.-T. *Tetrahedron* **2010**, *66*, 5277. (c) Roy, S. R.; Chakraborti, A. K. *Org. Lett.* **2010**, *12*, 3866. (d) O'Brien, J. M.; Hoveyda, A. H. *J. Am. Chem. Soc.* **2011**, *133*, 7712. (e) Kim, H.; Byeon, S. R.; Leed, M. G. D.; Hong, J. *Tetrahedron Lett.* **2011**, *52*, 2468. (f) Kang, Q.; Zhang, Y. *Org. Biomol. Chem.* **2011**, *9*, 6715.

²³⁶ Ranke, J.; Stolte, S.; Stormann, R.; Atning, J.; Jastorff, B. *Chem. Rev.* **2007**, *107*, 2183.

²³⁷ Smiglak, M.; Reichert, W. M.; Holbrey, J. D.; Wilkes, J. S.; Sun, L. J.; Thrasher, S.; Kirichenko, K.; Singh, S.; Katrizky, A. R.; Rogers, R. D. *Chem. Commun.* **2006**, 2554.

²³⁸ Costello, D. M.; Brown, L. M.; Lamberti, G. A. *Green Chem.* **2009**, *11*, 548.

²³⁹ Coleman, D.; Gathergood, N. *Chem. Soc. Rev.* **2010**, *39*, 600.

²⁴⁰ Sarkar, A.; Roy, S. R.; Parikh, N.; Chakraborti, A. K. *J. Org. Chem.* **2011**, *76*, 7132.

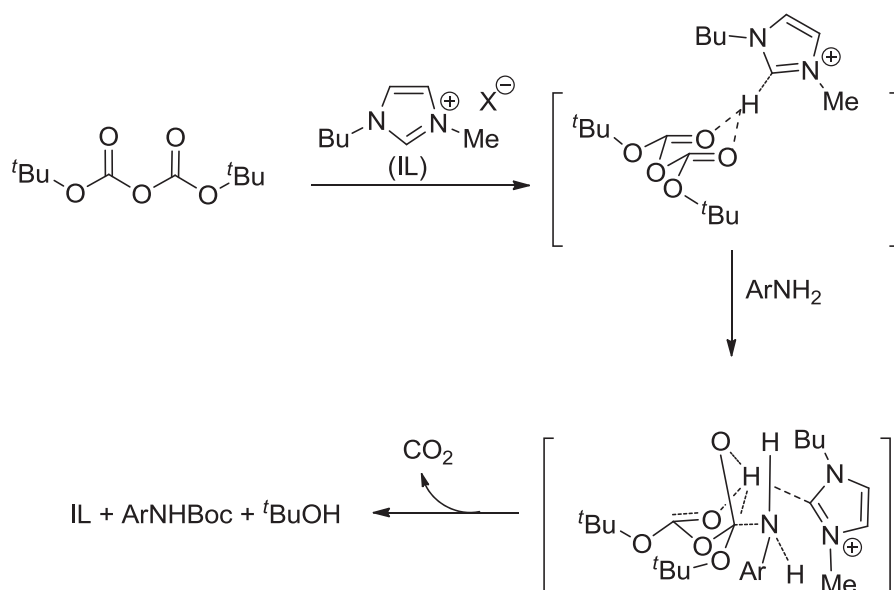
²⁴¹ Choi, D. S.; Kim, D. H.; Shin, U. S.; Deshmukh, R. R.; Lee, S.; Song, C. E. *Chem. Commun.* **2007**, 3467.

²⁴² (a) Aggarwal, A.; Kancaster, N. L.; Seth, A. R.; Welton, T. *Green Chem.* **2002**, *4*, 517. (b) Lungwitz, R.; Friedrich, M.; Linert, W.; Spange, S. *New J. Chem.* **2008**, *32*, 1493.

²⁴³ (a) Chakraborti, A. K.; Raha Roy, S.; Kumar, D.; Chopra, P. *Green Chem.* **2008**, *10*, 1111. (b) Chakraborti, A. K.; Raha Roy, S. *J. Am. Chem. Soc.* **2009**, *131*, 6902. (c) Raha Roy, S.; Chakraborti, A. K. *Org. Lett.* **2010**, *12*, 3866. (d) Sarkar, A.; Raha Roy, S.; Chakraborti, A. K. *Chem. Commun.* **2011**, *47*, 4538.

²⁴⁴ Steiner, T. *Angew. Chem., Int. Ed.* **2002**, *41*, 48.

²⁴⁵ Lungwitz, R.; Spange, S. *New J. Chem.* **2008**, *32*, 392.



Scheme 3.10. Role of the imidazolium-based IL in catalyzing the *N*-*t*-butyloxycarbonylation of amines

1.4 Supported NHC pre-catalysts

Most of the reported NHC catalyzed processes use soluble NHCs formed by deprotonation of the corresponding azolium salts. Although organocatalysis is considered to be free of the toxicity concerns that affect metal catalysis, these compounds are not innocuous and high catalyst loadings are used, which can complicate the separation protocols. Catalyst recovery and recycling remain a scientific challenge of economic and environmental relevance. One of the most widely used strategies to this purpose consists in immobilizing the homogeneous catalyst on an insoluble support. This immobilization allows an easy separation and the organic products are obtained without time-consuming chromatography. Therefore, over the past few years, some research groups have prepared and tested supported NHC catalysts to assess their recyclability.

Functionalization of commercial polymers such as PEG or polystyrene with NHC precursors has been tried.²⁴⁶ Storey reported the preparation of polymer-bound imidazolium salts (**SA1-SA3**) (Figure 3.6) (SA = supported azolium salt) and their application as supported pre-catalysts in benzoin condensation.^{246a} Polystyrene derivative **SA2** was recycled up to 3 cycles with a decrease of 10% yield after each cycle. Similarly, Zeitler described the obtention of heteroazolium salts linked to a MeOPEG-resin (**SA4-SA7**) (Figure 3.6).^{246b} In this case, MeOPEG-supported organocatalysts were tested in the intramolecular Stetter-type cyclization to form

²⁴⁶ (a) Storey, J.M.D.; Williamson, C. *Tetrahedron Lett.* **2005**, *46*, 7337. (b) Zeitler, K.; Mager, I. *Adv. Synth. Catal.* **2007**, *349*, 1851.

substituted chroman-4-one derivatives. They presented moderate to good yields despite the fact of a strong dependence on the reaction conditions. **SA4** could be recycled only once, as catalyst preservation was only achieved in the presence of EtOH, which lowered the yield.

Other polymeric NHC precursors have been reported, but they require the previous synthesis of specific monomers containing imidazolium moieties, or masked functionalities. Subsequent polymerization of those monomers by radical or ROMP processes were applied. These examples show good catalytic behavior but their recyclability has shown limited applicability in most cases.

The first example of these series was reported by Barrett which described the preparation of a high-loading ROMPgel-supported thiazolium iodide (**SA8**) derived from norbornene.²⁴⁷ ROMPgel **SA8** proved to be an efficient organocatalyst for Stetter reactions. 1,4-Dicarbonyl products were obtained in high yields and the catalyst could be reused up to four consecutive reaction cycles without significant loss of catalytic activity.

Buchmeiser described the preparation of a polymer-supported, CO₂-protected NHC (**SA9**) and its use in organocatalysis.²⁴⁸ The cyanosilylation²⁴⁹ and the trimerization of isocyanates²⁵⁰ were the reactions chosen to test the supported catalyst which showed excellent reactivity using low catalyst loadings. However, recyclability was not tested.

In the same manner, Taton and collaborators described the synthesis of a series of poly(NHC)s (**SA10-SA12** and **SA19**), poly(NHC) *N*-carboxylate adducts (**SA13-SA14**) and imidazolium hydrogencarbonates (**SA15-SA18**).²⁵¹ Both poly(NHC)s and their corresponding adducts were used as polymer-supported organocatalysts and precatalysts, respectively, in benzoin condensation, cyanosilylation and transesterification reactions. Both types of polymer-supported NHCs were recycled and

²⁴⁷ Barrett, A.G.M.; Love, A.C.; Tedeschi, L. *Org. Lett.* **2004**, *6*, 3377.

²⁴⁸ Pawar, G. M.; Buchmeiser, M. R. *Adv. Synth. Catal.* **2010**, *352*, 917

²⁴⁹ (a) Song, J. J.; Gallou, F.; Reeves, J. T.; Tan, Z.; Yee, N. K.; Senanayake, C. H. *J. Org. Chem.* **2006**, *71*, 1273. (b) Suzuki, Y.; Bakar, A.; Muramatsu, K.; Sato, M. *Tetrahedron* **2006**, *62*, 4227.

²⁵⁰ Bantu, B.; Pawar, G. M.; Decker, U.; Wurst, K.; Schmidt, A. M.; Buchmeiser, M. R. *Chem. Eur. J.* **2009**, *15*, 3103.

²⁵¹ (a) Pinaud, J.; Vignolle, J.; Gnanou, Y.; Taton, D. *Macromolecules*, **2011**, *44*, 1900. (b) Coupillaud, P.; Pinaud, J.; Guidolin, N.; Vignolle, J.; Fèvre, M.; Veaudecenne, E.; Mecerreyes, D.; Taton, D. *J. Pol. Sci., Part A: Pol. Chem.* **2013**, *51*, 4530. (c) Kuzmicz, D.; Coupillaud, P.; Men, Y.; Vignolle, J.; Vendramineto, G.; Ambrogi, M.; Taton, D.; Yuan, J. *Polymer* **2014**, *55*, 3423.

Chapter 3.1. Introduction

used several times, but the manipulation of poly(NHC)s (**SA10-SA12**) was more complicated owing to their air and moisture sensitivity. In this regard, zwitterionic poly(NHC-CO₂) adducts **SA13-SA14** could be easier manipulated than their bare poly(NHC) counterparts, providing good to excellent yields, in particular in the transesterification reaction.^{251a} Remarkably **SA14** could be reused up to 8 catalytic cycles. Although poly[NHC(H)][HCO₃] precursors exhibited a lower catalytic activity in all the reactions tested, a major advantage of these salts lies in their air stability in the solid state.²⁵² Authors postulated that the *in situ* generation of poly(NHC)s from **SA15-SA18** was not complete.^{251b} Good to excellent yields were obtained with **SA15-SA17** in tested reactions; however, recyclability was only achieved in cyanosilylations. Finally, for **SA19**, fairly good conversions were obtained in benzoin condensation and cyanosilylation reaction even after three cycles of organocatalysis.^{251c} The authors attributed the slight loss of efficiency in recyclability to a partial deactivation of NHC units.

Recently, Chung has presented poly(4-vinylimidazolium) iodide **SA20** as a highly recyclable organocatalyst precursor for benzoin condensation.²⁵³ Poly(4-vinyl NHC) obtained from **SA20** showed high catalytic activity and could be recovered and reused over seven times without loss of performance.

In the same way, Albéniz²⁵⁴ has reported the immobilization of imidazolium bromides in polynorbornene as a recyclable and recoverable pre-organocatalysts (**SA21-SA23**). Catalytic tests were performed for two different reactions. First, the conversion of α,β -unsaturated aldehydes into saturated esters was evaluated, where **SA22** and **SA23** became the best catalysts as a result of bulkier R groups and **SA22** could be reused up to 4 cycles. Then **SA22** was tested in the synthesis of γ -butyrolactones affording moderate yields.

²⁵² Fèvre, M.; Coupillaud, P.; Miqueu, K.; Sotiropoulos, J.-M.; Vignolle, J.; Taton, D. *J. Org. Chem.* **2012**, *77*, 10135.

²⁵³ Seo, U.R.; Chung, Y.K. *Adv. Synth. Catal.* **2014**, *356*, 1955.

²⁵⁴ Molina de la Torre, J.A.; Albéniz, A.C. *ChemCatChem* **2014**, *6*, 3547.

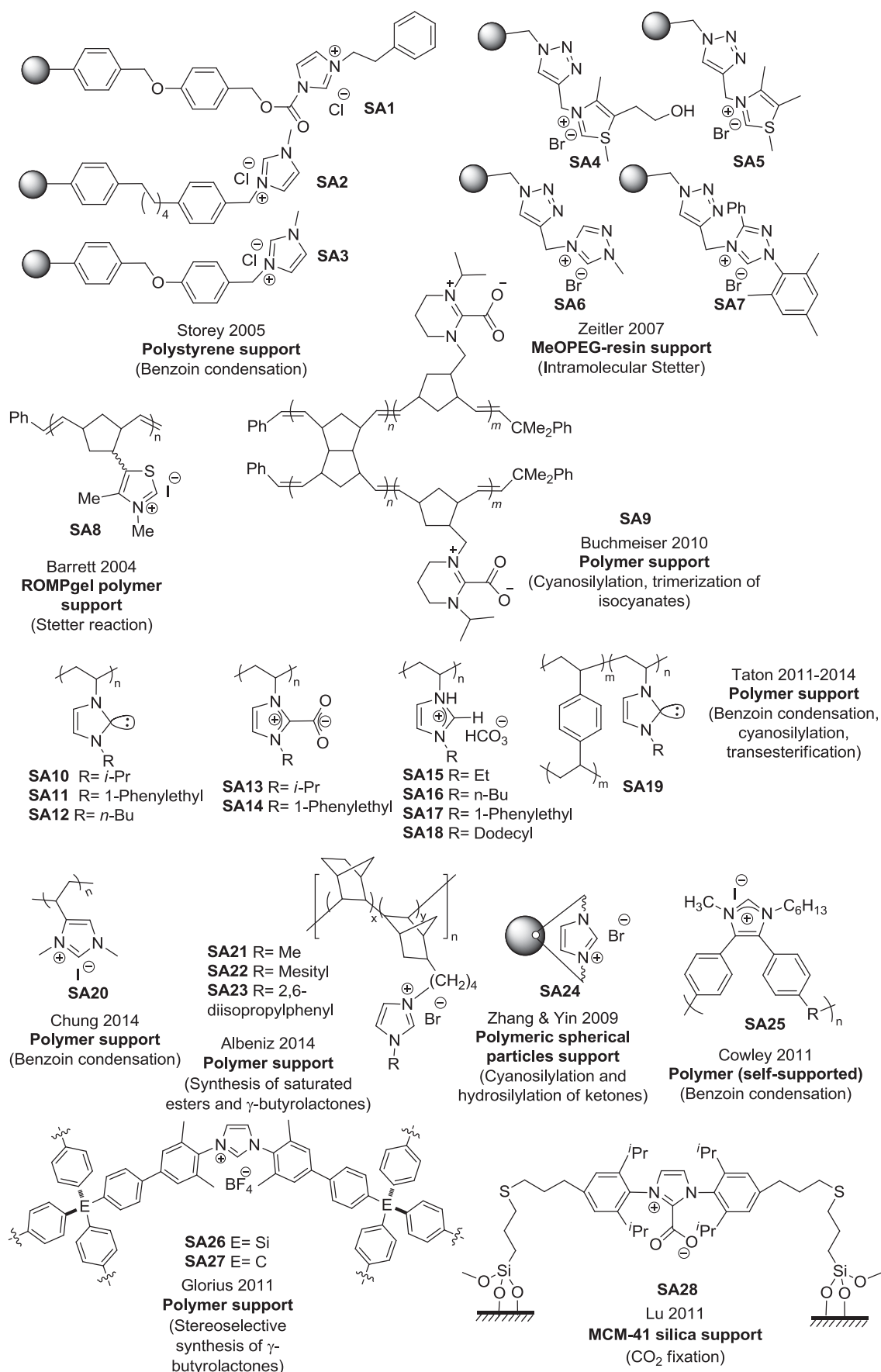


Figure 3.6. Examples of supported NHC catalysts and pre-catalysts.

Chapter 3.1. Introduction

Better results have been achieved using polymeric frameworks containing imidazolium salts in the main chain. Their preparation require a several step synthesis of specially designed monomers to give the polymeric framework by condensation or Suzuki coupling. In this way, symmetric substituted NHCs can be generated as part of the polymeric main chain. One of the examples of this type of supported catalysts is the poly-imidazolium bromide particles **SA24**²⁵⁵ which were tested in the cyanosilylation and hydrosilylation of ketones. Excellent catalytic activities were achieved and recyclability was possible up to 3 consecutive runs.

In 2011, Cowley reported the preparation of a recyclable, self-supported imidazolium iodide as precursor of NHC-organocatalyst (**SA25**).²⁵⁶ There was a repetition of imidazolium moieties positioned orthogonally with respect to the polymer backbone along the polymer chain. **SA25** was tested as pre-organocatalyst in the benzoin condensation, higher yields being achieved when electron-rich or electron-deficient benzaldehydes were employed due to synergistic effects between each repeating unit along the polymer chain and could result in higher efficiencies compared to monomeric analogues according to the authors. **SA25** was recovered and reused once with only a marginal loss of activity.

Glorius described the preparation of imidazolium tetrafluoroborates contained in organic frameworks (**SA26-SA27**) as heterogeneous organocatalysts.²⁵⁷ The catalytic activity of the *in situ* generated NHC species was tested in the conjugated umpolung of cinnamaldehyde and the stereoselective coupling with trifluoroacetophenone. The reusability of the heterogeneous catalyst was demonstrated in up to four cycles. The yields obtained with **SA26** varied from 69% to 84%, while they decreased from 65% to 46% in the case of **SA27**.

Finally, another type of immobilization was reported by Lu and coworkers. They investigated the catalytic performance of an MCM-41 functionalized organosilica containing an NHC-CO₂ adduct (**SA28**),²⁵⁸ which proved to be an effective catalyst precursor for the cycloaddition reaction of CO₂ with propylene oxide to produce cyclic carbonates. As expected, the reaction rate was lower than that of the reaction carried out with the homogeneous analogue, suggesting that the MCM-41 supported catalyst

²⁵⁵ Tan, M.X.; Zhang, .; Ying, J.Y. *Adv. Synth.Catal.* **2009**, *351*, 1390.

²⁵⁶ Powell, A.B.; Suzuki, Y.; Mitsuru, U.; Bielawski, C.W.; Cowley, A.H. *J. Am. Chem. Soc.* **2011**, *133*, 5218.

²⁵⁷ Rose, M.; Notzon, A.; Heitbaum, M.; Nickerl, G.; Paasch, S.; Brunner, E.; Glorius, F.; Kaskel, S. *Chem. Commun.* **2011**, *47*, 4814.

²⁵⁸ Zhou, H.; Wang, Y.-M.; Zhang, W.-Z.; Qu, J.-P.; Lu, X.-B. *Green Chem.* **2011**, *13*, 644.

suffered from diffusion resistance. Recycling studies were performed and supported catalyst could be reused up to 3 times.

1.5 Imidazolium and imidazolinium derived organosilicas. Precedents in the group

Although only one example of silica-supported NHC pre-catalyst has been found in the literature (**SA28**), there exist some other examples of organosilicas containing imidazolium salts which have been employed in organocatalysis not involving NHC species.²⁵⁹

Mizuno et al.²⁶⁰ reported the silica supported dihydroimidazolium salt **SA29** (Figure 3.7), which was prepared by grafting to silica gel, as a solid base catalyst for the cyanosilylation of cyclic and acyclic ketones, being reused in a second run. Material **SA29** was further employed for the epoxidation of some α,β -unsaturated cyclic ketones with H_2O_2 as an oxidant. No recycling experiments were mentioned for this last reaction.

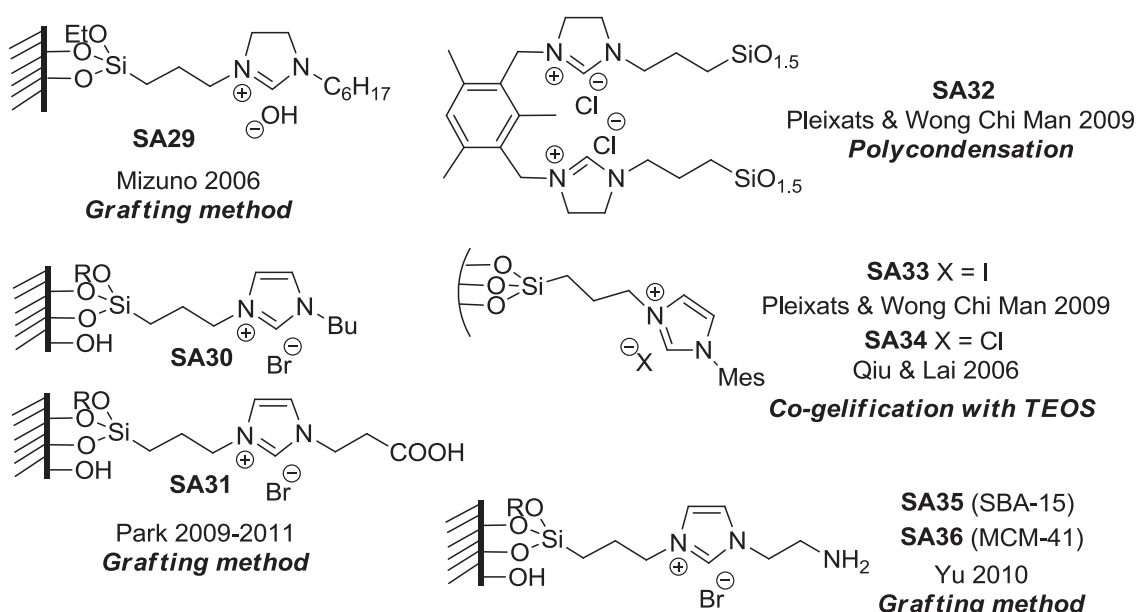


Figure 3.7. Examples of silica supported imidazolium salts-based organocatalysts.

Park and co-workers have studied several non-functionalized and functionalized imidazolium salts grafted onto silica gel, **SA30** and **SA31**, as heterogeneous catalysts in the cycloaddition reaction between epoxides and carbon dioxide to afford cyclic

²⁵⁹ Monge-Marcet, A.; Pleixats, R.; Cattoën, X.; Wong Chi Man, M. *Catal. Sci. Technol.* **2011**, *1*, 1544.

²⁶⁰ Yamaguchi, K.; Imago, T.; Ogasawara, Y.; Kasai, J.; Kotaniand, M.; Mizuno, N. *Adv. Synth. Catal.*, **2006**, *348*, 1516.

Chapter 3.1. Introduction

carbonates.²⁶¹ Material **SA30** offered moderate to excellent yields (64-94%) and was recycled up to 3 runs. The same material was also investigated in the copolymerization of phenylglycidyl ether and CO₂ with good results in terms of recycling and average of polymer length. Higher activity and selectivity in the formation of cyclic carbonates were obtained with the material **SA31** bearing a carboxyl group; the recycling of the catalyst was performed for 5 runs without loss of activity.

Some imidazolium or dihydroimidazolium-containing organosilicas **SA32-SA36** have been developed to facilitate the separation, recovery and recycling of the catalyst in Knoevenagel condensations. All these materials gave complete selectivity for the desired compound.

In our research group, hybrid silica materials **SA33** and **SA32** containing imidazolium and dihydroimidazolium salts in different dilutions were prepared using template-based sol-gel methodologies.²⁶² These materials were found to be active and reusable catalysts in the Knoevenagel condensations under solvent-free conditions at 100°C. Five consecutive cycles were performed with the same batch of catalyst. The immobilized catalysts showed higher activities for this transformation than other related homogeneous bis-imidazolium salts and were much more active than non-functionalized mesostructured MCM-41, which presented some residual activity. These facts suggest a certain degree of cooperativity between the surface of the inorganic matrix and the active sites and underline the crucial role of the (dihydro)imidazolium salt. Better performance was observed from the non-porous hybrid silica catalysts with higher organic loading, showing that the predominant factor is the concentration of the organics rather than the porosity of the materials under these neat conditions. Thus, the non-porous bridged silsesquioxane **SA32**, gave the best results in the reaction of a variety of aromatic aldehydes and active methylene compounds such as malonitrile and ethyl cyanoacetate.

Other examples are an imidazolium-functionalized SBA-15 type material **SA34** prepared by co-condensation with TEOS, which was described as a recyclable catalyst in the same type of reactions under neat conditions.²⁶³ Similarly, Shen and co-workers

²⁶¹ (a) Dharman, M. M.; Choi, H. J.; Park, S. W.; Park, D. W. *Top. Catal.*, **2010**, *53*, 462. (b) Han, L.; Choi, H. J.; Choi, S. J.; Liu, B. Y.; Park, D. W. *Green Chem.*, **2011**, *13*, 1023. (c) Han, L.; Park, S. W.; Park, D. W. *Energy Environ. Sci.*, **2009**, *2*, 1286. (d) Udayakumar, S.; Lee, M. K.; Shim, H. L.; Park, S. W.; Park, D. W. *Catal. Commun.*, **2009**, *10*, 659.

²⁶² Trilla, M.; Pleixats, R.; Wong Chi Man, M.; Bied, B. *Green Chem.*, **2009**, *11*, 1815.

²⁶³ (a) Liu, Y.; Peng, J. J.; Zhai, S. R.; Li, J. Y.; Mao, J. J.; Li, M. J.; Qiu, H. Y.; Lai, G. Q. *Eur. J. Inorg. Chem.*, **2006**, 2947. (b) Li, J. Y.; Peng, J. J.; Qiu, H. Y.; Jiang, J. X.; Wu, J. R.; Ni, Y.; Lai, G. Q. *Chin. J. Org. Chem.*, **2007**, *27*, 483.

reported similar results for a related material obtained by co-condensation of the same monomer with TEOS under acidic conditions without template assistance.²⁶⁴ Finally, task-specific basic imidazolium salts immobilized on mesoporous silicas SBA-15 and MCM-41 by a grafting procedure (**SA35-SA36**) were described as reusable catalysts for Knoevenagel condensations in aqueous media.²⁶⁵

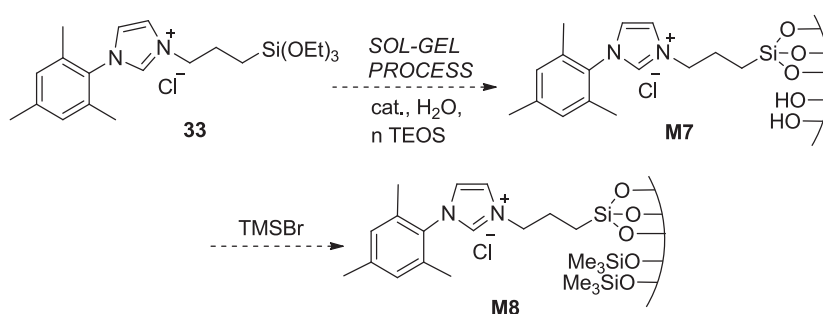
²⁶⁴ Lai, G. Q.; Peng, J. J.; Li, J. Y.; Qiu, H. Y.; Jiang, J. X.; Jian, K. Z.; Shen, Y. J. *Tetrahedron Lett.*, **2006**, *47*, 6951.

²⁶⁵ Zhao, H. H.; Yu, N. Y.; Ding, Y.; Tan, R.; Liu, C.; Yin, D. H.; Qiu, H. Y.; Yin, D. L. *Microporous Mesoporous Mater.*, **2010**, *136*, 10.

2. OBJECTIVES

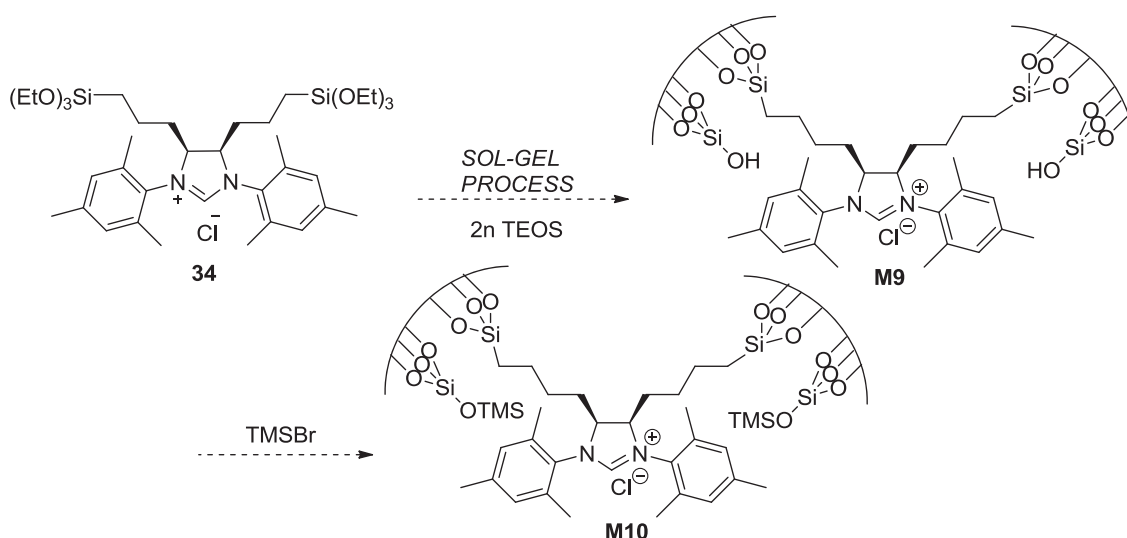
Following the interest of the group on recyclable organocatalysts based on imidazolium salts prepared by sol-gel methodologies, we aimed at the following:

a) The synthesis of the mono-silylated precursor **33** derived from an imidazolium salt, the subsequent preparation of organosilica **M7** using a sol-gel methodology, by co-condensation of **33** with TEOS under nucleophilic catalysis, and further protection of the free silanol groups present in the material **M7** to obtain the Si-OH capped material **M8** (Scheme 3.11).



Scheme 3.11. Silylated imidazolium salt precursor **33** and organosilicas **M7** and **M8**.

b) The synthesis of the bis-silylated precursor **34** derived from a dihydroimidazolium salt, the subsequent preparation of an organosilica **M9** using a sol-gel methodology involving co-condensation with TEOS. As in the previous case, free silanol groups would be protected in the form of trimethylsilyl ether groups to afford the organosilica **M10** (Scheme 3.12).



Scheme 3.12. Silylated dihydroimidazolium salt precursor **34** and organosilicas **M9** and **M10**.

c) The assay of these new hybrid silica materials (**M7**, **M8**, **M9**, **M10**) in organocatalysis. Supported NHC species would be generated *in situ* through the addition of a suitable base to Si-OH capped materials **M8** and **M10**. We envisaged to test the benzoin condensation and some other reactions proceeding through the formation of an homoenolate. We also planned to assay the *N*-tert-butylloxycarbonylation of amines, which takes place under catalysis by the imidazolium salt, without the need of an added base.

3. RESULTS AND DISCUSSION

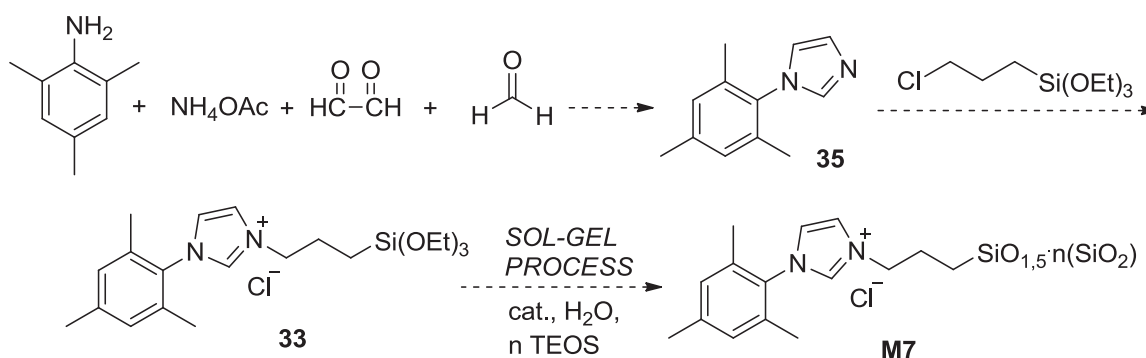
3.1 Immobilization of imidazolium and imidazolium salts

Imidazolium and imidazolium derived salts bearing trialkoxysilyl groups are prone to be immobilized by sol-gel methodology. This section will be divided in two parts according to the different azolium salts to be supported. The first part will focus on the preparation of an *N*-mesityl imidazolium supported pre-catalyst, while the second part will be dedicated to the immobilization of a *N,N'*-dimesityl imidazolium salt.

3.1.1 Hybrid silica materials derived from a mono-silylated *N*-mesityl imidazolium salt

3.1.1.1 Preparation of the hybrid silica material M7

The preparation of the monosilylated imidazolium chloride **33** and the hybrid silica material **M7** were envisaged as depicted in Scheme 3.13 following a procedure described by Dra. Guadalupe Borja for materials containing Pd-NHC moieties.²⁶⁶



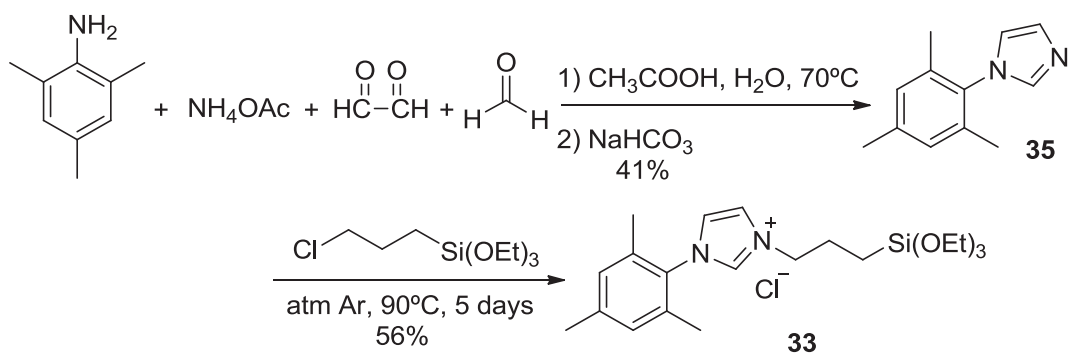
Scheme 3.13. Synthetic strategy for the preparation of **M7**.

Commercially available 2,4,6-trimethylaniline was treated with ammonium acetate, glyoxal and formaldehyde to achieve 1-mesitylimidazole **35** through an already described procedure,²⁶⁷ known as Debus-Radziszewski synthesis.²⁶⁸ Subsequent alkylation with 3-chloropropyltriethoxysilane in the absence of solvent at 90°C led to the obtention of the desired monosilylated precursor **33** (Scheme 3.14).

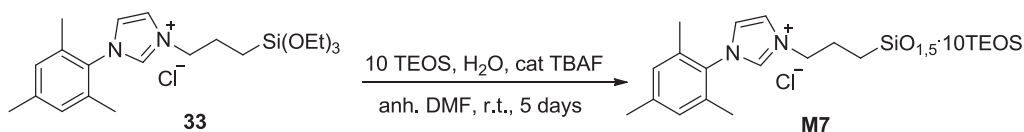
²⁶⁶ (a) Borja, G.; Monge-Marcet, A.; Pleixats, R.; Parella, T.; Cattoën, X.; Wong Chi Man, M. *Eur. J. Org. Chem.* **2012**, 3625. (b) Borja, G. *PhD Dissertation*, Universitat Autònoma de Barcelona, **2010**.

²⁶⁷ E.I. DU PONT DE NEMOURS AND COMPANY. "Process for the manufacture of imidazoles". Arduengo III, A. J.; Gentry Jr, F. P.; Taverkere, P. K.; Simmons III, H.E. United States. US Patent 6,177,575 B1, **2001**.

²⁶⁸ Maton, C.; De Vos, N.; Roman, B. I.; Vanecht, E.; Brooks, N.R.; Binnemans, K.; Schaltin, S.; Franser, J.; Stevens, C.V. *ChemPhysChem* **2012**, 13, 3146.

Scheme 3.14. Preparation of monosilylated imidazolium salt **33**.

Finally, the cogelification of monomer **33** with tetraethoxysilane (TEOS, molar ratio TEOS:**33** of 10:1) was performed in anhydrous DMF at room temperature under nucleophilic conditions using a stoichiometric amount of water (with respect to the ethoxy groups) and tetrabutylammonium fluoride as catalyst (1 mol% with respect to Si) (Scheme 3.15). The solution gellified after 2 hours and was aged for 5 days at room temperature. Then it was filtered, washed successively with water, ethanol and acetone. The resulting powder was dried overnight under vacuum at 50°C to afford **M7** as a white powder.

Scheme 3.15. Preparation of hybrid silica material **M7**.

This material was characterized by ^{13}C - and ^{29}Si -SSNMR, N_2 sorption measurements and elemental analysis. The ^{29}Si CP-MAS NMR spectrum (Figure 3.8 a) of **M7** confirmed the covalent bonding of the organic moiety to the silica matrix by the presence of T^2 and T^3 signals at -61.37 and -70.17 ppm respectively, in addition to the characteristic Q^2 , Q^3 and Q^4 signals corresponding to the condensed TEOS at -96.22 , -104.62 and -114.04 ppm. The ^{13}C -SSNMR spectrum showed broad signals at similar positions to those of the monosilylated precursor **33** (Figure 3.8 b) which constitutes also a prove that the organic functionality had been loaded in the final material. However, the dilution of the organic moiety in the inorganic matrix precluded the observation of the corresponding signals in the IR spectra.

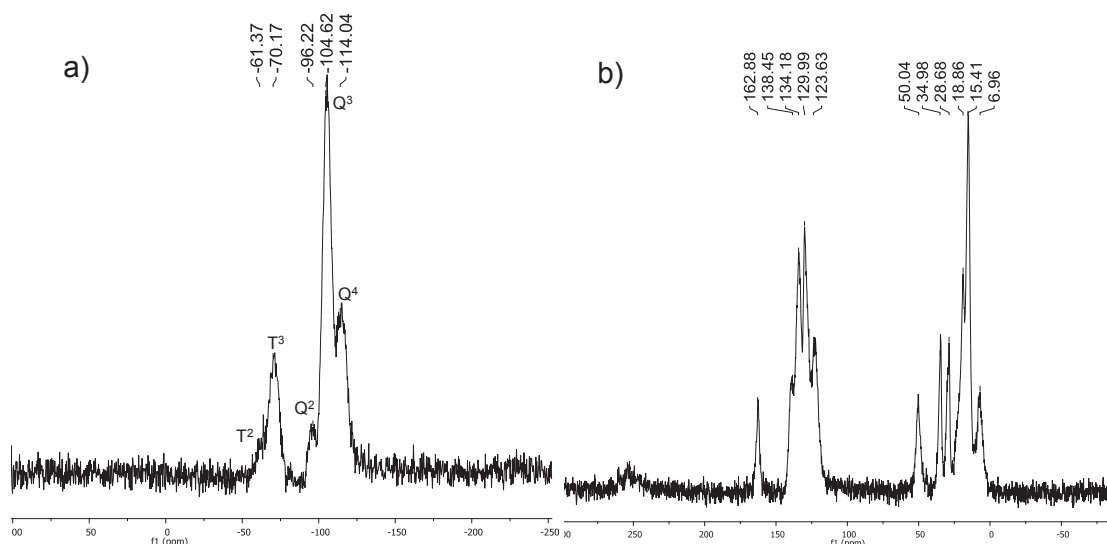


Figure 3.8. a) ^{29}Si -SSNMR of **M7**. b) ^{13}C -SSNMR of **M7**.

The N_2 adsorption-desorption measurements (Figure 3.9, left) of **M7** revealed a characteristic *type IV* isotherm, showing a hysteresis loop with a relatively large distribution of mesopores; the pore diameter distribution (Figure 3.9, right) was centered around 35 Å, with a total pore volume of $0.24 \text{ cm}^3/\text{g}$ and a BET surface area of $170 \text{ m}^2/\text{g}$. The imidazolium salt content was determined by elemental analysis of N and it was found to be 1.25 mmol of imidazolium salt/g.

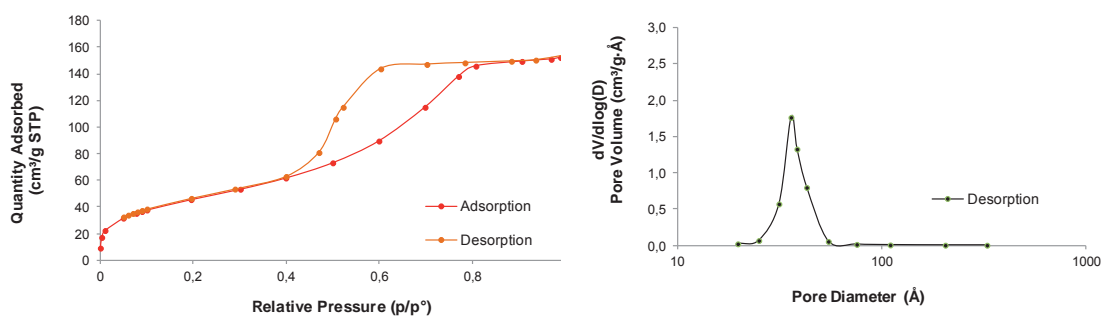


Figure 3.9. N_2 -sorption isotherm (left) and pore size distribution (right) of **M7**.

In agreement with the SEM and TEM images (Figure 3.10) and the p-XRD diffractogram (Figure 3.11) recorded for **M7**, we can conclude that organosilica **M7** is amorphous. This material does not present any organization as any structuring agent was used in its preparation; however in some cases bis- and tris-imidazolium salts can favour the self-organization of the organic fragment within the hybrid silica material.

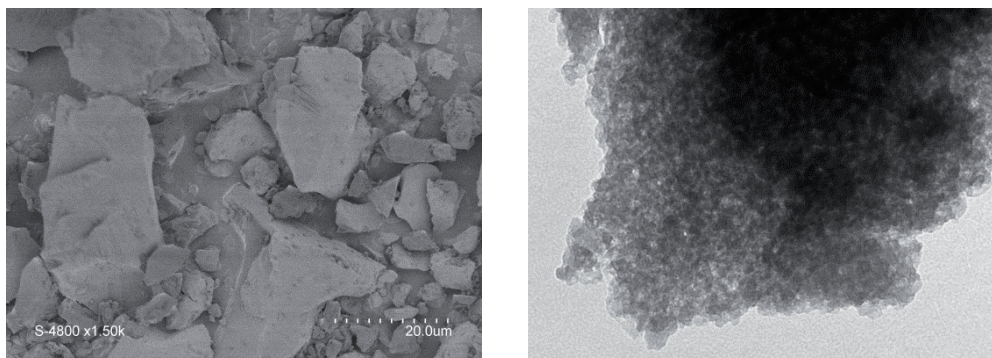


Figure 3.10. SEM (left) and TEM (right) images of material **M7**.

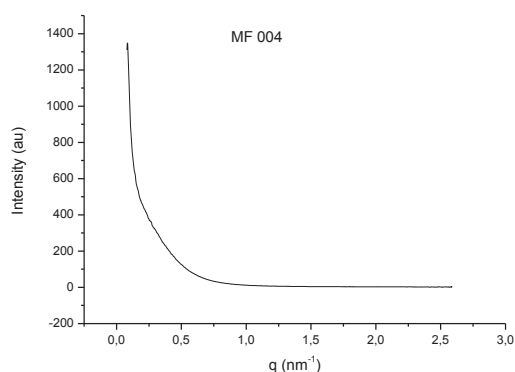


Figure 3.11. p-XRD diffractogram of **M7**.

3.1.1.2 Capping of surface silanol groups of hybrid silica material **M7**

Surface silanol groups can prevent the formation of the NHC carbene as they present an acidic character.²⁶⁹ Taking into account the fact that the ²⁹Si CP-MAS NMR spectrum (Figure 3.8 a) of **M7** presented the signals Q² and Q³ indicating that condensation of TEOS had not been complete, the presence of a considerable amount of free silanol groups was expected. At this point, we decided to protect them in the form of trimethyl silyl ethers.

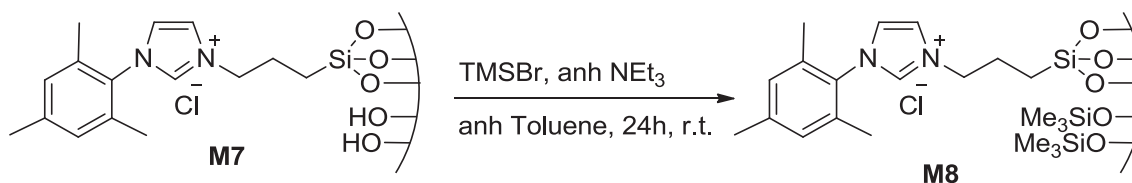
Thus, organosilica **M7** was treated with trimethylsilyl bromide in the presence of anhydrous triethylamine in anhydrous toluene at room temperature for 24 hours (Scheme 3.16), following an adapted procedure described in the literature.²⁷⁰ Then the

²⁶⁹ (a) Brinker, C. J.; Scherer, G. W. *Sol-Gel Science: the Physics and Chemistry of Sol-Gel Processing*, Academic Press, San Diego, **1990**. (b) Rosenholm, J. M.; Czuryzkiewicz, T.; Kleitz, F.; Rosenholm, J. B.; Lindén, M. *Langmuir*, **2007**, *23*, 4315. (c) Bass, J.D.; Solovyov, A.; Pascall, A.J.; Katz, A. *J. Am. Chem. Soc.* **2006**, *128*, 3737. (d) Brunelli, N. A.; Venkatasubbaiah, K.; Jones, C.W. *Chem. Mater.* **2012**, *24*, 2433.

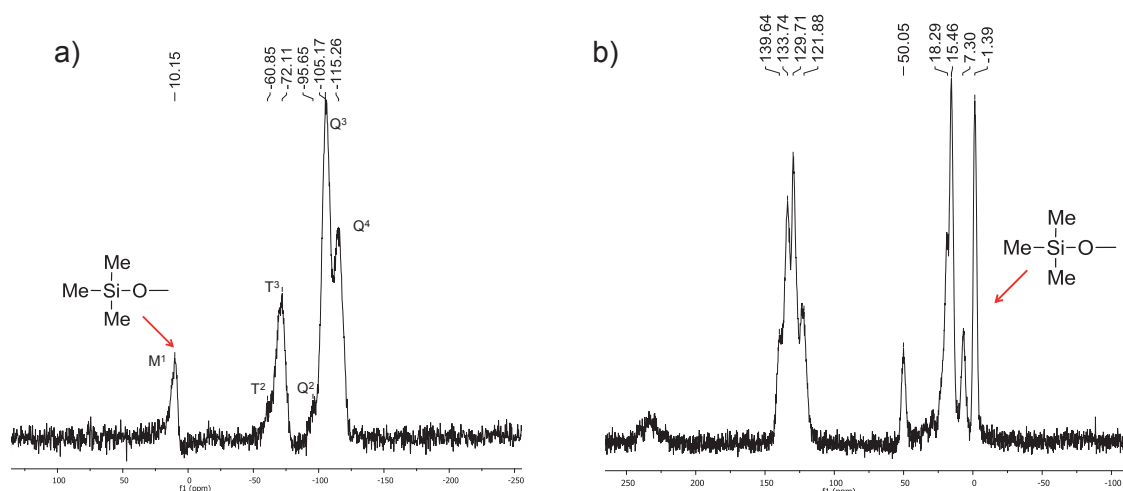
²⁷⁰ Karamé, I.; Boualleg, M.; Camus, J.-M.; Maishal, T.K.; Alauzun, J.; Basset, J.-M.; Copéret, C.; Corriu, R. J. P.; Jeanneau, E.; Mehdi, A.; Reyé, C.; Veyre, L.; Thieuleux, C. *Chem. Eur. J.* **2009**, *15*, 11820.

Chapter 3.3. Results and Discussion

solid was washed with toluene, methanol, diethyl ether and acetone and finally dried overnight under vacuum at 50°C to yield **M8** as a white powder.



Once material **M8** was obtained, it was characterized by ^{13}C - and ^{29}Si -SSNMR, N_2 sorption measurements and elemental analysis. The ^{29}Si CP-MAS NMR spectrum (Figure 3.12 a) of **M8** confirmed the protection of silanols by the appearance of the signal M^1 at 10.15 ppm corresponding to the new moieties $-\text{OSiMe}_3$. Furthermore, the ^{13}C CP-MAS NMR spectrum (Figure 3.12 b) exhibited a new signal corresponding to the methyl group linked to silicon.



The N_2 adsorption-desorption measurements (Figure 3.13) of **M8** showed the preservation of the characteristic *type IV* isotherm, showing again a hysteresis loop with a large distribution of mesopores; the pore diameter distribution (Figure 3.13) was centered around 35-45 Å, with a total pore volume of 0.22 cm^3/g and a BET surface area of 136 m^2/g . The imidazolium salt content was determined by elemental analysis of N and it was found to be 0.81 mmol of imidazolium salt/g.

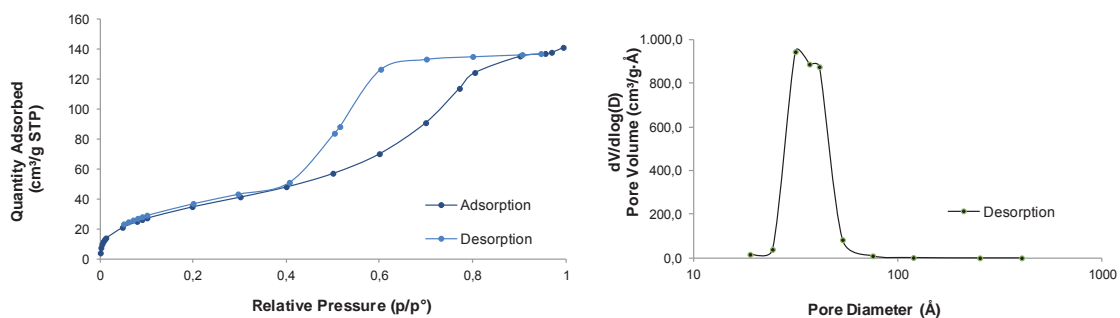
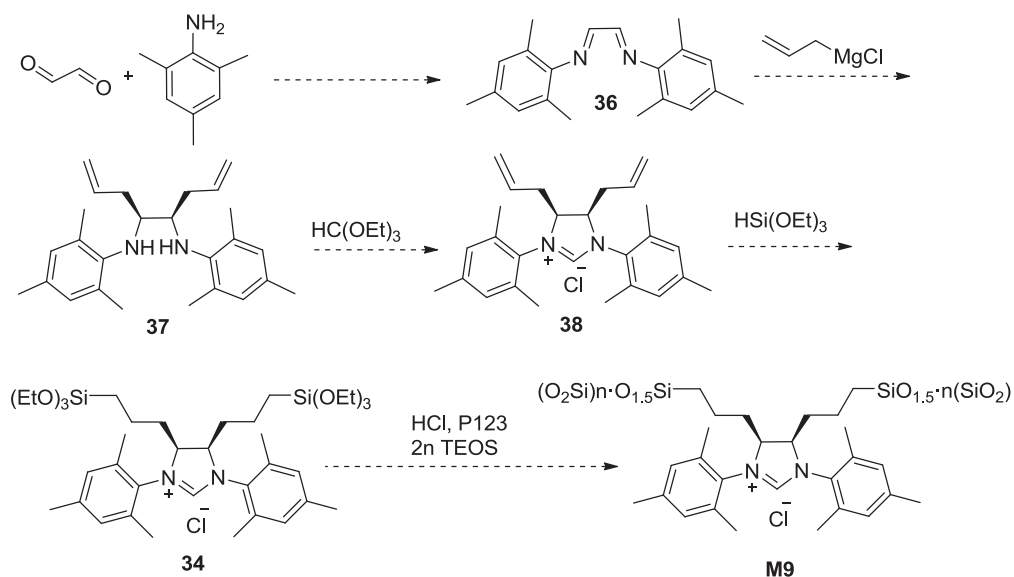


Figure 3.13. N_2 -sorption isotherm (left) and pore size distribution (right) of **M8**.

3.1.2 Hybrid silica materials derived from a bis-silylated N,N' -dimesityl imidazolium salt

3.1.2.1 Preparation of the hybrid silica material **M9**

The preparation of the bis-silylated dihydroimidazolium salt **34** and the hybrid silica material **M9** were envisaged as depicted in Scheme 3.17. The bis-silylated dihydroimidazolium salt had already been described by Dra. Amàlia Monge.²⁷¹



Scheme 3.17. Synthetic strategy for the preparation of **M9**.

The bis-imine **36** had already been described in the literature by Arduengo and was obtained from glyoxal and 2,4,6-trimethylaniline.²⁷² Subsequent addition of two mol of allylmagnesium chloride per mol of **36** led to a mixture of diastereomers, from which

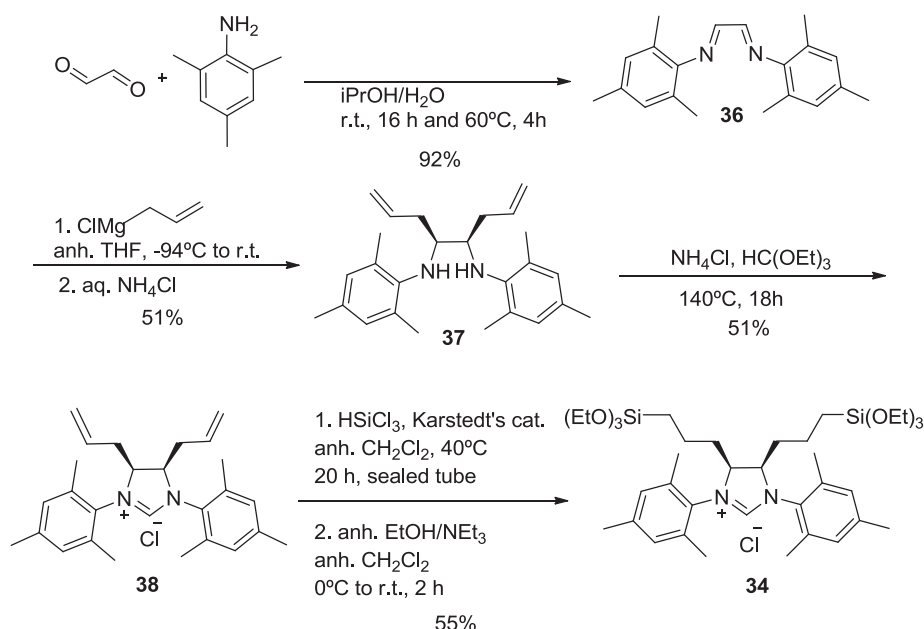
²⁷¹ Monge-Marcet, A.; Pleixats, R.; Cattoën, X.; Wong Chi Man, M. *J. Mol. Cat. A: Chem.* **2012**, *357*, 59.

²⁷² Arduengo III, A. J.; Krafczyk, R.; Schmutzler, R.; *Tetrahedron*, **1999**, *55*, 14523.

Chapter 3.3. Results and Discussion

the pure *meso* compound **37** was isolated by crystallization as previously reported.²⁷³ The diamine **37** underwent cyclization under standard conditions using triethylorthoformate and ammonium chloride to yield the corresponding dihydroimidazolium salt **38** (Scheme 3.18).

The hydrosilylation of compound **38** was carried out with trichlorosilane in the presence of Karstedt's catalyst, followed by treatment with ethanol and NEt_3 . This reaction was deeply investigated and optimized by Dr. Amàlia Monge²⁷⁴ and the method avoids the use of HSiOEt_3 in order to minimize the formation of side products derived from the reduction of the allyl chains under the hydrosilylation conditions. In brief, disilylated precursor **34** was obtained with a 13% overall yield.



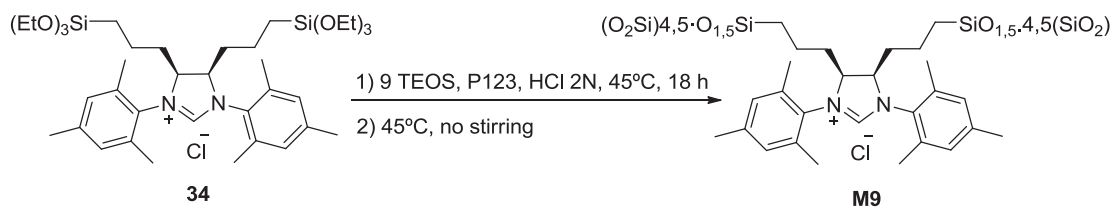
Scheme 3.18. Preparation of bis-silylated imidazolium chloride **34**.

The hydrolysis-polycondensation of **34** with tetraethoxysilane (TEOS:**34**, 9:1) was performed using HCl as catalyst (a 2M aqueous HCl solution) and in the presence of a structuring agent, the non ionic surfactant Pluronic® P123, (Scheme 3.19). This methodology has been described for the preparation of periodic mesoporous organosilicas (PMOs) containing bis-aryl-imidazolium entities.²⁷⁵

²⁷³ (a) Weigl, K.; Kohler, K.; Dechert, S.; Meyer, F. *Organometallics* **2005**, *16*, 4049. (b) Weigl, K. *PhD Dissertation*. University of Kaiserslautern, **2006**.

²⁷⁴ Monge, A. *PhD Dissertation*. Universitat Autònoma de Barcelona, **2011**.

²⁷⁵ Nguyen, T.-P.; Hesemann, P.; Gaveau, P.; Moreau, J. E. J. *J. Mater. Chem.* **2009**, *19*, 4164.



Scheme 3.19. Preparation of organosilica **M9** in a surfactant-assisted hydrolytic polycondensation process.

Under these conditions, a white solid was formed instead of a gel. The slurry was filtered and the resulting solid extracted with acidic EtOH in a Soxhlet apparatus for 48 hours in order to remove all the surfactant. The obtained solid was dried overnight under vacuum at 50°C to afford **M9** as a white powder.

This material was characterized by ^{13}C - and ^{29}Si -SSNMR, N_2 sorption measurements and elemental analysis. The ^{29}Si CP-MAS NMR spectrum (Figure 3.14 a) of **M9** showed the covalent bonding of the organic moiety to the silica matrix by the presence of T^2 and T^3 signals at -63.12 and -70.15 ppm respectively, in addition to the characteristic Q^3 and Q^4 signals corresponding to the condensed TEOS at -105.20 and -113.42 ppm.

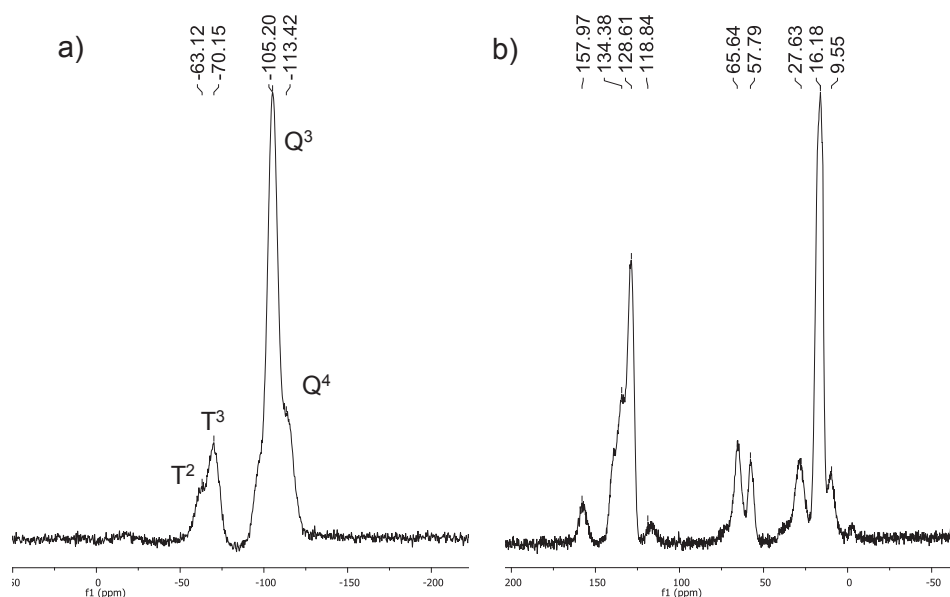


Figure 3.14. a) ^{29}Si -SSNMR of **M9**. b) ^{13}C -SSNMR of **M9**.

As in the case of **M7**, the ^{13}C -SSNMR spectrum of **M9** showed broad signals at similar positions to those of its corresponding precursor **34** (Figure 3.14 b), confirming that the organic functionality had been loaded in the final material. Similar to the previous case, the dilution of the organic moiety in the inorganic matrix precluded the observation of the corresponding signals in the IR spectra.

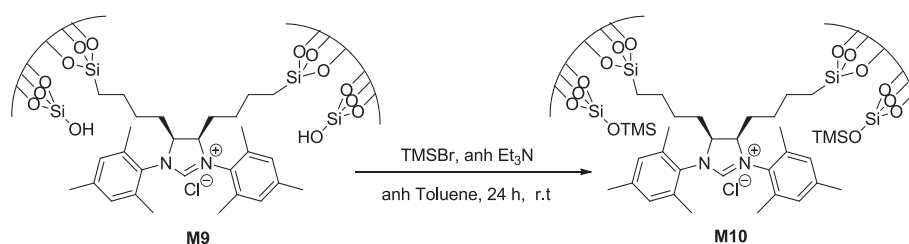
Chapter 3.3. Results and Discussion

N₂ adsorption desorption measurements indicated that **M9** was non-porous and, therefore, no organization had been generated in the material. Despite the use of a structuring agent,²⁷⁵ the high concentration of organic precursor might have avoided the formation of porosity. The dihydroimidazolium salt content was determined by elemental analysis of N and it was found to be 0.71 mmol of imidazolium salt/g.

3.1.2.2 Capping of surface silanol groups of hybrid silica material **M9**

As in the case of **M7**, the ²⁹Si CP-MAS NMR spectrum of **M9** (Figure 3.14 a) presented the signal Q³ indicating that condensation of TEOS had not been complete. For this reason, some silanol groups would be placed near the NHC carbene precursors and capping of these Si-OH groups was required for the stability of the *in situ* generated carbenes along the catalytic process.

Thus, the organosilica **M9** was treated with trimethylsilyl bromide in the presence of anhydrous triethylamine in anhydrous toluene at room temperature for 24 hours (Scheme 3.20). Then the solid was washed with toluene, methanol, diethyl ether and acetone. Finally it was dried overnight under vacuum at 50°C to yield **M10** as a white powder.



Scheme 3.20. Capping of silanols of **M9** to give **M10**.

The organosilica **M10** was characterized by elemental analysis and the organic fragment loading was found to be 0.68 mmol imidazolium salt/g material. N₂ sorption measurements were performed again to confirm the absence of porosity of the material.

3.2 Catalytic tests of materials **M7**, **M8** and **M10**.

Hybrid silica materials **M8** and **M10** with capped Si-OH groups were tested as precursors of NHC species to catalyze transformations such as benzoin condensation or annulation of enals and vinyl ketones. Taking into account the results obtained with them, we also decided to explore the ability of **M7** as recyclable organocatalyst in the *N*-*tert*-butyloxycarbonylation of amines.

3.2.1 Catalytic tests of materials M8 and M10 in NHC type reactions

3.2.1.1 Benzoin condensation

Commonly, benzoin condensation is catalyzed by thiazol- or triazol-2-ylidenes as mentioned in most of the reviews;²⁰¹ however some examples of imidazolium derived pre-catalysts have been found in the literature.^{256,276} Preliminary experiments were carried out in the presence of two different commercial pre-catalysts, IMesCl and SIMesCl (Figure 3.15) which are homogeneous analogues to the salts immobilized in the already prepared organosilicas **M7-M10**.

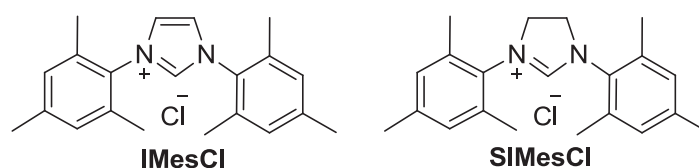
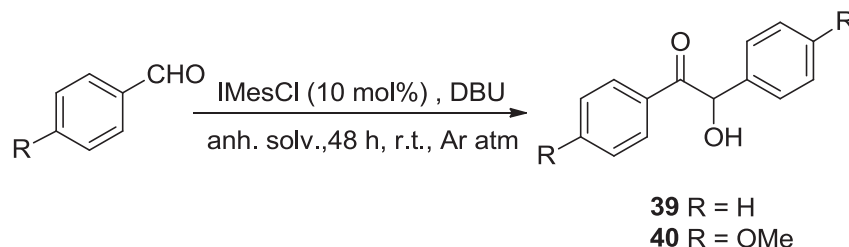


Figure 3.15. Homogeneous pre-catalysts IMesCl and SIMesCl.

To set the conditions, tests were performed in different anhydrous solvents and using DBU as a base to generate *in situ* the carbene catalytic species. Benzaldehyde and *p*-anisaldehyde were used as substrates (Table 3.1).

Table 3.1. Catalytic performance^[a] of homogeneous catalysts in the benzoin condensation of aromatic aldehydes.



Entry	R	solvent	Yield (%) ^[b]
1	H	DCM	20
2	H	DMSO	30
3	H	THF	33
4	OMe	DCM	10
5	OMe	DMSO	10
6	OMe	THF	42

^[a] Reaction conditions: 2.94 mmol of substrate, cat IMesCl (10 mol%), DBU (15 mol%) and dry solvent (2 mL) were stirred together for 48 h at room temperature under argon.

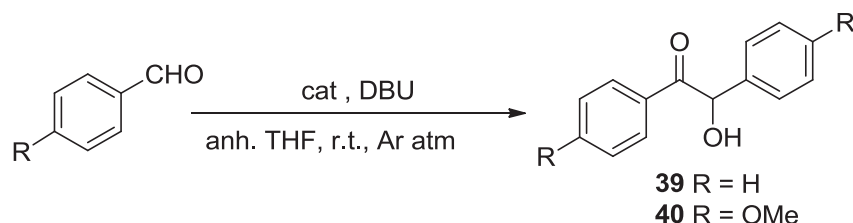
^[b] Determined by ¹H-NMR.

²⁷⁶ Iwamoto, K.-I.; Kimura, H.; Oike, M.; Sato, M. *Org. Biomol. Chem.* **2008**, 6, 912.

Chapter 3.3. Results and Discussion

THF was chosen as the best solvent to perform the catalytic tests. Then benzoin condensation of aromatic aldehydes was performed in presence of IMesCl and SIMesCl at different catalyst loadings (Table 3.2, Entries 1-4).

Table 3.2. Catalytic performance^[a] of homogeneous and heterogeneous catalysts in the benzoin condensation of aromatic aldehydes.



Entry	R	Cat (mol%)	time (h)	Yield (%) ^[b]
1	H	IMesCl (10)	72	14
2	H	IMesCl (18)	72	36
3	H	SIMesCl (10)	72	89
4	OMe	IMesCl (10)	72	20
5	H	M10 (20)	120	-
6	H	M10 (10)	120	-
7	H	M8 (20)	120	-
8	H	M8 (10)	120	-

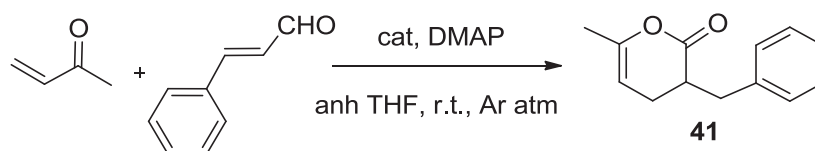
^[a] Reaction conditions: 1 equiv of substrate, cat (10-20 mol%), DBU (15-30 mol%) and dry THF were stirred together for the time indicated at room temperature under argon.

^[b] Determined by ¹H-NMR.

From these data, it seems clear that SIMesCl pre-catalyst presented higher activity than IMesCl. However, both pre-catalysts could facilitate the transformation. In conclusion, these results indicate that organosilicas **M8** and **M10** might be able to enable the reaction. Thus, materials **M8** and **M10** were tested as supported pre-catalysts in different catalyst loadings for the benzoin condensation of benzaldehyde. The tests were carried out under the same conditions used for its homogeneous analogues (Table 3.2, Entries 5-8). The reactions were followed by ¹H-NMR and, unfortunately, in any case the formation of the final product was observed. The expected slow reaction rates for heterogeneous catalysts and the fact that these type of precatalysts are not the most commonly used for the benzoin reaction might justify the bad performance of these materials. On the other hand, the uncertainty if some remaining free silanols may have consumed the base or the instability of the carbene species may explain as well the failure of the reaction.

3.2.1.2 Annulation reactions of enals and vinyl ketones

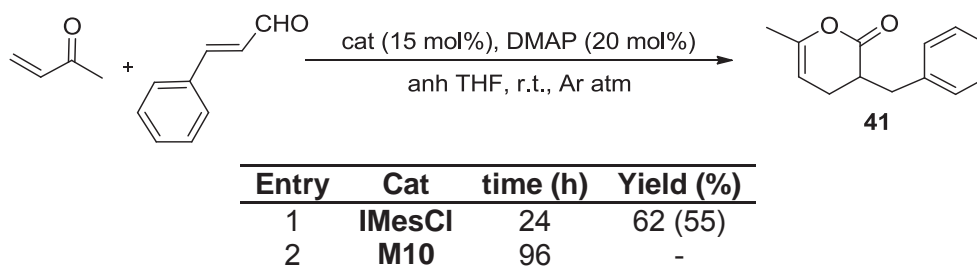
Homoenolate annulation of enals with vinyl ketones can lead to the selective synthesis of dihydropyranones (see scheme 3.8).²³² One example is the annulation of methyl vinyl ketone with cinnamic aldehyde to afford (2*H*)-pyranone **41** (Scheme 3.21). As described in the literature, when I*Me*sCl is used as pre-catalyst and DMAP as a base, the reaction works more efficiently.



Scheme 3.21. NHC catalyzed annulation of methyl vinyl ketone and cinnamic aldehyde for the formation of **41**.

Thus, the material **M10** derived from a S*IMe*s type salt was chosen to be tested as supported pre-catalyst to perform the reaction. Due to the fact that **M10** presents two mesityl groups which provide more steric hindrance than in the case of **M8** bearing only one bulky aryl substituent, it would stabilize better the generated carbene and it seemed to us the best candidate. Catalytic tests were performed for **I*Me*sCl** and **M10** under argon atmosphere in anhydrous THF using Schlenk techniques, in the presence of DMAP as a base (Table 3.3).

Table 3.3 Catalytic performance^[a] of **I*Me*sCl** and **M10** in the annulation of methyl vinyl ketone and cinnamaldehyde.



^[a] Reaction conditions: cinnamaldehyde (1.5 equiv), cat (0.15 equiv.) and methylvinylketone (1 equiv) were dissolved in anhydrous THF. After addition of DMAP (0.2 equiv.) the reaction was allowed to stir at room temperature for the indicated time under argon atmosphere.

^[b] Determined by ¹H-NMR. Isolated yield in brackets.

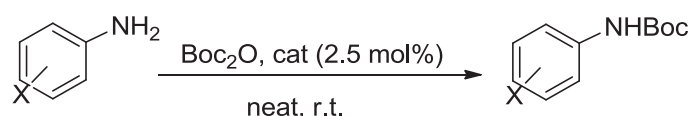
I*Me*sCl allowed the reaction to occur and afforded a 62% of conversion after 24 hours, with a 55% of isolated yield of **41**. Unfortunately, **M10** did not catalyze the reaction under the same conditions and the desired product **41** was not obtained. At this point, we decided that the type of immobilization may represent a drawback for the generation of carbenes. For this reason, we did not perform more catalytic tests.

3.2.2 Assay of M7 in imidazolium-based catalysis

3.2.2.1 Chemoselective *N*-*tert*-butyloxycarbonylation of amines

Modulating the reactivity of the amine functionality is a very frequent requisite exercise in the preparation of drug molecules.²⁷⁷ *N*-*tert*-butyloxycarbonylation is one of the preferred strategies for the protection of amines due to the stability of *tert*-butylcarbamates (*N*-*t*-Boc) toward a variety of routinely adopted experimental conditions and ease of regeneration of the parent amines under mild acidic conditions.

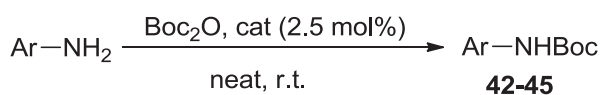
The increasing influence of green chemistry on the chemical research urges for greener reaction conditions. Recently, it has been described the nonsolvent application of 1-alkyl-3-methylimidazolium based Ionic Liquids as organocatalysts for chemoselective *N*-*t*-butyloxycarbonylation of various functionalized amines (Scheme 3.22).²⁷⁸ This kind of ILs exhibited from very good to excellent catalytic activity due to the acidic character of the C-2 hydrogen. They were found to be superior to the reported Lewis acid catalysts.



Scheme 3.22 . Chemoselective protection of *N*-*tert*-Butyloxycarbonylation of amines

For this reason, we planned to use our organosilica **M7** as recoverable organocatalyst for this reaction. Catalytic tests were performed with 2.5 mol% of catalyst at room temperature, in the absence of solvent (Table 3.4).

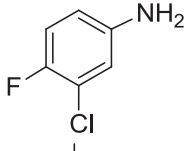
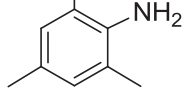
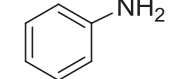
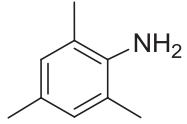
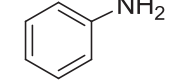
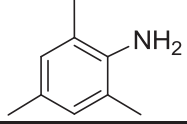
Table 3.4. Catalytic performance of **M7** and other catalysts in the chemoselective *N*-*tert*-butyloxycarbonylation of amines.



Entry ^[a]	Substrate	Cat	Prod	time	Yield (%) ^[b]
1		M7	42	10 min	92
2		M7	43	1 h	79

²⁷⁷ Carey, J.S.; Laffan, D.; Thomson, C.; Williams, M.T. *Org. Biomol. Chem.* **2006**, *4*, 2337.

²⁷⁸ Sarkar, A.; Roy, S.R.; Parikh, N.; Chakraborti, A.K. *J. Org. Chem.* **2011**, *76*, 7132.

3		M7	44	18 h	79
4		M7	45	24 h	90
5		[emim][Cl]	42	15 min	93 ^[c]
6		[emim][Cl]	45	45 min	85 ^[c]
7		SBA-15 (M5) ^[d]	42	30 min	92
8		SBA-15 (M5) ^[d]	45	24 h	82

^[a] Reaction conditions: the corresponding amine (2.5 mmol), (Boc)₂O (2.5 mmol, 1 equiv) and the corresponding catalyst (2.5 mol %) were stirred together at room temperature until complete conversion of substrates.

^[b] Isolated yield.

^[c] See ref. 278

^[d] 0.006 g of **M5**.

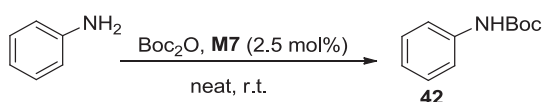
Aniline was converted to the desired product **42** in only 10 minutes using **M7** as supported catalyst (Table 3.4, Entry 1). This result is comparable to the one obtained by Sarkar *et al.*²⁷⁸ with [emim][Cl] (Table 3.4, Entry 5). No competitive formation of an O-*t*-Boc product was observed with 4-hydroxyaniline (Table 3.4, Entry 2), as it has already been described with homogeneous IL,²⁷⁸ due to the better nucleophilicity of the NH₂ group. Interestingly, challenging less nucleophilic anilines gave also good results. Thus, electron-deficient 3-chloro-4-fluoroaniline (Table 3.4, Entry 3) was obtained in 79% yield after 18 h of reaction. Sterically hindered 2,4,6-trimethylaniline (Table 3.4, Entry 4) was also successfully protected with Boc₂O, although requiring higher reaction times than those described by Sarkar for homogeneous IL (Table 3.4, Entry 6). These aniline derivatives had been described to give very low yields of *N-t*-Boc products in the absence of homogeneous IL.²⁷⁸ In order to check if the inorganic matrix did exert a cooperative effect²⁷ on the catalytic activity, we performed two essays using the mesostructured silica of SBA-15 type **M5** as catalyst. We found that **M5** was also able to catalyze the process with aniline and 2,4,6-trimethylaniline, although the reactions were somewhat slower (Table 3.4, Entries 7 and 8). This fact indicates that the acidity

Chapter 3.3. Results and Discussion

provided by the Si-OH groups of the silica matrix also enables the activation of the electrophile, Boc₂O.

Interestingly, catalyst **M7** could be reused in 5 consecutive cycles using aniline as substrate, with no significant loss in activity (Table 3.5).

Table 3.5. Recyclability of catalyst **M7** in the N-*tert*-butyloxycarbonylation of aniline.^[a]



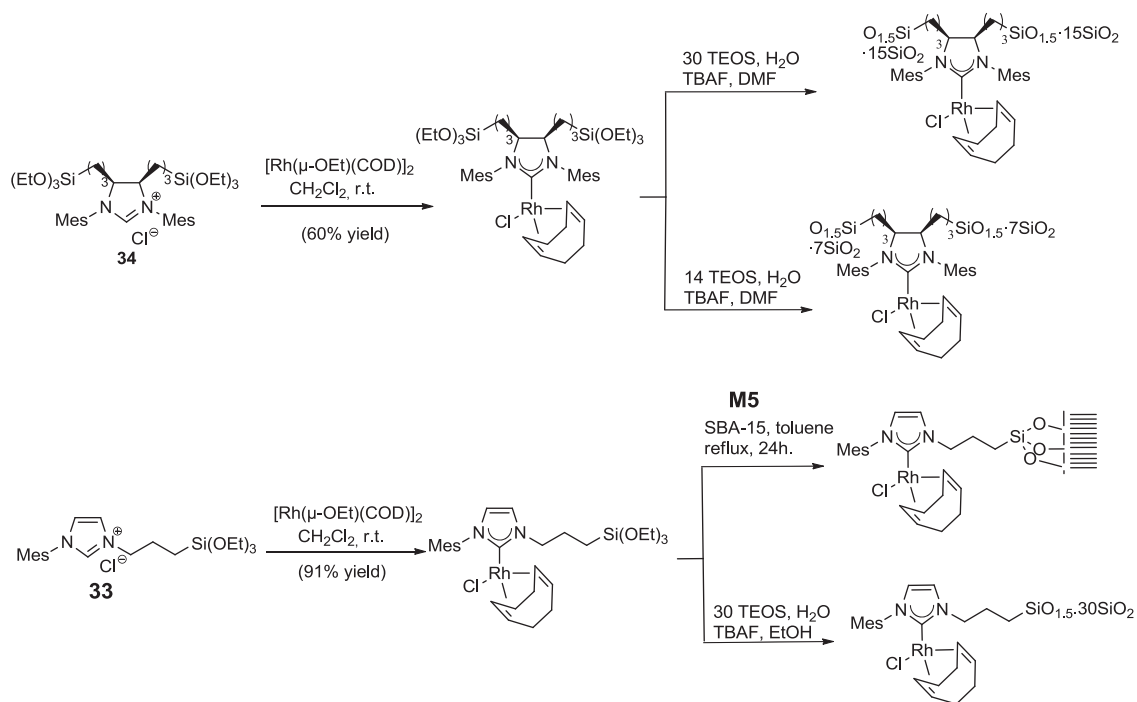
Cycle	time (min)	Yield (%) ^[b]
1	10	92
2	10	89
3	10	96
4	10	92
5	10	99

^[a] Reaction conditions: aniline (229 μL , 2.5 mmol), (Boc)₂O (574 μL , 2.5 mmol, 1 equiv) and **M7** (2.5 mol%) were stirred together at room temperature until complete conversion of substrates (10 minutes). After the time indicated, the reaction mixture was diluted with Et₂O, filtered and the catalytic material washed several times with Et₂O, dried under vacuum and directly used in the next cycle,

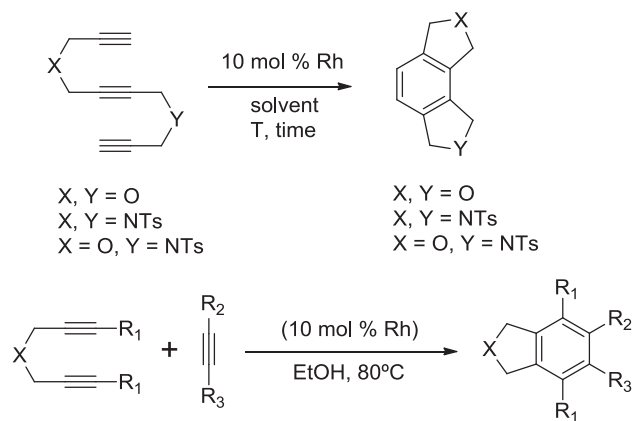
^[b] Isolated yield.

To finish this section I would like to mention that the silylated imidazolium and imidazolium salts **33** and **34** were used as ligands for the preparation of hybrid silica materials derived from Rhodium-NHC complexes. These complexes were synthesized by reacting the corresponding imidazolium salts with [Rh(μ -OEt)(COD)]₂ as depicted in Scheme 3.23. Hybrid silica materials were obtained by co-gelification of the corresponding complex with different amounts of TEOS or by *grafting* method with **M5** (SBA-15) (Scheme 3.23). Materials were used as recyclable catalysts for [2+2+2] cycloaddition reactions of alkynes (Scheme 3.24). This work has been conducted by Martí Fernández in *Universitat de Girona* within the framework of a collaboration of the group of Dra. Anna Roglans with our research group.²⁷⁹

²⁷⁹ Fernández, M.; Ferré, M.; Pla-Quintana, A.; Parella, T.; Pleixats, R.; Roglans, A. *Eur. J. Org. Chem.* **2014**, 6242.



Scheme 3.23. Preparation of hybrid silica materials derived from Rhodium(I) complexes.



Scheme 3.24. [2+2+2] cycloaddition reactions of alkynes catalyzed by hybrid materials derived from Rhodium(I) complexes.

4. CONCLUSIONS

A monosilylated imidazolium salt **33** and a bis-silylated imidazolium salt **34** have been synthesized and used as precursors to prepare azolium-derived organosilicas by sol-gel methodologies. Capping of the surface Si-OH groups of the resulting materials was also performed. Two families of *Class II* hybrid silica materials were obtained depending on the precursor: imidazolium salt-based (**M7-M8**) and dihydroimidazolium salt-based (**M9-M10**) hybrid silicas. Whereas the mesoporous material **M7** was obtained by sol-gel co-gelification of the monosilylated monomer with TEOS (ratio 1:10) under fluoride catalysis in the absence of surfactant, the material **M9** was formed by template-assisted hydrolytic polycondensation of the bis-silylated monomer with TEOS (ratio 1:9) under acidic conditions. Despite the use of the non-ionic surfactant P123, the material **M9** was found to be non-porous and no-structuration was achieved.

Materials **M8** and **M10** were tested as NHC-supported precatalysts, in the presence of a base, in the benzoin condensation, as well as in the annulation reaction of an enal with a vinyl ketone for the case of **M10**. However, the materials failed to catalyze these reactions. These results seem to indicate that the silica support is not suitable for the *in situ* generation of the NHCs. On one hand, diffusion resistance of reagents can decrease the reaction rates disfavoring the progress of reaction. On the other hand, despite of the capping of Si-OH groups, residual surface silanols could avoid the generation of the NHC.

Supported catalyst **M7** has been successfully applied to the chemoselective *N-tert*-butyloxycarbonylation of aromatic amines. This material **M7** efficiently promoted the reaction with challenging anilines (sterically hindered or electron-deficient) although with lower reaction rates compared with homogeneous imidazolium salts. Selective *N*-protection was obtained in the case of *p*-hydroxyaniline. Recyclability was achieved up to 5 consecutive runs without significant loss of activity using aniline as substrate. However, a cooperative effect of the acidic silica matrix was demonstrated, because non-functionalized mesostructured SBA-15 also catalyzed the reaction with aniline and 2,4,6-trimethylaniline.

5. EXPERIMENTAL SECTION

5.1. General remarks

Nuclear Magnetic Resonance (NMR). Spectra were recorded at the *Servei de Ressonància Magnètica Nuclear* of the *Universitat Autònoma de Barcelona*. ^1H -NMR, ^{13}C -NMR, ^1H - ^1H COSY, ^1H - ^1H NOESY, ^1H - ^{13}C HSQC, ^1H - ^{13}C HMBC and SELTOCSY spectra were recorded using Bruker instruments (DRX-250, DPX-360 and AVANCE-III 400). Chemical shifts (δ) are given in ppm using the residual non-deuterated solvent as internal reference.

The ^{29}Si and ^{13}C CP-MAS solid state NMR spectra were obtained in the *Servei de Ressonància Magnètica Nuclear* of the *Universitat Autònoma de Barcelona* from a Bruker AV400WB; the repetition time was 5 seconds with contact times of 5 milliseconds.

Infrared spectroscopy (IR). Spectra were usually recorded with a Bruker Tensor 27 spectrometer using a Golden Gate ATR module with a diamond window. When necessary, IR spectra were recorded using KBr pellets using a Thermo Nicolet IR2000 spectrometer.

Elemental Analysis (EA) of C, N, H and Si were performed by the *Serveis Científico-Tècnics* of the *Universitat de Barcelona (SCT-UB)*. The percentages of C, N and H were determined by combustion using an EA-1108 C.E. elemental analyser of Thermo Scientific using BBOT as internal standard. The content of Si was determined by Inductively Coupled Plasma (ICP) in a multichannel Perkin-Elmer Optima 3200 L instrument.

Thin-Layer Chromatography (TLC) was performed using 0.25 mm plates (Alugram Sil G/UV₂₅₄).

Flash Chromatography was performed under compressed air pressure on a *Macherey-Nagel GmbH & Co KG* silica gel which had a particle size of 230 – 400 mesh and pore volume of 0.9 mL/g.

Surface areas were determined by the Brunauer-Emmet-Teller (BET) method from N_2 adsorption-desorption isotherms obtained with a *Micromeritics ASAP2020* analyzer at the *Institut Charles Gerhardt de Montpellier* after degassing samples for 30h at 55°C under vacuum. The total pore volumes were evaluated by converting the volume adsorbed at p/p^0 0.98 to the volume of liquid adsorbed (single point adsorption total

Chapter 3.5. Experimental Section

pore volume of pores less than 4000 Å at $p/p^\circ \approx 0.98$). The pore size distributions for the materials were determined from the desorption branch using the Barrett-Joyner-Halenda (BJH) method²⁸⁰ which relies on the Kelvin equation to relate the width of the pores to the condensation pressure.

Electron Microscopy. Transmission Electron Microscopy (TEM) images were obtained with an instrument *JEOL 1200 EX II* equipped with a SIS Olympus Quemesa 11 Mpixel camera at *Université de Montpellier II*. Scanning Electron Microscopy (SEM) images were obtained at the *Institut Européen des Membranes* in Montpellier with a Hitachi S4800 apparatus after platinum metallization.

Other:

When required, experiments were carried out with standard high vacuum and Schlenk techniques under N₂ or Ar atmosphere using dry solvents and in some cases degassed by the freeze-and-thaw method and cannula or syringe-transferred.

Commercial reagents were directly used as received except for trichlorosilane which was purified first by distillation under vacuum; gaseous HCl was eliminated in a second step by performing 2 freeze-thaw cycles (this compound was always used with a secondary cold trap). Benzaldehyde, *p*-anisaldehyde and cinamaldehyde were purified by distillation. Aniline was distilled on CaH₂. Na₂SO₄ and MgSO₄ used to adsorb residual water of organic layers were anhydrous.

Dry solvents were obtained from two instruments: *PureSolv* (Innovative Technologies: THF, CH₂Cl₂ and pentane) and in some experiments from *MBraun SPS-800* (MBraun: THF).

Other dry solvents were prepared using standard methods: NEt₃ and DMF were distilled over CaH₂. Toluene and Et₂O were refluxed over Na/benzophenone, whereas ethanol and methanol were distilled on Mg/I₂. When needed, deuterated NMR solvents such as CDCl₃ were dried by distillation over CaH₂. For the preparation of hybrid silica materials, distilled and deionized water was used (*MilliQ H₂O*).

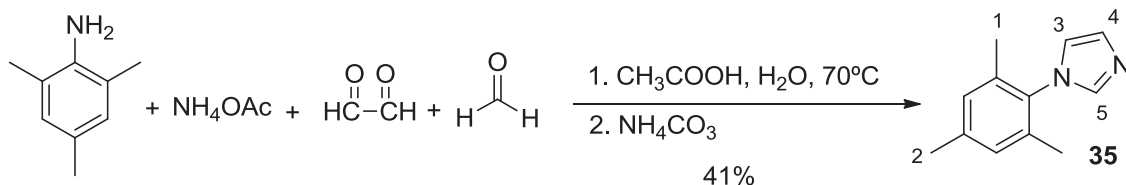
In this work some of the compounds prepared were already described in the literature. Therefore, only the physical and/or spectroscopic data necessary for their identification are presented. It has to be mentioned that the chemical shifts of the NCHN protons in

²⁸⁰ Barrett, E. P.; Joyner, L. G.; Halenda, P. P. *J. Am. Chem. Soc.*, **1951**, 73, 373.

imidazolium salts strongly depend on the concentration, thus their values might not match previously reported data.

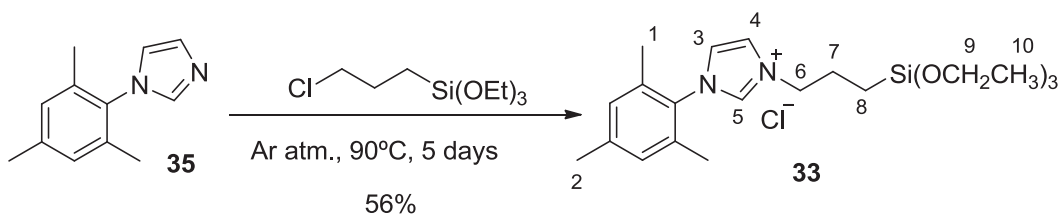
5.2 Preparation of hybrid silica materials

5.2.1. Preparation of 1-mesitylimidazole, **35**.²⁶⁷



To a solution of glacial acetic acid (10 mL), ammonium acetate (3.099 g, 40.2 mmol), water (1 mL) and 2,4,6-trimethylaniline 97% (5.6 mL, 0.94 g/cm³, 38.6 mmol), a solution formed by glacial acetic acid (10 mL), aqueous formaldehyde 35-40% (3 mL, 1.09 g/cm³, 40.3 mmol) and glyoxal (5.3 mL, 40 wt% aqueous solution, 1.27 g/cm³, 46.0 mmol) was added slowly (30 minutes) at room temperature. The mixture was stirred overnight at 70°C. Then the mixture was poured onto NaHCO₃ aqueous solution (29.570 g, 300 mL) and the resulting precipitate was filtered and washed with copious amounts of water. A brown solid was obtained, which was dried under vacuum and purified by column chromatography on silica gel (hexane:AcOEt 3:1 to 1:1). A pale brown solid was obtained, **35**²⁸¹ (2.947 g, Yield: 41%). **CF**: C₁₂H₁₄N₂. **MW**: 186,25 g/mol. **¹H-RMN (CDCl₃, 250 MHz) δ (ppm)**: 7.45 (s, 1H, H₃), 7.27 (s, 1H, H₄), 6.97 (s, 2H, H_{ar}), 6.90 (s, 1H, H₅), 2.34 (s, 3H, H₂₍₁₎), 1.99 (s, 6H, H₂₍₁₎).

5.2.2. Preparation of 1-mesityl-3-[3-(triethoxysilyl)propyl]-1*H*-imidazol-3-ium chloride, **33**.²⁶⁶



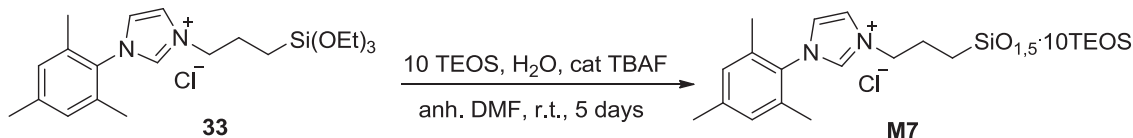
A mixture of 1-mesitylimidazole **35** (0.613 g, 3.29 mmol) and (3-chloropropyl)triethoxysilane (0.9 mL, 1.0 g/cm³, 3.55 mmol) was stirred under argon at 90°C for 5 days. The volatiles were removed under vacuum and the residue was thoroughly washed with anhydrous pentane to afford **33**²⁶⁶ as a solid (0.787 g, Yield: 56%). **¹HRMN (CDCl₃, 250 MHz) δ (ppm)**: 10.84 (s, 1H, H₅), 7.62 (s, 1H, H₃), 7.12 (s,

²⁸¹ Alcalde, E.; Dinarès, I.; Rodríguez, S.; Garcia, de Miguel, C. *Eur. J. Org. Chem.* **2005**, 1637.

Chapter 3.5. Experimental Section

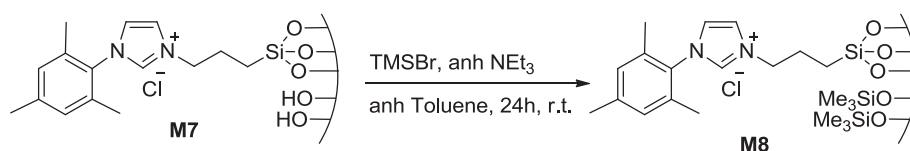
1H, H₄), 6.99 (s, 2H, H_{ar}), 4.77 (t, *J* = 7.5 Hz, 2H, H₆), 3.84 (q, *J* = 5.0 Hz, 6H, H₉), 2.33 (s, 3H, H₂), 2.07 (m, 8H, H₁+H₇), 1.21 (t, *J* = 7.5 Hz, 9H, H₁₀), 0.70-0.63 (t, *J* ca 7.5 Hz, 2H, H₈).

5.2.3. Preparation of hybrid silica material M7



To a stirred solution of **33** (0.787 g, 1.85 mmol) and TEOS 98% (4.2 ml, 0.94 g·cm⁻³, 18.54 mmol) in anhydrous DMF (10 mL) at room temperature was added a solution of distilled and deionized water (MilliQ) (1.4 mL, 79.7 mmol) and TBAF (1M solution in anhydrous THF, 0.2 mL, 0.2 mmol, 1 mol% F with respect so Si) in anhydrous DMF (10 mL). The resulting solution was stirred for 10 min at room temperature, then the stirring was stopped and after 2 hours a gel was formed, which was left to age at room temperature for 5 days. After this time, the gel was crushed, filtered off and washed with water (3 x 10 mL), EtOH (3 x 5 mL) and acetone (3 x 5 mL). The final solid was dried overnight at 55°C under vacuum (1.2 mbar) affording **M7** (1.686 g) as a white solid. **²⁹Si-CP-MAS NMR (79.5 MHz) δ:** -61.37 (T²), -70.17 (T³), -96.22 (Q²), -104.62 (Q³), -114.04 (Q⁴). **¹³C-CP-MAS NMR (100.62 MHz) δ:** 162.88, 138.45, 134.18, 129.99, 123.63, 50.04, 34.98, 28.68, 18.86, 15.41, 6.96. **IR (ATR) ν (cm⁻¹):** 3151, 2323, 1548, 1440, 1389, 1048, 960, 795, 666. **EA calculated for C₁₅H₂₀N₂SiClO_{1.5}·10 SiO₂** (considering complete conversion): 20.43% C, 2.27 % H, 3.18 % N, 35.1 % Si; **found:** 18.23 % C, 2.13 % H, 3.50 % N, 27.84 % Si (1.25 mmol imidazolium salt/g material). **BET** S_{BET}: 170 m²/g; pore diameter distribution centered around 35 Å; average pore diameter (4V/A, BET): 38 Å; pore volume: 0.24 cm³/g.

5.2.4. Preparation of hybrid silica material M8

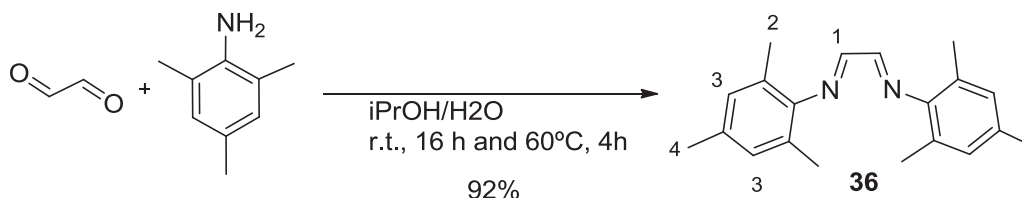


In a 50 mL Schlenk tube under nitrogen atmosphere was placed material **M7** (0.253 g) and anhydrous toluene (15 mL). Then TMSBr (1.0 mL, 1.16 g/cm³, 4.58 mmol, 1 mol TMS respect to 1 mol -OH²⁸²) and anh Et₃N (0.5 mL, 0.727 g/cm³, 7.58 mmol) were

²⁸² To calculate the maximum number of silanols to be protected, we supposed that all trialkoxy and tetraalkoxy groups present in the reactants had been hydrolyzed to silanols but not condensed, then each triethoxysilane moiety would give 3 silanols and each equivalent of TEOS would give 4 more Si-OH.

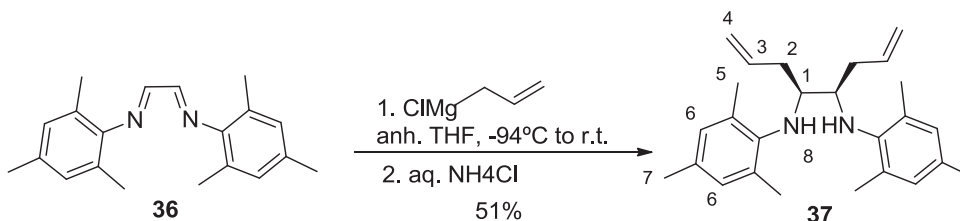
added and stirred at r.t. under Ar atmosphere for 24 h. Then, the material was filtered and washed with toluene (3 x 15 mL), methanol (3 x 15 mL) and Et₂O (3 x 15 mL) to afford **M8** as a white powder (0.1332 g). ²⁹Si-CP-MAS NMR (79.5 MHz) δ: 10.15 (M¹), -60.85 (T²), -72.11 (T³), -95.65 (Q²), -105.17 (Q³), -115.26 (Q⁴). ¹³C-CP-MAS NMR (100.62 MHz) δ: 139.64, 133.74, 129.71, 121.88, 50.05 18.29, 15.46, 7.30, 1.39. IR (ATR) (cm⁻¹): 3283, 2051, 1611, 1548, 1452, 1050, 846, 802. EA found: 16.21% C, 2.52% H, 2.26% N (0.81 mmol imidazolium salt/g material). BET S_{BET}: 136 m²/g; pore diameter distribution centered around 35-45 Å; average pore diameter (4V/A, BET): 39 Å; pore volume: 0.22 cm³/g.

5.2.5. Preparation of *N,N'*-(1*E*,2*E*)-(ethane-1,2-diylidene)bis(2,4,6-trimethylaniline), **36**.²⁷²



2,4,6-Trimethylaniline 97% (7.0 mL, 0.963 g/cm³, 49.9 mmol) was dissolved in 2-propanol (20 mL) and then a solution of glyoxal (3.40 mL, 40 wt% aqueous solution, 1.27 g/cm³, 29.8 mmol) in 2-propanol (10 mL) and water (5 mL) was added. The mixture was stirred at room temperature for 16h and then at 60°C for 4h. After this time, water (5 mL) was added and the resulting solid was filtered and recrystallized from hexane to afford **36**²⁷² as a yellow solid (6.71 g, Yield: 92%). CF: C₂₀H₂₄N₂. MW: 292.42 g/mol, m.p: 158 – 160°C (lit²⁷² m.p: 157-158°C). ¹H-NMR (CDCl₃, 400 MHz): 8.10 (s, 2H, H₁), 6.91 (s, 2H, H₃), 2.30 (s, 6H, H₄), 2.16 (s, 12H, H₂) ¹³CRMN (CDCl₃, 100.6 MHz): 164.19, 147.87, 134.60, 129.29, 126.85, 20.42, 17.84.

5.2.6. Preparation of (4*R*, 5*S*)-*N,N'*-dimesitylocta-1,7-diene-4,5-diamine, **37**.²⁷³

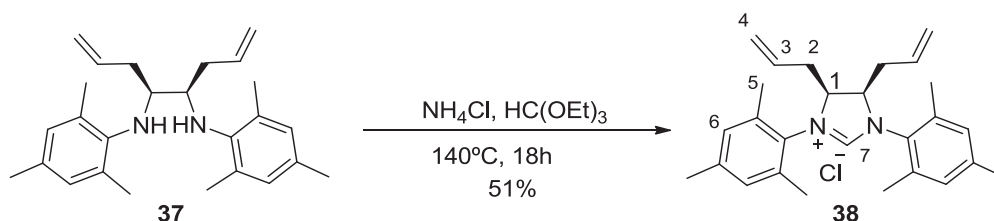


A solution of compound **36** (2.01 g, 6.87 mmol) was dissolved in dry THF (18 mL) and the mixture cooled to -94°C with a hexane/liquid N₂ bath. Under vigorous stirring allylmagnesium chloride (17.5 mL, commercial 2M solution in anh. THF,

Chapter 3.5. Experimental Section

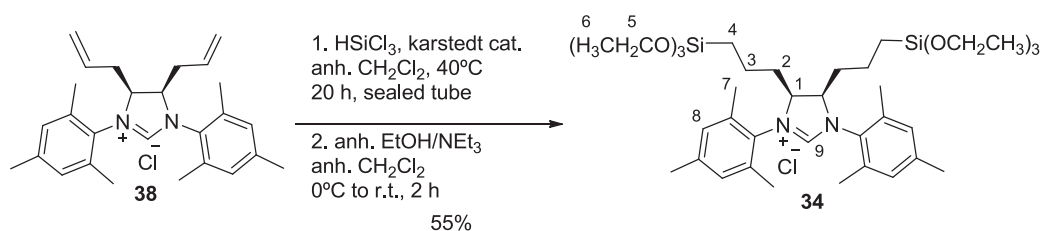
35.0 mmol) was slowly added and the mixture stirred overnight, allowing to reach the room temperature. After this time, the reaction mixture was cooled to 0°C with an ice bath and then NH₄Cl aqueous solution (2.22 g in 40 mL water) was carefully added. The organic phase containing the diastereomeric mixture of products was separated and the aqueous layer further extracted with Et₂O (3 x 25 mL). The combined organic layers were dried over Na₂SO₄ and concentrated under reduced pressure. A yellow oil was obtained, from which the *meso* product crystallized after 4 days at room temperature. After filtration and washing with cold MeOH compound **37**²⁷³ was obtained as a white solid (1.28 g, Yield: 51%). **CF**: C₂₆H₃₆N₂. **MW**: 376.6 g/mol, **m.p**: 77-78°C (lit²⁷³ m.p: 76°C). **¹H-NMR (CDCl₃, 400 MHz)**: 6.79 (s, 4H, H₆), 5.75 (ddt, 2H, J= 17.1 Hz, J= 10.0 Hz, J= 2.6 Hz, H₃), 5.06 (d, 2H, J= 17.1 Hz, H₄), 5.01 (d, 2H, J=10.0 Hz, H₄), 3.70 (m, 4H, H₈ + H₁), 2.26 (m, 4H, H₂, partially masked by the signal of H_{5/7}), 2.23 (s, 12 H, H₅), 2.22 (s, 6H, H₇). **¹³CRMN (CDCl₃, 62.5 MHz)**: 142.68, 136.88, 130.92, 130.50, 129.23, 117.23, 57.97, 35.12, 19.63, 18.56.

5.2.7. Preparation of (4*S*, 5*R*)-4,5-diallyl-1,3-dimesityl-4,5-dihydroimidazolium chloride, **38**.²⁷³



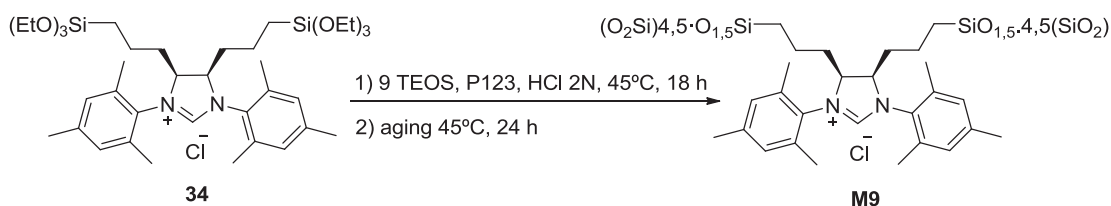
Compound **37** (1.82 g, 4.84 mmol) and NH₄Cl (0.31 g, 5.77 mmol) were stirred together in triethylorthoformate 98% (4.0 mL, 0.891 g/cm³, 24.0 mmol) at 140°C for 18h. After this time, the reaction mixture was cooled down to room temperature. The residue was dissolved in the minimum amount of CH₂Cl₂ and the excess of ammonium salt precipitated upon the addition of few drops of THF. The solid was separated by filtration and the filtrates were concentrated under vacuum. Pentane (5 mL) was added to the sticky residue until a new solid precipitated. This solid was filtered off and washed with pentane to afford the desired dihydroimidazolium salt, **38**²⁷³ (0.72 g, Yield: 51%). **CF**: C₂₇H₃₅ClN₂. **MW**: 423.0 g/mol, **m.p**: 258-259 °C (lit²⁷³ m.p: 258°C). **¹H-NMR (CDCl₃, 400 MHz)**: 10.40 (s, 1H, H₇), 6.96 (s, 2H, H₆), 6.93 (s, 2H, H₆), 5.48 (m, 2H, H₃), 5.07-4.94 (m, 6H, H₄ + H₁), 2.68 (m, 2H, H_{2a}), 2.47 (s, 6H, H₅), 2.38 (s, 6H, H₅), 2.28 (s, 6H, H₅), 2.34-2.22 (m, 2H, H_{2b}, masked by H₅ signals). **¹³CRMN (CDCl₃, 100.6 MHz)**: 160.62, 140.57, 135.74, 135.20, 132.14, 130.61, 130.43, 129.63, 119.00, 65.40, 31.10, 20.61, 18.75, 18.24.

5.2.8. Preparation of (4R, 5S)-1,3-dimesityl-4,5-bis[3-(triethoxysilyl)-propyl]-4,5-dihydroimidazolium chloride, **34**.²⁷¹



In a 100 mL sealable Schlenk tube, compound **38** (1.31 g, 3.10 mmol) was dissolved in dry CH₂Cl₂ (15 mL) under argon. To this solution Karstedt's catalyst (2.1 mL, 2.0% wt Pt solution in xylene, 0.19 mmol) and freshly distilled HSiCl₃ (8.0 mL, 1.34 g/cm³, 79.2 mmol) were added. The reaction was stirred under argon at 40°C for 20 h. After this time, excess HSiCl₃ was distilled off and collected in a secondary cold trap. The residue was re-dissolved in CH₂Cl₂ (30 mL) and the mixture was cooled to 0°C with an ice bath. At this temperature, a solution of anhydrous EtOH/NEt₃ (1/1, 18 mL) was added slowly and the mixture stirred at room temperature for 2 h. Then the volatiles were removed under vacuum, the residue was treated with dry toluene and filtered to separate the ammonium salt. The filtrates were concentrated under vacuum and dry pentane was added to precipitate the desired product, which was filtered off and washed with more pentane until the solid was colorless. Pure **34**²⁷¹ was isolated as a white solid (1.31 g, 1.75 mmol). Yield: 55%. **CF**: C₃₉H₆₇ClN₂O₆Si₂. **MW**: 751.6 g/mol. **¹H-NMR (CDCl₃, 250 MHz)**: 10.70 (s, 1H, H₉), 6.96 (s, 2H, H₈), 6.92 (s, 2H, H₈), 4.64 (m, 2H, H₁), 3.70 (q, 12H, J = 7.5 Hz, H₅), 2.47 (s, 6H, H₇), 2.35 (s, 6H, H₇), 2.26 (s, 6H, H₇), 1.84 (m, 4H, H₂), 1.69 (m, 4H, H₃), 1.15 (t, 18H, J = 7.5 Hz, H₆), 0.51 (m, 4H, H₄). **¹³CRMN (CDCl₃, 62.5 MHz)**: 161.19, 140.79, 136.49, 135.31, 131.10, 131.01, 130.63, 65.77, 58.09, 29.40, 20.19, 19.71, 18.27, 17.73, 17.38, 9.65.

5.2.9. Preparation of organosilica M9

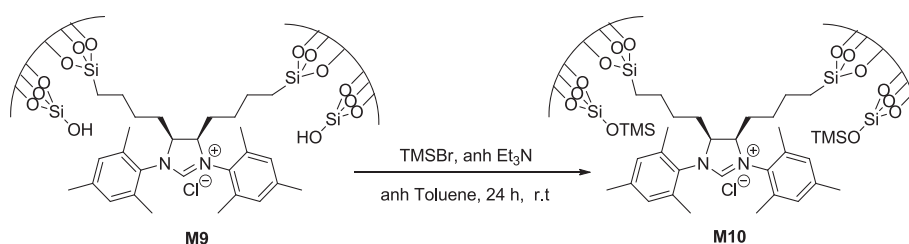


In a 250 mL round bottom flask equipped with magnetic stirring, P123 (0.372 g, 0.06 mmol) was dissolved in aqueous HCl (2M, 64.0 mL, 0.13 mmol) at 45°C. When the

Chapter 3.5. Experimental Section

solution was homogeneous, TEOS (3.6 mL, 0.940 g/cm³, 15.9 mmol) was added and the resulting suspension was stirred for 20 min at 45°C. At that time, a solution of **34** (1.335 g, 1.78 mmol) in a minimum amount of anhydrous EtOH (ca. 7 mL) was added and the final suspension stirred at 45°C for 18 h. Then the stirring was stopped and the mixture was aged at 45°C for 24 h. The mixture was cooled down to room temperature, then filtered and the solid was washed with water (3 x 30 mL), ethanol (3 x 30 mL) and acetone (3 x 30 mL). It was continuously extracted with acidic EtOH (10 v/v% conc. HCl/EtOH) for 48 h using a Soxhlet apparatus. After this time, the solid was filtered and dried overnight at 50°C under vacuum (1.2 mbar) and finally **M9** (1.691 g) was obtained as a white solid. **²⁹Si-CP-MAS NMR (79.5 MHz) δ:** -63.12 (T²), -70.15 (T³), -105.20 (Q³), -113.42 (Q⁴). **¹³C-CP-MAS NMR (100.62 MHz) δ:** 229.32, 157.97, 134.38, 128.61, 118.84, 65.64, 57.79, 27.63, 16.18, 9.55. **IR (ATR) (cm⁻¹):** 2974, 1623, 1045, 951, 793. **BET** S_{BET}: < 5 m²/g; non porous material. **EA calculated for C₂₇H₃₇N₂ClSi₃₂O₆₃** (considering complete conversion): 13.93% C, 1.60% H, 1.20%N, 38.46% Si; **found:** 24.44% C, 3.90% H, 2.00%N, 27.64% Si (0.71 mmol imidazolinium salt/g material).

5.2.10. Preparation of organosilica M10



In a 50 mL Schlenk tube under nitrogen atmosphere was placed material **M9** (0.507 g) and anhydrous toluene (30 mL). Then TMSBr (1.6 mL, 1.16 g/cm³, 12.1 mmol, 1 mol TMS respect to 1 mol -OH²⁸³) and anh Et₃N (0.5 mL, 0.727 g/cm³, 6.15 mmol) were added and the mixture stirred at r.t. under inert atmosphere for 24 h. Then, the material was filtered and washed with toluene (3 x 15 mL), methanol (3 x 15 mL), Et₂O (3 x 15 mL) and acetone (3 x 10 mL) to afford **M10** as a white powder (0.505 g). **IR (ATR) cm⁻¹:** 3234, 1623, 1045, 949, 848, 797. **EA found:** 23.12% C, 3.87% H, 1.91%N, 27.64% Si (0.68 mmol imidazolinium salt/g material). **BET** S_{BET}: < 5 m²/g; non porous material.

²⁸³ To calculate the maximum number of silanols to be protected, we supposed that all trialkoxy and tetraalkoxy groups present in the reactants had been hydrolyzed to silanols but not condensed, then each triethoxysilane moiety would give 3 silanols and each equivalent of TEOS would give 4 more Si-OH.

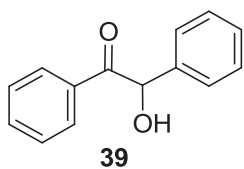
5.3 Catalytic tests

5.3.1 Assays in NHC-based catalytic reactions

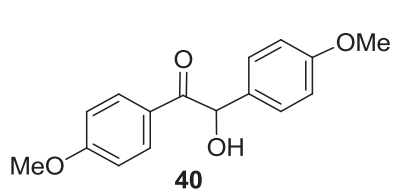
5.3.1.1 Benzoin condensation

General procedure for homogeneous catalysis. A 10 mL Schlenk flask was charged with the corresponding aromatic aldehyde (2.94 mmol) and the catalyst (10 mol%). Dry, degassed THF (2 mL) was added via syringe, followed by DBU (15 mol%). The reaction mixture was stirred for 72 h at room temperature under an atmosphere of argon. The product was then extracted with ethyl acetate (3 x 15 mL). The combined organic layers were washed with brine (3 x 20 mL) and dried with NaSO₄, filtered and concentrated under vacuum to yield a yellow oil. The crude product was analyzed by ¹HNMR.

General procedure for heterogeneous catalysis. A 10 mL Schlenk flask was charged with benzaldehyde (62 μL, 0.61 mmol) and the supported catalyst (20 mol%). Dry, degassed THF (0.5 mL) was added via syringe, followed by DBU (30 mol%). The reaction mixture was stirred for 5 days h at room temperature under an atmosphere of argon. Then the crude mixture was diluted with THF (2 mL) and filtered. The insoluble catalytic material was washed several times with THF (3 x 3 mL) and the combined filtrates were concentrated under vacuum to yield a yellow oil. The crude product was analyzed by ¹HNMR.



2-hydroxy-1,2-diphenylethanone, 39.²⁵⁶ CF: C₁₄H₁₂O₂. MW: 212,24 g/mol. ¹H-NMR (CDCl₃, 250 MHz) δ: 7.97-7.91 (m, 2H), 7.55-7.50 (m, 1H), 7.40-7.37 (m, 2H), 7.34-7.30 (m, 4H), 7.30-7.27 (m, 1H), 5.98 (s, 1H), 4.58 (br, 1H).

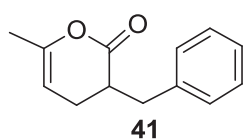


2-hydroxy-1,2-bis-(4-methoxyphenyl)ethanone, 40.²⁵⁶ CF: C₁₆H₁₆O₄. MW: 272,30 g/mol. ¹H-NMR (CDCl₃, 250 MHz) δ: 7.87-7.83 (m, 2H), 7.37-7.35 (m, 2H), 6.88-6.83 (m, 4H), 5.85 (s, 1H), 3.82 (s, 3H), 3.76 (s, 3H).

5.3.1.2 Annulation of enals and vinyl ketones

General procedure for homogeneous catalysis. A 10 mL Schlenk flask was charged with cinnamaldehyde (93 μL , 0.74 mmol), IMesCl (15 mol%) and methylvinylketone (41 μL , 0.49 mmol) and they were dissolved in dry and degassed THF (1 mL). Then DMAP was added (20 mol%) and the reaction mixture was stirred for 24 h at room temperature under an atmosphere of argon. Volatiles were removed under vacuum and the crude product was purified on column chromatography through silica gel (hexane:AcOEt 95:5) and **41** was obtained as a yellow liquid.

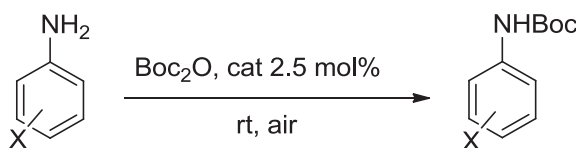
General procedure for heterogeneous catalysis: A 10 mL Schlenk flask was charged with cinnamaldehyde (86 μL , 1.05 g/cm³, 0.68 mmol), **M10** (15 mol%) and methylvinylketone (38 μL , 1.05 g/cm³, 0.45 mmol). They were dissolved in dry and degassed THF (1 mL). Then DMAP was added (20 mol%) and the reaction mixture was stirred for 5 days at room temperature under an atmosphere of argon. Then the crude mixture was diluted with THF (2 mL) and filtered. The insoluble catalytic material was washed several times with THF (3 x 3 mL) and the combined filtrates were concentrated under vacuum to yield a crude product which was analyzed by ¹H-NMR.



3-benzyl-6-methyl-3,4-dihydro-2H-pyran-2-one, 41.²³² **CF:** C₁₃H₁₄O₂. **MW:** 202,25 g/mol. **¹H-NMR (CDCl₃, 250 MHz) δ :** 7.29-7.14 (m, 5H), 4.74 (s, 1H), 3.19 (d, J= 9.3 Hz, 1H), 2.85-2.47 (m, 2H), 2.14-1.94 (m, 2H), 1.70 (s, 3H).

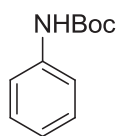
5.3.2 Assays in imidazolium-based catalytic reactions

5.3.2.1 Chemoselective *N*-*tert*-butyloxycarbonylation of amines.



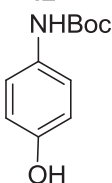
General Procedure. In a vial, to the mixture of the corresponding amine (2.5 mmol) and Boc₂O (2.5 mmol, 0.963 g/cm³, 1 equiv), **M7** (0.0629 g, 2.5 mol%) was added and the reaction mixture was stirred magnetically at r.t. After complete consumption of substrates (monitored by TLC), the crude mixture was diluted with Et₂O (5 mL) and filtered. The insoluble catalytic material was washed several times with Et₂O (3 x 10 mL) and the combined filtrates were concentrated under vacuum. From this residue,

the product was purified by column chromatography when necessary. The catalytic material was dried under vacuum and directly used in the next cycle.



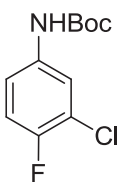
42

tert-butyl phenylcarbamate, 42.²⁷⁸ **CF:** C₁₁H₁₅NO₂. **MW:** 193.24 g/mol. **¹H-NMR (CDCl₃, 250 MHz) δ:** 7.38-7.29 (m, 4H), 7.06-7.01 (m, 1H), 6.46 (br, 1H), 1.52 (s, 9H). **¹³C-NMR (CDCl₃, 90 MHz) δ:** 153.19, 138.68, 129.28, 123.29, 118.75, 80.50, 28.02.



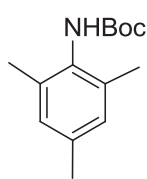
43

tert-butyl (4-hydroxyphenyl)carbamate, 43.²⁷⁸ **CF:** C₁₁H₁₅NO₃. **MW:** 209.24 g/mol. **¹H-NMR (CDCl₃, 250 MHz) δ:** 7.19 (d, J = 8.4 Hz, 2H), 6.77- 6.73 (m, 2H), 6.31 (br, 1H), 4.94 (br, 1H), 1.51 (s, 9H). **¹³C-NMR (CDCl₃, 90 MHz) δ:** 153.55, 152.25, 131.51, 121.41, 115.91, 82.38, 28.06.



44

tert-butyl (3-chloro-4-fluorophenyl)carbamate, 44.²⁷⁸ **CF:** C₁₁H₁₃ClFNO₂. **MW:** 245.68 g/mol. **¹H-NMR (CDCl₃, 250 MHz) δ:** 7.57-7.55 (m, 1H), 7.11-7.04 (m, 2H), 6.42 (br, 1H), 1.51 (s, 9H). **¹³C-NMR (CDCl₃, 90 MHz) δ:** 155.86, 153.14, 135.35, 120.88, 118.33, 116.84, 81.10, 27.94.



45

tert-butyl mesitylcarbamate, 45.²⁷⁸ **CF:** C₁₄H₂₁NO₂. **MW:** 235.32 g/mol. **¹H-NMR (CDCl₃, 250 MHz) δ:** 6.88 (s, 2H), 5.83 (br, 1H), 2.26 (s, 3H), 2.22 (s, 6H), 1.50 (s, 9H). **¹³C-NMR (CDCl₃, 90 MHz) δ:** 154.35, 136.77, 135.87, 131.69, 129.07, 79.42, 27.99, 20.49, 17.86.

CHAPTER 4

**Hybrid silica material derived from a [(NHC)AuCl]
complex.**

Applications as recyclable catalyst

1. INTRODUCTION

1.1 Gold catalysis

Since the first decade of 21st century, catalysis using gold has grown exponentially.²⁸⁴ Even though gold had been historically considered catalytically inert, this changed in 1973 when Bond *et al.* reported the hydrogenation of olefins over supported gold catalysts.²⁸⁵ More than a decade later, Haruta and Hutchings²⁸⁶ independently prognosticated that gold would be an extraordinary catalyst, with experimental demonstrations such as low-temperature oxidation of CO²⁸⁷ and hydrochlorination of acetylene to vinyl chloride,²⁸⁸ respectively, both reactions being performed under heterogeneous conditions. In addition, the early discovery by Ito *et al.*²⁸⁹ of a catalytic asymmetric aldol reaction established the first milestone of homogeneous gold catalysis. The next important step was done by Fukuda and Utimoto²⁹⁰ in 1991 with the catalytic hydration of alkynes promoted by Na[AuCl₄] which marked the beginning of the pursuit for novel catalytic applications of Au^I and Au^{III}. Gold is equally effective as an heterogeneous or an homogeneous catalyst.^{284a}

Reactivity of Au^I is based on its Lewis acid character due to relativistic effects.²⁹¹ Contraction of 6s orbitals and expansion of 5d orbitals characterize its reactivity. This fact justifies the low tendency of Au^I towards redox processes. In other words, Au^I complexes are good Lewis acids and present high affinity for unsaturated hydrocarbons such as alkynes, alkenes, enynes, allenes... activating them towards the addition of nucleophiles. This intrinsic π -activation property has shown remarkable

²⁸⁴ For reviews on gold catalysis see: (a) Hashmi, A. S. K; Hutchings, G.J. *Angew. Chem. Int. Ed.* **2006**, *45*, 7896. (b) Hashmi, A. S. K. *Chem. Rev.* **2007**, *107*, 3180. (c) Li, Z.; Brouwer, C.; He, C. *Chem. Rev.* **2008**, *108*, 3239. (d) Jiménez-Nuñez, E.; Echavarren, A.M. *Chem. Rev.* **2008**, *108*, 3326. (e) Arcadi, A. *Chem. Rev.* **2008**, *108*, 3266. (f) Fierro-Gonzalez, J.; Gates, B.C. *Chem. Soc. Rev.* **2008**, *37*, 2127. (g) Skouta, R.; Li, C.-J. *Tetrahedron*, **2008**, *64*, 4917. (h) Fürstner, A. *Chem. Soc. Rev.* **2009**, *38*, 3208. (i) Hashmi A.S.K.; Hubbert, C. *Angew. Chem. Int. Ed.* **2010**, *49*, 1010. (j) Hashmi A.S.K. *Angew. Chem. Int. Ed.* **2010**, *49*, 5232. (k) Corma, A.; Leyva-Pérez, A.; Sabater, M.J. *Chem. Rev.* **2011**, *111*, 1657. (l) Krause, N.; Winter, C. *Chem. Rev.* **2011**, *111*, 1994. (m) Bandini, M. *Chem. Soc. Rev.* **2011**, *40*, 1358. (n) Garayalde, D.; Nevado, C. *ACS Catal.* **2012**, *2*, 1462. (o) Rudolph, M.; Hashmi, A.S.K. *Chem. Soc. Rev.* **2012**, *41*, 2448. (p) Hashmi, A.S.K. *Acc. Chem. Res.* **2014**, *3*, 864. (q) Yang, W.; Hashmi, A.S.K. *Chem. Soc. Rev.* **2014**, *43*, 2941. For an example of early industrial research on cationic Au^I complexes, see: r) Teles, J.H.; Brode, S.; Chabanas, M. *Angew. Chem. Int. Ed.* **1998**, *37*, 1415.

²⁸⁵ Bond, G.C.; Sermon, P.A.; Webb, G.; Buchanan, D.A.; Wells, P.B. *J. Chem. Soc. Chem. Commun.* **1973**, 444.

²⁸⁶(a) Haruta, M. *Nature* **2005**, *437*, 1098. (b) Hutchings, G.J. *Catal. Today* **2005**, *100*, 55.

²⁸⁷ Haruta, M.; Kobayashi, T.; Sano, H.; Yamada, N. *Chem. Lett.* **1987**, *16*, 405.

²⁸⁸ Hutchings, G.J. *J. Catal.* **1985**, *96*, 292.

²⁸⁹ Ito, Y.; Sawamura, M.; Hayashi, T. *J. Am. Chem. Soc.* **1986**, *108*, 6405.

²⁹⁰ Fukuda, K.; Utimoto, K. *J. Org. Chem.* **1991**, *56*, 3729.

²⁹¹ (a) Fürstner, A.; Davies, P.W. *Angew. Chem. Int. Ed.* **2007**, *46*, 3410. (b) Gorin, D.J.; Toste, F.D. *Nature*, **2007**, *446*, 395. (c) Leyva-Pérez, A.; Corma, A. *Angew. Chem. Int. Ed.* **2012**, *51*, 614.

progress in various cyclization reactions, C-C bond formations and C-heteroatom bond-forming reactions.²⁹² Moreover, gold catalysis confers nonclassical cationic type intermediates, which in many cases allow access to cationic rearrangement cascades of the Wagner-Meerwein²⁹³ type, 1,2-alkyl shifts²⁹⁴ for example, to form interesting molecular frameworks.

Another key property, especially in Au^I catalysis, is the general tolerance of the catalytic system towards moisture and air.

1.2 General mechanism of gold(I) catalysis

Gold catalysis can be explained with the concept of *carbophilic π -acids* first introduced by Fürstner and Davies.^{291a}

To represent the basic mechanism of gold catalysis, Scheme 4.1 is based on a model substrate I. As mentioned before, a substrate suitable for Au^I catalysis requires the presence of a multiple bond such as alkynes, alkenes or allenes, containing an intramolecular nucleophile.²⁹⁵ The nucleophiles available in Au^I catalysis encompass a wide variety of compounds, including carbon nucleophiles, such as enolates, enamines, and electron-rich aromatic systems (Friedel-Crafts type reactions) as well as nucleophiles based on heteroatoms, such as nitrogen, sulphur, and oxygen.

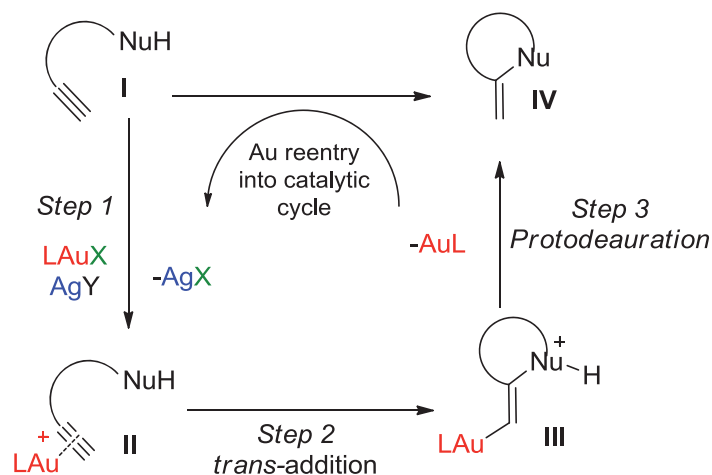
The Au^I catalyst precursor is normally denoted in the literature as LAuX, where X is often an halide such as chloride. This precursor does not contain a catalytic active site since Au^I is bidentate, and the abstraction of the halide with a co-catalyst is required before any catalysis can occur. Usually a silver salt bearing sterically hindered weakly binding counteranions (AgBF₄, AgSbF₆, AgOTf...) is used to abstract the halide and the thermodynamically stable AgX salt directly precipitates out from the reaction solvent. This ionic exchange pathway produces the catalytically active species LAu⁺, which in *step 1* activates the multiple bond due to its strong Lewis acidity to form the gold-alkyne complex II.

²⁹² Numerous examples can be found in ref 284. Some other selected examples are the following: (a) Marion, N.; Nolan, S.P. *Angew. Chem. Int. Ed.* **2007**, *46*, 2750. (b) Jiménez-Nuñez, E.; Echavarren, A.M. *Chem. Commun.* **2007**, 333. (c) Michelet, V.; Toullec, P.Y.; Genêt, J.P. *Angew. Chem. Int. Ed.* **2008**, *47*, 4268. (d) Shen, H.C. *Tetrahedron* **2008**, *64*, 3885. (e) Muzart, J. *Tetrahedron* **2008**, *64*, 5815. (f) Shen, H.C. *Tetrahedron* **2008**, *64*, 7847. (g) Rudolph, M.; Hashmi, A.S.K. *Chem. Commun.* **2011**, *47*, 6536. (h) Brenzovich, W.E. Jr. *Angew. Chem. Int. Ed.* **2012**, *51*, 8933. (i) Zhang, D.H.; Zhang, Z.; Shi, M. *Chem. Commun.* **2012**, *48*, 10271. (j) Braun, I.; Asiri, A.M.; Hashmi, A.S.K. *ACS Catal.* **2013**, *3*, 1902.

²⁹³ Zweifel, T.; Hollmann, D.; Prüger, B.; Nielsen, M.; Jørgensen, K.A. *Tetrahedron Asymm.* **2010**, *21*, 1624.

²⁹⁴ Crone, B.; Kirsch, S.F. *Chem. Eur. J.* **2008**, *14*, 3514.

²⁹⁵ Loh, C.C.J.; Enders, D. *Chem. Eur. J.* **2012**, *18*, 10212.



Scheme 4.1. Basic principles in Au catalysis according to ref 295.

The π -activation of the alkyne allows the nucleophile to attack through a *trans*-addition pathway in *step 2*, thereby generating the vinyl-Au intermediate **III**, in which an Au-C covalent bond is formed. Such intermediates are nonclassical cationic in nature, which are able to undergo cationic skeletal rearrangements.

In last step, the Au-C covalent bond has to be cleaved before the Au catalyst can reenter into the catalytic cycle. Unlike the commonly known Pd catalysis, where a *reductive elimination* can occur due to its ease in switching between oxidation states, Au catalysis is resistant to oxidation state switching. By contrast, a proton transfer process occurs, known as *protodeauration*, leading to product **IV** (Scheme 4.1, *step 3*). In other words, either an intramolecular or intermolecular proton shift allows the Au-C bond cleavage to regenerate the catalytically active Au^I species.

1.3 NHC-Au(I) complexes

Similarly to other transition metals, the stability, reactivity (Lewis acidity) and selectivity of the gold complexes are strongly dependent on the ligands bonded to the metallic center.^{296,297b} Furthermore, when the mono-ligated cationic catalyst is generated, it requires strong electronic and steric stabilization from its ancillary ligand.

In this sense, *N*-heterocyclic carbene ligands have generated a great interest for the past few years.²⁹⁷ This family of ligands shows strong σ -donation and weak π -

²⁹⁶ (a) Gorin, D.J.; Sherry, B.D.; Toste, F.D. *Chem. Rev.* **2008**, *108*, 3351. (b) Wang, W.; Hammond, G.B.; Xu, B. *J. Am. Chem. Soc.* **2012**, *134*, 5697.

²⁹⁷ For reviews on (NHC)-Au catalysis see: (a) Marion, N.; Nolan, S.P. *Chem. Soc. Rev.* **2008**, *37*, 1776. (b) Nolan, S.P. *Acc. Chem. Res.* **2011**, *44*, 91. (c) Gaillard, S.; Cazin, C.S.J.; Nolan, S.P. *Acc. Chem. Res.* **2012**, *45*, 778.

retrodonation compared to tertiary phosphines.²⁹⁸ Consequently they offer higher stability (as increases the strength of metal-ligand bond) and different chemical properties to the metal center (higher electron density to the metal center).

Fischer²⁹⁹ reported the first stable transition metal complexes bearing carbene ligands in 1964, and ten years later, Schrock³⁰⁰ isolated a different type of alkylidene complex. Meanwhile, Wanzlick³⁰¹ and Öfele³⁰² had also reported independently their studies on (NHC)-transition metal complexes in 1968. However, no isolation of a monomeric carbene ligand was achieved at that time. It was not until 1991 when Arduengo *et al.*³⁰³ described the isolation of a free imidazol-2-ylidene which provided access to numerous transition metal carbenes. Although the first NHC-gold(I) complex was isolated in 1973,³⁰⁴ it is only recently that these compounds have gained popularity, mainly as species of formula [(NHC)AuCl].

NHC ligands have been found to be excellent σ -donors to metals. To date, all theoretical and experimental evidences indicated that, in order to form a stable carbene, the carbenic carbon needs to be bonded to strong π -donor atoms.³⁰⁵ Thus, the stability of an NHC is largely due to the π -donation from the lone pairs of the adjacent nitrogen atoms to the empty p orbitals of the carbene (Figure 4.1). However, recent theoretical and structural evidences have suggested that π -back-donation plays a larger role than previously thought. The degree of back-donation is dependent upon the metal in question.

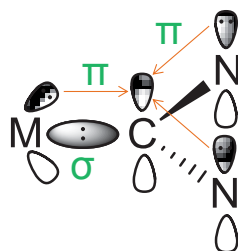


Figure 4.1. Orbital diagram of N-heterocyclic carbenes.

²⁹⁸ (a) Garrison, J.C.; Youngs, W.J. *Chem. Rev.* **2005**, *105*, 3978. (b) Hu, X.; Castro-Rodriguez, I.; Olsen, K.; Meyer, K. *Organometallics* **2004**, *23*, 755. (c) Nemcsok, D.; Wichmann, K.; Frenking, G. *Organometallics* **2004**, *23*, 3640.

²⁹⁹ Fischer, E.O.; Maasböl, A. *Angew. Chem. Int. Ed.* **1964**, *3*, 580.

³⁰⁰ Schrock, R.R. *J. Am. Chem. Soc.* **1974**, *96*, 6796.

³⁰¹ Wanzlick, H.W.; Schönherr, H.J. *Angew. Chem. Int. Ed.* **1968**, *7*, 141.

³⁰² Öfele, K. *J. Organomet. Chem.* **1968**, *12*, P42.

³⁰³ Arduengo III, A.J.; Harlow, R.L.; Kline, M.A. *J. Am. Chem. Soc.* **1991**, *113*, 361.

³⁰⁴ Minghetti, G.; Bonati, F. *J. Organomet. Chem.* **1973**, *54*, C62-C63.

³⁰⁵ Díez-González, S.; Nolan, S.P. *Coord. Chem. Rev.* **2007**, *251*, 874.

Despite the existence of several families of stable carbenes, only the five-membered cyclic diamino carbenes have found numerous applications. Structures for the most commonly employed carbene ligands are represented in Figure 4.2.

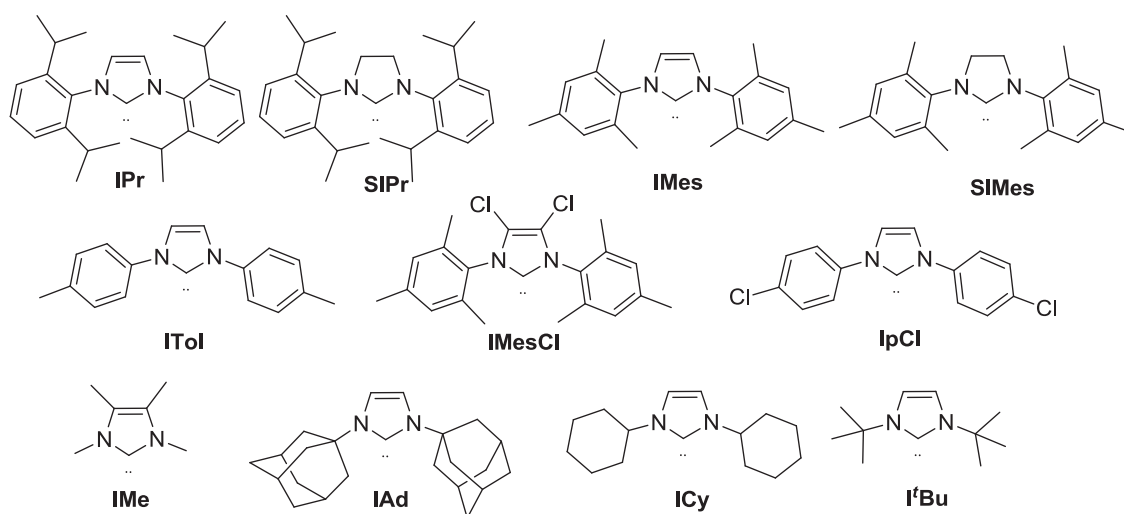


Figure 4.2. Structures of N-heterocyclic carbene ligands.

Additional steric protection from the N-substituents may enhance the stability of the carbenes and it might compensate for less electronic stabilization. Bulkiness of the groups bound to the nitrogen atoms of the NHC ligands and more importantly, the short metal-carbon distances in these complexes, increase the steric congestion around the metal center when compared to tertiary phosphines.

In order to quantify the steric requirements of these ligands, a numerical model was designed by Nolan: the *Buried Volume* method (Figure 4.3). The method quantifies the steric demand of various NHCs by representing the part of a sphere around a metal (with a certain radius r) that is buried by the atoms of the ligand under investigation. The more sterically demanding (within the coordinating sphere of the metal) a ligand, the larger the $\%V_{Bur}$ value.³⁰⁶ This model allows comparison with other ligands, particularly tertiary phosphines. The model also takes into account the high asymmetry of these ligands. The right combination of electronic and steric factors characterizing NHCs has been key to rationalize the stabilization of otherwise highly reactive species.

³⁰⁶ Dröge, T.; Glorius, F. *Angew. Chem. Int. Ed.* **2010**, *49*, 6940.

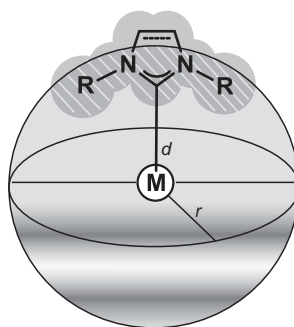


Figure 4.3. Graphical illustration of the buried volume ($\% V_{Bur}$) concept.³⁰⁶

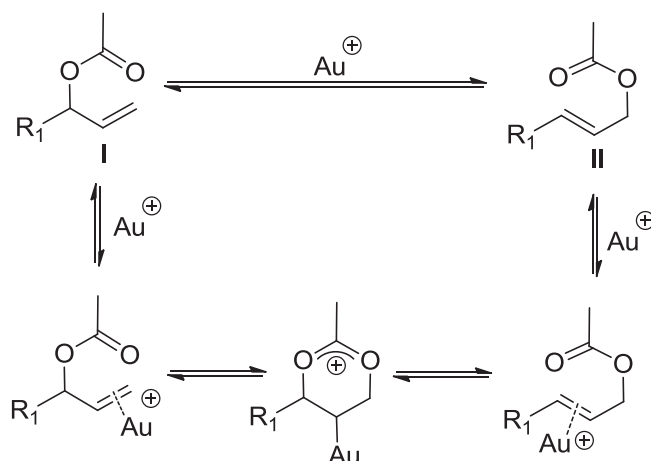
1.4 Reactivity of NHC-Au(I) complexes

As mentioned before, NHC-Au catalysis encompasses a wide variety of reactions such as skeletal rearrangements, cycloisomerizations, addition of water to alkynes and nitriles, and C-H bond activation. These processes are quite atom-economical, and in the most recent C-H reactions the only byproduct is water.

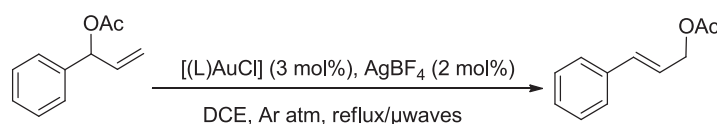
The following sections describe some of these reactions as well as the state-of-the-art methodology, which involves single-component catalysts, precluding the need for costly silver co-catalysts.

1.4.1 Allylic ester rearrangement (alkene activation)

Similarly to propargylic esters, an acetate moiety can undergo a 1,3-shift upon complexation of Au^+ fragment onto the alkene, resulting ultimately in the formation of an isomerized allylic acetate. This reaction provides an efficient and atom-economical access to primary oxo-derivatives. The mechanism is believed to proceed *via* initial π -coordination of the alkene **I** to the cationic gold center. π -Activation of the C=C bond triggers an intramolecular attack by the carbonyl oxygen, leading to a 6-membered stabilized 1,3-acetoxonium. Regeneration of the carbonyl bond affords the isomerized olefin **II**. (Scheme 4.2).

Scheme 4.2. Allylic ester rearrangement mechanism.³⁰⁷

Nolan reported a series of [(NHC)AuCl] complexes which, in conjunction with a silver salt, efficiently catalyze the isomerization of allylic acetates under thermal or microwave-assisted conditions (Scheme 4.3 and Table 4.1).³⁰⁷



Scheme 4.3. Allylic ester rearrangement of 1-phenylallyl acetate.

Table 4.1. Influence of the ligand on the rearrangement.³⁰⁷

Entry	Ligand	Yield (%)	Entry	Ligand	Yield (%)
1	none	<5	6	I ^t Bu	98
2	IPr	99	7	ICy	61
3	SIPr	98	8	IMe	56
4	IMes	95	9	PPh ₃	53
5	IAd	97			

It was observed that, in this particular transformation, the steric hindrance of the ligand, more than its electronic properties, was a key parameter. Hence, bulky ligands, such as I^tBu and IAd performed better than smaller ones like IMe, ICy or PPh₃ (Table 4.1). The authors proposed that a bulky ligand, rather than having an effect on the catalytic reaction itself, would shield the cationic gold center more efficiently than a smaller ligand and prevent catalyst decomposition. Interestingly, the reaction could be carried out under microwave heating without alteration of the yield or the purity of the products. This highlights the robustness of the NHC-Au^I bond and the interest in

³⁰⁷ Marion, N.; Gealageas, R.; Nolan, S.P. *Org. Lett.* **2007**, 9, 2653. Additions and corrections, *Org. Lett.* **2008**, 10, 1037.

employing this type of catalyst when somewhat harsh conditions are required for a given transformation. The scope of this reaction was found to be quite broad, notably including trisubstituted olefins, with the exception of nitrile-containing substrates, which probably hinder catalysis by N-coordination to gold.

1.4.2 NHC-Au-OH as precatalyst

Pursuing the synthesis of new gold complexes, Nolan has reported the preparation of a series of mononuclear Au-NHC hydroxide complexes (Scheme 4.4).³⁰⁸ The achievement of these compounds has allowed the development of new silver-free gold-catalyzed protocols.³⁰⁹



Scheme 4.4. NHC-Au-OH preparation method described by Nolan.^{308b}

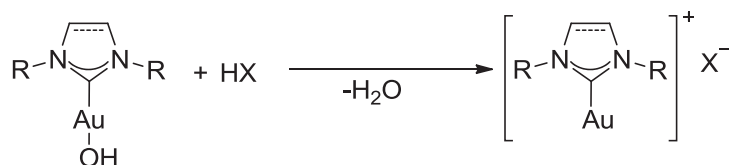
Avoiding the use of silver salts decreases costs and makes handling easier, as they can be sensitive to light and moisture. Moreover, they may also persist as impurities in the catalyst and, therefore, cause confusion about the identity of the active catalytic species when the cationic gold(I) species has been generated by halide abstraction using silver,³¹⁰ as they are known to be σ - and π -system activating agents.

The activation of gold(I) complex by formation of $[\text{LAu}]^+$ can be easily obtained by simple protonolysis of $[(\text{NHC})\text{-Au-OH}]$ in the presence of a Brønsted acid (HX) such as HBF_4 , HSbF_6 or HNTf_2 (Scheme 4.5). A slight excess of acid is necessary to ensure complete formation of the active species in the reaction medium, otherwise active species can be found in equilibrium.³⁰⁹ A second advantage of this activation type is that water is the only co-product formed, which is in any case a reagent or even the reaction solvent.

³⁰⁸ (a) Gaillard S.; Slawin, A. M. Z.; Nolan, S.P. *Chem. Commun.* **2010**, 46, 2742. (b) Patrick, S.R.; Gómez-Suárez, A.; Slawin, A.M.Z.; Nolan, S.P. *Organometallics* **2014**, 33, 421.

³⁰⁹ (a) Gaillard S.; Bosson, J.; Ramón, R.S.; Nun, P.; Slawin, A. M. Z.; Nolan, S.P. *Chem. Eur. J.* **2010**, 16, 13729. (b) Nun, P.; Ramón, R.S.; Gaillard S.; Nolan, S.P. *J. Organomet. Chem.* **2011**, 696, 7.

³¹⁰ Wang, D.; Cai, R.; Sharma, S.; Jirak, J.; Thummanapelli, S.K.; Akhmedov, N.G.; Zhang, h.; Petersen, J.L.; Shi, X. *J. Am. Chem. Soc.* **2012**, 134, 9012.



Scheme 4.5. Generation of [(NHC)Au]⁺X⁻ via acid activation.

The catalytic activity of [(IPr)AuOH] was evaluated in a number of important organic transformations such as nitrile and alkyne hydration, conversion of propargylic acetates into enones, skeletal rearrangement and alkoxy cyclization of enynes, 3,3-rearrangement of allylic acetates, intramolecular hydroamination of alkenes and a Beckman-type rearrangement.³⁰⁹ Complex [(IPr)AuOH] was found to be efficient in all of them.

1.4.3 NHC-Au(I) catalysis in aqueous media

The development of organic transformations in aqueous media has become one of the major keystones in modern chemistry.³¹¹ The use of water as an alternative, available, safe and cost-effective solvent fulfills the principles of "Green Chemistry",³¹² offering a surrogate to the growing concerns associated with the environmental impact of chemical processes. Water is non-toxic and non-flammable, has high heat capacity, and is relatively inexpensive. However, water has some significant drawbacks, one of them is the fact that it is a poor solvent for most organic molecules.

Design of catalysts containing ligands with hydrophilic substituents has been the most common approach to prepare catalysts that operate in the aqueous phase of a biphasic reaction. Such ligands have been typically based on phosphine derivatives and nitrogen ligands, however, increasing efforts are devoted to the development of hydrophilic analogues such as *N*-heterocyclic carbenes (NHC).³¹³ One of the most common strategy for this type of ligands to be used in aqueous media is the introduction of ionic moieties in their molecular structure.³¹⁴ Concerning NHC-Au complexes, some examples are represented in Figure 4.4. However, only the sulfonated derivatives **D-G** have been employed in catalysis applications. Joó and co-

³¹¹ (a) *Organic Reactions in Water*; Lindström, U.M., Ed. Blackwell Publishing; Oxford, 2007. (b) *Alternative Solvents for Green Chemistry*; Kerston, F.M. Ed.; RSC Publishing, Cambridge, UK, 2009.

³¹² Sheldon, R.A.; Arends, I.; Hanefeld, U. *Green Chemistry and Catalysis*; Wiley-VCH: Weinheim, 2007.

³¹³ Velazquez, H.D.; Verport, F. *Chem. Soc. Rev.* **2012**, 41,7032.

³¹⁴ (a) Schaper, L.A.; Hock, S.J.; Herrmann, W.A; Kühn, F.E.; *Angew. Chem. Int. Ed.* **2013**, 52, 270. (b) Fliedel, C.; Braunstein, P. *J. Organomet. Chem.* **2014**, 751, 286.

workers³¹⁵ used complexes **D-F** as catalysts in the Markovnikov hydration of terminal alkynes in aqueous media and **G** complexes were described by Cadierno³¹⁶ to facilitate de cycloisomerization of γ -alkynoic acids.

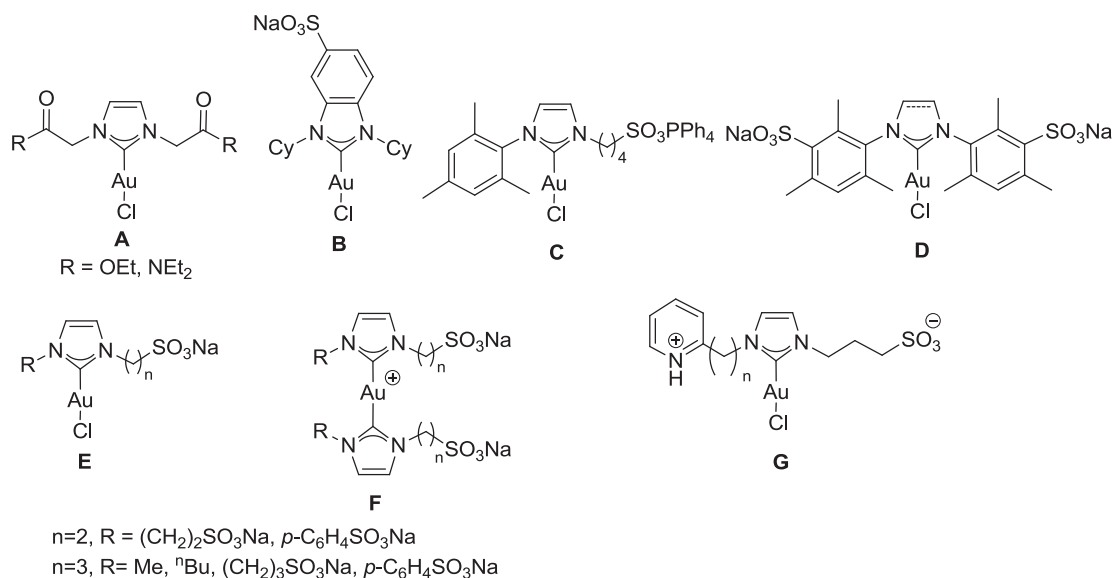
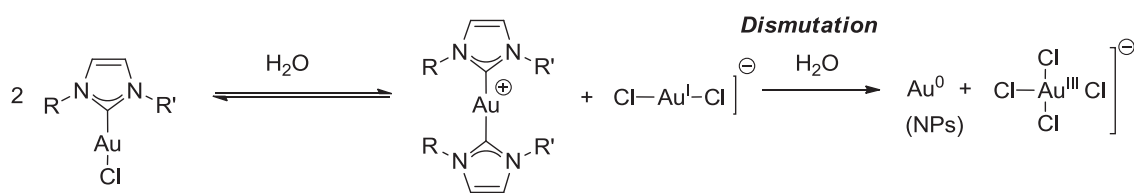


Figure 4.4. Molecular structure of hydrophilic [(NHC)-Au(I)] complexes **A-G**.

However, complexes represented by the formula [(NHC)AuCl] have shown very low stability in water as they usually decompose generating the corresponding biscarbenes [Au(NHC)₂]⁺ and gold nanoparticles, the latter being the result of the anion [AuCl₂]⁻ dismutation (Scheme 4.6).³¹⁷ In fact, Cadierno performed the reactions in a biphasic toluene/water system.



Scheme 4.6. Equilibrium between *mono*- and *bis*-carbenic gold(I) species and dismutation process of the [AuCl₂]⁻ species.

³¹⁵ (a) Almásy, A.; Nagy, C.E.; Bényei, A.C.; Joó, F. *Organometallics* **2010**, *29*, 2484. (b) Czégéni, C.E.; Papp, G.; Kathó, A.; Joó, F. *J. Molec. Catal. A: Chem.* **2011**, *340*, 1.

³¹⁶ Tomás-Mendivil, E.; Toullec, P.Y.; Borge, J.; Conejero, S.; Michelet, V.; Cadierno, V. *ACS Catal.* **2013**, *3*, 3086.

³¹⁷ (a) Gammons, C.H.; Yu, Y.; Williams-Jones, A.E.; *Geochim. Cosmochim. Acta* **1997**, *61*, 1971. (b) Bergamini, P.; Ceroni, V.; Balzani, M.; Gingras, M.; Raimundo, J.M.; Morandic, V.; Merli, P.G.; *Chem. Commun.* **2007**, 4167. (c) English, M.D.; Waclawik, E.R. *J. Nanopart. Res.* **2012**, *14*, 650.

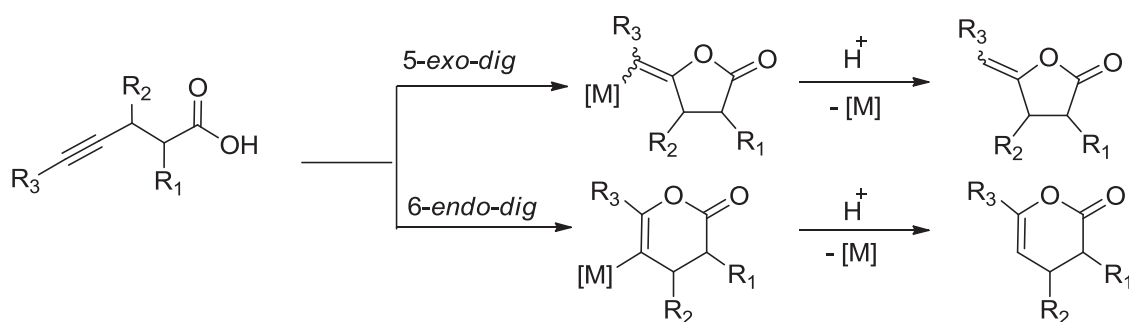
Due to the low number of examples of [(NHC)-Au(I)] complexes which have been investigated as aqueous phase catalysts, this opens an enormous window of opportunities in this field. A better understanding of the role of water as a reaction medium may improve the performance of the chemical processes, such as product separation, treatment of by-products and recycling of catalysts and solvent.

Moreover, formation of cationic [LAu]⁺ is very likely in the polar aqueous media, and some reactions can be run in the absence of a silver(I) salt for a chloride abstraction.^{315b,316}

1.4.4 Catalytic cycloisomerization of γ -alkynoic acids into enol-lactones in aqueous media

Catalytic cycloisomerization of γ -alkynoic acids is one attractive process for the formation of *exo*-cyclic 5-membered ring enol-lactones (γ -butirolactones) as it exhibits excellent atom economy.³¹⁸ γ -Butirolactones are present in numerous skeletons of natural organic molecules³¹⁹ as well as in synthetic key intermediates of great interest.³²⁰

Importantly, it is worth to remind that in this reaction, apart from obtaining the desired 5-membered ring enol-lactone coming from a *5-exo-dig* cyclization, it can be generated a 6-membered ring derived from the corresponding *6-endo-dig* cyclization according to the Baldwin rules (Scheme 4.7).³²¹ Usually the *5-exo-dig* cyclization is favored for terminal alkynes.



Scheme 4.7. Cycloisomerization products according to Baldwin rules.

As mentioned above, Cadierno and collaborators have reported the synthesis and characterization of novel Au(I) derivatives containing related water soluble NHC ligands

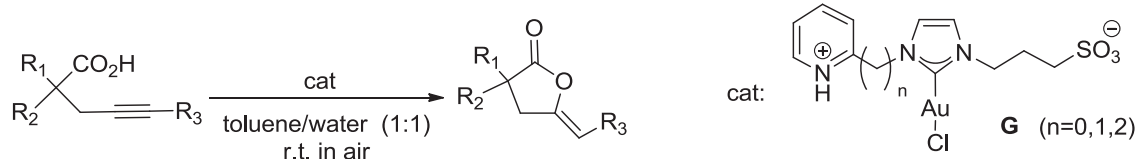
³¹⁸ Alonso, F.; Beletskaya, I.P.; Yus, M. *Chem. Rev.* **2004**, *104*, 3079.

³¹⁹ (a) Negishi, E.I.; Kitora, M.; *Tetrahedron*, **1997**, *53*, 6707.

³²⁰ (a) Padwa, A.; Rashatasakhon, P.; Rose, M. *J. Org. Chem.* **2003**, *68*, 5139. (b) Yang, T.; Campbell, L.; Dixon, D.J. *J. A. Chem. Soc.* **2007**, *129*, 12070.

³²¹ Baldwin, J.E. *J. Chem. Soc., Chem. Commun.* **1976**, 734.

with the ability to promote the cycloisomerization of γ -alkynoic acids in a biphasic system toluene/water (Scheme 4.8).³¹⁶



Scheme 4.8. γ -Alkynoic acids cycloisomerization described by Cadierno.

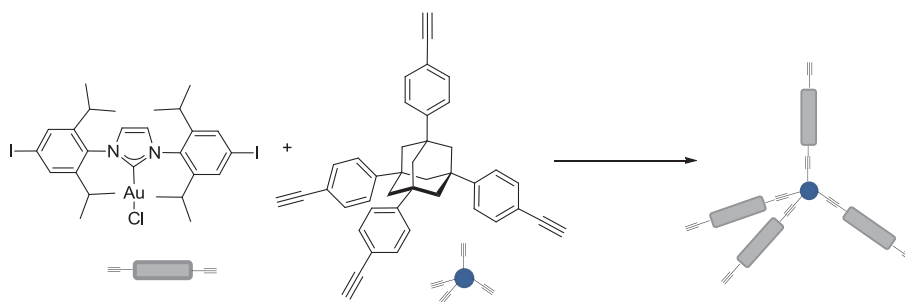
Despite the great tendency shown by gold complexes to promote the hydration of $C\equiv C$ bonds, competing alkyne hydrations were not observed using the zwitterionic **G** catalysts. Thus, Au(I) derivatives proved to be active and selective in the cycloisomerization of 4-pentynoic acid (TOF = 40 h⁻¹). Some of these catalysts could be reused up to 5 runs. The high reactivity of these Au(I) complexes merits to be highlighted since the participation of a chloride abstractor was not required. Easy dissociation of the chloride ligand in the polar aqueous medium, leading to the effective generation of active $[Au(NHC)]^+$ species, can be evoked to explain the catalytic activity observed. Remarkably, the presence of a NHC ligand in the catalysts was crucial, as the efficiency and selectivity of the reaction were markedly lower using simple AuCl₃ or AuCl salts.

1.5 Supported NHC-Au(I) catalysts.

Heterogenization of [(NHC)-Au] catalysts represents a reinforcement of the "greenness" of the catalytic processes. To our knowledge, only two different examples of immobilized [NHC-Au] catalysts have been described in the literature.

Li and collaborators³²² have recently reported (when this PhD work was in course) a direct controllable synthesis of [(IPr)-Au] derived catalysts immobilized in different porous organic polymers (POPs). POPs present high surface area as well as hydrothermal stability and chemical robustness. The supported catalysts were prepared from a [(IPr)-Au-Cl] derivative as *building block* and *via* Sonogashira coupling by varying the monomer strut length and concentration during polymerization (Scheme 4.9). Alkyne monomers with different lengths were selected as linkers to tune the physical properties.

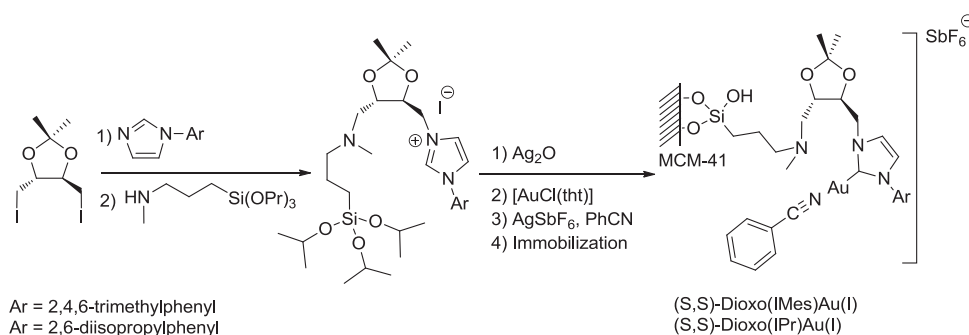
³²² Wang, W.; Zheng, A.; Zhao, P.; Xia, C. Li, F. *ACS Catal.* **2014**, *4*, 321.



Scheme 4.9. Synthesis of one example of Au-NHC@POPs1 described by Li.

The materials were found to be efficient, recoverable and reusable heterogeneous catalysts in alkyne hydration reactions. However, in reactions carried out in pure water, no product was observed, possibly due to the hydrophobicity of the materials. The best conditions were found to be MeOH/H₂O (2:1), 0.6 mol% Au together with AgSbF₆ as co-catalyst, at reflux temperature, yielding up to 86% of final product. No by-products were formed, suggesting that all these catalysts were selective. The alkyne hydration could not be realized in the absence of AgSbF₆. AuNHC@POPs precipitated from the reaction mixture, then they were collected by centrifugation and reused for the next run. AgSbF₆ had to be reloaded each cycle. Catalyst AuNHC@POPs1 could be reused up to five times without significant loss of activity.

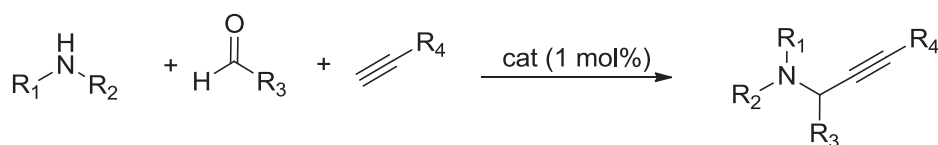
On the other hand, Sánchez, Iglesias *et al.* reported the preparation of *N*-heterocyclic carbene-dioxolane Au(I) complexes immobilized on mesoporous silica support MCM-41 to catalyze a multicomponent reaction (MCR).³²³ Gold complexes ((*S,S*)-dioxo-(IMes)Au(I), (*S,S*)-dioxo-(IPr)Au(I)) were prepared by a sequence involving formation of the NHC-Ag complexes from the corresponding silylated imidazolium salts, subsequent transmetalation with AuCl(tht), addition of a silver salt and benzonitrile to generate the cationic NHC-Au(I) species, and final immobilization on MCM-41 by a *grafting* method (Scheme 4.10).



Scheme 4.10. Supported NHC-Au(I) catalysts described by Iglesias and Sánchez.

³²³ Villaverde, G.; Corma, A.; Iglesias, M.; Sánchez, P. *ACS Catal.* **2012**, *2*, 399.

Supported catalysts were tested in the one-pot, three component coupling reaction of various aldehydes, amines and terminal alkynes for the synthesis of propargylamines (Scheme 4.11). In the benchmark reaction, benzaldehyde, piperidine and phenylacetylene were used as substrates. The optimal reaction conditions were established as follows: 1:1.2:1.5 molar ratio of aldehyde:amine:acetylene, 1 mol% of Au catalyst, in chloroform at 70°C for 24 h.



Scheme 4.11. NHC-Au(I) catalyzed three-component synthesis of propargylamines.

As expected for MCRs in which three molecules have to meet within the support pores, the pore size of MCM-41 have a marked influence on the reaction efficiency. No conversion was found in the absence of catalyst under identical conditions and a KAuCl₄ catalyzed reaction yielded only a 63% of the product. These results clearly emphasized the role of the support itself and the nature of gold complex. Catalysts were filtered after centrifugation and reused after each run, although a reactivation step was needed, which consisted in a treatment with benzonitrile at 70°C for 5 h. They could be reused for six reaction cycles, in which gold reduction was not observed and only a loss of 10.0% of the initial amount of Au was detected. Remarkably, no external ligands/additives or inert atmosphere were needed to promote the reaction, and a low loading of gold was sufficient to efficiently catalyze the reactions.

1.6 Precedents in the research group on the immobilization of NHC-metal complexes.

In our research group, Dra. Amalia Monge immobilized NHC-ruthenium alkylidene complexes through the NHC ligands by forming hybrid silica materials, in order to obtain reusable metathesis catalysts (Figure 4.5). To achieve this goal, triethoxysilyl groups were introduced into the NHC moieties by different methods.

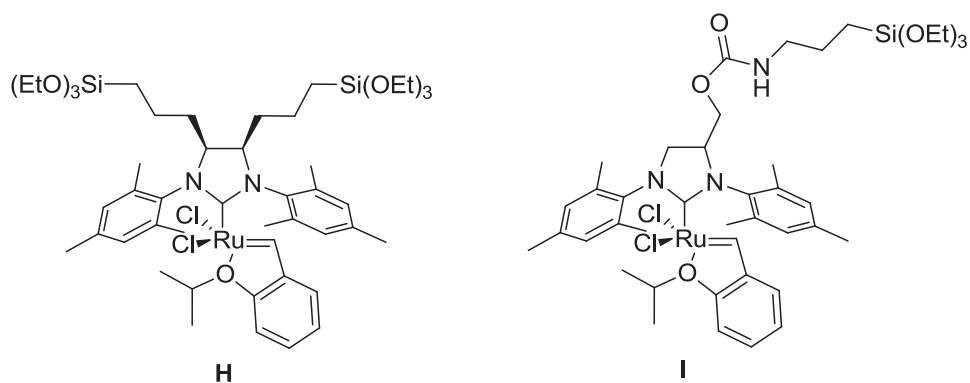
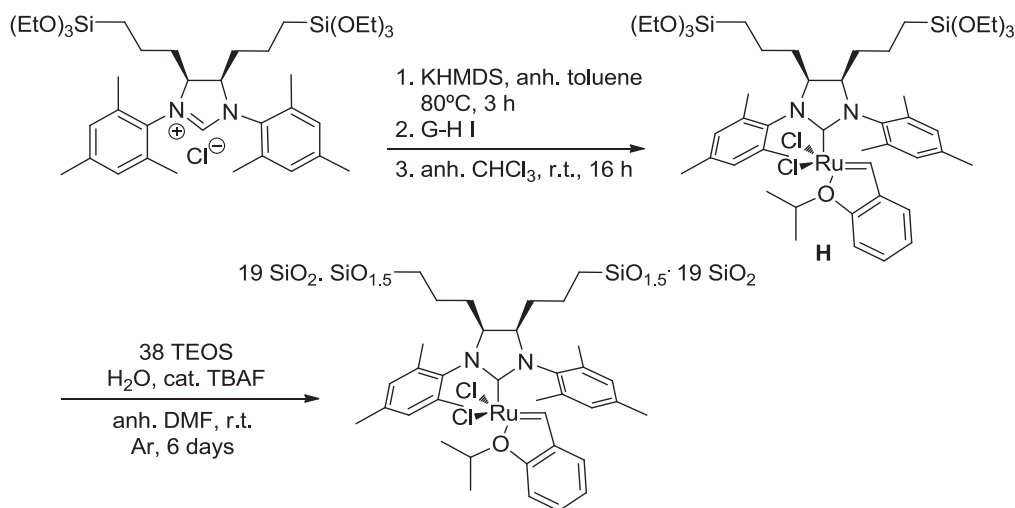


Figure 4.5. Precursors for NHC-immobilized 2nd generation Grubbs-Hoveyda catalysts.

Among them, we would like to remark complex **H**³²⁴ as its preparation resulted to be easier compared to that of **I**.³²⁵ Complex **H** was obtained through treatment of the first generation Grubbs-Hoveyda catalyst (G-H **I**) with the free carbene, previously generated from a bis-silylated dihydroimidazolium salt in the presence of a strong base (Scheme 4.12). The corresponding derived hybrid silica material was prepared by sol-gel process performed on the bis-silylated ruthenium alkylidene, namely by co-gelification with tetraethoxysilane (TEOS, molar ratio 1:38) in anhydrous DMF under argon atmosphere, using nucleophilic catalysis (TBAF). This catalytic material efficiently promoted diene ring-closing metathesis reactions (RCM) and could be reused up to 5 cycles.^{324,326}



Scheme 4.12. Preparation of a bis-silylated NHC-Ru alkylidene and a sol-gel derived hybrid silica material.

³²⁴ Monge-Marcet, A.; Pleixats, R.; Cattoën, X.; Wong Chi Man, M. *J. Molec. Catal. A Chem* **2012**, 357, 59.

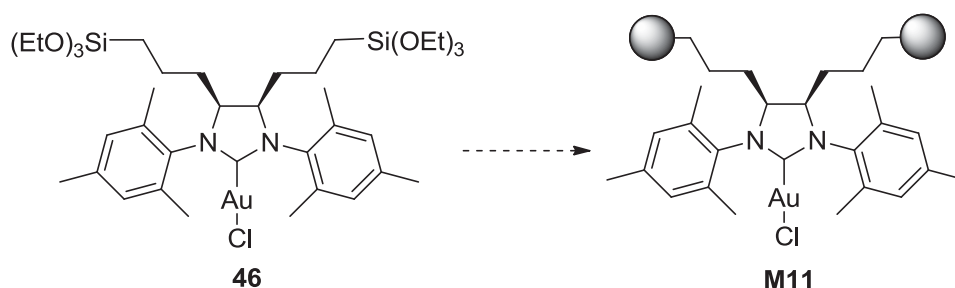
³²⁵ Monge-Marcet, A.; Pleixats, R.; Cattoën, X.; Wong Chi Man, M. *Tetrahedron* **2013**, 69, 341.

³²⁶ Monge-Marcet, A.; Pleixats, R.; Cattoën, X.; Wong Chi Man, M. *Catal.Sci. Technol.*, **2011**, 1, 1544.

2. OBJECTIVES

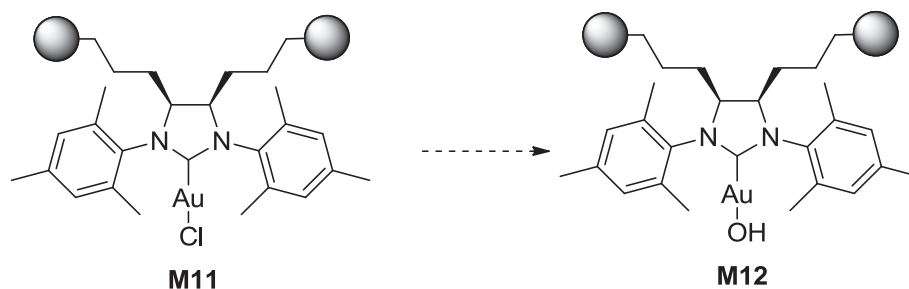
Continuing the studies of the group on recyclable catalysts based on NHC-late transition metals prepared by sol-gel methodologies for catalytic purposes, we aimed at the following:

a) The preparation of a bis-silylated [(NHC)AuCl] complex **46** and its immobilization through the NHC ligand by sol-gel co-gelification with TEOS to afford the hybrid silica material **M11**. Linking the catalyst to the matrix through NHC-ligands is particularly promising because the metal-NHC bond is very strong and the NHC less labile than other ligands; therefore leaching of the catalyst can be minimized. On the other hand, the triethoxysilyl groups were chosen to be tethered on the backbone of the 5-membered imidazolinyldene ring because this leads to geometrical features which are similar to those of the non-silylated ligand. An incorporation of the silylated groups on the *N*-aryl moieties would result in a different geometry of the heterogenized complex which would affect the catalytic activity.



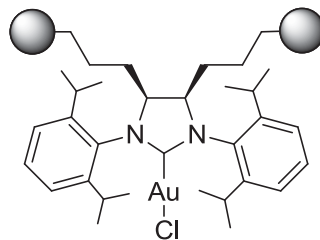
Scheme 4.13. Hybrid silica material **M11** derived from a bis-silylated NHC-Au-Cl complex

b) The exchange of the chloride ligand of **M11** for a hydroxide ligand (-OH) to afford the immobilized mononuclear NHC-Au-OH complex **M12**. The development of this material would allow us to avoid the use of silver salts and inert atmosphere in its catalytic applications, contributing to the achievement of *greener processes*.



Scheme 4.14. Anion exchange on hybrid silica **M11** to obtain **M12**.

c) The preparation of [(NHC)AuCl] immobilized catalyst **M13** through a [1,3-bis-(2,6-diisopropylphenyl)imidazolinyliidene] (SIPr) moiety instead of a SIMes as was the case for **M11**. In most of Nolan's publications, SIPr ligand seems to provide the better gold(I) catalysts .



M13

Figure 4.6. Hybrid silica material **M13**

d) The evaluation of the prepared materials **M11**, **M12** and **M13** as reusable catalysts in several NHC-Au(I) promoted reactions such as rearrangement of allylic acetates and cycloisomerization of γ -alkynoic acids.

3. RESULTS AND DISCUSSION

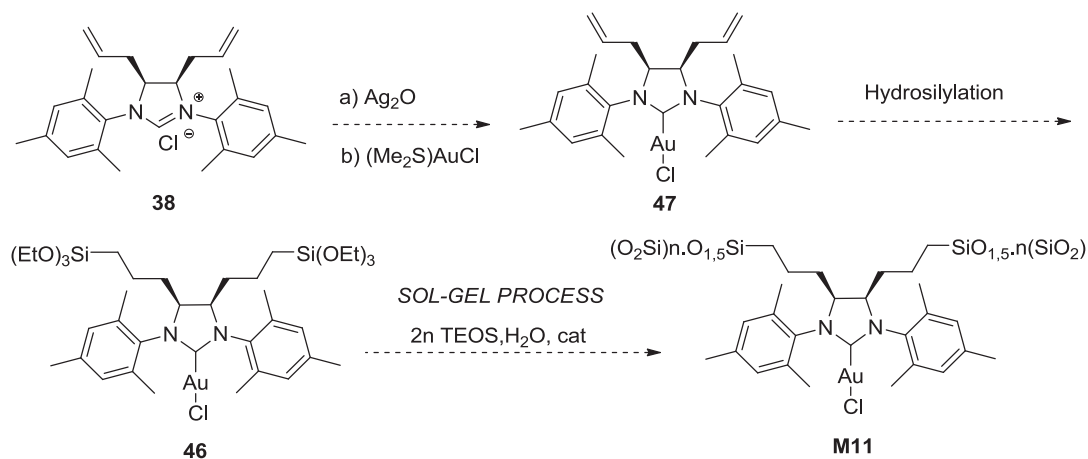
3.1 Immobilization of NHC-Au(I) complexes

Two different [(NHC)-Au(I)] complexes bearing two triethoxysilyl groups were planned to be synthesized and evaluated. In the first part of this section, the preparation of a material derived from a disilylated bis-mesityl substituted NHC-Au complex by using the already prepared compound **38** will be detailed. In the second part, the attempt of preparation of a material derived from a disilylated bis-SIPr substituted NHC-Au complex will be described.

3.1.1 Hybrid silica material M11 derived from a disilylated bis-mesityl NHC-Au complex

3.1.1.1. Preparation of the disilylated NHC-Au-Cl monomer **46**

Taking advantage of the already prepared compound **38** (see Section 3.3), we decided to synthesize the NHC-Au-Cl complex **47** via transmetallation of the corresponding [(NHC)-Ag] species with $(\text{Me}_2\text{S})\text{AuCl}$, following a methodology previously described by Nolan.³²⁷ Hydrosilylation of the two C=C bonds of complex **47** under platinum catalysis would afford the disilylated precursor **46** needed for the formation of hybrid material **M11** (Scheme 4.15).



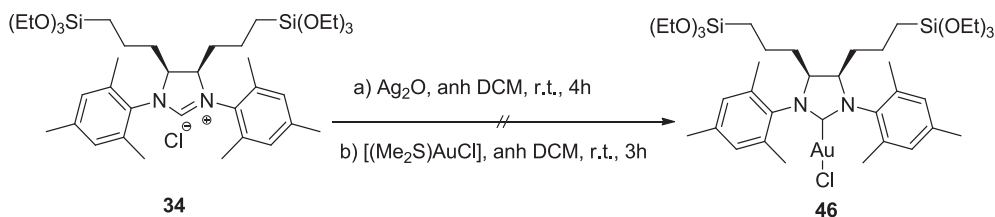
Scheme 4.15. Initial synthetic strategy for the preparation of **M11**.

The decision of introducing the alkoxy-silyl groups at the end of the synthetic route was due to the fact that the alternative preparation of this complex **46** through carbene transfer from the corresponding Ag-NHC complex derived from disilylated dihydroimidazolium salt **34** had already been investigated by Roland Wedekind³²⁸ in

³²⁷ De Frémont, P.; Scott, N. M.; Stevens, E. D.; Nolan, S. P. *Organometallics* **2005**, *24*, 2411.

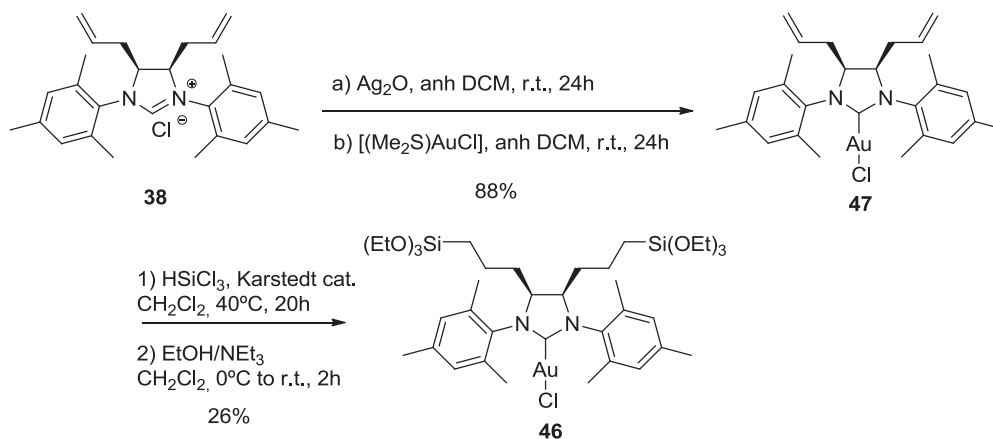
³²⁸ Wedekind, R. *Bachelor Thesis. École Nationale Supérieure de Chimie de Montpellier*, 2012.

Wong Chi Man's group, leading to decomposition and formation of pinkish solution (Scheme 4.16).



Scheme 4.16. Attempt to prepare compound **46** by Roland Wedekind.

Thus, taking into account this result, we prepared complex **47** in 88% yield from **38** as planned in Scheme 4.15. Then, hydrosilylation of compound **47** with HSiCl_3 in the presence of Karstedt catalyst, followed by treatment with EtOH/NEt_3 led to the formation of **46** in 26% yield (Scheme 4.17).

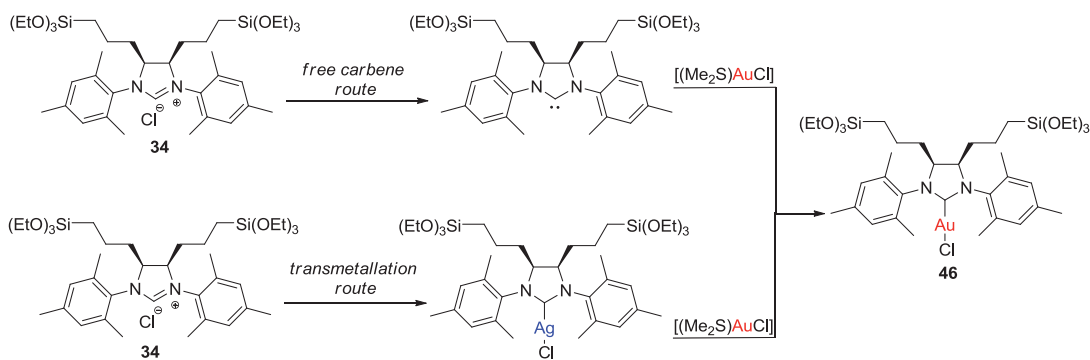


Scheme 4.17. Preparation of compounds **47** and **46**.

The poor yield of this hydrosilylation reaction might be explained by the low stability of compound **46** and to the formation of gold nanoparticles during the treatment with EtOH/NEt_3 due to the presence of a polar media.³²⁹ Noteworthy, a dark reddish precipitate was always obtained in this reaction. With the purpose of improving the yield of **46**, we decided to prepare it from its silylated precursor **34** avoiding the transmetalation reaction, *via* free carbene route (Scheme 4.18).

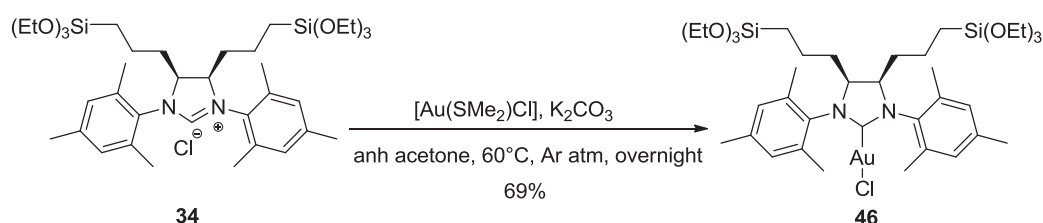
³²⁹ Alvarado, E.; Badaj, A.C.; Larocque, T.G.; Lavoie, G.G. *Chem. Eur. J.* **2012**, *18*, 12112.

Chapter 4. 3. Results and Discussion



Scheme 4.18. Synthetic routes for the preparation of $[\text{Au}(\text{NHC})\text{Cl}]$ complex **46**.

The first attempt of the straightforward synthesis of **46** was performed following a methodology recently described by Nolan.³³⁰ The free carbene of **34** was generated by using K_2CO_3 as a base and, after the addition of $[(\text{Me}_2\text{S})\text{AuCl}]$, the gold complex **46** was achieved in 69% yield (Scheme 4.19).



Scheme 4.19. Preparation of complex **46** via free carbene route.

Even though this reaction presented a higher yield at low scale (84 mg), when we scaled it up (~300 mg), we did not obtain the desired product, the solution became dark pinkish, indicating the possible formation of gold nanoparticles³¹⁷ among other decomposition products.³²⁷

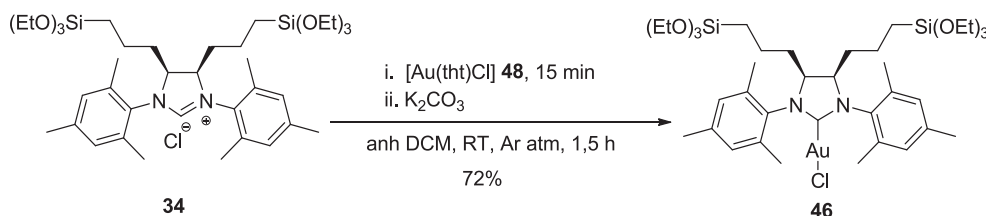
Interestingly, Koželj³³¹ and collaborators described the NHC catalyzed preparation of polyhedral silsesquioxanes (PSS) via condensation of silanol species from trihalo- and trialkoxysilanes. They used NHC-silver complexes as reagents to generate *in situ* the free carbenes.³³² For this reason, we think that some part of the undesired products obtained in the process leading to **46** might be PSS formed by the generation of free NHC in the reaction medium.

³³⁰ Collado, A.; Gómez-Suárez, A.; Martín, A.R.; Slawin, A.M.Z.; Nolan, S.P. *Chem. Commun.* **2013**, *49*, 5541..

³³¹ Koželj, M.; Orel, B. *Dalton Trans.* **2013**, *42*, 9432.

³³² Sentman, A.C.; Csihony, S.; Waymouth, R.M.; Hedrick, J.L. *J. Org. Chem.* **2005**, *70*, 2391.

In a second attempt to prepare **46** *via* free carbene route, we changed the source of gold and we used the complex [Au(tht)Cl], **48**, as it has recently been described in an efficient and facile route for the preparation of [Au(NHC)Cl] complexes.³³³ The authors proposed the stabilization of the imidazolium salt [(NHC)-H]⁺ with [AuCl₂]⁻ acting as a counter-anion, which after a subsequent deprotonation would lead to the desired [(NHC)AuCl] complex. The reaction performed in small scale (76 mg) presented a remarkable 72% yield (Scheme 4.20) but, unfortunately, after two days the isolated product got black and decomposed, indicating the presence of some impurity which had not been detected by ¹H-NMR in the freshly synthesized compound. At this point, we decided not to scale up this reaction and to give up the synthesis of the disilylated gold complex by this free carbene strategy.



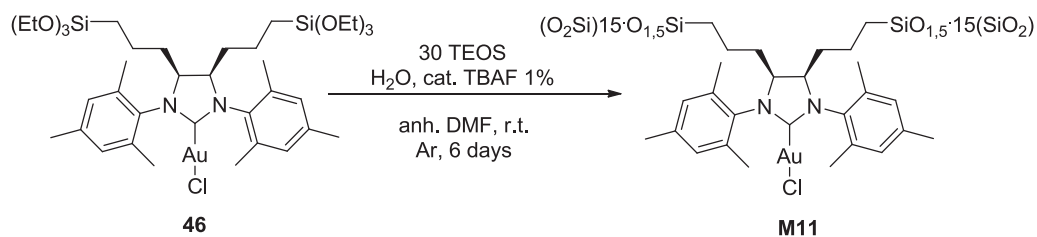
Scheme 4.20. Second attempt of preparation of complex **46** *via* free carbene route.

After the previously described results, the preparation of disilylated [(NHC)AuCl] complex **46** was best performed by the transmetalation route as indicated in Scheme 4.17 in a scale of 300 mg and once enough precursor was achieved, the corresponding hybrid silica material was prepared.

3.1.1.2 Preparation of hybrid silica material M11

The cogelification of **46** with tetraethoxysilane (TEOS, molar ratio 1:30) was performed under argon atmosphere in anhydrous and degassed DMF at room temperature, using a stoichiometric amount of water (with respect to the ethoxy groups) and tetrabutylammonium fluoride as a nucleophilic catalyst (1 mol% with respect to Si) (Scheme 4.21). The solution gellified after half an hour and was aged for six days at room temperature under argon atmosphere (Figure 4.7). Then it was filtered, washed successively with dry ethanol, acetone and diethyl ether. The resulting powder was dried overnight under vacuum to afford **M11** as a white powder (Figure 4.7).

³³³ Visbal, R.; Laguna, A.; Gimeno, M.C. *Chem. Commun.* **2013**, 49, 5642.



Scheme 4.21. Preparation of hybrid silica material **M11**.



Figure 4.7. Gel formed from **46** and TEOS (left) and final hybrid silica material **M11** (right).

This material was characterized by ^{29}Si -SSNMR, N_2 sorption measurements, TEM and SEM microscopies, EDX and elemental analysis. The ^{29}Si CP-MAS NMR (Figure 4.8) of **M11** confirmed the covalent bonding of the organic moiety to the silica matrix by the presence of T^3 signal at -66.0 ppm, in addition to the characteristic Q^3 and Q^4 signals corresponding to the condensed TEOS at -104.0 and -110.0 ppm respectively. The high dilution of the organic moiety in the organic matrix precluded the observation of the corresponding signals in the solid state ^{13}C -SSNMR and IR spectra.

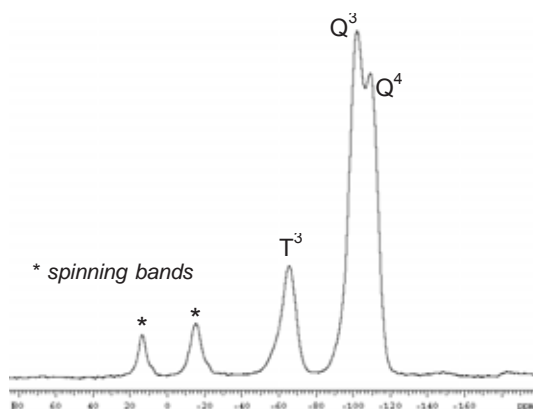


Figure 4.8. ^{29}Si -SSNMR of material **M11**.

The N_2 adsorption-desorption isotherm (Figure 4.9) of **M11** is of *Type IV*, representative of a mesoporous material with a sharp pore diameter distribution (Figure 4.9) is centered around 35 Å, with a total pore volume of 0.62 cm^3/g and a BET surface area of 818 m^2g^{-1} .

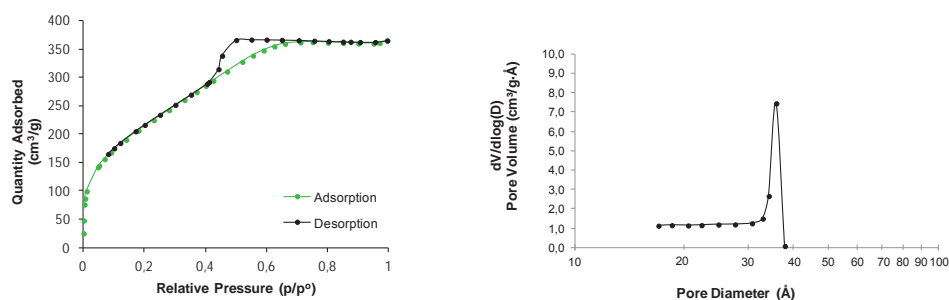


Figure 4.9. N₂-sorption isotherm (left) and pore size distribution (right) of **M11**.

The gold content was determined by inductively coupled plasma (ICP-MS) analysis (2.99% w/w, 0.15 mmol [(NHC)Au]/g material). The elemental analysis revealed a Au/Si ratio of 1/66, while theoretical value should be 1/32 (considering a complete condensation). Consequently, it is likely that incomplete condensation (as determined by the ²⁹Si solid state NMR, Figure 4.8) and partial loss of the metal had occurred during the formation of the material by the sol-gel process.

Neither SEM nor TEM images of **M11** showed a clear evidence of the presence of gold nanoparticles in the material as a result of partial decomposition of **46** during the sol-gel process (Figure 4.10).

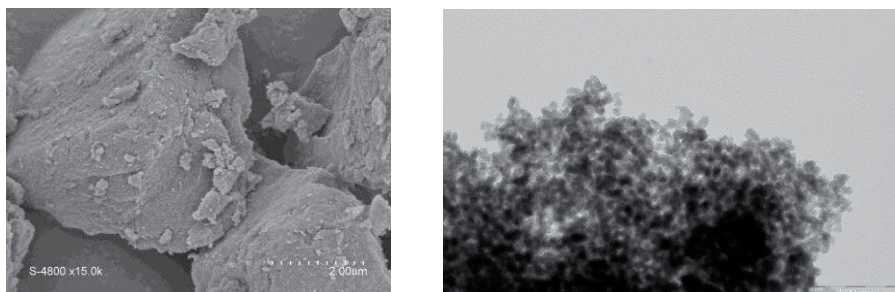
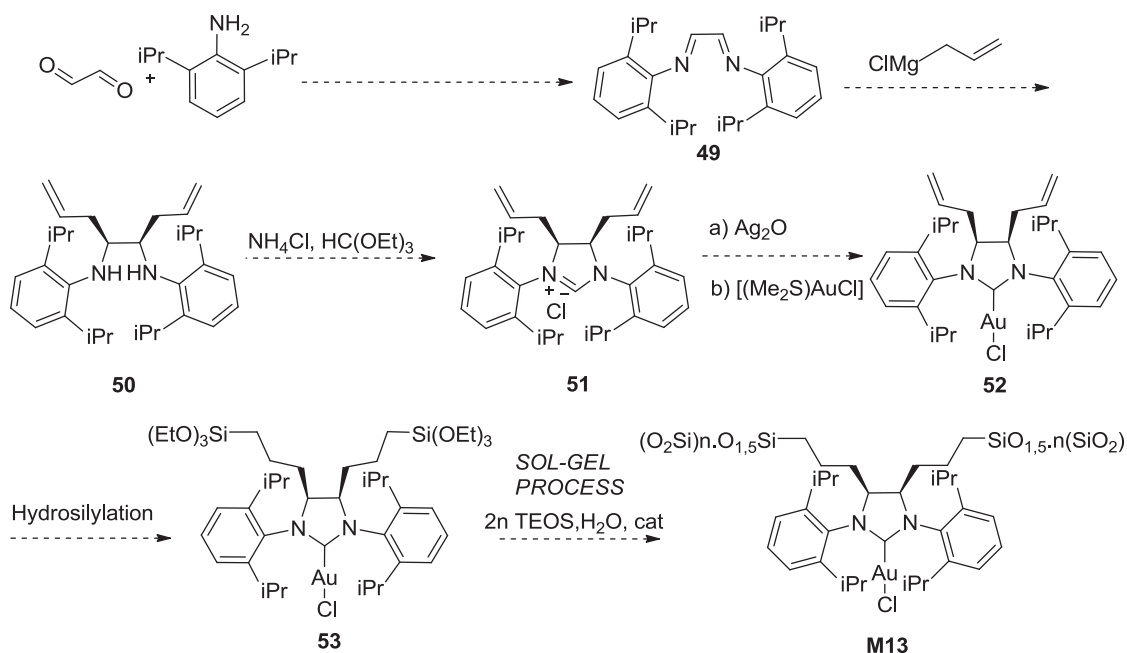


Figure 4.10. SEM (left) and TEM (right) images of **M11**.

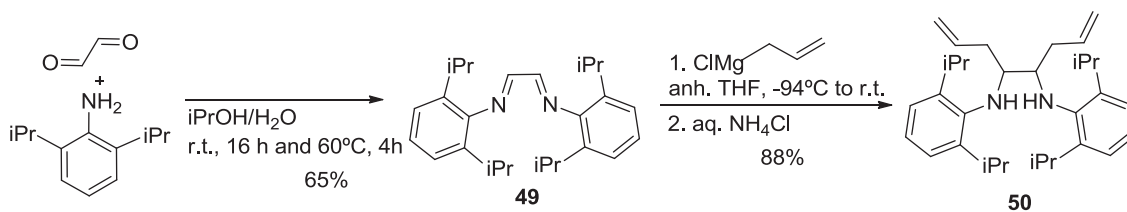
3.1.2 Studies towards the formation of hybrid silica material **M13** derived from a disilylated bis-SIPr (NHC)-Au complex

The synthetic strategy envisaged for the obtention of **M13** is analogous to the previously described for **M11** and is depicted in Scheme 4.22. The bis-imine **49** would be prepared from glyoxal and 2,6-diisopropylaniline. Then, a reaction with allylmagnesium chloride would afford the diamine **50**. Further treatment with triethyl orthoformate would enable the cyclization to the dihydroimidazolium salt **51**, from which the [(NHC)-Au(I)] complex **52** would be prepared *via* a transmetalation route. Subsequent hydrosilylation would afford the bis-silylated precursor **53**, which would be submitted to the sol-gel process to give **M13**.



3.1.2.1 Attempts for the preparation of the disilylated NHC-Au-Cl monomer **53**

For the preparation of new hybrid silica material **M13** we first needed to obtain the dihydroimidazolium salt **51**. As its analogous product described in chapter 3, the bis-imine **49** had already been described in the literature by Arduengo³³⁴ and we reproduced this procedure. Subsequent addition of two allylmagnesium chloride equivalents led to the formation of **50** as a yellow oil as a mixture of *meso* and *d,l* diastereoisomers, which crystallized after 24 h at room temperature. In principle, we supposed that the crystallized product was the *meso* diastereoisomer by analogy with the synthetic route for the analogous diamine bearing mesityl groups (Scheme 4.23).



As by NMR spectroscopy we could not elucidate which of the isomers we had obtained, we performed a chiral HPLC chromatography in order to determine if our product was a mixture of enantiomers (*d, l*) or not (Figure 4.11). We got a single peak

³³⁴ Arduengo III, A. J.; Krafczyk, R.; Schmutzler, R.; *Tetrahedron*, **1999**, *55*, 14523.

which would indicate that diamine **50** was in *meso* form. However, as the product is not described in the literature we could not confirm these results as we were not sure of having found the right conditions for the separation of the enantiomers. Then we tried to analyze the product by X-Ray powder diffraction to get the crystal structure, in collaboration with Oriol Vallcorba at ICMAB. Unfortunately, it was impossible to get the unit cell of the sample to elucidate the structure.

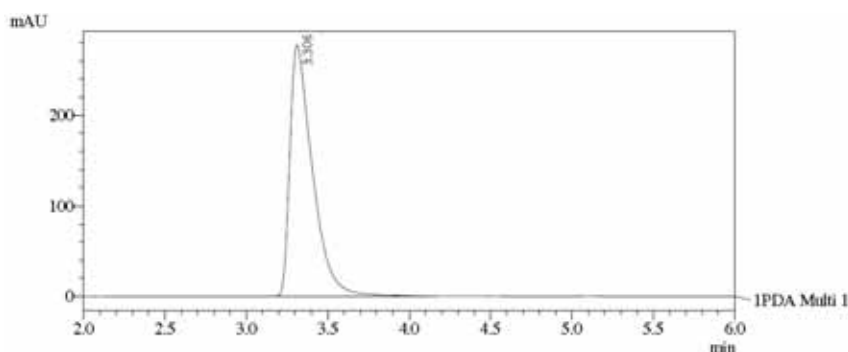
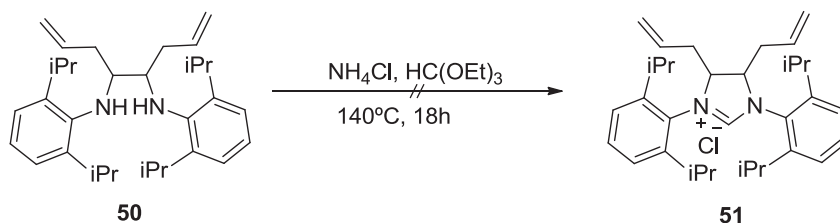


Figure 4.11. HPLC chromatogram of **50** (OD-H hexane: isopropanol 99:1 1 mL/min).

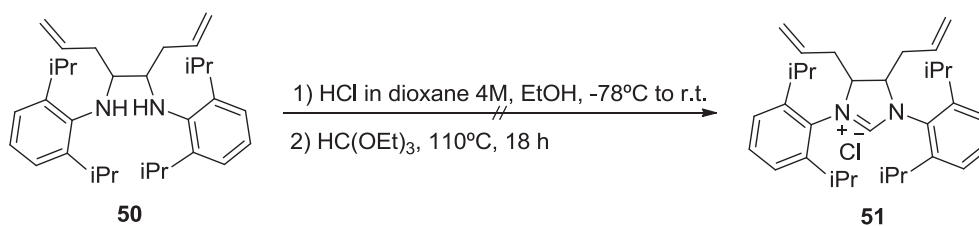
At this point, we pretended that diamine **50** underwent cyclization under standard conditions using triethylorthoformate and ammonium chloride to yield the corresponding dihydroimidazolium salt **51** (Scheme 4.24). Unfortunately, the desired compound was not achieved.



Scheme 4.24. Attempt to prepare compound **51**.

Another attempt of preparation of compound **51** was performed following a procedure described in the literature for the cyclization of similar salts.³³⁵ It consisted on a first treatment of the amine with HCl in dioxane, followed by addition of triethylorthoformate (Scheme 4.25). However, as in the previous case, the desired product was not formed.

³³⁵ Khan, R.K.M.; Zhugralin, A.R.; Torker, S.; O'Brien, R.V.; Lombardi, S.P.; Hoveyda, A.H. *J. Am. Chem. Soc.*, **2012**, *134*, 12438.



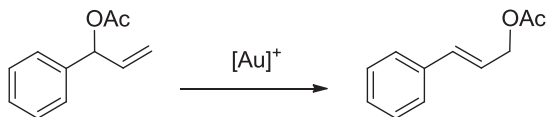
Scheme 4.25. Second attempt to prepare compound 51.

As a result of the above mentioned unsuccessful experiments, we abandoned at this point our synthetic route for the obtention of disilylated monomer **53**. At present we do not know the reason for the different behaviour of diamines **37** and **50** towards the cyclization reaction with triethylorthoformate.

3. 2 Applications of M11 as recyclable catalyst

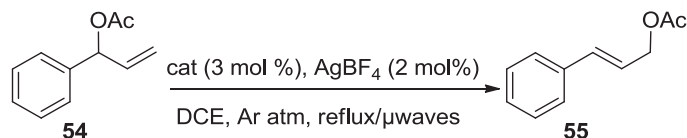
3.2.1. Rearrangement of allylic acetates

Allylic acetate moieties can undergo an 1,3-shift upon complexation of Au^+ fragment onto the alkene, resulting in the formation of an isomerized olefin (Scheme 4.26). This reaction provides an efficient and atom-economical access to derivatives of primary allylic alcohols.



Scheme 4.26. Allylic acetate rearrangement.

$[(\text{NHC})\text{AuCl}]$ complexes, in conjunction with a silver salt, efficiently catalyze the isomerization of allylic acetates under thermal or microwave-assisted conditions.³⁰⁷ For this reason, we decided to assess hybrid material **M11** as a supported catalyst of this reaction. However, first we tested an homogeneous analogue (compound **47**, see scheme 4.17) in the rearrangement of 1-phenylallyl acetate **54** to cinnamyl acetate **55** in order to optimize the reaction conditions (Table 4.2). All catalytic tests were carried out under argon atmosphere and protection from light to avoid damages to the silver salt.

Table 4.2. Catalytic performance^[a] of **47** in the allylic acetate rearrangement of compound **54**.

Exp.	Cat	Heating conditions	Conv. (%) ^[c]	Yield (%) ^[d]	Time
1	47	reflux	5	-	48 h
2	47	microwaves ^[b]	100	17 ^[e]	30 min
3	47	microwaves	100	15	12 min

^[a] Reaction conditions: a) *Reflux heating*: 1 mmol allylic acetate, 0.03 mmol of **47**, 0.02 mmol AgBF₄, 15 mL anh DCE; b) *Microwaves heating*: 1 mmol allylic acetate, 0.03 mmol of **47**, 0.02 mmol AgBF₄, 2.5 mL anh DCE.

^[b] Microwave conditions: 80°C, 200W for the indicated time.

^[c] Calculated from ¹H-NMR spectroscopy.

^[d] Isolated yield.

^[e] Side product and decomposition products were formed due to excess of time heating.

An experiment performed with 3 mol% of **47** and 2 mol% of AgBF₄ under refluxing dichloroethane (Table 4.2, Exp.1) led to very low conversion of **54**. However, experiments performed under microwave heating showed complete conversion of starting product. Excess of microwave heating time led to the formation of decomposition products (Table 4.2, Exp. 2). Then, the reaction time was reduced to 12 min, but the formation of a side product could not be avoided. In conclusion, the use of homogeneous NHC-Au-Cl complex **47** hardly produced the isomerized product and led mainly to oligomerization.

Then, hybrid silica material **M11** was tested as supported catalyst of the same reaction (Table 4.3). Heating time was optimized to 40 min and no formation of side-products was observed. Moreover, the reusability of the catalyst was evaluated. Supported catalyst **M11** could be reused up to 3 consecutive runs without loss of activity. It is worth to point out that a precipitate of AgCl resulting from activation of the catalyst remained entrapped into the material along the performed tests as a consequence of its insolubility. This fact might explain the catalyst deactivation after the third cycle.

Table 4.3. Catalytic performance of **M11**^[a] in the allylic acetate rearrangement of compound **54**.

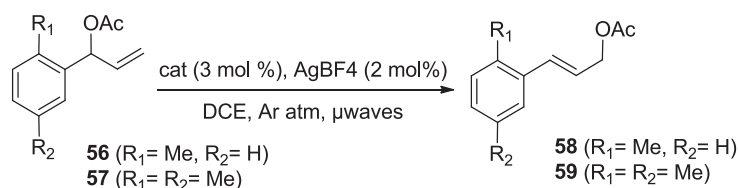
Cat	Cycle	Time (min)	Conv. (%) ^[b]	Yield (%) ^[c]
M11	1	40	100%	93
	2	40	100%	94
	3	40	100%	83

^[a] Reaction conditions: 0.25 mmol allylic acetate, 0.05 g **M11** (3 mol% Au), AgBF₄ (2 mol%), 0.6 mL anhydrous DCE, microwave conditions: 80°C, 200W for the indicated time.

^[b] Calculated from ¹H-NMR spectroscopy.

^[c] Isolated yield.

Encouraged with these results, we decided to enlarge the reaction scope with other substrates. Substitution patterns on the phenyl ring did not alter the activity of the catalyst; this was the case of 1-(*o*-tolyl)allyl acetate **56** and 1-(2,5-dimethylphenyl)allyl acetate **57** which experimented 1,3-rearrangement under similar conditions (Table 4.4).

Table 4.4. Catalytic performance of **M11**^[a] in the allylic acetate rearrangement of compounds **56** and **57**.

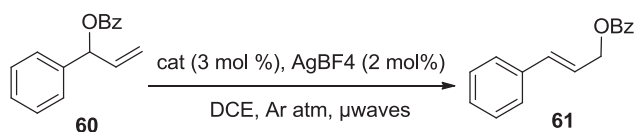
Entry	Cat	Cycle	R ₁	R ₂	Time (min)	Conv (%) ^[b]	Yield (%) ^[c]
1	M11	1	Me	H	40	100	83
2		2	Me	H	40	100	79
3		3	Me	H	40	100	71
4	M11	1	Me	Me	40	100	71
5		2	Me	Me	40	100	72
6		3	Me	Me	40	100	59

^[a] Reaction conditions: 0.25 mmol allylic acetate, 0.05 g **M11** (3 mol% Au), AgBF₄ (2 mol%), 0.6 mL anhydrous DCE, microwave conditions: 80°C, 200W for the indicated time.

^[b] Calculated from ¹H-NMR spectroscopy.

^[c] Isolated yield.

Further expanding the scope of the reaction, a benzoate group at the allylic position isomerized as well (Table 4.5). Secondary allylic benzoate **60** could be rearranged in 60 min under microwave heating conditions to the cinnamyl benzoate **61**.

Table 4.5. Catalytic performance of **M11**^[a] in the allylic benzoate rearrangement of compound **60**.

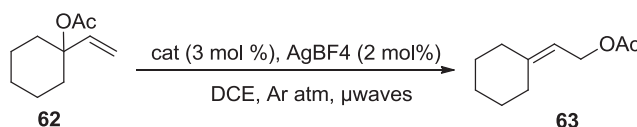
Cat	Cycle	Time (min)	Yield (%)
M11	1	75	69
	2	60	74
	3	60	74

^[a] Reaction conditions: 0.25 mmol allylic benzoate, 0.05 g **M11** (3 mol%), AgBF₄ (2 mol%), 0.6 mL anhydrous DCE, microwave conditions: 80°C, 200W for the indicated time.

^[b] Calculated from ¹H-NMR spectroscopy.

^[c] Isolated yield

However, the formation of a tri-substituted olefin **63** from the allylic acetate **62** derived from a tertiary alcohol presented moderate yields (Table 4.6).

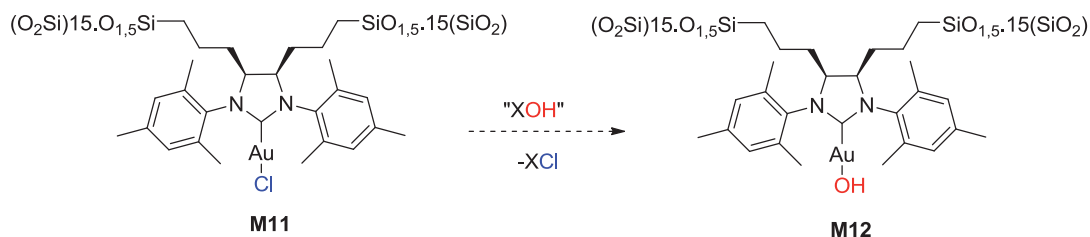
Table 4.6. Catalytic performance of **M11**^[a] in the allylic acetate rearrangement of compound **62**.

Cat	Cycle	time (min)	Yield (%)
M11	1	40	40
	2	40	57
	3	40	-

It is worth to point out that the formation of oligomerization products was not observed in any of the catalytic tests performed with **M11**. Moreover, very good yields were obtained for the products **55**, **58**, **59** and **61**. However, reusability was not achieved for more than 3 consecutive runs. This can be explained by the formation of AgCl as mentioned before; as it is a very insoluble salt, it remained mixed with the supported catalyst and could poison the [(NHC)AuCl] complex.

The use of silver salts cannot be avoided as they act as a chloride abstractor. Nevertheless they represent a drawback in our catalytic system as they remain entrapped in the materials, in addition to its economic cost. Taking benefit from the

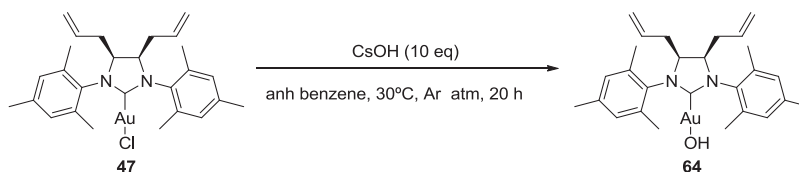
recent description of the [(NHC)Au(OH)] complexes and their catalytic activity,³³⁶ we reasoned that one solution to this problem would be to exchange the chloride ligand of **M11** for an hydroxide to afford **M12** (Scheme 4.27).



Scheme 4.27. Ligand exchange of **M11**.

To carry out this reaction, it must be taken into account that free silanols would consume the XOH used, for this reason previous capping of silanols could be suitable. Moreover, due to the high dilution of the organometallic moiety in **M11** it would be very difficult to ensure the change of the chloride to hydroxide ligand by IR spectroscopy or ¹H-SS NMR. For this reason, before performing the ligand exchange with **M11** we decided to optimize the reaction conditions using homogeneous (NHC)AuCl complex **47** as a model for this reaction.

Following the already described methodology to prepare [(NHC)AuOH] complexes,^{336c} compound **47** was treated with 10 eq of CsOH in anhydrous benzene at 30 °C for 20 h to afford **64** (Scheme 4.28).



Scheme 4.28. Preparation of compound **64**.

Neither the ¹H-NMR nor the IR spectra showed significant differences between **47** and the presumed **64** (Figure 4.12). This compound **64** should present a characteristic O-H stretching band at around 3627 cm⁻¹.^{336a} As the transformation of **47** to **64** was not clear, we did not perform the ligand exchange reaction with **M11**.

³³⁶ a) Gaillard, S.; Slawin, A.M.Z.; Nolan, S.P. *Chem. Commun.* **2010**, 46, 2742. b) Gaillard, S.; Bosson, J.; Ramón, R.S.; Nun, P.; Slawin, A.M.Z.; Nolan, S.P. *Chem. Eur. J.* **2010**, 16, 13729. c) Patrick, S.R.; Gómez-Suárez, A.; Slawin, A.M.Z.; Nolan, S.P. *Organometallics* **2014**, 33, 421.

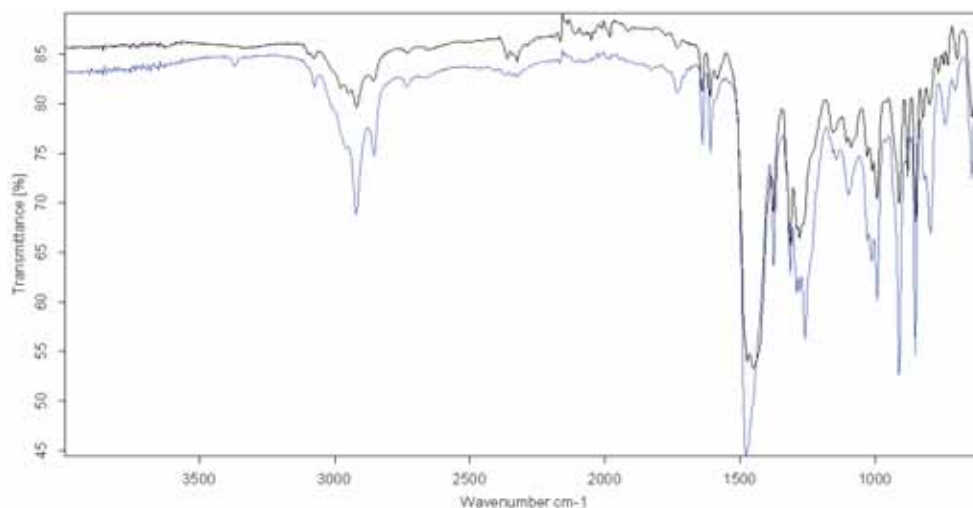
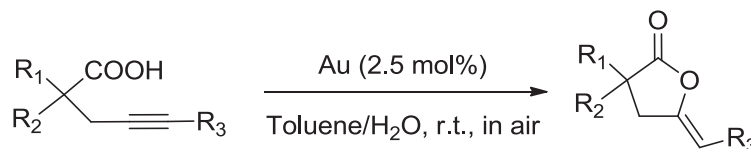


Figure 4.12. Comparison of the IR spectra of **47** (blue) and **64** (black).

3.2.2 Cycloisomerization of γ -alkynoic acids

Recently, it has been described the cycloisomerization of γ -alkynoic acids into enol-lactones, catalyzed by [(NHC)AuCl] and [(NHC)AuCl₃] complexes in a biphasic system water/toluene (Scheme 4.29).³³⁷



Scheme 4.29. Cycloisomerization of γ -alkynoic acids.

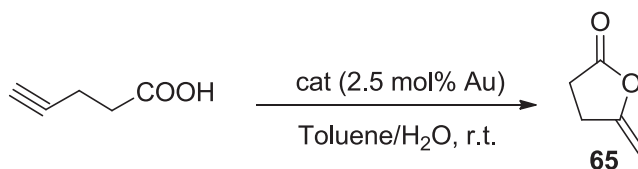
The reaction obviously presents economic and environmental advantages as it is performed in the presence of water to liberate the chloride ligand and generate the true catalyst, the species [(NHC)Au]⁺. This fact prompted us to test our supported catalyst **M11** in aqueous media in this transformation.

First, the ability of homogeneous [(NHC)AuCl] complex **47** to promote the cycloisomerization of 4-pentynoic acid was evaluated for comparative purposes (Table 4.7). Then, **M11** was tested under the same conditions. Thus, in a first set of experiments (entries 1-2), we found that the commercially available 4-pentynoic acid, in a biphasic 1:1 water/toluene mixture under magnetic stirring, led to the selective formation of the desired 5-methylene-dihydrofuran-2-one **65** only under catalysis by **47**.

³³⁷ Tomás-Mendivil, E.; Toullec, P.Y.; Borge, J.; Conejero, S.; Michelet, V.; Cadierno, V. *ACS Catalysis* **2013**, *3*, 3086.

Heterogeneous catalyst **M11** did not allow the formation of **65** and became a pinkish material.

Table 4.7. Catalytic performance^[a] of **47** and **M11** in cycloisomerization of 4-pentynoic acid.



Entry	Cat	Cycle	Time (h)	Yield (%) ^[b]	TON ^[c]	TOF (h ⁻¹) ^[d]
1	47	-	4	>99 (80)	40	10
2	M11	1 ^[e]	18	-	-	-
3	M11	1 ^[f]	48	>99 (75)	40	0.83
4	M11	2 ^[f]	48	>99 (77)	40	0.83
5	M11	3 ^[f]	48	>99 (76)	40	0.83
6	M11	4 ^[f]	48	>99 (78)	40	0.83
7	M11	5 ^[f]	48	>99 (70)	40	0.83
8	M11	6 ^[f]	48	>99 (65)	40	0.83

^[a] Reaction conditions: 0.15 mmol of γ -alkynoic acid, 0.025 g of **M11** (2.5 mol% of Au), 0.5 mL toluene, 0.5 mL water at r.t. under aerobic conditions for the indicated time.

^[b] Full conversion determined by TLC or ¹H-NMR spectroscopy. Isolated yields are given in brackets.

^[c] Turnover number (mol product/mol Au) calculated on the basis of the ¹H NMR yield

^[d] Turnover frequencies (TON/time) were calculated at the time indicated in each case using the ¹H NMR yield.

^[e] Under magnetic stirring the catalyst decomposed and no conversion was achieved.

^[f] Stirring with a wrist type shaker

The catalyst need to be in the presence of water to liberate the chloride ligand and also in contact with the substrate, soluble in the organic solvent, in order to catalyze the reaction. At the same time, a polar media might promote the formation of gold nanoparticles. Moreover, we observed that the supported catalyst **M11**, as a result of its insolubility in both solvents, remained in the interphase between the aqueous and the organic layers (Figure 4.13). These facts led us to think that the kind of stirring was an important parameter that could determine the success of the reaction. At this point, we decided to use a wrist type shaker (or rocking mixer vibromatic (Figure 4.13)) instead of magnetic stirring to obtain a good mixing of the immiscible layers and to enable the material to be in contact both with water and with the organic phase containing the substrate. Under these conditions compound **65** was obtained in 48 h with total conversion (entry 3 of Table 4.7).

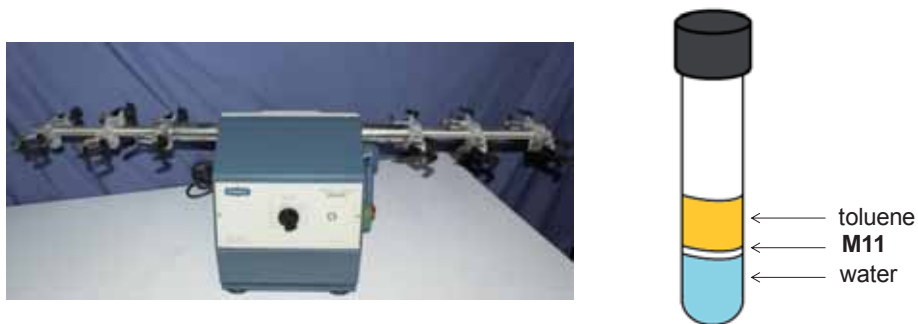


Figure 4.13. Wrist type shaker (left) and biphasic catalyst system (right).

Isolation of **65** was carried out by simple decantation of the organic phase. At that point, material **M11** presented the same white color as in the beginning of the test, which would indicate the preservation of the catalyst and the avoidance of nanoparticles formation. For this reason, we decided to study its recyclability, separating the organic phase at the end of each cycle and adding a fresh load of γ -alkynoic acid in toluene to the aqueous phase in which surface remained **M11**. Successfully, **M11** could be reused up to 5 times without any loss of activity or selectivity. After the fifth run, the material started to get a light pink color as a result of being 12 days in contact with water.

To define the scope of this catalytic transformation, other γ -alkynoic acids were subjected to the action of **M11**. First, compounds **66** and **67**, bearing two and one terminal alkyne units respectively, were tested (Table 4.8, entries 1 and 7), affording selectively the desired five-membered enol-lactones **68** and **69**. Furthermore, recycling of **M11** was successfully achieved.

Similar to the previous case, **M11** was able to be used in 6 consecutive runs without loss of activity (Table 4.8, entries 1-6). In the case of **67** the reuse was also possible but we only performed two consecutive runs (Table 4.8, entries 7-8). The TON and TOF values were similar to those obtained with 4-pentynoic acid.

In contrast, diyne **70** containing internal 2-butynyl units, was transformed to the desired five-membered enol-lactone **71**, but also experimented a competing 6-*endo-dig* cyclization to give the 6-membered enol-lactone **71'** (Table 4.9). Attempts to separate these products by column chromatography through silica gel failed as indicated in the literature.^{337,338} The molar ratios **71**:**71'** were determined by ¹H-NMR. The selectivity decreased in the second cycle.

³³⁸ Tomás-Mendivil, E.; Toullec, P.Y.; Díez, J.; Conejero, S.; Michelet, V.; Cadierno, V. *Org. Lett.* **2012**, *14*, 2520-2523.

Apart from water, the use of other green and bio-renewable solvents still remains a lasting challenge, even when the environmental and safety problems associated with conventional hazardous organic volatile solvents (VOCs) are well established. In this sense, deep eutectic solvents (DES) have been used as environmental-friendly solvents in a variety of applications including biological transformations, metal deposition, metal-oxide dissolutions, purification of bio-diesel, synthetic processes and materials chemistry.³³⁹ However, only a few examples of applications of DES as solvents of catalytic processes have been described.³⁴⁰

DESs are mostly obtained by mixing a quaternary ammonium salt with a hydrogen-bond donor that can form a complex with the halide anion of the ammonium salt. A common preparation of DESs involves the use of the low-cost and readily available ammonium salt choline chloride (ChCl), which in combination with biorenewable and environmentally benign hydrogen-bond donors (namely, glycerol (Gly), lactic acid (LA), urea or water) can form eutectic mixtures (Figure 4.14).³⁴¹

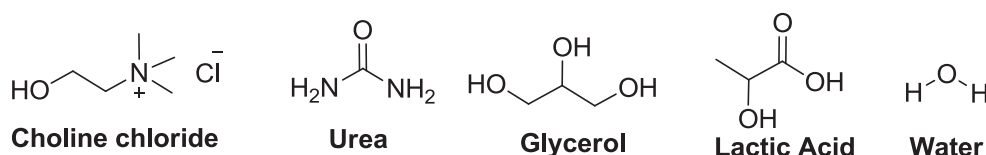


Figure 4.14. Compounds used in the synthesis of the DESs.

Thus, following our interest in green catalytic systems, we decided to test a non conventional DES solvent (1 ChCl / 2 Urea) as a reaction media in the cycloisomerization of γ -alknoic acids under catalysis by **M11**. This deep eutectic mixture was kindly provided by Joaquín García-Alvarez, from the University of Oviedo.

We first tested **M11** with alkynoic acids **66** and **67** (Table 4.10). Complete conversions were achieved in both cases despite an increase of the reaction time with respect to the toluene/water system (144 h *versus* 48 h). It is worth to mention that in this case we used magnetic stirring and no decomposition of the catalyst was observed due to the absence of water.

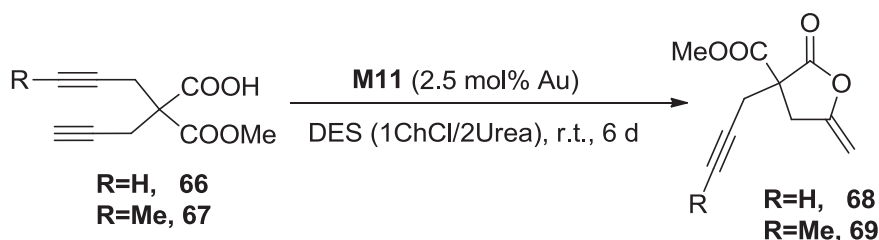
³³⁹ (a) Zhang, Q.; Vigier, K. O.; Royer, S.; Jérôme, P. *Chem. Soc. Rev.* **2012**, *41*, 7108. (b) Carriazo, D.; Serrano, M. C.; Gutiérrez, M.C.; Ferrer, M.L.; Del Monte, P. *Chem. Soc. Rev.* **2012**, *41*, 4996. (c) Abbott, A.P.; Harris, R. C.; Ryder, K.S.; D'Agostino, C.; Gladden, L.P.; Mantle, M.D. *Green Chem.* **2011**, *13*, 82. (d) Ruß, C.; König, B. *Green Chem.* **2012**, *14*, 2969.

³⁴⁰ (a) Imperato, G.; Höger, S.; Lenoir, D.; König, B. *Green Chem.* **2006**, *8*, 1051. (b) Imperato, G.; Vasold, R.; König, B. *Adv. Synth. Cat.* **2006**, *348*, 2243. (c) Ilgen, F.; König, B. *Green Chem.* **2009**, *11*, 848. (d) Vidal, C.; Suárez, F.J.; García-Álvarez, J. *Catal. Commun.* **2014**, *44*, 76.

³⁴¹ Vidal, C.; García-Álvarez, J.; Hernán-Gómez, A.; Kennedy, A. R.; Hevia, E. *Angew. Chem. Int. Ed.* **2014**, *53*, 5969.

The long reaction times discouraged us to perform more than 2 consecutive runs, but remarkably any pinkish coloration was observed along any of the cycles, indicating the good preservation of the catalyst under these conditions.

Table 4.10. Catalytic performance^[a] of **M11** in the cycloisomerization of **66** and **67**.



Entry	Substrate	Product	Cycle	Conv (%) ^[b]	TON ^[c]	TOF (h ⁻¹) ^[d]
1	66	68	1	>99	40	0.28
2	66	68	2	>99	40	0.28
3	67	69	1	>99	40	0.28
4	67	69	2	>99	40	0.28

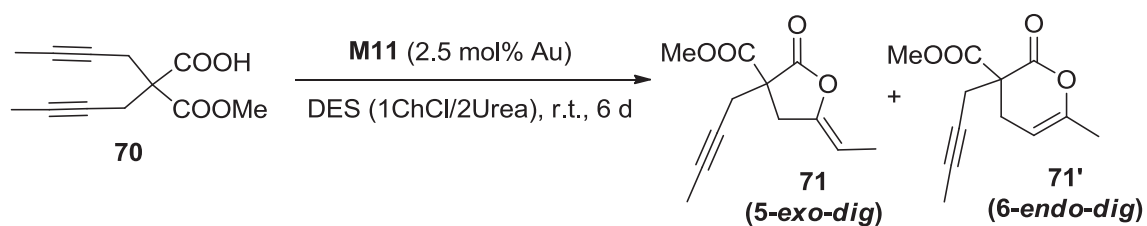
^[a] Reaction conditions: 0.15 mmol of γ -alkynoic acid, 0.025 g of **M11** (2.5 mol%), 0.150 g DES at r.t. under aerobic conditions for 144 h.

^[b] Conversion determined by ¹H-NMR spectroscopy.

^[c] Turnover number (mol product/mol Au)

^[d] Turnover frequencies (TON/time)

Alkynoic acid **70** was also tested to assess the selectivity towards the formation of the five-membered enol-lactone **71** or the 6-membered ring **71'** (Table 4.11). In this case, the selectivity in the first cycle was the same attained with the toluene/water system, showing again a preference for the formation of the 5-membered ring **71**. Interestingly, the selectivity remained unchanged in both cycles.

Table 4.11. Catalytic performance^[a] of **M11** in the cycloisomerization of **70**.

Entry	Cycle	Conv (%) ^[b]	77:77' ^[c]	TON ^[d]	TOF (h ⁻¹) ^[e]
1	1	>99	4:1	40	0.28
2	2	>99	4:1	40	0.28

^[a] Reaction conditions: 0.15 mmol γ -alkynoic acid, 0.025 g **M11** (2.5 mol%), 0.150 g DES at r.t. under aerobic conditions for the indicated time.

^[b] Conversion determined by ¹H-NMR spectroscopy.

^[c] Determined by ¹H-NMR spectroscopy

^[d] Turnover number (mol product/mol Au)

^[e] Turnover frequencies (TON/time).

4. CONCLUSIONS

The preparation of bis-silylated (NHC)AuCl complex **46** has been achieved from the dihydroimidazolium salt **38** by a synthetic route involving formation of (NHC)Ag species, transmetalation to (NHC)AuCl and subsequent hydrosilylation of the two olefinic moieties. Reversal of the order of steps was found to be unsatisfactory. Thus, when the formation of the gold(I) complex was attempted on the silylated dihydroimidazolium salt **34**, either *via* a free carbene route or *via* a transmetalation route, extended decomposition was observed, with formation of gold nanoparticles.

A *class II* hybrid silica material **M11** has been prepared by sol-gel co-gelification of bis-silylated monomer **46** with TEOS under fluoride catalysis. To the best of our knowledge, this material represents the first example of [(NHC)AuCl] supported catalyst prepared by sol-gel process. Material **M11** has shown to be stable towards air and moisture and has been characterized by ²⁹Si-SSNMR, N₂ sorption measurements, TEM microscopy and elemental analysis. It was found to be mesoporous.

Material **M11** has been successfully tested as recyclable catalyst in two different reactions. First, it has proved to be an efficient catalyst, in conjunction with a silver salt, for the rearrangement of allylic esters. Interestingly, **M11** exhibited much better performance than its homogeneous analogue **47**. Thus, polymerization side-product formed under homogeneous conditions was avoided by the use of the silica-supported catalyst. The catalyst was reused up to three runs. Remarkably, catalyst **M11** enabled the formation of a tri-substituted olefin.

Moreover, material **M11** has presented high efficiency in the cycloisomerization of γ -alkynoic acids to 5-membered enol-lactones in a toluene/water biphasic medium at room temperature, avoiding the use of silver salts. The employment of an appropriate stirring method (wrist type shaker) was found to be a key factor for the success of the reaction and the preservation of the catalyst along the process. Catalyst **M11** has demonstrated to be a recyclable catalyst as it has been reused up to 6 cycles. Additionally it presents high chemoselectivity under the mentioned conditions, as ketones derived from alkyne hydration were not formed. Furthermore, a deep eutectic solvent (DES) (1 ChCl/2 urea) has also been successfully tested as green reaction medium for this process. However, in this case the reaction times required for complete conversion increased substantially.

5. EXPERIMENTAL SECTION

5.1. General remarks

Nuclear Magnetic Resonance (NMR). Spectra were recorded at the *Servei de Ressonància Magnètica Nuclear* of the *Universitat Autònoma de Barcelona*. ^1H -NMR, ^{13}C -NMR, ^1H - ^1H COSY, ^1H - ^{13}C HSQC, ^1H - ^{13}C HMBC and SELTOCSY spectra were recorded using Bruker instruments (DRX-250, DPX-360 and AVANCE-III 400). Chemical shifts (δ) are given in ppm using the residual non-deuterated solvent as internal reference. The ^{29}Si CP-MAS spectra were recorded at the *Université de Montpellier II* with a Varian VNMRs 400 MHz instrument.

Infra-red spectroscopy (IR). Spectra were recorded with a Bruker Tensor 27 spectrometer using a Golden Gate ATR module with a diamond window. When necessary, IR spectra were recorded using KBr pellets using a Thermo Nicolet IR2000 spectrometer.

Mass-spectrometry (MS). Low- and high-resolution mass spectra were obtained by direct injection of the sample with electrospray techniques in a Hewlett-Packard 5989A and *microTOF-Q* instruments respectively. These analyses have been performed by the *Servei d'Anàlisi Química (SAQ)* of the *Universitat Autònoma de Barcelona*.

Elemental Analysis (EA) of C, N, H and Si were performed by the *Serveis Científico-Tècnics* of the *Universitat de Barcelona (SCT-UB)*. The percentages of C, N and H were determined by combustion using a EA-1108 C.E. elemental analyser of Thermo Scientific using BBOT as internal standard. The content of Si was determined by Inductively Coupled Plasma (ICP) in a multichannel Perkin-Elmer Optima 3200 L instrument.

Thin-Layer Chromatography (TLC) was performed using 0.25 mm plates (Alugram Sil G/UV₂₅₄).

Flash Chromatography was performed under compressed air pressure on a *Macherey-Nagel GmbH & Co KG* silica gel which had a particle size of 230 – 400 mesh and pore volume of 0.9 mL/g.

Surface areas were determined by the Brunauer-Emmet-Teller (BET) method from N_2 adsorption-desorption isotherms obtained with a *Micromeritics ASAP2020* analyzer after degassing samples for 30 h at 55 °C under vacuum. The total pore volumes were evaluated by converting the volume adsorbed at p/p^0 0.98 to the volume of liquid

adsorbed (single point adsorption total pore volume of pores less than 4000 Å at $p/p^\circ \approx 0.98$). The pore size distributions for the materials were determined from the desorption branch using the Barrett-Joyner-Halenda (BJH) method³⁴² which relies on the Kelvin equation to relate the width of the pores to the condensation pressure.

Electron Microscopy. Transmission Electron Microscopy (TEM) images were obtained with an instrument *JEOL 1200 EX II* equipped with a SIS Olympus Quemesa 11 Mpixel camera at the *Université de Montpellier II*. Scanning Electron Microscopy (SEM) images were obtained at the *Institut Européen des Membranes* in Montpellier with a Hitachi S4800 apparatus after platinum metallization.

Microwave assisted reactions were performed using a *CEM Discover®* Microwave instrument, which operates between 0 and 300 W. The reactions were conducted in a 10 mL sealed reactor. Temperature was measured with an infrared sensor placed under the reactor. During the experiments compressed nitrogen was used to cool the reactor when necessary. We thank Dr. Ramon Alibés for allowing its use.

Other:

When required, experiments were carried out with standard high vacuum and Schlenk techniques under N₂ or Ar atmosphere using dry solvents, which were degassed by the freeze-and-thaw method and cannula or syringe-transferred.

Commercial reagents were directly used as received except for trichlorosilane, which was purified first by distillation under vacuum; gaseous HCl was eliminated in a second step by performing 2 freeze-thaw cycles (this compound was always used with a secondary cold trap). Na₂SO₄ and MgSO₄ used to adsorb water of organic layers were anhydrous.

Dry solvents were obtained from two instruments: *PureSolv* (Innovative Technologies: THF, CH₂Cl₂ and pentane) and in some experiments from *MBraun SPS-800* (MBraun: pentane, CHCl₃, CH₂Cl₂, THF, Et₂O, and toluene).

Other dry solvents were prepared using standard methods: ClCH₂CH₂Cl, NEt₃ and DMF were distilled over CaH₂. Toluene, benzene and Et₂O were refluxed over Na/benzophenone whereas ethanol and methanol were distilled on Mg/I₂. Acetone was distilled over K₂CO₃. When needed, deuterated NMR solvents such as CDCl₃ and

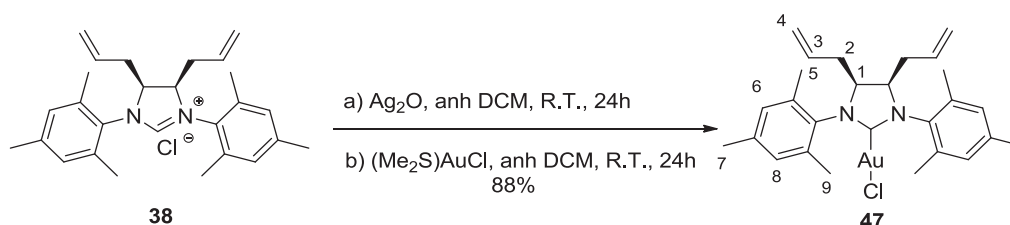
³⁴² Barrett, E. P.; Joyner, L. G.; Halenda, P. P. *J. Am. Chem. Soc.*, **1951**, 73, 373.

CD_2Cl_2 were dried by distillation over CaH_2 . For the preparation of hybrid silica materials, distilled and deionized water was used (*MilliQ H₂O*).

In this work some of the compounds prepared were already described in the literature. Therefore, only the physical and/or spectroscopic data necessary for their identification are presented. It has to be mentioned that the chemical shifts of the NCHN protons in imidazolium salts strongly depend on the concentration, thus their values might not match previously reported data.

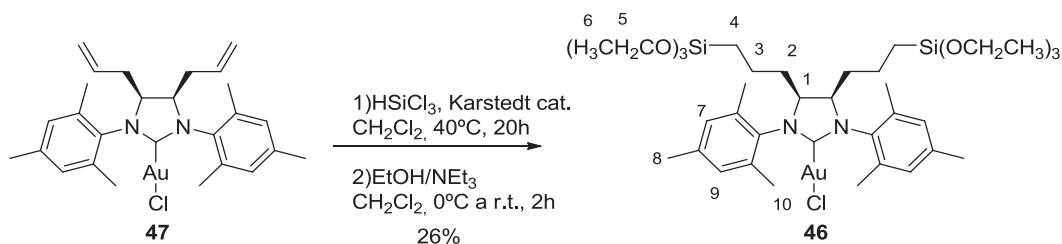
5.2 Immobilization of (NHC)AuCl complexes

5.2.1 Synthesis of ((4*R*,5*S*)-4,5-diallyl-1,3-dimesitylimidazolidin-2-yl)gold(I) chloride, **47**



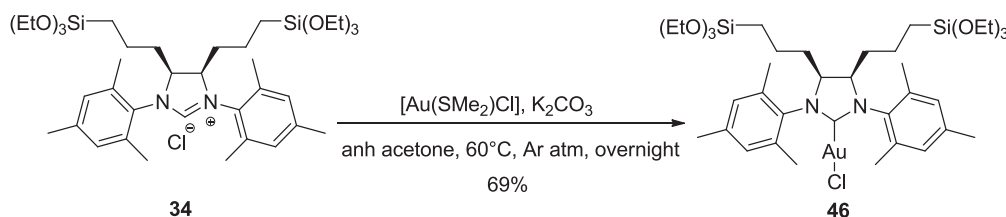
In a 250 mL Schlenk tube protected from light with an aluminium foil, a mixture of silver(I) oxide (0.318 g, 1.37 mmol) and (4*R*, 5*S*)-4,5-diallyl-1,3-dimesityl-4,5-dihydroimidazolium chloride **38** (0.983 g, 2.32 mmol) in dry CH_2Cl_2 (200 mL) was stirred overnight at room temperature under argon. After this time, the mixture was filtered *via* a canula to another light protected Schlenk tube, and (dimethylsulfide)gold(I) chloride (0.669 g, 2.27 mmol) was added. The resulting mixture was stirred for 24 h at room temperature under argon. Activated carbon was added and the mixture was filtered through Celite. The filtrates were concentrated under vacuum. The residue was purified by flash chromatography using dichloromethane as eluent to afford **47** as a white solid (1.235 g, Yield: 87.9%). **CF**: $\text{C}_{27}\text{H}_{34}\text{AuClN}_2$. **MW**: 618.99 g/mol. **¹H RMN (CDCl₃, 400 MHz) δ (ppm)**: 6.92 (s, 2H, H₆), 6.91 (s, 2H, H₈), 5.47 (m, 2H, H₃), 4.97 (m, 4H, H₄), 4.42 (m, 2H, H₁), 2.62-2.57 (m, 2H, H_{2a}), 2.39 (s, 6H, H₇), 2.36-2.32 (m, 2H, H_{2b}), 2.28 (s, 6H, H_{5/9}), 2.27 (s, 6H, H_{5/9}). **¹³C RMN (CDCl₃, 100.6 MHz)**: 195.20, 139.05, 136.82, 135.50, 133.77, 130.28, 130.25, 118.05, 85.02, 31.56, 20.67, 19.06, 17.94. **IR (ATR) ν (cm⁻¹)**: 2918, 1639, 1610, 1376, 1316, 1260, 1091, 994, 913, 852, 799, 642. **HRMS (ESI)**: calculated for [¹²C₂₇H₃₄Au³⁵ClN₂+Na]⁺: 641.1968; found: 641.1974.

5.2.2 Preparation of ((4*R*,5*S*)-1,3-dimesityl-4,5-bis(3-(triethoxysilyl)propyl)imidazolidin-2-yl)gold(I) chloride, **46**, from gold complex **47**



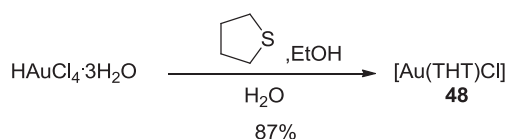
In a 100 mL sealable Schlenk tube protected from light with an aluminium foil, compound **47** (0.961 g, 1.55 mmol) was dissolved in dry CH_2Cl_2 (20 mL) under argon. To this solution freshly distilled HSiCl_3 (3.2 mL, 1.34 g/cm³, 31.6 mmol) and Karstedt's catalyst (1.0 mL, 2% Pt, 0.08 mmol Pt) were added. The reaction mixture was stirred under argon at 40°C for 3 h. After this time, excess HSiCl_3 was distilled off and collected in a secondary cold trap. The residue was redissolved in dry CH_2Cl_2 (20 mL) and the mixture was cooled to 0°C with an ice bath. Then, anhydrous EtOH/NEt_3 (1/1, 12 mL) was added slowly and the mixture stirred at room temperature for 2 h. Then the volatiles were removed under vacuum, the residue was treated with dry toluene and filtered to separate the ammonium salt. The filtrates were concentrated under vacuum and the resulting brown solid was digested with dry pentane (3 x 20 mL) and filtered *via* a canula each time to another Schlenk tube. Filtrates were concentrated under vacuum to afford a white solid **46** (0.386 g, Yield: 26%). The product was stored under Argon and protected from light at room temperature. **CF**: $\text{C}_{39}\text{H}_{66}\text{AuClN}_2\text{O}_6\text{Si}_2$. **MW**: 947.54 g/mol. **¹H RMN (CDCl₃, 400 MHz) δ (ppm)**: 6.92 (s, 2H, H₇), 6.90 (s, 2H, H₉), 4.25 (br, 2H, H₁), 3.71 (q, 12H, J = 6.9 Hz, H₅), 2.39 (s, 6H, H₈), 2.28 (s, 12H, H₁₀), 1.79 (m, 2H, H_{2a}), 1.63 (m, 2H, H_{2b}), 1.27 (m, 4H, H₃), 1.17 (t, 18H, J = 6.9 Hz, H₆), 0.51 (m, 4H, H₄). **¹³C RMN (CDCl₃, 100.6 MHz)**: 194.77, 138.71, 136.89, 135.43, 134.88, 130.25, 130.19, 65.25, 58.20, 31.65, 30.72, 29.41, 26.77, 20.67, 20.45, 18.95, 17.97, 17.88, 10.35. **IR (ATR) ν (cm⁻¹)**: 2963, 2923, 1482, 1389, 1259, 1166, 1075, 1022, 954, 793. **HRMS (ESI)**: calculated for [¹²C₃₉H₆₆Au³⁵CIN₂O₆Si₂+Na]⁺: 969.3706; found: 969.3706.

5.2.3 First preparation of ((4*R*,5*S*)-1,3-dimesityl-4,5-bis(3-(triethoxysilyl)propyl)imidazolidin-2-yl)gold(I) chloride, **46**, from silylated dihydroimidazolium salt **34**.



In a 10 mL Schlenk tube protected from light with an aluminium foil, a mixture of **34** (0.0964 g, 0.128 mmol), (dimethylsulfide)gold(I) chloride (0.0403 g, 0.137 mmol) and potassium carbonate (0.0191 g, 0.138 mmol) in dry acetone (2 mL) was stirred overnight at 60°C under argon. The suspension turned from white to violet. After this time, the mixture was filtered over Celite to another light protected Schlenk tube. Celite path was washed several times with dry dichloromethane and the resulting combined filtrates were concentrated under vacuum and afforded **46** as a white solid (0.084 g, Yield: 69%).

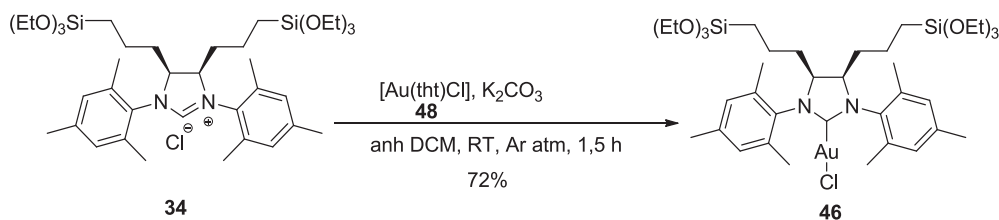
5.2.4 Synthesis of [Au(tht)Cl], **48**.³⁴³



In a 50 mL round bottom flask H[AuCl₄·3H₂O] (1.085 g, 2.75 mmol) was dissolved in a mixture of 10 mL of water and EtOH (2.5 mL). Then tetrahydrothiophene (0.66 mL, 1 g/cm³, 7.49 mmol) was added dropwise and the yellow solution became colourless and a precipitate appeared, which was filtered off and dried under vacuum. The complex[(tht)AuCl] **48** was obtained as a colourless powder (0.764 g, Yield: 87%). The product was stored under Argon and protected from light in the freezer. **CF**: C₄H₈AuClS. **MW**: 320.59 g/mol. **m.p**: 128-130°C (decomposition). (m.p. lit³⁴³: 130°C (decomposition)). ¹HRMN (CDCl₃, 250 MHz) δ (ppm): 3.81-3.05 (br, 4H, SCH₂CH₂), 2.51-1.81 (br, 4H, SCH₂CH₂).

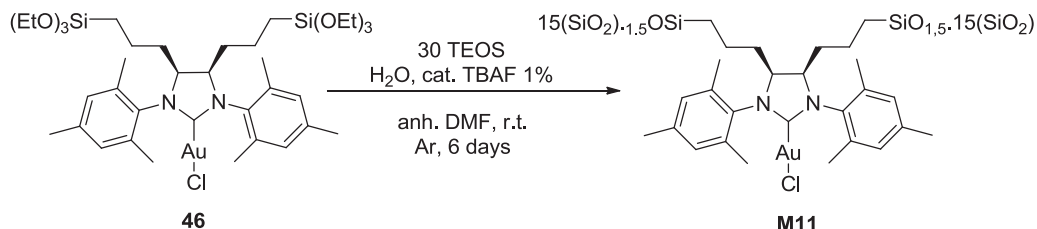
³⁴³ Hashmi, A.S.K.; Braun, I.; Rudolph, M.; Rominger, F. *Organometallics*, **2012**, *31*, 644.

5.2.5 Second preparation of ((4*R*,5*S*)-1,3-dimesityl-4,5-bis(3-(triethoxysilyl)propyl)imidazolidin-2-yl)gold(I) chloride, **46**, from silylated dihydroimidazolium salt **34**



In a 10 mL Schlenk tube protected from light with an aluminium foil, a mixture of **34** (0.0832 g, 0.111 mmol) and [(tht)AuCl] **48** (0.0367 g, 0.115 mmol) was stirred in dry CH₂Cl₂ for 15 minutes at room temperature under Ar. After this time, potassium carbonate (0.206 g, 1.495 mmol) was added and the suspension was stirred in the same conditions for 1.5 h. The suspension turned from white to red. The mixture was filtered over Celite to another light protected Schlenk tube. Celite path was washed several times with dry dichloromethane and the resulting combined filtrates were concentrated under vacuum and afforded **46** as a white solid (0.076 g, Yield: 72%). The obtained product turned from white to black color in 2 days.

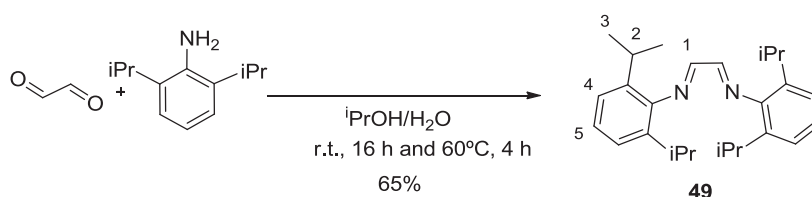
5.2.6 Preparation of hybrid silica material M11



Under argon, a solution of complex **46** (0.772 g, 0.815 mmol) and TEOS (5.5 mL, 0.94 g/cm³, 24.8 mmol) in dry and degassed DMF (20 mL) was prepared in a 250 mL schlenk round bottom flask. Under stirring, a solution of TBAF (0.26 mL, commercial solution 1M in anh THF, 0.26 mmol, 1 mol% F respect to Si) and MilliQ water (1.9 mL, 105 mmol, H₂O/EtO = 1) in dry DMF (5 mL) was added to the first solution. The mixture was stirred at room temperature for 15 min, then the stirring was stopped. A gel formed within 20 min and was left to age at room temperature under argon atmosphere and protected from light for 6 days. At this time, the gel was pulverized, filtered, washed *via canula* with dry and degassed EtOH (3 x 15 mL), dry and degassed acetone (3 x 15 mL) and dry and degassed diethyl ether (3 x 15 mL). Then the solid was washed with dry and degassed CHCl₃ with a Soxhlet apparatus for 48 h in order to remove the residual DMF entrapped in the material. After drying overnight at 40°C under vacuum

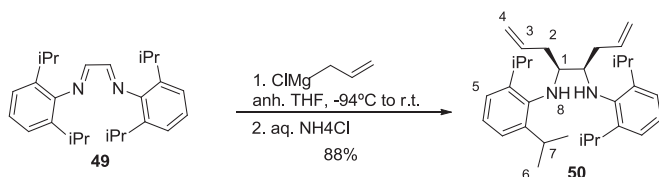
M11 was obtained (1.419 g) as a white solid. ²⁹Si-CP-MAS NMR (79.5 MHz) δ : -66.0 (T³), -104.0 (Q³), -110.0 (Q⁴). IR (ATR) (cm⁻¹): 2977, 1468, 1053, 801. BET S_{BET}: 818 m²/g; pore diameter distribution centered around 35 Å; average pore diameter (4V/A, BET): 29 Å; pore volume: 0.62 cm³/g. EA calculated for C₂₇H₃₆N₂ClAuSi₃₂O₆₃ (considering complete condensation): 12.85% C, 1.44% H, 1.11%N, 7.80% Au, 35.47% Si; found: 17.72% C, 2.91 % H, 1.06 %N, 2.99% Au, 28.0% Si (0.15 mmol [(NHC)Au]/g material).

5.2.7 Preparation of glyoxal bis[(2,6-diisopropylphenyl)imine], **49**.



2,6-Diisopropylaniline 97% (10.0 mL, 0.94 g/cm³, 53.0 mmol) was dissolved in 2-propanol (20 mL) and then a solution of glyoxal (4.0 mL, 40 wt% solution, 1.27 g/cm³, 35.0 mmol) in 2-propanol (10 mL) and water (5 mL) was added. The mixture was stirred at room temperature for 16 h and then at 60°C for 4 h. After this time, water (5 mL) was added and the resulting solid was filtered and recrystallized from ethanol to afford **49** as a yellow solid (6.52 g, 17.3 mmol). Yield: 65%. CF: C₂₆H₃₆N₂. MW: 376.6 g/mol, m.p: 70-72°C (lit³³⁴ m.p: 71-73°C). ¹H-NMR (CDCl₃, 400 MHz): 8.10 (s, 2H, H₁), 7.21-7.13 (m, 6H, H₄+H₅), 2.94 (sept, 4H, J= 6.9 Hz, H₂), 1.21 (d, J= 6.9 Hz, 24H, H₃). ¹³CRMN (CDCl₃, 100.6 MHz): 163.61, 148.44, 137.06, 125.40, 123.45, 27.73, 23.04.

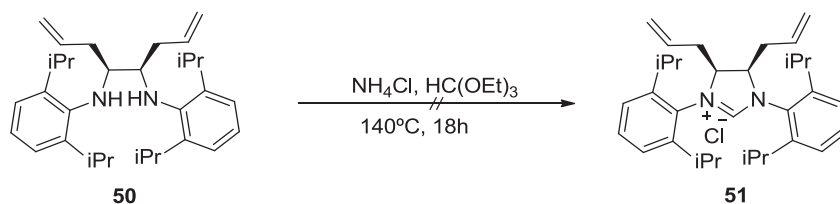
5.2.8 Preparation of (4R, 5S)-N,N'-dimesitylocta-1,7-diene-4,5-diamine, **50**.



Compound **49** (4.26 g, 11.3 mmol) was dissolved in dry THF (30 mL) and the solution was cooled to -94°C with a hexane/liquid N₂ bath. Under vigorous stirring allylmagnesium chloride (54.0 mL, commercial 2M solution in anh. THF, 108 mmol) was slowly added and the mixture stirred overnight, allowing to reach the room temperature. After this time, the reaction mixture was cooled to 0°C with an ice bath and then NH₄Cl aqueous solution (3.44 g in 60 mL water) was carefully added. The organic phase containing a diastereomeric mixture was separated and the aqueous layer further extracted with Et₂O (3 x 25 mL). The combined organic layers were dried

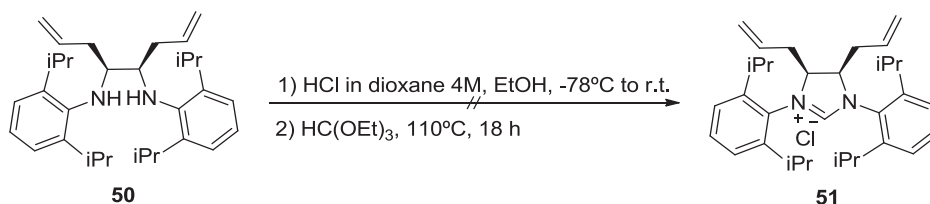
over Na_2SO_4 and concentrated under reduced pressure. A yellow oil was obtained which crystallized after one night at room temperature affording a pale yellow solid of the *meso* diastereoisomer **50** (4.54 g, 9.85 mmol). Yield: 88%. **CF**: $\text{C}_{32}\text{H}_{48}\text{N}_2$. **MW**: 460.7 g/mol. **$^1\text{H-NMR}$ (CDCl_3 , 400 MHz)**: 7.11 (m, 4H, $\text{H}_{\text{aromatic}}$), 7.03 (m, 2H, $\text{H}_{\text{aromatic}}$), 5.73 (ddt, 2H, $J = 17.2$ Hz, $J = 9.6$ Hz, $J = 7.3$ Hz, H_3), 5.07 (d, 2H, $J = 17.2$ Hz, H_{4a}), 5.02 (d, 2H, $J = 9.6$ Hz, H_{4b}), 3.77 (br, 2H, H_8), 3.57 (t, 2H, $J = 6$ Hz, H_1), 3.36 (sept, 4H, $J = 6.8$ Hz, H_7), 2.31 (ap t, $J = 6.8$ Hz, 4H, H_2), 1.25 (d, $J = 6.8$ Hz, 12H, H_6), 1.22 (d, 12H, $J = 6.8$ Hz, H_6). **$^{13}\text{CRMN}$ (CDCl_3 , 100.6 MHz)**: 142.02, 141.66, 136.59, 123.82, 122.82, 116.90, 61.79, 35.33, 27.46, 23.94, 23.49.

5.2.9 First attempt to prepare (4*S*,5*R*)-4,5-diallyl-1,3-bis(2,6-diisopropylphenyl)-4,5-dihydro-1*H*-imidazol-3-ium chloride, **51**.



A mixture of compound **50** (1.02 g, 2.21 mmol), NH_4Cl (0.145 g, 2.71 mmol) and triethylorthoformate 98% (1.8 mL, 0.891 g/cm³, 9.84 mmol) were stirred at 140°C for 24 h. A TLC of the crude mixture did not show any evidence of the formation of a new compound. After this time, the reaction mixture was cooled down to room temperature. The residue was dissolved in the minimum amount of CH_2Cl_2 and the excess of ammonium salt precipitated upon the addition of few drops of THF. The solid was separated by filtration and the filtrates were concentrated under vacuum. $^1\text{HNMR}$ of the residue did not present any signal of formation of **51**, but the presence of the starting materials.

5.2.10 Second attempt to prepare (4*S*,5*R*)-4,5-diallyl-1,3-bis(2,6-diisopropylphenyl)-4,5-dihydro-1*H*-imidazol-3-ium chloride, **51**.



In a 30 mL Schlenk tube under nitrogen atmosphere compound **50** (0.556 g, 1.20 mmol) was dissolved in anhyd EtOH (20 mL). The mixture was allowed to cool to -78°C, after which it was added dropwise a solution of HCl in dioxane (4 M, 5 mL, 20.0 mmol).

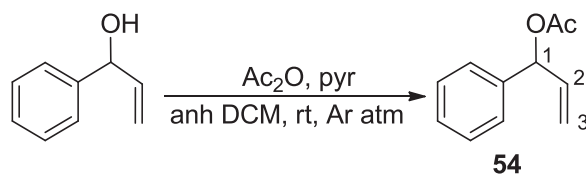
The mixture was allowed to stir 30 min at -78°C and then allowed to warm to room temperature by stirring overnight. The volatiles were removed in vacuo to give a white powder, which was further washed with Et_2O (3 mL) and pentane (3 mL). The resulting solid was dried under high vacuum for 48 hours. After this time, it was transferred to a round bottom flask equipped with a condenser containing triethylorthoformate (2.00 mL, 0.891 g/cm^3 , 12.1 mmol) and stirred at 110°C overnight. Then it was allowed to cool to 22°C , and the remaining triethylorthoformate was removed under vacuum giving a brownish solid. $^1\text{H-NMR}$ of this solid did not present any signal of formation of **51**, but the presence of the starting materials.

5.3 Catalytic tests with homogeneous [(NHC)Au] complexes and with silica-supported [(NHC)AuCl], M11

5.3.1 Rearrangement of allylic esters

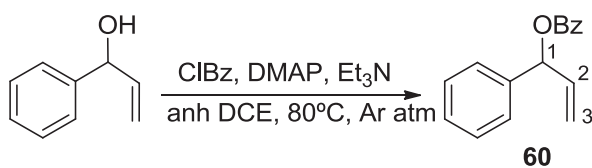
5.3.1.1 Preparation of the substrates

Preparation of 1-phenylallyl acetate, **54**.³⁴⁴

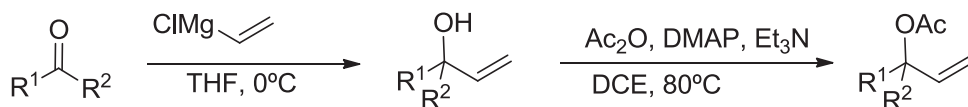


To a solution of commercial α -vinylbenzyl alcohol (1.463 g, 10.9 mmols) in anhydrous DCM (8 mL), Ac_2O (1.5 mL, 1.08 g/cm^3 , 11.0 mmols) and pyridine (1.3 mL, 0.978 g/cm^3 , 16.1 mmols) were added and the mixture was stirred under argon atmosphere at room temperature until TLC showed no evidence of the starting product. Additional DCM was added and the organic layer was washed with saturated NaHCO_3 aqueous solution (3 x 10 mL), HCl 1.0 M (3 x 10 mL) and H_2O (3 x 10 mL). The organic layers were dried over anhydrous sodium sulphate and evaporated, giving a colorless liquid **54**³⁰⁷ (1.083 g, Yield: 56%). **CF:** $\text{C}_{11}\text{H}_{12}\text{O}_2$. **MW:** 176.21 g/mol. **$^1\text{H-NMR}$ (CDCl_3 , 400 MHz):** 7.37-7.29 (m, 5H, H_{ar}), 6.27 (d, $J = 6.2\text{ Hz}$, 1H, H_1), 6.00 (ddd, $J = 16.9\text{ Hz}$, $J = 11.0\text{ Hz}$, $J = 6.2\text{ Hz}$, 1H, H_2), 5.32-5.24 (m, 2H, H_3), 2.12 (s, 3H, OCOCH_3). **$^{13}\text{C-NMR}$ (CDCl_3 , 100.6 MHz):** 170.52, 139.26, 136.63, 128.85, 128.46, 127.43, 117.13, 76.16, 20.90.

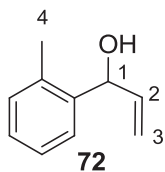
³⁴⁴ Villarroya, M. *PhD Dissertation*, Universitat Autònoma de Barcelona 1995.

Preparation of 1-phenylallyl benzoate, **60**.³⁰⁷

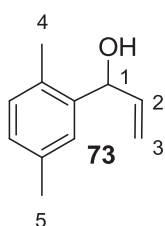
α -Vinylbenzyl alcohol (1.35 g, 10.0 mmol), DCE (60 mL), DMAP (0.72 g, 6.0 mmol), Et₃N (11.2 mL, g/cm³, 80 mmol) and benzoyl chloride (6.8 mL, 1.2 g/cm³, 60 mmol) were added successively to a round bottom flask equipped with a condenser. The reaction mixture was heated overnight at 80°C. The reaction was then quenched with a saturated NH₄Cl aqueous solution (40 mL) and extracted with diethyl ether (3 x 30 mL). The organic layers were washed with brine (3x 30 mL) and dried over anhydrous sodium sulphate, filtered and evaporated to give the crude product that was purified by flash chromatography (pentane/Et₂O 95/5) yielding a colorless liquid **60**³⁰⁷ (0.63 g, Yield: 42%). **CF**: C₁₆H₁₄O₂. **MW**: 238.28 g/mol. **¹H-NMR (CDCl₃, 400 MHz)**: 8.12-8.10 (m, 2H, H_{ar}), 7.47-7.43 (m, 1H, H_{ar}), 7.42-7.30 (m, 7H, H_{ar}), 6.52 (d, J = 5.8 Hz, 1H, H₁), 6.13 (ddd, J = 16.5, 10.6, 5.8 Hz, 1H, H₂), 5.43-5.29 (m, 2H, H₃). **¹³CRMN (CDCl₃, 100.6 MHz)**: 166.03, 139.32, 136.66, 133.39, 130.60, 130.03, 128.91, 128.69, 128.50, 127.42, 117.29, 76.65.

General procedure for the preparation of substrates **56**, **57** and **62**.³⁰⁷

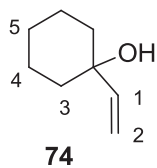
Alkenylation (GP 1). In a flame dried round-bottom flask under nitrogen atmosphere, a solution of the aldehyde/ketone (30 mmol) in anhydrous THF (40 mL) was stirred for 10 minutes at 0°C. To the reaction mixture, vinylmagnesium chloride (22.5 mL, commercial 1.6M solution in anhydrous THF, 36 mmol) was added dropwise and the reaction was then allowed to warm up to r.t. and stirred for further 2 hours. Then the reaction was quenched with a saturated NH₄Cl aqueous solution (50 mL) and extracted with diethyl ether (3 x 30 mL). The organic layers were washed with brine (3x 30 mL) and dried over anhydrous sodium sulfate, filtered and evaporated to give the crude allylic alcohol that was engaged in the next step without further purification.



1-(o-Tolyl)prop-2-en-1-ol, 72.³⁰⁷ Yellow oil (4.34 g, Yield: 98%). **CF:** C₁₀H₁₂O. **MW:** 148.20 g/mol. **¹H-NMR (CDCl₃, 400 MHz):** 7.46 (d, J= 9.2 Hz, 1H, H_{ar}), 7.26-7.16 (m, 3H, H_{ar}), 6.04 (ddd, J= 16.7, 10.8, 6.2 Hz, 1H, H₂), 5.42 (d, J= 5.4 Hz, 1H, H₁), 5.32 (d, J= 7.0 Hz, 1H, H_{3a}), 5.21 (d, J= 9.9 Hz, 1H, H_{3b}), 2.37 (s, 3H, H₄), 2.21 (br, 1H, OH). **¹³CRMN (CDCl₃, 100.6 MHz):** 140.77, 139.69, 135.60, 130.73, 127.81, 126.50, 126.09, 115.32, 71.85, 18.66.

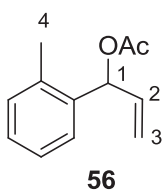


1-(2,5-Dimethylphenyl)prop-2-en-1-ol, 73.³⁰⁷ Yellow oil (4.78 g, Yield: 99%). **CF:** C₁₁H₁₄O. **MW:** 162.23 g/mol. **¹H-NMR (CDCl₃, 400 MHz):** 7.31 (s, 1H, H_{ar}), 7.09 (d, J= 7.9 Hz, 1H, H_{ar}), 7.05 (d, J= 7.9 Hz, 1H, H_{ar}), 6.05 (ddd, J= 16.3, 10.7, 6.5 Hz, H₂), 5.37 (d, J= 4.8 Hz, 1 H, H₁), 5.34 (d, J= 17.2 Hz, 1H, H_{3a}), 5.23 (d, J= 10.4 Hz, 1H, H_{3b}), 2.62 (br, 1H, OH), 2.38 (s, 3H, H₄), 2.34 (s, 3H, H₅). **¹³CRMN (CDCl₃, 100.6MHz):** 140.51, 139.76, 135.83, 132.27, 130.55, 128.34, 126.69, 114.95, 71.67, 20.57, 18.09.



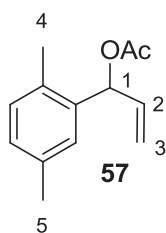
1-Vinylcyclohexanol, 74.³⁰⁷ Brown oil (3.13 g, Yield: 86%). **CF:** C₈H₁₄O. **MW:** 126.20 g/mol. **¹H-NMR (CDCl₃, 400 MHz):** 5.93 (dd, J= 17.5, 10.8 Hz, 1H, H₁), 5.20 (d, J= 17.6 Hz, 1H, H_{2a}), 4.99 (d, J= 10.8 Hz, 1H, H_{2b}), 2.65 (br, 1H, OH), 1.72-1.56 (m, 2H, H₃), 1.56-1.46 (m, 8H, H₄+H₃+H₅). **¹³CRMN (CDCl₃, 100.6 MHz):** 146.26, 111.65, 71.71, 37.17, 25.10, 21.56.

Acylation (GP 2). The allylic alcohol (30 mmol), DCE (90 mL), DMAP (9 mmol, 0.3 equiv), Et₃N (120 mmol, 4 equiv) and Ac₂O (60 mmol, 2 equiv) were successively added to a round bottom flask equipped with a condenser. The reaction mixture was heated overnight at 80°C. The reaction was then quenched with a saturated NH₄Cl aqueous solution (50 mL) and extracted with diethyl ether (3 x 30 mL). The organic layers were washed with brine (3x 30 mL) and dried over anhydrous sodium sulphate, filtered and evaporated to give the crude product that was purified by flash chromatography.

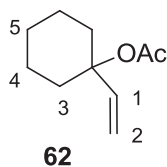


1-(o-Tolyl)allyl acetate, 56.³⁰⁷ The **GP 2** procedure yielded, after a flash chromatography on silica gel (gradient pentane/Et₂O 95/5 to 90/10), 3.16 g, Yield: 57%). **CF:** C₁₂H₁₄O₂. **MW:** 190.24 g/mol. **¹H-NMR (CDCl₃, 400 MHz):** 7.38-7.36 (m, 1H, H_{ar}), 7.22-7.16 (m, 3H, H_{ar}), 6.45 (d, J=5.0 Hz, 1H, H₁), 6.00 (ddd, J= 16.5, 11.5, 6.5 Hz, 1H, H₂), 5.25-5.18 (m, 2H, H₃), 2.38 (s,

3H, H₄), 2.11 (s, 3H, OAc). ¹³CRMN (CDCl₃, 100.6 MHz): 170.51, 137.36, 136.08, 136.05, 130.84, 128.32, 127.15, 126.48, 117.15, 73.35, 20.84, 18.84.



1-(2,5-Dimethylphenyl)allyl acetate, 57.³⁰⁷ The **GP 2** procedure yielded, after a flash chromatography on silica gel (pentane/Et₂O 80/20), 4.48 g, Yield: 74%). **CF:** C₁₃H₁₆O₂. **MW:** 204.26 g/mol. **¹H-NMR (CDCl₃, 400 MHz):** 7.17 (s, 1H, H_{ar}), 7.06-7.01 (m, 2H, H_{ar}), 6.42 (d, J= 5.4Hz, 1H, H₁), 5.99 (ddd, J= 16.8, 11.1, 6.0 Hz, 1H, H₂), 5.24-5.19 (m, 2H, H₃), 2.32 (s, 6H, H₄+H₅), 2.12 (s, 3H, OAc). ¹³CRMN (CDCl₃, 100.6 MHz): 170.52, 137.05, 136.13, 135.99, 132.93, 130.79, 129.08, 127.84, 116.92, 73.42, 20.87, 20.69, 18.38.



1-Vinylcyclohexyl acetate, 62.³⁰⁷ The **GP 2** procedure yielded, after a flash chromatography on silica gel (gradient pentane/Et₂O 95/5 to 80/20), 2.113 g, Yield: 50%). **CF:** C₁₀H₁₆O₂. **MW:** 168.23 g/mol. **¹H-NMR (CDCl₃, 400 MHz):** 6.11 (dd, J= 17.0, 10.7 Hz, 1 H, H₁), 5.16 (d, J= 16.6 Hz, 1H, H_{2a}), 5.12 (d, J= 10.3 Hz, 1H, H_{2b}), 2.20-2.13 (m, 2H, H₃), 2.02 (s, 3H, OAc), 1.62-1.50 (m, 6H, H₃+H₄), 1.34-1.22 (m, 2H, H₅). ¹³CRMN (CDCl₃, 100.6 MHz): 170.49, 142.35, 113.75, 81.81, 34.62, 25.03, 21.78, 21.53.

5.3.1.2 General procedures for catalytic tests

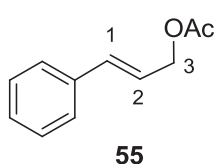
General procedure for the catalytic tests with homogeneous gold(I) complex 47.

Under light protection and inert atmosphere, to a dry DCE solution (1.7 mL) of **47** (0.019 g, 0.03 mmol, 3 mol%) in a microwave-designed vial, AgBF₄ (3.9 mg, 0.02 mmol, 2 mol%) was added. The solution instantly became cloudy and the reaction mixture was stirred for 1 min before a dry DCE solution (0.6 mL) of the corresponding allylic ester (1 mmol, 1 equiv) was added. The vial was then placed in a microwave reactor and heated at 80°C for the time indicated in tables. The resulting mixture was dissolved in pentane, filtered through celite and evaporated. The crude product was purified by flash chromatography on silica gel when necessary.

General procedure for the catalytic tests with the silica-supported gold(I) complex, M11.

Under light protection and inert atmosphere, to a dry DCE solution (1.7 mL) of **M11** (0.019 g, 0.03 mmol, 3 mol%) in a microwave-designed vial, AgBF₄ (3.9 mg, 0.02 mmol, 2 mol%) was added. The solution instantly became cloudy and the reaction was stirred for 1 min before a dry DCE solution (0.6 mL) of the corresponding allylic ester (1

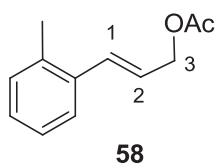
mmol, 1 equiv) was added. The vial was then placed in a microwave reactor and heated at 80°C for the time indicated in tables. Then the crude mixture was diluted with CH₂Cl₂ (2 mL) and filtered. The insoluble catalytic material was washed several times with CH₂Cl₂ (3 x 3 mL) and the combined filtrates were concentrated under vacuum yielding the desired product. The catalytic material was dried under vacuum and directly used in the next cycle.



55

Cinnamyl acetate, 55.³⁰⁷ **CF:** C₁₁H₁₂O₂. **MW:** 176.21 g/mol. **¹H-NMR (CDCl₃, 400 MHz):** 7.40-7.39 (m, 2H, H_{Ar}), 7.35-7.31 (m, 3H, H_{Ar}), 6.65 (d, 1H, J= 15.7 Hz, H₁), 6.29 (dt, 1H, J= 15.7 Hz, J= 6.5 Hz, H₂), 4.73 (d, 2H, J= 6.5 Hz, H₃), 2.10 (s, 3H, OAc).

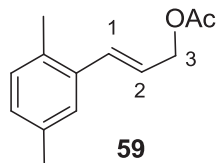
¹³CRMN (CDCl₃, 100.6 MHz): 171.41, 136.55, 134.56, 128.91, 128.38, 126.90, 123.44, 64.99, 20.66.



58

(E)-3-(o-tolyl)allyl acetate, 58.³⁰⁷ **CF:** C₁₂H₁₄O₂. **MW:** 190.24 g/mol. **¹H-NMR (CDCl₃, 400 MHz):** 7.44-7.42 (m, 1H, H_{Ar}), 7.18-7.11 (m, 3H, H_{Ar}), 6.86 (d, J= 15.8 Hz, 1H, H₁), 6.16 (dt, J= 15.8, 6.4 Hz, 1H, H₂), 4.73 (dd, J= 6.4, 1.2 Hz, 2H, H₃), 2.34 (s, 3H, Me), 2.09 (s, 3H, OAc).

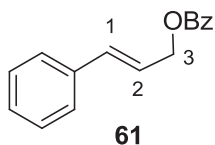
¹³CRMN (CDCl₃, 100.6 MHz): 171.46, 135.95, 135.60, 132.41, 130.59, 128.21, 126.37, 126.05, 124.68, 65.23, 20.62, 19.32.



59

(E)-3-(2,5-dimethylphenyl)allyl acetate, 59.³⁰⁷ **CF:** C₁₃H₁₆O₂. **MW:** 204.26 g/mol. **¹H-NMR (CDCl₃, 400 MHz):** 7.26 (s, 1H, H_{Ar}), 7.02 (d, J= 7.8 Hz, 1H, H_{Ar}), 6.97 (dd, J= 7.8, 1.5 Hz, 1H, H_{Ar}), 6.84 (d, J= 15.8 Hz, 1H, H₁), 6.16 (dt, J= 15.8, 6.6 Hz, 1H, H₂), 4.73 (dd, J=

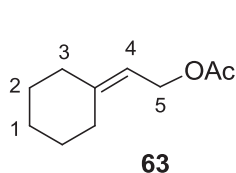
6.5, 1.4 Hz, 2H, H₃), 2.29 (s, 6H, Me), 2.09 (s, 3H, OAc). **¹³CRMN (CDCl₃, 100.6 MHz):** 171.44, 135.78, 135.33, 132.89, 132.56, 130.52, 129.00, 126.68, 124.37, 65.30, 20.63, 20.58, 18.83.



61

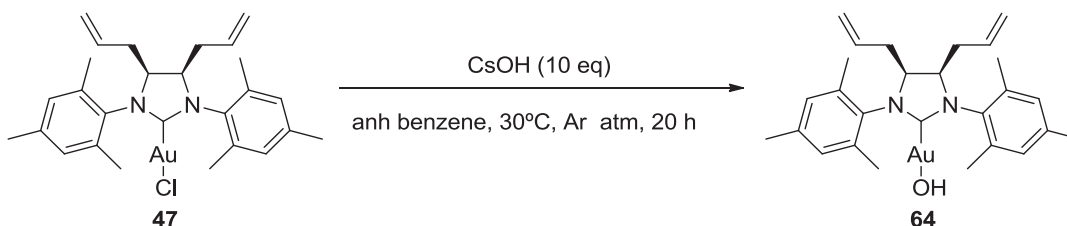
Cinnamyl benzoate, 61.³⁰⁷ **CF:** C₁₆H₁₄O₂. **MW:** 238.28 g/mol. **¹H-NMR (CDCl₃, 400 MHz):** 8.07 (d, 2H, J= 8.1 Hz, H_{Ar}), 7.58-7.51 (m, 1H, H_{Ar}), 7.46-7.39 (m, 4H, H_{Ar}), 7.35-7.21 (m, 3H, H_{Ar}, masked by CDCl₃ signal), 6.73 (d, 1H, J= 15.8 Hz, H₁), 6.39 (dt, J=

15.8 Hz, J=6.4 Hz, H₂), 4.97 (d, 2H, J= 6.4 Hz, H₃). **¹³CRMN (CDCl₃, 100.6 MHz):** 166.91, 136.54, 134.58, 133.30, 129.94, 128.89, 128.65, 128.36, 126.91, 123.49, 65.43.



2-(Cyclohexylidene)ethyl acetate, 63.³⁰⁷ **CF:** C₁₀H₁₆O₂. **MW:** 168.23 g/mol. **¹H-NMR (CDCl₃, 400 MHz):** 5.29 (td, J= 7.3, 1.2 Hz, 1H, H₄), 4.58 (d, J= 7.2 Hz, 2H, H₅), 2.19 (m, 2H, H₃), 2.12 (m, 2H, H₃), 2.05 (s, 3H, OAc), 1.56 (m, 6H, H₂+H₁).

5.3.2 Attempted preparation of ((4*R*,5*S*)-4,5-diallyl-1,3-dimesitylimidazolidin-2-yl)(hydroxy)gold(I), 64, for silver-free catalytic tests

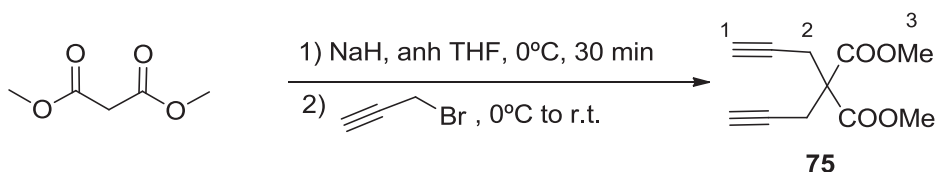


In a 100 mL Schlenk tube under argon atmosphere, cesium hydroxide (0.263 g, 2.00 mmol, 10 equiv.) was added to a stirred solution of **47** (0.115 g, 0.19 mmol) in dry benzene (16 mL, 0.01 mol L⁻¹). The reaction mixture was stirred at 30°C for 20 h and then filtered through Celite. The eluted fraction was concentrated, dry diethyl ether was added and a precipitation of a solid occurred, which was collected by filtration. The solvent was removed from filtrates. Both the precipitate and the residue from filtrates were dried under vacuum and analyzed by IR and ¹H-NMR (CD₂Cl₂ previously filtered through a plug of basic alumina to avoid the presence of any traces of HCl in the NMR solvent). Any of the spectra showed clear evidences of the formation of the desired compound **64**.

5.3.3 Cycloisomerization of γ -alkynoic acids

5.3.3.1 Preparation of the substrates

Preparation of dimethyl 2,2-di(prop-2-yn-1-yl)malonate, **75**³⁴⁵

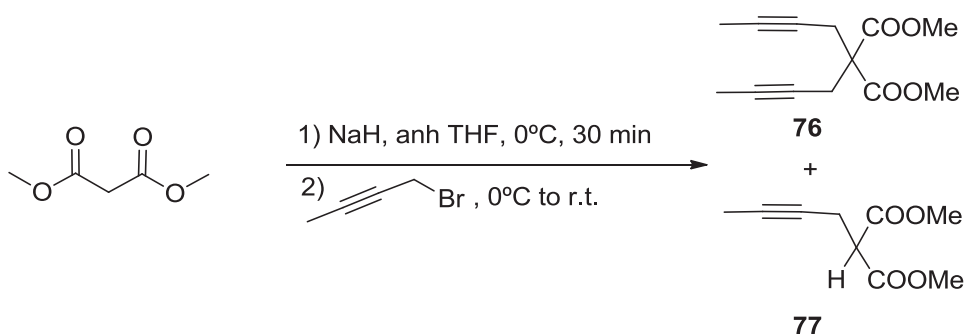


To a solution of NaH (3.00 g, 60% dispersion in mineral oil, 75 mmol) in dry THF (90 mL), dimethyl malonate (3.4 mL, 1.154 g/cm³, 30.0 mmol) was added at 0°C under Ar atmosphere. The mixture was stirred for 30 minutes allowing the temperature to warm

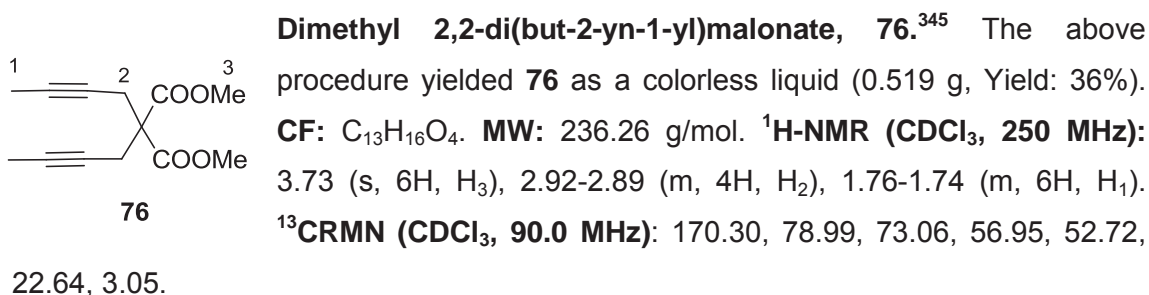
³⁴⁵ Wilking, M.; Mück-Lichtenfeld, C.; Daniliuc, C.G.; Ulrich, H. *JACS* **2013**, *135*, 8133-36.

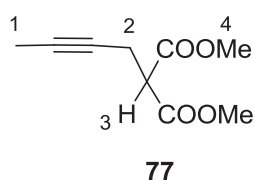
up to r.t. After cooling down to 0°C, propargyl bromide (10.0 mL, 80% in toluene, 1.335 g/cm³, 90 mmol) was added. The solution was stirred overnight while warming up to r.t. The reaction mixture was poured into a saturated aqueous solution of NH₄Cl (100 mL) and the aqueous layer was extracted with CH₂Cl₂ (3 x 30 mL). The combined organic layers were dried over anhydrous sodium sulphate, filtered and evaporated to give a pale yellow solid **75**³⁴⁵ (5.14 g, Yield: 83%). **CF**: C₁₁H₁₂O₄. **MW**: 208.21 g/mol. **¹H-NMR (CDCl₃, 250 MHz)**: 3.76 (s, 6H, H₃), 3.00 (d, J = 2.5 Hz, 4H, H₂), 2.03 (t, J = 2.5 Hz, 2H, H₁). **¹³CRMN (CDCl₃, 90.0 MHz)**: 169.38, 78.23, 71.70, 56.24, 52.95, 22.25.

Preparation of dimethyl 2,2-di(but-2-yn-1-yl)malonate, 76 and dimethyl 2-(but-2-yn-1-yl)malonate, 77.



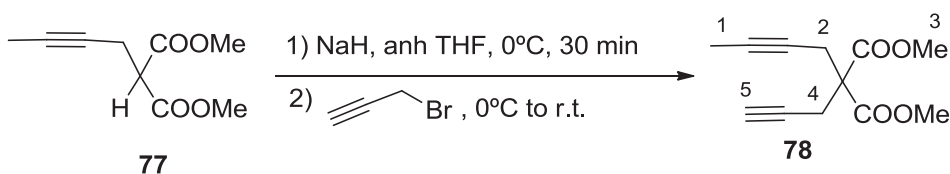
To a solution of NaH (0.586 g, 60% dispersion in mineral oil, 14.6 mmol) in dry THF (20 mL), dimethyl malonate (0.7 mL, 1.154 g/cm³, 6.12 mmol) was added at 0°C under Ar atmosphere. The mixture was stirred for 30 minutes allowing the temperature to warm up to r.t. After cooling down to 0°C, 1-bromo-2-butyne (1.5 mL, 1.52 g/cm³, 17.1 mmol) was added. The solution was stirred overnight while warming up to r.t. The reaction mixture was poured into saturated aqueous solution of NH₄Cl (30 mL) and the aqueous layer was extracted with CH₂Cl₂ (3 x 30 mL). The combined organic layers were dried over anhydrous sodium sulphate, filtered and evaporated to give a crude mixture of *mono- 77* and *di- 76* substituted products which were separated by flash chromatography (pentane/Et₂O 95/5 to 80/20).





Dimethyl 2-(but-2-yn-1-yl)malonate, 77. The above procedure yielded **77** as a colorless liquid (0.508 g, Yield: 45%). **CF:** C₉H₁₂O₄. **MW:** 184.19 g/mol. **¹H-NMR (CDCl₃, 250 MHz):** 3.76 (s, 6H, H₄), 3.55 (t, J= 7.5 Hz, 1H, H₃), 2.74-2.70 (m, 2H, H₂), 1.74 (s, 3H, H₁). **¹³CRMN (CDCl₃, 90.0 MHz):** 169.12, 77.88, 74.44, 52.52, 51.22, 18.45, 2.96.

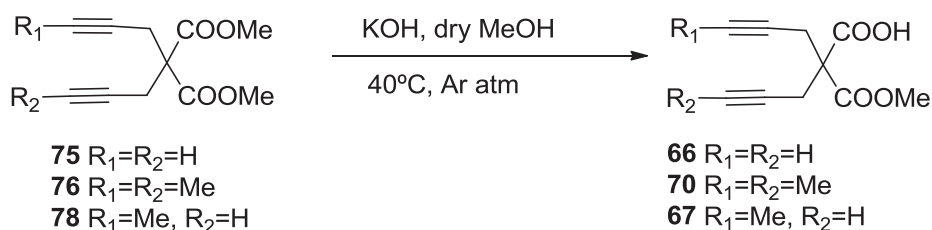
Preparation of dimethyl 2-(but-2-yn-1-yl)-2-(prop-2-yn-1-yl)malonate, 78.



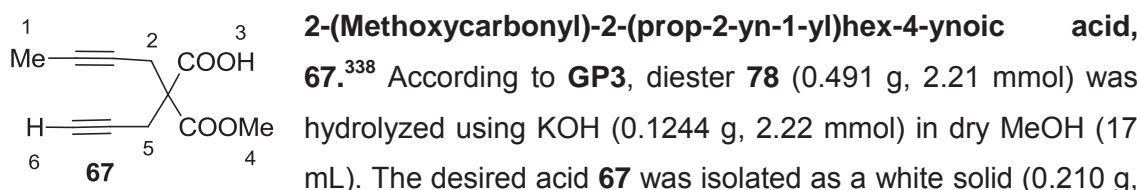
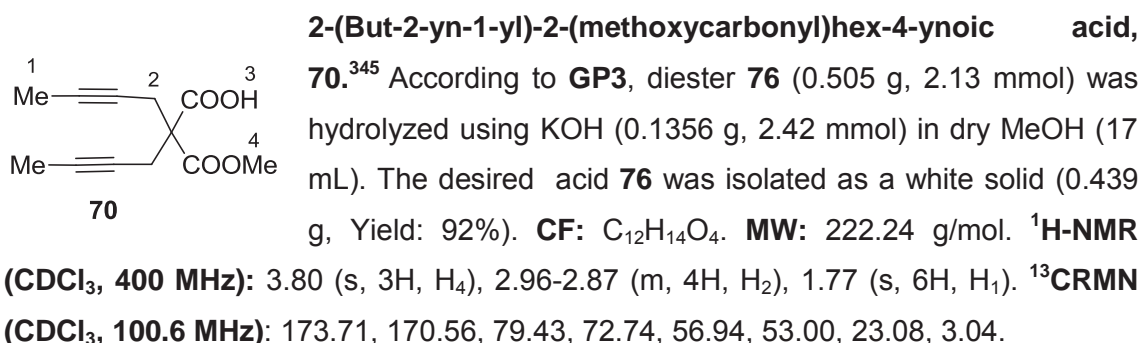
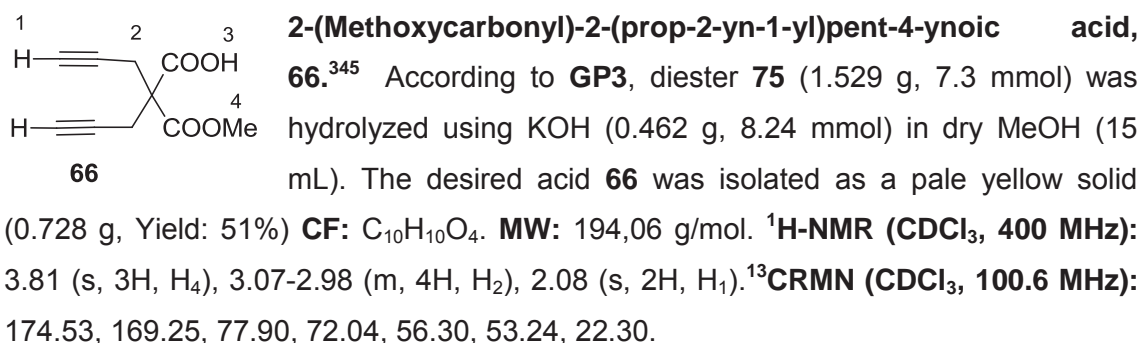
To a solution of NaH (0.137 g, 60% dispersion in mineral oil, 3.42 mmol) in dry THF (5 mL), diester **77** (0.501 g, 2.72 mmol) was added at 0°C under Ar atmosphere. The mixture was stirred for 30 minutes allowing the temperature to warm up to r.t. After cooling down to 0°C, propargyl bromide (0.4 mL, 80% in toluene, 1.335 g/cm³, 3.59 mmol) was added. The solution was stirred overnight while warming up to r.t. The reaction mixture was poured into saturated aqueous NH₄Cl (10 mL) and the aqueous layer was extracted with CH₂Cl₂ (3 x 15 mL). The combined organic layers were dried over anhydrous sodium sulphate, filtered and evaporated to give a colorless liquid **78**³⁴⁶ (0.491 g, Yield: 82%). **CF:** C₁₂H₁₄O₄. **MW:** 222,24 g/mol. **¹H-NMR (CDCl₃, 250 MHz):** 3.75 (s, 6H, H₃), 2.97-2.95 (m, 4H, H₂+H₄), 2.00 (m, 1H, H₅), 1.74 (m, 3H, H₁). **¹³CRMN (CDCl₃, 90.0 MHz):** 169.94, 79.28, 78.63, 72.71, 71.44, 56.60, 52.85, 22.64, 22.29, 3.02.

³⁴⁶ Shimamoto, T.; Chimori, M.; Sogawa, H.; Yamamoto, K. *J. Am. Chem. Soc.* **2005**, *127*, 16410.

General procedure for the monohydrolysis of dimethyl 2,2-disubstituted malonates (GP 3)



In a round bottom flask, the corresponding dimethyl 2,2-disubstituted malonate was dissolved in dry MeOH, KOH was added (1.1 eq) and the reaction mixture was stirred at 40°C under Ar atmosphere. After the completion of the reaction (TLC monitoring), volatiles were removed under vacuum and the residue was dissolved in a saturated NaHCO₃ aqueous solution. The aqueous layer was extracted with Et₂O to remove residual starting diester. The aqueous layer was acidified to pH=1 with HCl_{aq} (5M) and was extracted with CH₂Cl₂. The combined dichloromethane layers were dried over anhydrous sodium sulphate, filtered and evaporated to give the desired product.



Yield: 46%). **CF**: C₁₁H₁₂O₄. **MW**: 208.21 g/mol. **¹H-NMR (CDCl₃, 400 MHz)**: 3.79 (s, 3H, H₄), 2.98-2.93 (m, 4H, H₂+H₅), 2.04 (s, 1H, H₆), 1.76 (s, 3H, H₄). **¹³C-NMR (CDCl₃, 100.6 MHz)**: 174.62, 169.76, 79.61, 78.33, 72.46, 56.65, 53.06, 22.76, 22.35, 3.00.

5.3.3.2 General procedures for catalytic tests

*General procedure for the catalytic tests with the homogeneous catalyst **47**.*

To a biphasic system composed of 1 mL of toluene and 1 mL of distilled water, 0.3 mmol of 4-pentynoic acid and the homogeneous catalyst **47** (2.5 mol% Au) were added. The resulted mixture was magnetically stirred under air at room temperature until complete conversion of the alkynoic acid was observed by TLC (hexane:AcOEt 9:1). The organic phase was then separated, the aqueous layer was extracted with Et₂O (3 x 1.5 mL), and the combined organic extracts were dried over anhydrous MgSO₄ and filtered over a short pad of silica gel using DCM as eluent. The volatiles were removed under vacuum to yield the corresponding lactone.

*General procedure for the catalytic tests in toluene/water biphasic system with **M11**.*

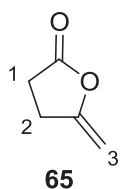
To a biphasic system composed of 0.5 mL of toluene and 0.5 mL of distilled water, 0.15 mmol of the corresponding alkynoic acid and the heterogeneous catalyst **M11** (2.5 mol% Au) were added. The resulted mixture was stirred by a laboratory wrist type shaker apparatus under air at room temperature until complete conversion of the alkynoic acid was observed by TLC (hexane: AcOEt 9:1). The organic phase was then separated, the aqueous layer was extracted with Et₂O (3 x 1.5 mL), and the combined organic extracts were dried over anhydrous MgSO₄. The volatiles were removed under vacuum to yield the corresponding lactone. Recyclability tests were performed by recharging the system (water + solid **M11**) with toluene and the corresponding alkynoic acid.

*General procedure for the catalytic tests in eutectic solvents with **M11**.*

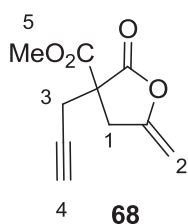
In a vial, 0.15 mmol of the corresponding alkynoic acid were dissolved in 0.150 g of DESCl and then heterogeneous catalyst **M11** (2.5 mol% Au) was added. The resulted mixture was magnetically stirred under air at room temperature until complete conversion of the alkynoic acid was observed by TLC (hexane: AcOEt 9:1). The reaction mixture was then extracted with Et₂O (3 x 1.5 mL), and the combined organic extracts were dried over anhydrous MgSO₄. The volatiles were removed under vacuum

to yield the corresponding lactone. Recyclability tests were performed by recharging the system (DES + solid **M11**) with the corresponding alkynoic acid.

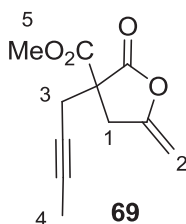
The identity of the known lactones was assessed by comparison of their ^1H and ^{13}C NMR spectroscopic data with those reported in the literature.^{337,338}



5-Methylenedihydrofuran-2(3H)-one, 65. CF: $\text{C}_5\text{H}_6\text{O}_2$. MW: 98,10 g/mol. $^1\text{H-NMR}$ (CDCl_3 , 250 MHz): 4.82 (m, 1H, H_{3a}), 4.39 (m, 1H, H_{3b}), 2.98-2.91 (m, 2H, H_1), 2.77-2.71 (m, 2H, H_2).

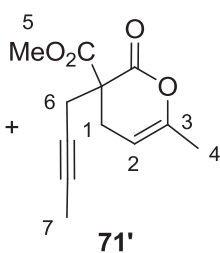
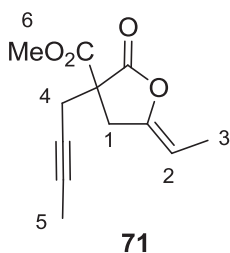


Methyl 5-Methylene-2-oxo-3-(prop-2-yn-1-yl)tetrahydrofuran-3-carboxylate, 68. CF: $\text{C}_{10}\text{H}_{10}\text{O}_4$. MW: 194.18 g/mol. $^1\text{H-NMR}$ (CDCl_3 , 250 MHz): 4.85 (m, 1H, H_{2a}), 4.42 (m, 1H, H_{2b}), 3.81 (s, 3H, H_5), 3.36-3.18 (m, 2H, H_3/H_1), 2.91 (m 2H, H_1/H_3), 2.09 (t, $J = 2.7$ Hz, 1H, H_4) $^{13}\text{C-NMR}$ (CDCl_3 , 62.5 MHz): 172.69, 169.74, 153.44, 89.98, 77.51, 72.28, 54.03, 53.30, 34.03, 22.92.



Methyl 3-(but-2-yn-1-yl)-5-methylene-2-oxotetrahydrofuran-3-carboxylate, 69. CF: $\text{C}_{11}\text{H}_{12}\text{O}_4$. MW: 208.21 g/mol. $^1\text{H-NMR}$ (CDCl_3 , 250 MHz): 4.81 (m, 1H, H_{2a}), 4.39 (m, 1H, H_{2b}), 3.78 (s, 3H, H_5), 3.26-3.17 (m, 2H, H_3/H_1), 2.89-2.82 (m, 2H, H_1/H_3), 1.75 (t, $J = 2.5$ Hz, 3H, H_4). $^{13}\text{C-NMR}$ (CDCl_3 , 62.5 MHz): 173.08, 169.05, 153.72, 89.32,

79.88, 71.89, 54.35, 53.08, 33.95, 23.27, 1.87.



Methyl 3-(but-2-yn-1-yl)-5-ethylidene-2-oxotetrahydrofuran-3-carboxylate (71) + methyl 3-(but-2-yn-1-yl)-6-methyl-2-oxo-3,4-dihydro-2H-pyran-3-carboxylate (71'). CF: $\text{C}_{12}\text{H}_{14}\text{O}_4$. MW: 222.24 g/mol. $^1\text{H-NMR}$ (CDCl_3 ,

250 MHz): (**71**): 4.74-4.66 (m, 1H, H_2), 3.78 (s, 3H, H_6), 3.27-3.08 (m, 2H, H_4/H_1), 2.90-2.80 (m, 2H, H_1/H_4), 1.75 (t, $J = 2.5$ Hz, 3H, H_5), 1.70 (dt, $J = 6.9$ Hz, $J = 1.7$ Hz, 3H, H_3). (**71'**): 5.00 (m, 1H, H_2), 3.75 (s, 3H, H_5), 2.80-2.77 (m, 2H, H_6/H_1), 2.77-2.56 (m, 2H, H_1/H_6), 1.87 (m, 3H, H_7), 1.77 (m, 3H, H_4).

GENERAL CONCLUSIONS

The present thesis deals with the preparation and application of different recyclable heterogeneous catalysts which were fixed on a silica matrix. A brief introduction to the field of hybrid silica materials, with a special emphasis on their preparation and characterization, is given in Chapter 1. We have applied most of the methodologies described therein to immobilize the different catalysts, sol-gel process has been used in Chapters 2, 3 and 4, an example of *grafting* can be found in Chapter 2 and a template-assisted hydrolytic polycondensation is described in Chapter 3.

This thesis encompasses different fields of catalysis. First, asymmetric organocatalysis has been approached by supported catalysts derived from proline mimetics. Organosilicas derived from proline sulfonamides have shown good performances in direct asymmetric aldol reactions under mild conditions (in water at room temperature, absence of co-catalyst, relatively low amount of catalyst) allowing their recycling up to 5 consecutive runs. We have observed that the characteristics of the matrix, the nature and length of the linker and the site of immobilization to the inorganic matrix within the catalytic organic moiety, affects the catalytic performance of the material. However, these supported catalysts showed lower efficiency and/or selectivity in other asymmetric reactions such as aza-Diels Alder reactions.

Secondly, NHC-based organocatalysis has been attempted with two different materials derived from imidazolium and imidazolinium salts by the *in situ* addition of a base. Unfortunately, it has not been possible to generate supported free NHC species to catalyze the benzoin condensation or the annulation reaction of an enal with a vinyl ketone despite the protection of acidic free silanol groups of the silica material. Alternatively, imidazolium supported organocatalyst has been successfully used as a recyclable catalyst for the chemoselective *N-tert*-butyloxycarbonylation of aromatic amines. Contrary to the previous case, it was found that the acidity of the support brings a cooperative effect as simple mesostructured silica of SBA-15 type also catalyzed the reaction, although at lower reaction rate.

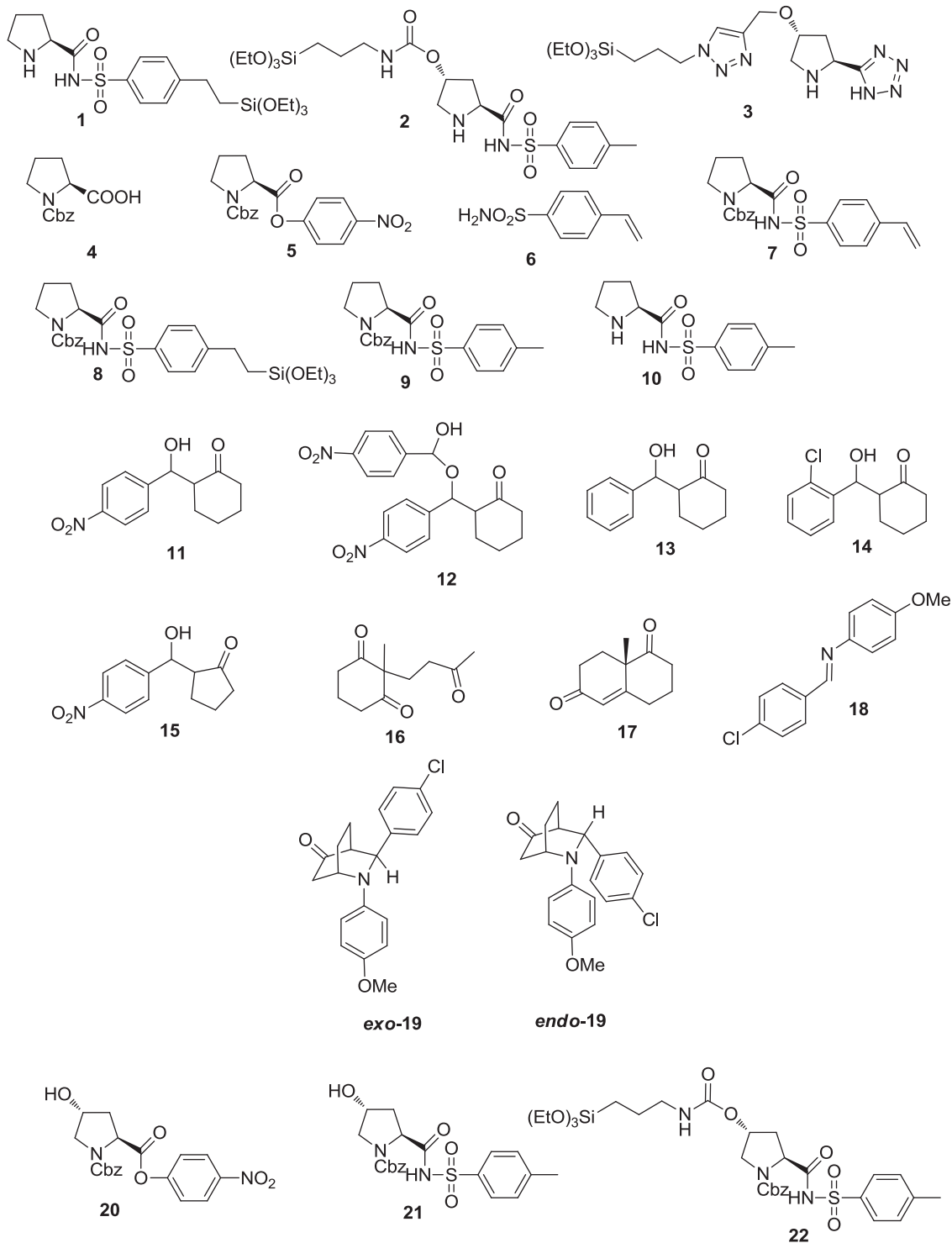
On the other hand, organometallic catalysis by [(NHC)Au(I)] species has also been treated. We have achieved for the first time the preparation of a silica-supported [(NHC)AuCl] catalyst by a sol-gel co-condensation process. A synergistic effect was observed for this hybrid silica material as the [(NHC)AuCl] immobilized complex showed higher stability and a much better performance than its homogeneous

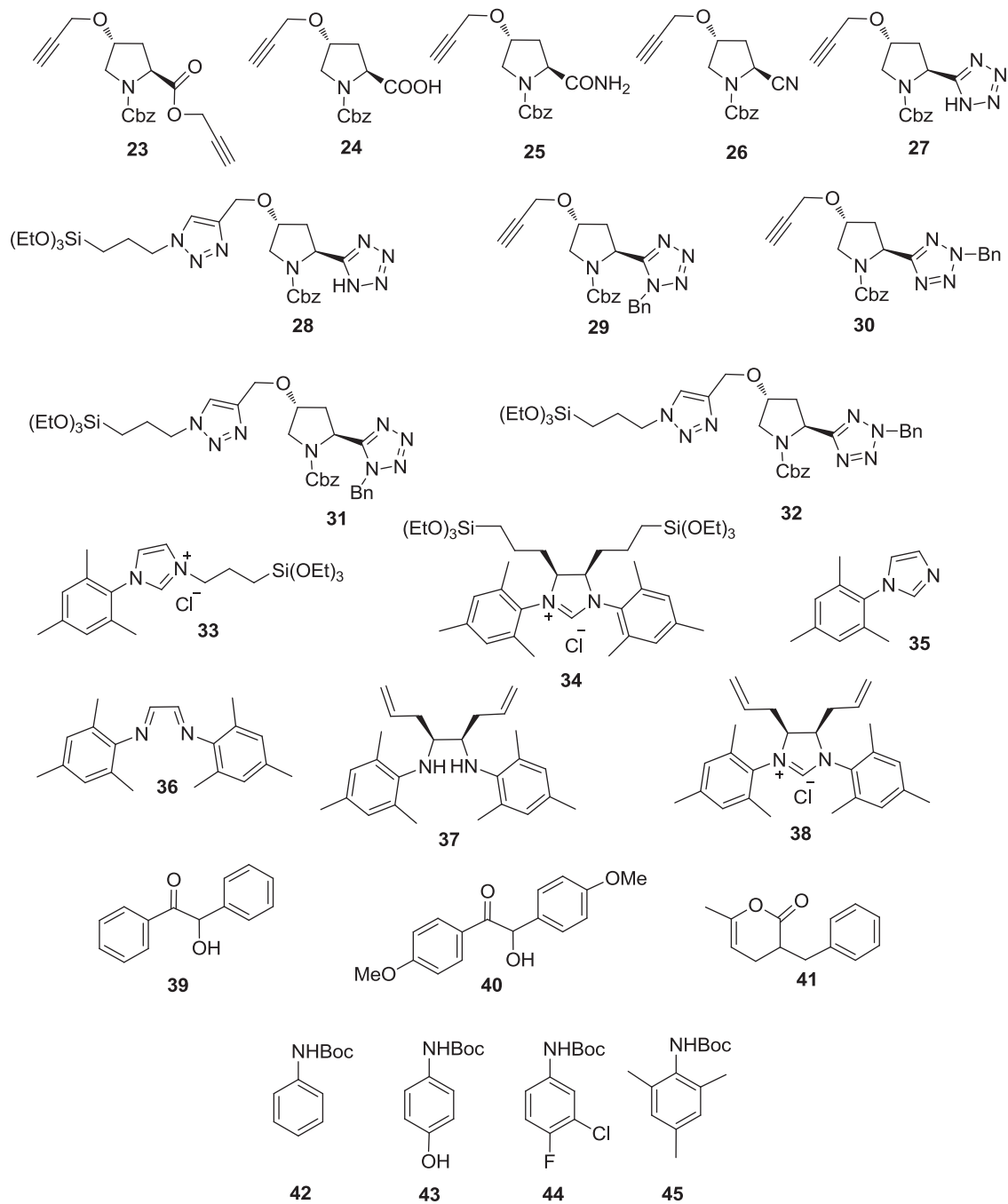
General Conclusions

analogue in the catalytic assays. First, it was tested in the rearrangement of allylic esters in conjunction with a silver salt. More interestingly, it showed an excellent performance in the cycloisomerization of γ -alkynoic acids to 5-membered enol-lactones in a toluene/water biphasic medium at room temperature, avoiding the use of silver salts and allowing its reuse up to 6 cycles.

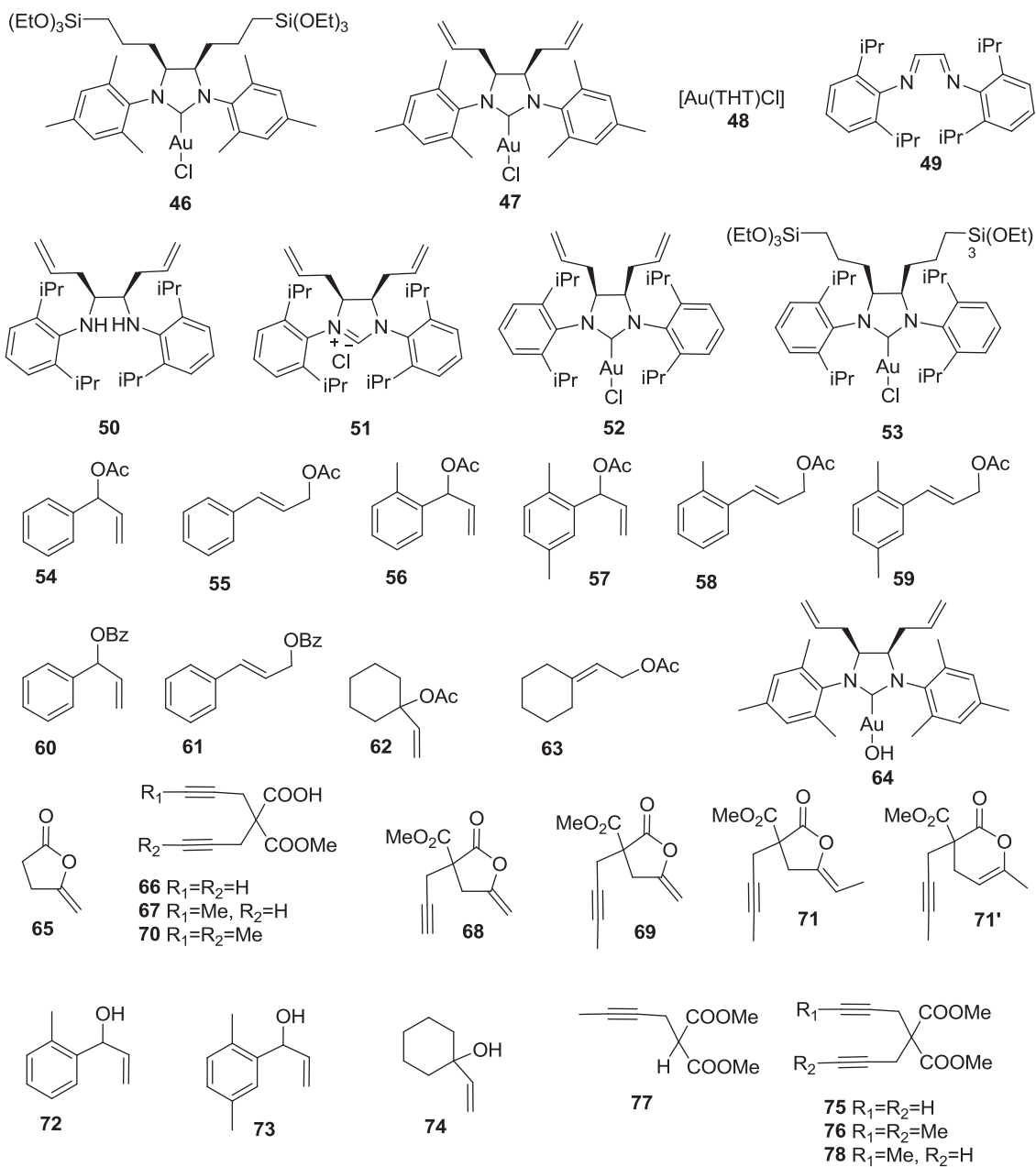
In summary, we have presented the usefulness of the sol-gel process and grafting methods for the development of different silica-supported catalysts from the corresponding silylated precursors. Some of these catalytic materials have shown good recycling profiles and an easy recovery.

FORMULA INDEX





Formula Index



MATERIALS